

**FIRING RATE ANALYSIS FOR A LINEAR
INTEGRATE-AND-FIRE NEURONAL MODEL**

by

Ryan M. O'Grady

B.S., Allegheny College, 2002

M.A., University of Pittsburgh, 2009

Submitted to the Graduate Faculty of
the Department of Mathematics in partial fulfillment
of the requirements for the degree of

Doctor of Philosophy

University of Pittsburgh

2011

UNIVERSITY OF PITTSBURGH
MATHEMATICS DEPARTMENT

This dissertation was presented

by

Ryan M. O'Grady

It was defended on

April 22, 2011

and approved by

William C. Troy, Department of Mathematics

Brent Doiron, Department of Mathematics

Gunduz Caginalp, Department of Mathematics

Satish Iyengar, Department of Statistics

Dissertation Director: William C. Troy, Department of Mathematics

FIRING RATE ANALYSIS FOR A LINEAR INTEGRATE-AND-FIRE NEURONAL MODEL

Ryan M. O'Grady, PhD

University of Pittsburgh, 2011

We investigate a stochastic linear integrate-and-fire (IF) neuronal model and use the corresponding Fokker-Planck equation (FPE) to study the mean firing rate of a population of IF neurons. The firing rate (or emission rate) function, $\nu(t)$, is given in terms of an eigenfunction expansion solution of the FPE. We consider two parameter regimes of current input and prove the existence of infinitely many branches of eigenvalues and derive their asymptotic properties. We use the eigenfunction expansion solution to prove asymptotic properties of the firing rate function, $\nu(t)$. We also perform a numerical experiment of 10,000 IF neurons and show that our simulation is in agreement with our theoretical results. Finally, we state several open problems for future research.

TABLE OF CONTENTS

PREFACE	x
1.0 INTRODUCTION	1
1.1 The Mean Firing Rate in Neurons	1
1.2 Mathematical Models	2
1.2.1 The Integrate-and-Fire Model	3
1.2.2 The Leaky Integrate-and-Fire Model	3
1.2.3 The Hodgkin-Huxley Equations: The Space Clamped Simplification	4
1.2.4 Simplifications of the Hodgkin-Huxley Equations	4
1.3 Stochastic Integrate-and-Fire Models	5
1.3.1 Why study integrate-and-fire models rather than HH type models	6
1.4 The Focus of This Thesis	11
1.5 Our Mathematical Results	13
1.5.1 Thesis Goals and Results	13
1.5.2 Chapter Outline	14
2.0 LEAKY (LIF) AND LINEAR (IF) MODELS: A COMPARISON	17
2.1 The Leaky Integrate-and-Fire Model	18
2.1.1 The Fokker-Plank Equation FPE for the LIF Model	18
2.1.2 The Firing Rate Function for the LIF Model	19
2.1.3 The FPE BVP for the LIF Model	20
2.2 The Linear Integrate-and-Fire Model	20
2.2.1 The Fokker-Plank Equation for the IF Model	21
2.2.2 The Firing Rate Function for the IF Model	22

2.2.3	The FPE Boundary Value Problem for the IF Model	22
2.3	Eigenfunction Expansion for the LIF Model	23
2.3.1	The ODE BVP for Eigenfunctions of the LIF Model	24
2.3.2	Stationary Solution of the FPE of the LIF Model	25
2.3.3	Behavior of the Stationary Solution of the LIF	29
2.3.4	Numerical Exploration of the Neighborhood U	33
2.3.5	The Difficulty in the LIF Eigenvalue Problem	34
2.4	The Eigenfunction Expansion for the IF Model	34
2.4.1	The ODE BVP for Eigenfunctions of the IF Model	36
2.4.2	ODE Eigenvalue Problem for the Case $V_L = V_R$	37
2.4.3	The Eigenvalue Problem for the IF in the General Case	42
2.4.4	The Stationary Solution when $V_L = -\infty$	47
2.5	Conclusion and Open Problem	49
3.0	BACKGROUND PROPERTIES OF THE IF MODEL WHEN $V_L = V_R$	50
3.1	The Linear Integrate and Fire (IF) FPE Boundary Value Problem	51
3.2	The Operators L and L^+ when $V_L = V_R = 0$	55
3.3	The Eigenfunction Expansion When $V_L = V_R$	57
3.4	The Mattia-Del Giudice Conjecture	58
4.0	THE MAIN RESULTS: EXISTENCE OF EIGENVALUES WHEN	
	$V_L = V_R$	59
4.1	Eigenvalue Structure of the IF When $V_L = V_R$	60
4.1.1	The Fokker Planck Problem When $-\infty < V_L = V_R < \theta$	60
4.1.2	The Eigenvalue Problem When $V_L = V_R$	61
4.1.3	The Nonlinear Eigenvalue Equation	62
4.1.4	The Eigenfunctions ϕ_n of L and ψ_n of L^+	64
4.2	Eigenvalues for the IF model when $\mu = 0$	66
4.2.1	The ODE Boundary Value Problem	66
4.2.2	The Main Theoretical Result	67
4.3	Eigenvalues for the IF model when $z = \frac{\mu\theta}{\sigma^2} > 0$	77
4.3.1	The Nonlinear Algebraic Equations for γ_1 and γ_2	78

4.3.2	ODEs for γ_1 and γ_2	79
4.3.3	Infinitely Many Initial Values for the (γ_1, γ_2) ODEs.	80
4.3.3.1	Outline of the Proof of Theorem 3	81
4.3.3.2	Proof of Theorem 3.	81
4.3.4	Infinitely many $C^1((0, \infty))$ solutions of the ODEs.	93
4.3.5	Properties of $\lambda_1^n(z)$ and $\lambda_2^n(z)$ as $z = \frac{\mu\theta}{\sigma^2} \rightarrow 0^+$	106
4.4	Eigenvalues for the IF model when $z = \frac{\mu\theta}{\sigma^2} < 0$	110
4.4.1	Existence and Asymptotic Behavior When $z = \frac{\mu\theta}{\sigma^2} < 0$	111
4.4.1.1	Proof of Theorem 8.	113
4.4.1.2	Proof of Theorem 9.	116
4.4.1.3	Proof of Theorem 10.	129
4.4.1.4	Proof of Theorem 11.	132
4.5	Partial Proof of the Mattia-Del Giudice Conjecture when $\mu > 0$	135
4.5.1	All Eigenvalues are Complex When $\mu > 0$	136
4.5.2	The Real Parts of the Eigenvalues are Negative	142
4.5.3	Open Problem: Real parts of the Eigenvalues are Negative	143
4.6	Partial Proof of the Mattia-Del Giudice Conjecture when $\mu < 0$	144
4.6.1	Eigenvalues are Negative when $\gamma_1 = 0$	144
4.6.2	Open Problem: The Eigenvalues are Real and Negative	145
5.0	THE FIRING RATE	146
5.1	Numerical Simulations for IF when $\mu > 0$	146
5.1.1	Numerical Computation of the Eigenvalues.	147
5.1.1.1	Remarks About the Eigenvalue Tables	148
5.1.2	The Firing Rate Function	149
5.1.2.1	Numerical Simulation of a Population of IF neurons	149
5.2	Firing Rate Analysis when $\mu > 0$	150
5.2.1	The Firing Rate function generated by the FPE.	150
5.2.2	Asymptotic Results for the Firing Rate Function	152
5.2.3	Relative Error Between Theoretical and Numerical Values of $\nu(\infty)$	153
5.3	Firing Rate when $\mu(t)$ is a step function	153

5.3.1	Theoretical Firing rate	154
5.3.2	Population Firng Rate	155
5.4	Proof that $E([\nu_N(t) - \nu(t)]^2) \approx \frac{\nu(t)}{N\Delta t}$, $N \gg 1$	156
6.0	OPEN PROBLEMS AND FUTURE RESEARCH	170
6.1	Open Problem 1: Extremum properties of the Stationary Solution for the LIF FPE	170
6.2	Open Problem 2: Existence of eigenvalues and eigenfunctions for the LIF FPE	171
6.3	Open Problem 3: Resolution of the Mattia-Del Giudice Conjecture for the IF Model	171
	APPENDIX. NUMERICAL CODES	173
A.1	Reproducing the plots of the stationary solutions for the LIF and IF	173
A.2	Numerical Investigation of the Neighborhood U	180
A.3	The functions $\gamma(z)$ and $\lambda(z)$	181
A.4	Calculating the Eigenvalues for the FPE of the IF model	188
A.5	The Firing Rate Function	190
A.5.1	Calculating the Theoretical Firing Rate, $\nu(t)$	190
A.5.2	Simulation of the Population Firing Rate	193
	BIBLIOGRAPHY	197

LIST OF TABLES

1	Gamma Values when $\mu = 20$	158
2	Eigenvalues when $\mu = 20$	159
3	Gamma Values when $\mu = 5$	160
4	Eigenvalues when $\mu = 5$	161
5	Gamma Values when $\mu = 1$	162
6	Eigenvalues when $\mu = 1$	163
7	Gamma Values when $\mu = 0.1$	164
8	Eigenvalues when $\mu = 0.1$	165
9	Relative Error	169

LIST OF FIGURES

1	The firing rate when $\mu(t)$ is a step function	10
2	Stationary solution of the LIF when $\tau = 1$	27
3	Stationary solution of the LIF when $\tau = 20$	28
4	The neighborhood U	35
5	Stationary solution of the IF when $V_L = V_R$	41
6	Stationary solution of the IF when $V_L < V_R$	48
7	The rectangle B_n	82
8	The rectangle D_n and the initial point for the ODE	95
9	The functions $\gamma_1(z)$ and $\gamma_2(z)$	96
10	The eigenvalues $\lambda_1(z)$ and $\lambda_2(z)$	107
11	$\gamma_1(z)$, $\gamma_2(z)$ and corresponding eigenvalues for $\mu < 0$	114
12	Theoretical Firing Rate	166
13	Firing Rate: Population versus Theoretical	167
14	Firing Rate as μ varies	168
15	The firing rate when $\mu(t)$ is a step function	169

PREFACE

The completion of this thesis would not have been possible without the assistance and support of several people.

Most importantly, I would like to thank my advisor Professor William C. Troy. His insight, guidance, and patience are truly invaluable.

To my committee members, Professors Brent Doiron, Gunduz Caginalp, and Satish Iyengar: thank you for being excellent teachers and mentors. Your courses and personal discussions have been helpful and productive.

I would also like to thank Dr. Cheng Ly, Dr. Mark DeSantis, Sashi Marella, and Justin Dunmyre. Each of you has been a great help over the last few years. Your insight and suggestions were greatly appreciated.

The Pitt math department faculty, staff, and students: you have all made the last few years challenging and exciting. Thank you!

Lastly, I must thank my family and friends, especially Amy. You have know clue what it is that I do, yet you only complain some of the time. I wish this thesis could serve as proof that I have actually worked over the last few years. However, I am quite sure you won't understand a word that follows this!

1.0 INTRODUCTION

The purpose of this thesis is to provide mathematical analysis of the firing rate of a linear integrate-and-fire neuronal model (1.10). In this chapter we introduce the notion of mean firing rate of a neuron, its importance, and how it is studied mathematically. Next, goals and mathematical results are discussed. In particular, we do the following:

1.1 This section gives a motivation of the main problem in this thesis: mean firing rate analysis of a neuron.

1.2 This section gives a description of the important mathematical models used to study the mean firing rate over the last 104 years.

1.3 This section introduces the two stochastic integrate-and-fire neuronal models analyzed in this thesis. We describe the advantages and disadvantages of studying these models.

1.5 This section describes our main mathematical results. An outline is given which describes the results proved in each chapter.

1.1 THE MEAN FIRING RATE IN NEURONS

The concept of mean firing rate in neurons has been a central focus of experimental studies ever since the pioneering work of Adrian and Zotterman [1, 2] in 1926. These authors gave evidence which showed how frog muscle responded to stimulation of single motor neuron nerve fibers. The stimulation they used included the pressure on the muscle, as well as pricking the muscle with a needle. Their recordings “showed that the firing rate of stretch receptor neurons in the muscles is related to the force applied to the muscle” (Gerstner and

Kistler [13]). In 1928 Adrian and Bronk [3] extended the experimental techniques in [1, 2] to record the firing rate response of skin to a stimulus of constant intensity. Due to the ease of measuring firing rates experimentally, this method has been widely used over the last 83 years [13]. As pointed out by Gerstner and Kistler in their 2002 textbook [13], a central modern day issue is to understand the role of mean firing rate in the mammalian brain, which “contains more than 10^{10} densely packed neurons that are connected to an intricate network. In every small volume of cortex, thousands of spikes are emitted each millisecond.” These large scale neuronal firing properties have led to the following fundamental questions (e.g. see Gerstner and Kistler [13], Haken [14], Tuckwell [35]):

- **Question 1.** What is the information contained in a spatio-temporal pattern of pulses?
- **Question 2.** What is the code used by the neurons to transmit the information in a spatio-temporal pattern of pulses?
- **Question 3.** How might other neurons decode the signal?
- **Question 4.** As external observers, can we read the code and understand the message of the neuronal activity pattern?

An important approach to answering **Questions 1-4** is to investigate firing rate phenomena in mathematical models. Below, we describe relevant models.

1.2 MATHEMATICAL MODELS

A first step in addressing the issues raised in **Questions 1-4** above is to combine experimental results, together with mathematical modeling, in order to understand underlying mechanisms responsible for firing rate phenomena in neuronal settings. Thus, in this section our goal is to give a brief description of mathematical models that have been used during the last 100 years to understand firing rate phenomena.

1.2.1 The Integrate-and-Fire Model

One of the earliest models (e.g. see Tuckwell [35], Cronin [8]) of neuronal firing is the equation

$$C_m \frac{dV_m}{dt} = I(t), \quad (1.1)$$

where $V_m(t)$ and $I(t)$ are the transmembrane voltage and current, respectively. This model, which was proposed in 1907 by Louis Lapicque [21], results from taking the time derivative of the law of capacitance $C_m V_m(t) = Q(t)$. When a positive constant current I is applied in equation (1.1), the membrane voltage increases with time until $V_m(t_T) = \text{threshold} = V_T$ at a time t_T . At t_T a delta function spike occurs and the voltage $V_m(t)$ is reset to its resting potential, $V = V_R < V_T$, after which the model again determines the behavior of $V_m(t)$. As the input current $I(t)$ is increased the firing frequency of the neuron also increases. One way to improve the biological accuracy of this model is to introduce a refractory period $T_R > 0$, which limits the frequency of firing during a period of length T_R immediately following the voltage reset after the neuron fires[35]. Thus, when $T_R > 0$, the maximum firing frequency of the neuron is $1/T_R$. In a recent review article by Brunel and Van Rossum [6], they point out that “the simplicity of equation (1.1) makes it one of the most popular models of neuronal firing to this day: it has been used in computational neuroscience for both cellular and neural networks studies, as well as in mathematical neuroscience.”

1.2.2 The Leaky Integrate-and-Fire Model

A more biologically accurate model is the leaky integrate-and-fire model (e.g. see [35]) given by the equation

$$C_m \frac{dV_m}{dt} + \frac{V_m(t)}{R_m} = I(t). \quad (1.2)$$

R_m is the membrane resistance. As with the integrate-and-fire model (1.1), the membrane voltage increases with time until $V_m(t_T) = \text{threshold} = V_T$ at a time t_T . At t_T a delta function spike occurs and the voltage $V_m(t)$ is reset to its resting potential, $V = V_R$, after which the model (1.2) again determines the behavior of $V_m(t)$.

1.2.3 The Hodgkin-Huxley Equations: The Space Clamped Simplification

In 1952 Hodgkin and Huxley [16] introduced the following nonlinear system to model a space clamped axon:

$$\begin{aligned}\frac{dV}{dt} &= \frac{1}{C_M} [I - \bar{g}_{Na}m^3h(V - V_{Na}) - \bar{g}_Kn^4(V - V_K) - \bar{g}_l(V - V_l)], \\ \frac{dm}{dt} &= \alpha_m(1 - m) - \beta_m m, \\ \frac{dh}{dt} &= \alpha_h(1 - h) - \beta_h h, \\ \frac{dn}{dt} &= \alpha_n(1 - n) - \beta_n n.\end{aligned}$$

Here, V is membrane potential, and the variables m , n , and h were proposed by Hodgkin and Huxley to control the conductance of sodium and potassium ions. The functions α_m , β_m , α_h , β_h , α_n , β_n in the odes for m , n , and h are assumed to be functions of V . The Hodgkin-Huxley (HH) equations model the variations of the membrane potential and ion conductance that occur at a fixed point of the neuron [8]. The difficulty in analytically studying neuronal mean firing rate in the HH system is that the functions α_m , β_m , α_h , β_h , α_n , β_n are transcendental [14]. Also, experimental indicates that the threshold is not well defined, hence the maximum voltage varies during a spike [17].

1.2.4 Simplifications of the Hodgkin-Huxley Equations

The FitzHugh-Nagumo Model

To aid in the study of the HH equations, simplifications have been made [8, 14, 35]. A fundamentally important example is the two-dimensional model developed independently by Fitzhugh [10] and Nagumo [26] given by the system

$$\begin{aligned}\frac{dV}{dt} &= V - \frac{1}{3}V^3 - W + I, \\ \frac{dW}{dt} &= \phi(V + a - bW),\end{aligned}$$

where a , b , and ϕ are positive constants. As before, I is the membrane current and V is the membrane potential. The new function W is a recovery variable.

The Morris-Lecar Equations

In 1981 Morris and Lecar combined Hodgkin-Huxley and FitzHugh-Nagumo into a voltage-gated calcium channel model with a delayed-rectifier potassium channel, represented by

$$\begin{aligned} C \frac{dV}{dt} &= -I_{ion}(V, w) + I \\ \frac{dw}{dt} &= \phi \frac{w_{\infty} - w}{\tau_w(V)} \end{aligned}$$

where

$$I_{ion}(V, w) = \bar{g}_{Ca} m_{\infty}(V)(V - V_{Ca}) + \bar{g}_K w(V - V_K) + \bar{g}_L(V - V_L).$$

Other two variable models similar to the FitzHugh-Nagumo equations, and the Morris-Lecar system, have been developed by Hindmarsh-Rose [15] in 1984, Rinzel [29] in 1985 and Wilson [36] in 1999.

1.3 STOCHASTIC INTEGRATE-AND-FIRE MODELS

As Tuckwell [35] points out (see page 111 in Vol II), the deterministic models discussed in Section 1.2 are inadequate when describing firing rate behavior (and hence address **Questions 1-4**) for a real neuron. In particular, sequences of firing times in experimentally studied neurons are random. This is due to thermo-molecular processes and channel noise. The overwhelming source of randomness is from synaptic transmission (e.g. the random arrival of synaptic events, and/or synaptic failure). This randomness in firing rate characterizes the behavior of realistic neurons, hence realistic models should be stochastic. Stochastic firing rate models were first introduced by Gerstein and Mandelbrot [12] in 1964, and subsequently by Stein [32] in 1965, and Knight [18] in 1972. Fusi and Mattia [11] introduced refractory barriers in stochastic integrate-and-fire models in 1999. Two of the most widely studied stochastic integrate-and-fire models are known as leaky integrate-and-fire (LIF) model and the linear integrate-and-fire (IF) model. These models, which are the focus of this thesis, are extensions of equations (1.1) and (1.2), and are described below:

I. The stochastic linear integrate-and-fire (IF) model, which is an extension of (1.1) consists of the stochastic differential equation (SDE)

$$dV = \mu(t)dt + \sigma(t)dW. \quad (1.3)$$

Here, the membrane potential $V(t)$ satisfies $V \in [V_L, V_T]$, where $V_L \leq V_R < V_T$, $\sigma(t)dW$ represents Brownian motion, and the function $\mu(t)$ describes the input of current. The parameter V_L represents the lowest possible value of transmembrane potential. For a real neuron, $V_L \approx -85 \text{ mV}$, which corresponds to the reversal potential for potassium (see Section 2.2 for further discussion). Descriptions of this model, together with the eigenfunction-eigenvalue expansion approach to its analysis, were given by Knight [18, 19] in 1972 and 2000, and by Mattia and Del Giudice [24] in 2002.

II. The stochastic leaky integrate-and-fire (LIF) model, which is an extension of (1.2) consists of the SDE

$$dV = \left(\mu(t) - \frac{V}{\tau} \right) dt + \sigma(t)dW, \quad (1.4)$$

where $-\frac{V}{\tau}$ is a leakage term that is not present in the IF model (1.3). A complete description of this spiking model is given by Gerstner and Kistler [13].

1.3.1 Why study integrate-and-fire models rather than HH type models

As pointed out by Tuckwell [35], Cronin [8], Lindner [22] and Izhikevich [17], integrate-and-fire models are not as biologically accurate as conductance based HH type models described above in Section 1.2. The obvious question arises: why study integrate-and-fire models rather than HH type models? Three important reasons for studying integrate-and-fire models are the following:

I. Computational efficiency. In 2004 Izhikevich [17] published the paper “Which Model to Use for Cortical Spiking Neurons?” in which compared the efficiency and accuracy of firing rates in a multitude of diverse models. These include integrate-and-fire models, the Hodgkin Huxley equations, the FitzHugh-Nagumo system, and the Morris-Lecar model. He found that integrate-and-fire models were computationally very efficient, whereas Hodgkin-Huxley

type systems were extremely inefficient, for recording firing rates in populations of large numbers of neurons. For example, a $1ms$ simulation of an IF model requires approximately 5 flops¹ while a Hodgkin-Huxley simulation for $1ms$ requires approximately 1200 flops.

II. Applicability. Below, we describe five examples of recent studies which have successfully made use of integrate-and-fire models to understand firing rate phenomena in biological systems.

(A.) In 2006 Doiron, Rinzel and Reyes used a multi-layer IF model to show that interaction between populations of spiking neurons in the cortex may depend critically on the size of the populations. In particular, they performed a simulation of 10 layers of 500 IF neurons. Their results agreed with experimentally observed behavior in a rat somatosensory cortex [28].

(B.) In 2008, Mullenwey and Iyengar [25] studied maximum likelihood estimates of a leaky integrate-and-fire neuron. They develop an algorithm for estimating parameters when only the firing rate is known. Their results were in agreement with previously published theoretical results.

(C.) In 2009 Ly and Doiron [23] used integrate-and-fire models to successfully estimate dynamic neural response in normal sensory and motor behavior. In particular, they construct an integrate-and-fire model with realistic, time varying inputs that agree with clamp experimental data in rat somatosensory cortex [7].

(D.) In 2009, Okamoto and Fukai [27] make use of integrate-and-fire model to study neuronal firing rate behavior in rat prefrontal and entorhinal cortex. Their results suggest that populations of neurons (in various brain areas) can act like non-leaky integrate-and-fire neurons at the population level. In addition, their results are in agreement with in agreement with experimental observations.

(E.) In his 2011 PH.D. thesis, Sashi Morelli [] obtained theoretical predictions of the firing rate of IF and LIF model neurons receiving mean or variance coded time-varying inputs. These predictions were tested via real neurons in the somatosensory cortex of a rat.

III. Mathematical tractability. Because of the simplicity of stochastic integrate-and-

¹The number of flops represents the number of floating point operations required for a simulation

fire models, they are much easier to analyze than systems of nonlinear HH conductance type models which have large numbers of functions and constants. To study stochastic integrate-and-fire type models, Knight [18, 19], as well as Mattia and Del Giudice [24], have successfully made use of eigenfunction expansion methods to study solutions of the Fokker Planck Equation (FPE) corresponding to the IF SDE (1.3):

$$\frac{\partial}{\partial t}\rho = -\mu(t)\frac{\partial}{\partial V}\rho + \frac{\sigma^2(t)}{2}\frac{\partial^2}{\partial V^2}\rho + \nu(t)\delta(V - V_R), \quad (1.5)$$

where $V(t) \in [V_L, V_T]$, and $V(t)$ satisfies a reflective boundary condition at V_L . An eigenfunction expansion solution of the FPE1.5, which has the form

$$\rho(V, t|V_0, 0) = \sum_{\lambda} A_n(t)e^{\lambda t}\phi_n(V), \quad (1.6)$$

has allowed these authors to successfully investigate the behavior of the firing rate (or emission rate) function

$$\nu(t) = -\frac{\sigma^2}{2}\frac{\partial}{\partial V}\rho(V_T, t|V_0, 0). \quad (1.7)$$

Question: What is the connection between the mean firing rate of a population of real neurons and the mean firing rate constructed by using the eigenfunction expansion method?

In real nervous systems neurons react to inputs from dynamic environments (e.g. sensory, memory recall). The input statistics for a given neuron change during the course of a task. Thus, in the context of the stochastic IF SDE equation (1.3), $\mu(t)$ and/or $\sigma(t)$ are time dependent quantities. A simple example illustrating this property is when the neuron input $\mu(t)$ is a step function, e.g.

$$\mu(t) = \begin{cases} 0 & 0 \leq t < T^* = 1000 \text{ msec.}, \\ 25 & t \geq T^*, \end{cases} \quad (1.8)$$

and $\sigma(t)$ is constant, e.g.

$$\sigma(t) = 1 \quad \forall t \geq 0. \quad (1.9)$$

The left panel of Figure 1 illustrates a simulation of population mean firing rate, $\nu_N(t)$, for $N = 10,000$ neurons. Here, we assume that each neuron satisfies the initial condition

$V(0) = V_R = 0$. Over the subinterval $0 \leq t < T^* = 1000$ the neurons receive constant input $\mu = 0$, and the population mean firing rate quickly relaxes to the equilibrium level $\nu_N(\infty) \approx 1$. When $t \geq 1000$ the input discontinuously jumps to the new constant level $\mu = 25$. In response to this discontinuous change of input, the population mean firing rate initially undergoes oscillations (i.e. ringing) with peaks that decrease in amplitude during a transition period of length approximately 200 *msecs*. By the end of this transition interval, the firing rate has relaxed to its equilibrium level, $\nu_N \approx 25$. The right panel shows the theoretical mean firing rate, $\nu(t)$, resulting from the eigenfunction expansion method. During the transition interval, $[1000, 1200)$, the theoretical firing rate $\nu(t)$ also undergoes oscillations, with peaks that decrease to zero in amplitude as the $\nu(t)$ relaxes to its equilibrium level, $\nu \approx 25$ (see Section 5.2.2). A major thrust of this thesis is to give a firm foundation to the use of the eigenfunction expansion to understand non equilibrium behavior of firing rate when μ and σ are constant during the two subintervals $[0, T^*)$ and $[T^*, \infty)$. Our study includes the parameter regime $\mu > 0$ and $\sigma > 0$, and also the regime $\mu < 0$ and $\sigma > 0$. Eigenfunction expansions have played an important role in several of the neuronal studies described above (e.g. studies **(A)**, **(C)** and **(E)**). In each application, numerical simulations led the authors to assume, without proof, that branches of eigenvalues, and corresponding eigenfunctions actually exist. However, to our knowledge there has been no rigorous analysis which establishes their existence. Thus, the focus of this thesis is to rigorously establish the existence of branches of eigenvalues and eigenfunctions. This will give a firm mathematical foundation for using eigenvalue/eigenfunction expansions to investigate firing rate properties in the stochastic models described above. The first step is to investigate these issues for the IF model, for both $\mu > 0$ and $\mu < 0$. It is hoped that our results will form a baseline from which we can gain insight for future analytical studies of the more complicated LIF model. Our approach is described below.

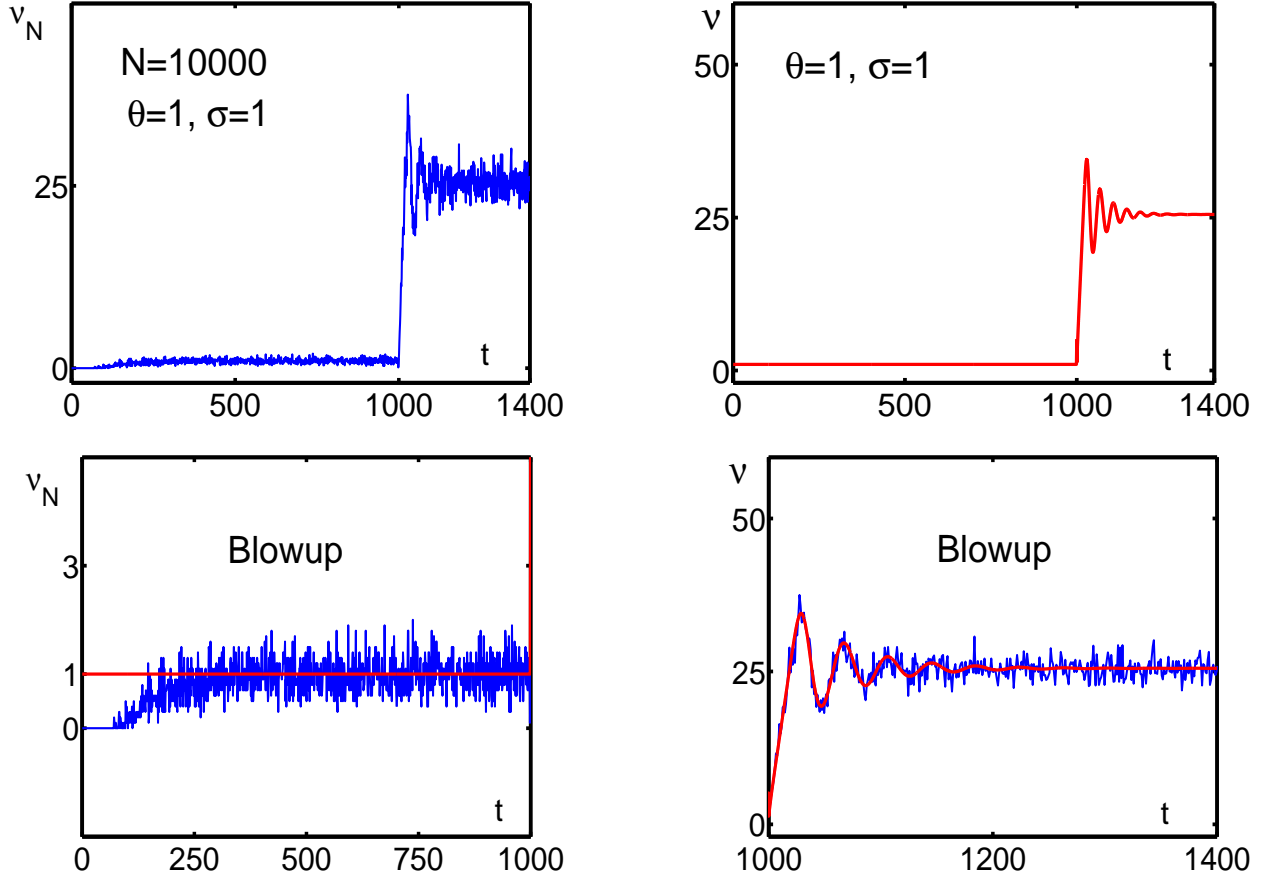


Figure 1: **Left Panel:** population mean firing rate, $\nu_N(t)$, (see formula (5.9)) for $N = 10,000$ neurons when $\sigma(t) \equiv 1$, and $\mu(t)$ is the step function defined in (1.8), i.e $\mu(t) = 0 \forall t \in [0, 1000)$, and $\mu(t) = 25 \forall t \in [1000, \infty)$. **Right Panel:** Theoretical mean firing rate, $\nu(t)$, of the FPE (1.5) constructed using the eigenfunction expansion method. See text.

1.4 THE FOCUS OF THIS THESIS

In this thesis we fix $\mu(t)$ and $\sigma(t)$ to be constant, hence the stochastic IF model (1.3) becomes

$$dV = \mu dt + \sigma dW, \tag{1.10}$$

with corresponding FPE

$$\frac{\partial}{\partial t} \rho = -\mu \frac{\partial}{\partial V} \rho + \frac{\sigma^2}{2} \frac{\partial^2}{\partial V^2} \rho + \nu(t) \delta(V - V_R). \tag{1.11}$$

Interpretation of μ and σ

We now discuss the interpretation of μ and σ in equations (1.10) and (1.11). Each neuron in a neural network has a base (or intrinsic) current β that defines its resting state [22, 35]. The neuron also receives input current from other neurons via synapses. Each synapse is characterized as either excitatory or inhibitory depending on the electric and chemical signal it sends to a connected neuron. The total input current to a neuron modeled by equation (1.10) is

$$I = \mu + \sigma \xi, \tag{1.12}$$

where we decompose μ as

$$\mu = \beta + \mu_{exc} + \mu_{inh}. \tag{1.13}$$

In equation (1.13) β is the intrinsic current characteristic of the neuron, μ_{exc} represents the average input current over all excitatory synapses, and μ_{inh} represents the average input current over all inhibitory synapses. Finally, the parameter σ represents the total magnitude of the variances of the summed input currents. Below, we describe values of μ and σ in two different physical settings, namely slice (i.e. “in vitro”) experiments, and living brain (i.e. “in vivo”) experiments.

- **In vitro:** In general, for slice experiments, synaptic input current is negligible. Thus, $\mu_{exc} = \mu_{inh} = 0$, and equation (1.13) reduces to

$$\mu = \beta, \tag{1.14}$$

and (1.12) reduces to

$$I = \beta + \sigma\xi. \tag{1.15}$$

In equation (1.15), $\sigma > 0$ represents natural fluctuations in input current due to remnant synaptic contributions. This suggests that σ is relatively small compared to in-vivo experiments. For cortical slice experiments, an external current is often required to force the transmembrane potential above the resting level so that the neuron fires. This suggests that the intrinsic current, β , is negative in equations (1.14) and (1.15). However, a recent study of auditory cortex, (Tzounopoulos, Leao, Lie and Doiron[34] forthcoming) have shown that there is a neuronal population for which $\beta > 0$, and also a population for which $\beta < 0$.

- **In vivo:** Experimental evidence indicates that cortical neurons receive both excitable and inhibitory synaptic inputs, and that these inputs cancel each other out, i.e. $\mu_{exc} + \mu_{inh} = 0$ [5, 20, 33]. Thus, (1.13) reduces to

$$\mu = \beta, \tag{1.16}$$

and (1.12) reduces to

$$I = \beta + \sigma\xi. \tag{1.17}$$

The value of the intrinsic current, β , in (1.16) and (1.17) could be either positive or negative depending on the specific experimental preparation. Finally, the variances of the intrinsic, excitable and inhibitory currents are all positive, and therefore the value of σ in (1.17) can be relatively large compared to in-vitro experiments.

1.5 OUR MATHEMATICAL RESULTS

Mattia and Del Giudice [24] consider equations (1.10) when $V_L = V_R$, and derive the following nonlinear equation for the eigenvalues of the FPE (1.11):

$$\lambda = \frac{\sigma^4(\gamma_1^2 - \gamma_2^2) - \mu^2 V_T^2}{2V_T^2 \sigma^2} + i \frac{\gamma_1 \gamma_2 \sigma^2}{V_T^2}, \quad (1.18)$$

where

$$z = \frac{\mu V_T}{\sigma^2}, \quad \gamma = \gamma_1 + i\gamma_2 = \frac{V_T}{\sigma^2} \sqrt{\mu^2 + 2\lambda\sigma^2}, \quad (1.19)$$

and

$$\gamma e^z = \gamma \cosh(\gamma) + z \sinh(\gamma). \quad (1.20)$$

Mattia and Del Giudice [24] make the following conjecture:

The Mattia-Del Giudice Conjecture for problem (1.18)-(1.19)-(1.20)

(a) When $\mu > 0$ the eigenvalues are complex with negative real parts, and the corresponding eigenfunctions ‘form a complete set.’

(b) When $\mu < 0$ the eigenvalues are real and negative, and the corresponding eigenfunctions ‘form a complete set.’

Mattia and Del Giudice [24] also claim that this conjecture is true when $V_L < V_R$ (see Section 3.4 for details).

1.5.1 Thesis Goals and Results

The main mathematical goals of this thesis are the following:

- (I) Resolve the Mattia-Del Giudice conjecture.
- (II) Use the Theorems proved in part (I) to analyze the firing rate function.

Our main mathematical advances:

- **(I)** We give a rigorous proof of existence of eigenvalues of problem (1.18)-(1.19)-(1.20). Although many authors (e.g. Knight [19], Doiron [9], Mattia and Del Giudice [24], Cheng, Tranchina) have simulated these eigenvalues, to date there has been no rigorous analysis of this fundamental problem. In Chapter 4 we investigate the Mattia-Del Giudice eigenvalue problem and prove that infinitely many branches of solutions do exist. Our results apply to both the $\mu > 0$ and $\mu < 0$ settings.
- **(II)** We make use of the Theorems proved in part **(I)** to give a rigorous analysis of the firing rate function of the IF SDE model (1.10). Chapter 5 contains all of these results.

1.5.2 Chapter Outline

Chapter 2: Comparison of the IF and LIF Models

The goal of Chapter 2 is to exhibit the difficulties in studying the LIF model, and hence explain why we focus on the IF model. We begin by introducing the complete SDEs for both the LIF and IF models, as well as the corresponding Fokker-Planck equation (FPE). We follow Knight [18, 19], as well as Mattia and Del Giudice [24], and investigate the existence of eigenfunction expansion solutions of (1.11) under appropriate boundary conditions. Next, we derive the corresponding FPE boundary value problems for the LIF and IF models and derive two identities involving the firing rate, $\nu(t)$. We also derive a formula for the stationary solution (time-independent solution), $\phi_0(V)$, of the LIF model and point out the prohibitive difficulties of finding solutions of the eigenfunctions corresponding to non-zero eigenvalues. A particular parameter region is considered where it is proved that the slope of the stationary solution at reset changes sign exactly once as a function of the input current, μ . Our numerical experiments lead to a conjecture on the size of this parameter region. In Section 2.4 we investigate the existence of eigenfunction expansion solutions to the IF FPE boundary value problem. We derive formulas for the stationary solution in two different regimes:

$$-\infty < V_L = V_R < V_T \quad \text{and} \quad -\infty < V_L < V_R < V_T.$$

In both cases we derive nonlinear algebraic equations that describe the eigenvalues of the corresponding FPE boundary value problem. Lastly, in Section 2.5 we offer a brief discussion

on the difficulties of studying the LIF model analytically.

Chapter 3: Background Properties of the IF Model

We consider the IF model (1.10) when $\infty < V_L \leq V_R < V_T$, $V \in [V_L, V_i]$ and μ and σ constant. We follow Mattia and Del Giudice [24] and develop the FPE boundary value problem in two cases:

$$V_L < V_R < V_T \quad \text{and} \quad V_L = V_R < V_T.$$

In the case $V_L = V_R < V_T$ we follow Knight [19], as well as Mattia and Del Giudice [24], and develop ODE boundary value problems for the eigenvalues of the FPE (1.11). In Section 3.4 we state the Mattia-Del Giudice conjecture in detail.

Chapter 4: Existence Theorems

This Chapter contains our main mathematical results. In particular, our goal is to determine the behavior of solutions of the FPE (1.11) for the IF model (1.10) when $V_L = V_R$. First, we follow Mattia and Del Giudice [24] and derive the nonlinear eigenvalue problem (1.18)-(1.19)-(1.20). Next, we analyze this problem in three parameter regimes:

Case I, $\mu > 0$: In Theorem 5 we give a rigorous proof that equation (1.20) has infinitely many branches of solutions, and hence there exist infinitely many branches of eigenvalues. We prove asymptotic results for the eigenvalues. In Section 4.5 we provide a partial proof of the Mattia-Del Giudice conjecture (see Section 3.4).

Case II, $\mu < 0$: In Theorems 8 and 9 we assume that the eigenvalues are real² and give a rigorous proof that equation (1.20) has infinitely many branches of solutions, and hence there exist infinitely many eigenvalues. We prove asymptotic properties of the eigenvalues and provide a partial proof of the Mattia-Del Giudice conjecture (see Section 3.4) for $\mu < 0$.

Case III, $\mu = 0$: In Theorem 2 we prove that the eigenvalues are real and negative. We also show that an eigenfunction expansion solution of the FPE boundary value problem does not exist.

²This assumption is based upon numerical calculations and the implication that the eigenvalues are real.

Chapter 5: Analysis of the Firing Rate Function

We begin Chapter 5 by calculating the eigenvalues of the FPE in different parameter regimes. Next, we perform a numerical simulation of 10,000 IF neurons and compare the mean firing rate of the population with our theoretical results from Chapter 4. We prove asymptotic results of the theoretical mean firing rate in terms of the parameters μ and σ .

Chapter 6: Open Problems

For completeness we state open problems and discuss future research possibilities for the IF and LIF models. In particular, we discuss the next step towards answering **Questions 1-4** above.

Appendix : Matlab Programs

In the appendix we provide instructions and Matlab code to reproduce all the figures and numerical experiments.

2.0 LEAKY (LIF) AND LINEAR (IF) MODELS: A COMPARISON

In this chapter we compare the eigenvalue problem for two neuronal models: the leaky integrate-and-fire (LIF) and the linear integrate-and-fire (IF). In particular, we do the following:

2.1 We state the complete SDE for the leaky integrate-and-fire (LIF) model. We then state the associated Fokker-Planck equation (FPE) and derive the complete FPE boundary value problem.

2.2 We state the complete SDE for the linear integrate-and-fire (IF) model. We then state the associated FPE and derive the complete FPE boundary value problem.

2.3 We look for eigenfunction expansion solutions to the associated FPE of the LIF model. We derive stationary solutions and investigate the behavior of these solutions both analytically, and numerically.

2.4 We look for eigenfunction expansion solutions to the associated FPE of the IF model. We derive stationary solutions and investigate the behavior of these solutions both analytically, and numerically.

2.5 We discuss the difficulty in studying the LIF model and point out why the IF is more accessible for analytic results. We also discuss the difficulties that arise in giving a complete, general analysis of the IF model.

2.1 THE LEAKY INTEGRATE-AND-FIRE MODEL

The first model we consider is the leaky integrate-and-fire model (LIF):

$$dV = \left(\mu - \frac{V}{\tau} \right) dt + \sigma dW, \quad -\infty < V(0) = V_0 \leq V_T. \quad (2.1)$$

It is assumed [9], [24], [19] that there exists a value $V_R \in (-\infty, V_T)$ where V_R is a reset value defined as follows:

$$\text{if } V(t^-) = V_T, \text{ then } V(t^+) = V_R, \quad (2.2)$$

where V_T is the “threshold” and where the neuron fires. The range of $V(t)$ is

$$-\infty < V(t) \leq V_T, \quad \forall t \geq 0. \quad (2.3)$$

Goals: In the remainder of this section our goals are:

2.1.1 State the Fokker-Planck Equation (FPE) for $\rho(V, t|V_0, 0)$, the conditional probability density function which is used to determine the probable value of $V(t)$.

2.1.2 We develop a formula for $\nu(t)$, the firing rate emission function.

2.1.3 We state the full FPE boundary value problem associated with the LIF model.

2.1.1 The Fokker-Planck Equation FPE for the LIF Model

A standard approach [9], [24], [19] in determining the most probable value of $V(t)$ is to make use of the associated Fokker-Planck equation (FPE) [30]

$$\frac{\partial \rho}{\partial t} = -\frac{\partial}{\partial V} \left[\left(\mu - \frac{V}{\tau} \right) \rho \right] + \frac{\sigma^2}{2} \frac{\partial^2 \rho}{\partial V^2} + \nu(t) \delta(V - V_R). \quad (2.4)$$

The relevant solution of (2.4), which is used to determine the probable value of $V(t)$, is denoted by the conditional probability density function $\rho(V, t|V_0, 0)$. It satisfies

$$\left(\rho(V, t|V_0, 0), \frac{\partial}{\partial V} \rho(V, t|V_0, 0) \right) \rightarrow (0, 0) \text{ as } V \rightarrow -\infty, \quad \forall t > 0, \quad (2.5)$$

the initial condition

$$\rho(V, 0|V_0, 0) = \delta(V - V_0), \quad (2.6)$$

the absorbing condition

$$\rho(V_T, t|V_0, 0) = 0, \quad \forall t \geq 0, \quad (2.7)$$

and the normalizing condition

$$\int_{-\infty}^{V_T} \rho(V, t|V_0, 0) dV = 1, \quad \forall t > 0. \quad (2.8)$$

Proving the existence and behavior of $\rho(V, t|V_0, 0)$ is a formidable analysis problem. A standard approach is to express $\rho(V, t|V_0, 0)$ as an eigenfunction expansion. The relevant eigenfunctions satisfy an ODE boundary value problem. The difficulty in studying the resultant ODE boundary value problem is discussed in Section 2.3. In particular, see Section 2.3.5.

2.1.2 The Firing Rate Function for the LIF Model

To develop the formula for $\nu(t)$, we proceed as follows: first, an integration of (2.4) with respect to V from $-\infty$ to V_T , together with (2.5), (2.7) and (2.8), gives the formula

$$\nu(t) = -\frac{\sigma^2}{2} \frac{\partial}{\partial V} \rho(V_T, t|V_0, 0), \quad \text{for all } t > 0. \quad (2.9)$$

Next, integrate (2.4) with respect to V from $V_R - \epsilon$ to $V_R + \epsilon$, let $\epsilon \rightarrow 0^+$, and obtain the equivalent formula

$$\nu(t) = -\frac{\sigma^2}{2} \left[\frac{\partial}{\partial V} \rho(V_R^+, t|V_0, 0) - \frac{\partial}{\partial V} \rho(V_R^-, t|V_0, 0) \right], \quad \forall t > 0. \quad (2.10)$$

2.1.3 The FPE BVP for the LIF Model

Equations (2.9) and (2.10) give two representations of $\nu(t)$. Therefore, we replace the term $\nu(t)\delta(V - V_R)$ in (2.4) by the boundary condition

$$\frac{\partial}{\partial V}\rho(V_T, t|V_0, 0) = \frac{\partial}{\partial V}\rho(V_R^+, t|V_0, 0) - \frac{\partial}{\partial V}\rho(V_R^-, t|V_0, 0). \quad (2.11)$$

Thus, the FPE boundary value problem for the LIF model is

$$\left\{ \begin{array}{l} \frac{\partial \rho}{\partial t} = -\frac{\partial}{\partial V} \left[\left(\mu - \frac{V}{\tau} \right) \rho \right] + \frac{\sigma^2}{2} \frac{\partial^2 \rho}{\partial V^2} \\ (\rho(V, t|V_0, 0), \frac{\partial}{\partial V}\rho(V, t|V_0, 0)) \rightarrow (0, 0) \text{ as } V \rightarrow -\infty, \quad \forall t > 0 \\ \rho(V, 0|V_0, 0) = \delta(V - V_0) \\ \rho(V_T, t|V_0, 0) = 0, \quad \forall t > 0 \\ \int_{-\infty}^{V_T} \rho(V, t|V_0, 0) dV = 1, \quad \forall t > 0 \\ \frac{\partial}{\partial V}\rho(V_T, t|V_0, 0) = \frac{\partial}{\partial V}\rho(V_R^+, t|V_0, 0) - \frac{\partial}{\partial V}\rho(V_R^-, t|V_0, 0), \quad \forall t > 0. \end{array} \right. \quad (2.12)$$

2.2 THE LINEAR INTEGRATE-AND-FIRE MODEL

For comparison with the LIF model we state the complete linear integrate-and-fire (IF) SDE [9],[24],[19] problem:

$$dV = \mu dt + \sigma dW, \quad V_L \leq V(0) = V_0 \leq V_T. \quad (2.13)$$

where $V_L < V_T$. The possible range of values for V_L depend critically on the choice of μ . When $\mu < 0$ we require V_L to be finite. As we show below, this constraint is necessary to construct a stationary solution of the FPE boundary value problem (see Section 2.4.4). When $\mu \geq 0$ it is theoretically possible that $V_L = -\infty$, since a stationary solution of the FPE problem can be constructed in this case. However, as pointed out in the introduction, the lowest possible value of V_L for a real neuron is $V_L \approx -85 \text{ mV}$. Thus, in the remainder of this thesis we follow Mattia [24] (see p. 051917-3) and focus only on the case $-\infty < V_L \leq V_R$.

The next assumption, as with the LIF model (see equation (2.2) in Section 2.1), is that there exists $V_R \in (V_L, V_T)$ where V_R is a reset value defined as follows:

$$\text{if } V(t^-) = V_T, \text{ then } V(t^+) = V_R. \quad (2.14)$$

When V_L is finite the range of $V(t)$ is

$$V_L \leq V(t) \leq V_T, \quad \forall t \geq 0, \quad (2.15)$$

and we assume reflective boundary conditions when $V(t) = V_L$.

Goals: In the remainder of this section our goals are

2.2.1 State the associated Fokker-Planck Equation (FPE) for $\rho(V, t|V_0, 0)$, the conditional probability density function which is used to determine the probable value of $V(t)$.

2.2.2 We develop a formula for $\nu(t)$, the firing rate emission function for the IF model.

2.2.3 We state the full FPE boundary value problem associated with the IF model.

2.2.1 The Fokker-Planck Equation for the IF Model

The FPE associated with the IF model is given by

$$\frac{\partial}{\partial t} \rho = -\mu \frac{\partial}{\partial V} \rho + \frac{\sigma^2}{2} \frac{\partial^2}{\partial V^2} \rho + \nu \delta(V - V_R), \quad (2.16)$$

where $V_L < V(t) < V_T$ and $t > 0$. Again, as with the LIF model, the solution to (2.16) is denoted by $\rho(V, t|V_0, 0)$ and it satisfies the initial condition

$$\rho(V, 0|V_0, 0) = \delta(V - V_0), \quad (2.17)$$

the absorbing condition

$$\rho(V_T, t|V_0, 0) = 0, \quad \forall t \geq 0, \quad (2.18)$$

and the normalizing condition

$$\int_{V_L}^{V_T} \rho(V, t|V_0, 0) dV = 1, \quad \forall t > 0. \quad (2.19)$$

2.2.2 The Firing Rate Function for the IF Model

Exactly as in the case of the LIF model, the firing rate, $\nu(t)$, satisfies two identities:

$$\nu(t) = -\frac{\sigma^2}{2} \frac{\partial}{\partial V} \rho(V_T, t | V_0, 0), \quad \forall t > 0, \quad (2.20)$$

and

$$\nu(t) = -\frac{\sigma^2}{2} \left[\frac{\partial}{\partial V} \rho(V_R^+, t | V_0, 0) - \frac{\partial}{\partial V} \rho(V_R^-, t | V_0, 0) \right], \quad \forall t > 0. \quad (2.21)$$

2.2.3 The FPE Boundary Value Problem for the IF Model

As with the LIF, the equations (2.20) and (2.21) give the boundary condition

$$\frac{\partial}{\partial V} \rho(V_T, t | V_0, 0) = \frac{\partial}{\partial V} \rho(V_R^+, t | V_0, 0) - \frac{\partial}{\partial V} \rho(V_R^-, t | V_0, 0). \quad (2.22)$$

Since V_L is finite, the reflecting boundary condition at V_L implies [24, 35]

$$0 = -\mu \rho(V_L, t) + \frac{\sigma^2}{2} \frac{\partial}{\partial V} \rho(V_L, t) \quad \forall t \geq 0, \quad (2.23)$$

which we do not have in the Leaky case.

Remark: The probability current function [24, 35], $S_\rho(V, t)$, is given by

$$S_\rho(V, t) = \frac{\sigma^2}{2} \frac{\partial}{\partial V} \rho(V, t) - \mu \rho(V, t). \quad (2.24)$$

It should be noted that (2.23) is equivalent to the net flux at V_L being zero, i.e.

$$S_\rho(V_L, t) = 0. \quad (2.25)$$

It follows that, when V_L is finite, the complete FPE boundary value problem for the IF model is

$$\left\{ \begin{array}{l} \frac{\partial}{\partial t} \rho = -\mu \frac{\partial}{\partial V} \rho + \frac{\sigma^2}{2} \frac{\partial^2}{\partial V^2} \rho \\ \rho(V, 0|V_0, 0) = \delta(V - V_0) \\ \rho(V_T, t|V_0, 0) = 0, \quad \forall t > 0 \\ 0 = -\mu \rho(V_L, t) + \frac{\sigma^2}{2} \frac{\partial}{\partial V} \rho(V_L, t), \quad \forall t \geq 0 \\ \int_{V_L}^{V_T} \rho(V, t|V_0, 0) dV = 1, \quad \forall t > 0 \\ \frac{\partial}{\partial V} \rho(V_T, t|V_0, 0) = \frac{\partial}{\partial V} \rho(V_R^+, t|V_0, 0) - \frac{\partial}{\partial V} \rho(V_R^-, t|V_0, 0), \quad \forall t > 0. \end{array} \right. \quad (2.26)$$

Now that we have derived the boundary value problems for both the LIF and the IF models, we turn our attention to their respective eigenvalue problems.

2.3 EIGENFUNCTION EXPANSION FOR THE LIF MODEL

A standard approach [9], [24], [19] to solving a FPE boundary value problem is to assume that $\rho(V, t|V_0, 0)$ has an eigenfunction/eigenvalue expansion of the form

$$\rho(V, t|V_0, 0) = \sum_{n=-\infty}^{\infty} A_n \phi_n(V) e^{\lambda_n t}. \quad (2.27)$$

Goals: In the remainder of this section we do the following:

2.3.1 Develop the ODE boundary value problem associated with the eigenvalues λ_n and corresponding eigenfunctions ϕ_n .

2.3.2 Derive the stationary solution, $\phi_0(V)$, corresponding to the eigenvalue $\lambda = 0$. In particular, we show that

$$\phi_0(V) = \begin{cases} A e^{-\frac{\tau}{\sigma^2} (\mu - \frac{V}{\tau})^2}, & V < V_R \\ \frac{A}{B} e^{-\frac{\tau}{\sigma^2} (\mu - \frac{V}{\tau})^2} \int_V^{V_T} e^{\frac{\tau}{\sigma^2} (\mu - \frac{x}{\tau})^2} dx, & V_R < V \leq V_T. \end{cases} \quad (2.28)$$

where A and B are positive constants. In Figures 2 and 3 we plot $\phi_0(V)$ in different parameter regions.

2.3.3 We set $V_R = 0$, $V_T = 1$ and study $\phi'_0(0^+)$ as a function of τ , σ and μ . The main result, Theorem 1, is fundamental to answering questions about the maximum value of $\phi_0(V)$.

2.3.4 We perform numerical computations to gain confidence of the results proved in Section 2.3.3. A conjecture is made on the size of the parameter space in which Theorem 1 holds.

2.3.5 We discuss the difficulty in finding closed form expressions for the eigenfunctions $\phi_n(V)$ when $n \geq 0$.

2.3.1 The ODE BVP for Eigenfunctions of the LIF Model

A standard approach to analyze (2.12) is to look for solutions of the form

$$\rho(V, t|V_0, 0) = \phi(V)e^{\lambda t}. \quad (2.29)$$

The first step is to replace ρ in (2.12) with (2.29), and obtain the ODE

$$\phi''(V) - \frac{2}{\sigma^2} \left(\mu - \frac{V}{\tau} \right) \phi'(V) + \frac{2}{\sigma^2} \left(\frac{1}{\tau} - \lambda \right) \phi(V) = 0, \quad (2.30)$$

with boundary conditions

$$\begin{cases} (\phi(V), \phi'(V)) \rightarrow (0, 0) \text{ as } V \rightarrow -\infty \\ \phi(V_T) = 0 \\ \phi'(V_T) = \phi'(V_R^+) - \phi'(V_R^-). \end{cases} \quad (2.31)$$

Thus, the complete boundary value problem for eigenfunctions is (2.30)-(2.31).

2.3.2 Stationary Solution of the FPE of the LIF Model

The first step in studying (2.30) and (2.31) is to let $n = 0$, and to look for a stationary solution, $\phi_0(V)$, corresponding to the eigenvalue $\lambda_0 = 0$. Our goal is to show that the stationary solution is given by

$$\phi_0(V) = \begin{cases} Ae^{-\frac{\tau}{\sigma^2}(\mu-\frac{V}{\tau})^2}, & V < V_R \\ \frac{A}{B}e^{-\frac{\tau}{\sigma^2}(\mu-\frac{V}{\tau})^2} \int_V^{V_T} e^{\frac{\tau}{\sigma^2}(\mu-\frac{x}{\tau})^2} dx, & V_R < V \leq V_T. \end{cases} \quad (2.32)$$

where A and B are positive constants.

To find the solution $\phi_0(V)$ we first set $\lambda = 0$ in (2.30) and obtain

$$\phi_0'' - \frac{2}{\sigma^2} \left[\left(\mu - \frac{V}{\tau} \right) \phi_0 \right]' = 0. \quad (2.33)$$

First, we focus on the interval $V_R < V < V_T$. From (2.33) it follows that

$$\phi_0' - \frac{2}{\sigma^2} \left(\mu - \frac{V}{\tau} \right) \phi_0 = C. \quad (2.34)$$

Since $\phi_0(V_T) = 0$ it follows that $\phi_0'(V_T) = C$. Integration of (2.34) from V to V_T , along with $\phi_0(V_T) = 0$, yields

$$\phi_0(V) = -Ce^{-\frac{\tau}{\sigma^2}(\mu-\frac{V}{\tau})^2} \int_V^{V_T} e^{\frac{\tau}{\sigma^2}(\mu-\frac{x}{\tau})^2} dx, \quad V_R < V \leq V_T. \quad (2.35)$$

To solve (2.33) for $V < V_R$, we integrate (2.33) from $-\infty$ to V . The condition

$$(\phi(V), \phi'(V)) \rightarrow (0, 0) \quad \text{as } V \rightarrow -\infty$$

yields a first order ODE with solution

$$\phi_0(V) = Ae^{-\frac{\tau}{\sigma^2}(\mu-\frac{V}{\tau})^2}, \quad V < V_R. \quad (2.36)$$

For the solution to be continuous at V_R it must be that $\phi_0(V_R^+) = \phi_0(V_R^-)$. That is,

$$-CB = A \quad \text{where } B = \int_{V_R}^{V_T} e^{\frac{\tau}{\sigma^2}(\mu-\frac{x}{\tau})^2} dx \in \mathbb{R}. \quad (2.37)$$

Therefore,

$$\phi_0(V) = \begin{cases} Ae^{-\frac{\tau}{\sigma^2}(\mu-\frac{V}{\tau})^2}, & V < V_R \\ \frac{A}{B}e^{-\frac{\tau}{\sigma^2}(\mu-\frac{V}{\tau})^2} \int_V^{V_T} e^{\frac{\tau}{\sigma^2}(\mu-\frac{x}{\tau})^2} dx, & V_R < V \leq V_T. \end{cases} \quad (2.38)$$

To solve for A recall the normality condition, $\int_{-\infty}^{V_T} \phi_0(V) dV = 1$, [30]. Thus,

$$A = \frac{1}{I_1 + \frac{1}{B}I_2} \quad (2.39)$$

where

$$I_1 = \int_{-\infty}^{V_R} e^{-\frac{\tau}{\sigma^2}(\mu-\frac{V}{\tau})^2} dV \quad \text{and} \quad (2.40)$$

$$I_2 = \int_0^{V_T} e^{-\frac{\tau}{\sigma^2}(\mu-\frac{V}{\tau})^2} \int_V^{V_T} e^{\frac{\tau}{\sigma^2}(\mu-\frac{x}{\tau})^2} dx dV. \quad (2.41)$$

Finally, a straightforward calculation shows that the jump condition $\phi'(V_T) = \phi'(V_R^+) - \phi'(V_R^-)$ is satisfied. Therefore, the stationary solution is given by (2.38)-(2.39)-(2.40)-(2.41).

In Figures 2 and 3 we plot the stationary solution given by (2.38)-(2.39)-(2.40)-(2.41) for two different parameter sets.

The Most Probable Value of $V(t)$: Recall that $V(t)$ is the membrane potential of a neuron and that $\rho(V, t|V_0, 0)$ is used to find the probable value of $V(t)$. If the real part of the eigenvalues, λ_n , of the FPE are negative, then

$$\rho(V, t|V_0, 0) = \phi_0(V) + \sum_{n \neq 0} A_n(V) e^{\lambda_n t} \phi_n(V) \rightarrow \phi_0(V) \quad \text{as } t \rightarrow \infty. \quad (2.42)$$

Thus, **the most probable value of $V(t)$** is given by critical V_{crit} where $\phi_0(V)$ achieves a maximum. The numerical simulations (See Figures 2 and 3) provide evidence that V_{crit} is a decreasing function of μ .

Remark: The leaky integrate-and-fire (LIF) ODE boundary value problem (2.30)-(2.31) is especially difficult to solve when $n \neq 0$. **The analytic difficulty is due to the presence of the “leaky term” $-\frac{V}{\tau}\phi'(V)$ in equation (2.30).** To our knowledge there are no proofs of the existence of closed form solutions for $\phi_n(V)$, $n \geq 1$.

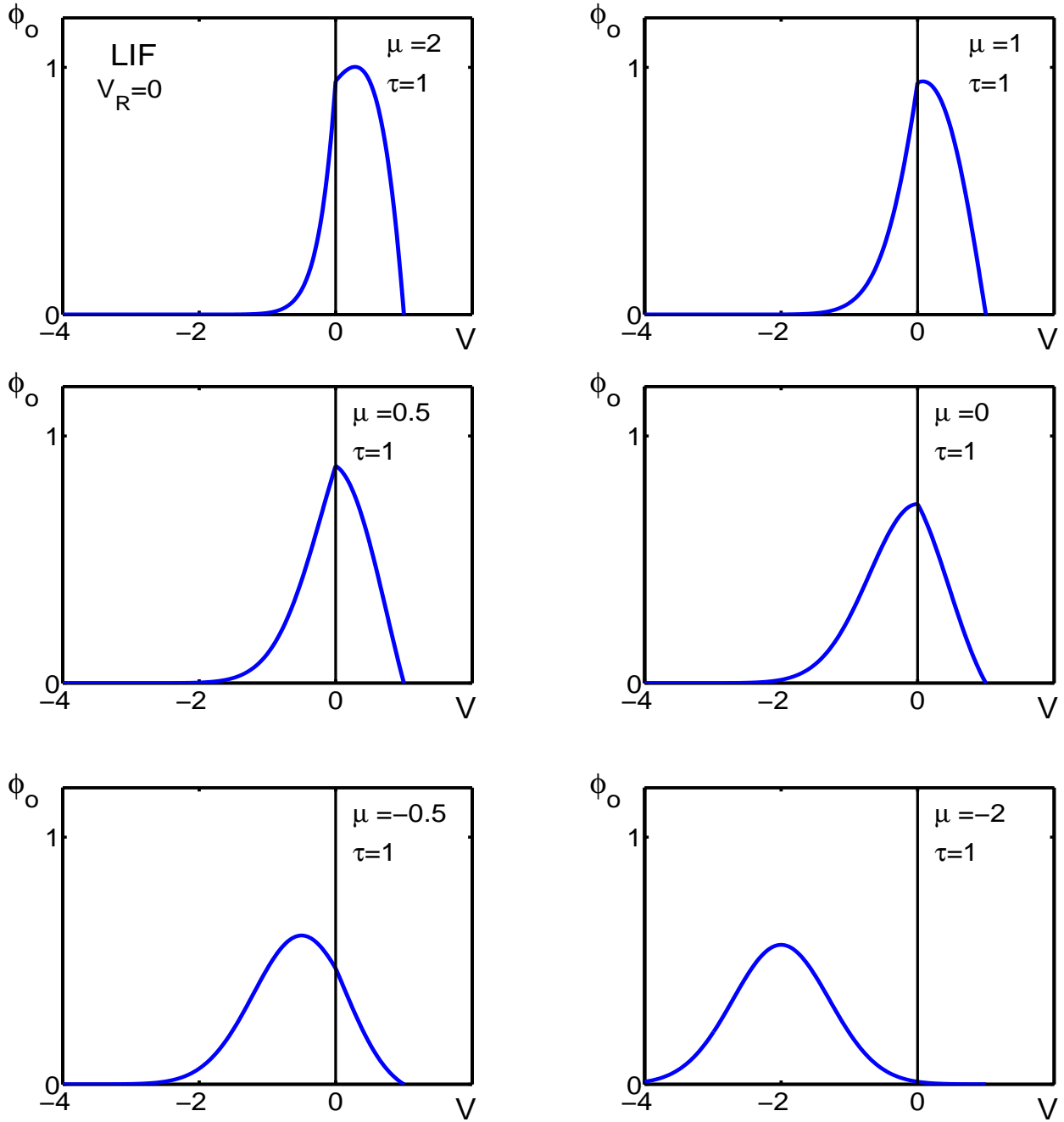


Figure 2: Stationary solutions for the LIF model defined by (2.38)-(2.39)-(2.40)-(2.41). Parameters: $\tau = 1$, $V_R = 0$, $\theta = \sigma = 1$ and μ decreases from $\mu = 2$ (upper left) to $\mu = -0.5$ (lower right). The value $V = V_\mu$ where the peak occurs is a continuous function of μ . We think that $V_\mu \rightarrow -\infty$ as $\mu \rightarrow -\infty$ and $V_\mu \rightarrow 0$ as $\mu \rightarrow \infty$. See Listing .7 in Appendix A.1 for the Matlab code.

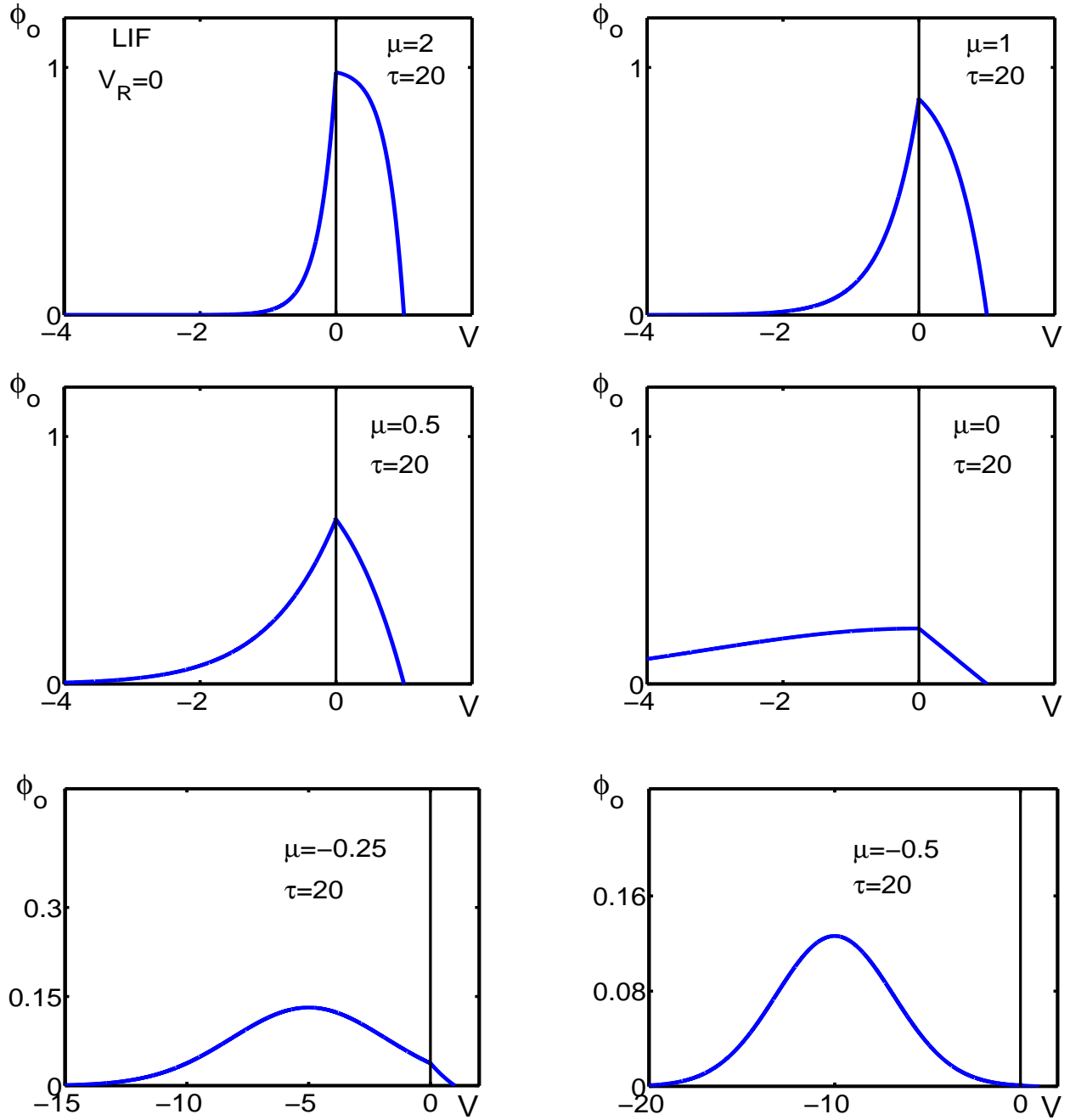


Figure 3: (Stationary solutions for the LIF model defined by (2.38)-(2.39)-(2.40)-(2.41). Parameters: $\tau = 20$, $V_R = 0$, $\theta = \sigma = 1$ and μ decreases from $\mu = 2$ (upper left) to $\mu = -0.5$ (lower right). The value $V = V_\mu$ where the peak occurs is a continuous function of μ . We think that $V_\mu \rightarrow -\infty$ as $\mu \rightarrow -\infty$ and $V_\mu \rightarrow 0$ as $\mu \rightarrow \infty$. See Listing .7 in Appendix A.1 for the Matlab code.

2.3.3 Behavior of the Stationary Solution of the LIF

In this section we study the behavior of the solution (2.38)-(2.39)-(2.40)-(2.41). Notice that (see Figures 2 and 3), for fixed τ and σ , $\phi'_0(0^+)$ changes sign as μ decreases from 2 to 0. In what follows we will prove the following

Theorem 1. *Let $V_R = 0$ and $V_T = 1$. Then, there exists a neighborhood U in the (τ, σ) plane, and a unique $\mu^* \in (0, 1)$, such that $(1, 1) \in U$ and $\phi'_0(0^+) = 0$ when $\mu = \mu^*$. Furthermore, there exists a unique*

$$\mu^*(\tau, \sigma) \in \mathcal{C}^1(U, \mathbb{R}) \quad (2.43)$$

such that $\phi'_0(0^+) = 0$ when $\mu = \mu^(\tau, \mu)$ for all $(\tau, \sigma) \in U$. In particular, $\phi'_0(0^+) > 0$ when $\mu > \mu^*$ and $\phi'_0(0^+) < 0$ when $\mu < \mu^*$.*

Proof. We prove Theorem 1 in the following four steps:

Step I. Fix $\tau = 1 = \sigma$. Prove that there exists μ_1 and μ_2 such that $\phi'_0(0^+) < 0$ when $\mu = \mu_1$ and $\phi'_0(0^+) > 0$ when $\mu = \mu_2$.

Step II. Show that $\phi'_0(0^+)$ is a continuous function of μ . Therefore, by Step I, the intermediate value theorem guarantees $\mu^* \in (\mu_1, \mu_2)$ such that $\phi'_0(0^+) = 0$ provided $\mu = \mu^*$.

Step III. Prove that μ^* is unique.

Step IV. Use the implicit function theorem to show that the unique μ^* exists in a neighborhood U of $\tau = 1, \sigma = 1$.

Proof of Step I. Fix $\tau = \sigma = 1$ and assume that $0 < V < 1$. It follows from (2.38) that

$$\phi_0(V) = \frac{A}{B} e^{-\frac{\tau}{\sigma^2}(\mu - \frac{V}{\tau})^2} \int_V^1 e^{\frac{\tau}{\sigma^2}(\mu - \frac{x}{\tau})^2} dx, \quad (2.44)$$

and thus

$$\phi'_0(V) = \frac{A}{B} \left[\frac{2}{\sigma^2} \left(\mu - \frac{V}{\tau} \right) e^{-\frac{\tau}{\sigma^2}(\mu - \frac{V}{\tau})^2} \int_V^1 e^{\frac{\tau}{\sigma^2}(\mu - \frac{x}{\tau})^2} dx - 1 \right]. \quad (2.45)$$

The function of importance is

$$\phi'_0(0^+) = \frac{A}{B} \left[\frac{2\mu}{\sigma^2} e^{-\frac{\tau\mu^2}{\sigma^2}} \int_0^1 e^{\frac{\tau}{\sigma^2}(\mu - \frac{x}{\tau})^2} dx - 1 \right]. \quad (2.46)$$

Recall that A and B are positive constants. To study equation (2.46) we set

$$F(\mu, \tau, \sigma) = \frac{2\mu}{\sigma^2} e^{-\frac{\tau\mu^2}{\sigma^2}} \int_0^1 e^{\frac{\tau}{\sigma^2}(\mu - \frac{x}{\tau})^2} dx. \quad (2.47)$$

To complete **Step I** we prove two technical lemmas.

Lemma 1. *Let $\tau = \sigma = 1$ and $\mu = 0$. Then $\phi'_0(0^+) < 0$.*

Proof. A direct evaluation of (2.47) gives $F(0, 1, 1) = 0$. Combine (2.46) with the fact that $A > 0$ and $B > 0$ to obtain the desired result. \square

Lemma 2. *Let $\tau = \sigma = 1$ and $\mu = 1$. Then $\phi'_0(0^+) > 0$.*

Proof. It is enough to show that $F(1, 1, 1) > 1$. We produce two proofs.

Proof 1: Notice that

$$F(1, 1, 1) = \frac{2}{e} \int_0^1 e^{(1-x)^2} dx. \quad (2.48)$$

By Jensen's inequality we have that

$$F(1, 1, 1) > \frac{2}{e} \exp\left(\int_0^1 (1-x)^2 dx\right) = 2e^{-\frac{2}{3}} > 1. \quad (2.49)$$

Proof 2: A change of variable shows that

$$F(1, 1, 1) = 2e^{-1} \int_0^1 e^{y^2} dy. \quad (2.50)$$

It follows that

$$\begin{aligned} F(1, 1, 1) &> \frac{2}{e} \int_0^1 \left(1 + y^2 + \frac{y^4}{2}\right) dy \\ &= \frac{2}{e} \left(1 + \frac{1}{3} + \frac{1}{10}\right) \\ &= \frac{2}{e} \frac{43}{10} > 1, \end{aligned} \quad (2.51)$$

as claimed. \square

This completes the proof of **Step I**.

Proof of Step II. Notice that F is the product of three continuous functions and hence continuous on $[0, \infty) \times (0, \infty) \times \mathbb{R}$. An application of the intermediate value theorem, combined with Lemmas 1 and 2, proves the following

Lemma 3. *Let $\tau = \sigma = 1$. Then there exists $\mu^* \in (0, 1)$ such that $F(\mu^*, 1, 1) = 1$. In particular,*

$$\phi'_0(0^+) = 0 \quad \text{when } \mu = \mu^*. \quad (2.52)$$

Proof of Step III. We show that μ^* is unique:

Lemma 4. *Let $\tau = \sigma = 1$. Then there exists a unique $\mu^* \in (0, 1)$ such that $F(\mu^*, 1, 1) = 1$. In particular, $\phi'_0(0^+) = 0$ when $\mu = \mu^*$. Furthermore, for $\mu > \mu^*$, $\phi'_0(0^+) > 0$ while $\phi'_0(0^+) < 0$ for $\mu \in (0, \mu^*)$.*

Proof. We set $G(x) = F(x, 1, 1)$ and show that if there exists $x^* \geq 0$ such that $G(x^*) = 1$, then $G'(x^*) > 0$. Thus, once F crosses the line $F = 1$ it can not cross the line $F = 1$ again. This implies that $\phi'_0(0^+) = 0$ only once. To complete the proof of Lemma 4 we need two lemmas.

Lemma 5. *The function $H(x) = 1 - 2x^2e^{1-2x}$ on \mathbb{R}^+ obtains a minimum at $x = 1$ and $H(1) > 0$.*

Proof. First notice that $H(0) = 1 = H(\infty)$. Since $H'(x) = 4x(x-1)(1-e^{-2x})$, it follows that H achieves a minimum at $x = 1$. As $H(1) = 1 - \frac{2}{e} < H(0)$ we conclude that H is bounded below $1 - \frac{2}{e}$. \square

Lemma 6. *Let $\tau = \sigma = 1$ and $\mu > 0$. Also, suppose that $G(x) = 1$. Then, $G'(x) > 0$.*

Proof. A differentiation of (2.47), with $\tau = 1 = \sigma$, shows that G satisfies the ODE

$$G' = \frac{F}{\mu} - 2\mu G - 2\mu e^{-\mu^2} \left[e^{(\mu-1)^2} - e^{\mu^2} \right]. \quad (2.53)$$

Suppose that $G(x) = F(x, 1, 1) = 1$. An application of Lemma 5 gives the desired result:

$$G' = \frac{1}{\mu} (1 - 2\mu^2 e^{1-2\mu}) > 0. \quad (2.54)$$

This completes the proof of Lemma 6. \square

It follows that there exists a unique $\mu^* \in (0, 1)$ such that $\phi'_0(0^+) = 0$ when $\mu = \mu^*$. Furthermore, if $0 < \mu < \mu^*$, then $\phi'_0(0^+) < 0$. If $\mu > \mu^*$, then $\phi'_0(0^+) > 0$. This completes the proof of Lemma 4. \square

This completes the Proof of **Step III**.

Proof of Step IV. Thus far, we have shown that there exists a unique $\mu^* \in (0, 1)$ such that $F(\mu^*, 1, 1) = 1$. It remains to show that $\frac{\partial}{\partial \mu} F(\mu^*, 1, 1) \neq 0$. Notice that

$$\begin{aligned} \frac{\partial}{\partial \mu} F(\mu, \tau, \sigma) &= \frac{1}{\mu} F(\mu, \tau, \sigma) - \frac{2\mu\tau}{\sigma^4} F(\mu, \tau, \sigma) \\ &\quad + \frac{2\mu}{\sigma^2} e^{-\frac{\tau\mu^2}{\sigma^2}} \int_0^1 \frac{2\tau}{\sigma^2} \left(\mu - \frac{x}{\tau} \right) e^{\frac{\tau}{\sigma^2}(\mu - \frac{x}{\tau})} dx \\ &= \frac{1}{\mu} F(\mu, \tau, \sigma) - \frac{2\mu\tau}{\sigma^4} F(\mu, \tau, \sigma) \\ &\quad - \frac{2\mu\tau}{\sigma^2} e^{-\frac{\tau\mu}{\sigma^2}} \left(e^{\frac{\tau}{\sigma^2}(\mu - \frac{1}{\tau})^2} - e^{\frac{\tau\mu^2}{\sigma^2}} \right) \\ &= \frac{1}{\mu} F(\mu, \tau, \sigma) - \frac{2\mu\tau}{\sigma^4} F(\mu, \tau, \sigma) - \frac{2\mu\tau}{\sigma^2} \left(e^{\frac{1}{\sigma^2}(1-2\mu)} - 1 \right). \end{aligned}$$

It follows from Lemma 5 that

$$\begin{aligned} \frac{\partial}{\partial \mu} F(\mu^*, 1, 1) &= \frac{1}{\mu^*} F(\mu^*, 1, 1) - 2\mu^* F(\mu^*, 1, 1) - 2\mu^* \left(e^{(1-2\mu^*)} - 1 \right) \\ &= \frac{1}{\mu^*} - 2\mu^* e^{(1-2\mu^*)} \\ &= \frac{1}{\mu^*} \left(-2(\mu^2)^* e^{(1-2\mu^*)} \right) > 0. \end{aligned}$$

The implicit function theorem applies: there exists a neighborhood U of $(1, 1)$ in the (τ, σ) plane, and a continuously differentiable function $\mu^*(\tau, \sigma) \in \mathbb{C}^1(U, \mathbb{R})$ such that

$$F(\mu^*(\tau, \sigma), \tau, \sigma) = 1. \tag{2.55}$$

This completes the proof of **Step IV** as well as the proof of Theorem 1. \square

Question: How large is the neighborhood U ?

To investigate this question we perform a numerical experiment.

2.3.4 Numerical Exploration of the Neighborhood U

In this section we use a numerical experiments to investigate the neighborhood U . These experiments lead us to make the following conjecture:

Conjecture: Let $V_R = 0$ and $V_T = 1$. Then, for each $\tau > 0$ and $\sigma > 0$ we conjecture that there is a unique $\mu^* > 0$ such that $\phi'_0(0^+) = 0$. In fact, $\phi'_0(0^+) > 0$ when $\mu > \mu^*$ and $\phi'_0(0^+) < 0$ when $\mu < \mu^*$.

The Mathematical Setting: To verify this conjecture numerically, we need to analyze the equation

$$F(\mu^*(\tau, \sigma), \tau, \sigma) = 1. \quad (2.56)$$

That is, for a given parameter set (τ, σ) , a solution $\mu^*(\tau, \sigma)$ of (2.56) gives a μ value such that $\phi'_0(0^+) = 0$. We claim that a solution $\mu^*(\tau, \sigma)$ of (2.56) is unique for each $\sigma > 0$ and $\tau > 0$. To check this claim numerically we develop an algorithm to compute $\mu^*(\tau, \sigma)$ as a function of τ when σ is fixed, and also as a function of σ when τ is fixed. For this, we differentiate (2.56) with respect to both τ and σ and obtain the two ODES

$$\frac{d\mu^*}{d\tau} = -\frac{F_\tau}{F_\mu} \quad \text{and} \quad \frac{d\mu^*}{d\sigma} = -\frac{F_\sigma}{F_\mu}. \quad (2.57)$$

In particular,

$$\frac{\partial F}{\partial \mu} = F \left(\frac{1}{\mu^*} - \frac{2\mu^*\tau}{\sigma^2} \right) - \frac{2\mu^*\tau}{\sigma^2} \left[e^{\frac{1}{\sigma^2}(\frac{1}{\tau} - 2\mu^*)} - 1 \right], \quad (2.58)$$

$$\frac{\partial F}{\partial \sigma} = F \left(\frac{2(\mu^*)^2\tau}{\sigma^3} - \frac{1}{\sigma} \right) + \frac{2\mu^*\tau}{\sigma^3} \left[\left(\mu^* - \frac{1}{\tau} \right) e^{\frac{1}{\sigma^2}(\frac{1}{\tau} - 2\mu^*)} - \mu^* \right], \quad (2.59)$$

$$\frac{\partial F}{\partial \tau} = F \left(\frac{1}{2\tau} - \frac{(\mu^*)^2}{\sigma^2} \right) - \frac{\mu^*}{\sigma^2} e^{\frac{1}{\sigma^2}(\frac{1}{\tau} - 2\mu^*)} \left[\mu^* + \frac{1}{\tau} \right] + \frac{(\mu^*)^2}{\sigma^2}. \quad (2.60)$$

The Numerical Experiment First, fix $\tau = 1$ and solve the equation $\frac{d\mu}{d\sigma} = -\frac{F_\sigma}{F_\mu}$ with initial value $(\sigma, \mu) = A_1 = (1, .743622)$. The next step is to choose a σ value. In particular, we chose $\sigma = 2.5$ and $\sigma = 5$. These σ values correspond to the points A_1 , A_2 and A_3 in Figure 4. We start by fixing $\sigma = 1$ and solve the equation $\frac{d\mu}{d\tau} = -\frac{F_\tau}{F_\mu}$ with initial point A_1 . Perform a similar computation with $\sigma = 2.5$ and $\sigma = 5$. In all three cases the results imply that $\mu^*(\tau)$

exists throughout U (see Figure 4). The numerical code to perform this computation and reproduce Figure 4 can be found in Listing ?? in the Appendix . We plot these solutions below. It appears, see Figure 4, that the solutions exist for each $\tau > 0$ and $\sigma > 0$. That is, the neighborhood U is actually all of the first quadrant: $U = (0, \infty) \times (0, \infty)$.

Open Problem: It remains to prove that $U = (0, \infty) \times (0, \infty)$.

2.3.5 The Difficulty in the LIF Eigenvalue Problem

As we pointed out at the end of Section 2.3.2, to our knowledge there are no rigorous proofs of the existence of eigenvalues, and corresponding eigenfunctions, for problem (2.30)-(2.31) when $n \geq 1$. **What makes this problem mathematically formidable is the presence of the “leaky” term $-\frac{V}{\tau}\phi'(V)$ in (2.30).** However, Apfaltrer, Ly and Tranchina [4] have performed extensive numerical calculations of the eigenvalues and eigenfunctions for a problem which is equivalent to (2.30)-(2.31).

2.4 THE EIGENFUNCTION EXPANSION FOR THE IF MODEL

A standard approach [9], [24], [19] to solving a FPE boundary value problem is to assume that $\rho(V, t|V_0, 0)$ has an eigenfunction/eigenvalue expansion of the form

$$\rho(V, t|V_0, 0) = \sum_{n=0}^{\infty} A_n(V)\phi_n(V)e^{\lambda_n t}. \quad (2.61)$$

Goals: In the remainder of this section we consider the following:

2.4.1 Develop the ODE boundary value problem associated with the eigenvalues λ_n and corresponding eigenfunctions ϕ_n .

2.4.2 We consider the eigenvalue problem in the case $-\infty < V_L = V_R$. In particular, we derive the nonlinear algebra equation that describes the eigenvalues. We also compute the eigenfunctions and plot the stationary solution for different parameter values (see Figure 5).

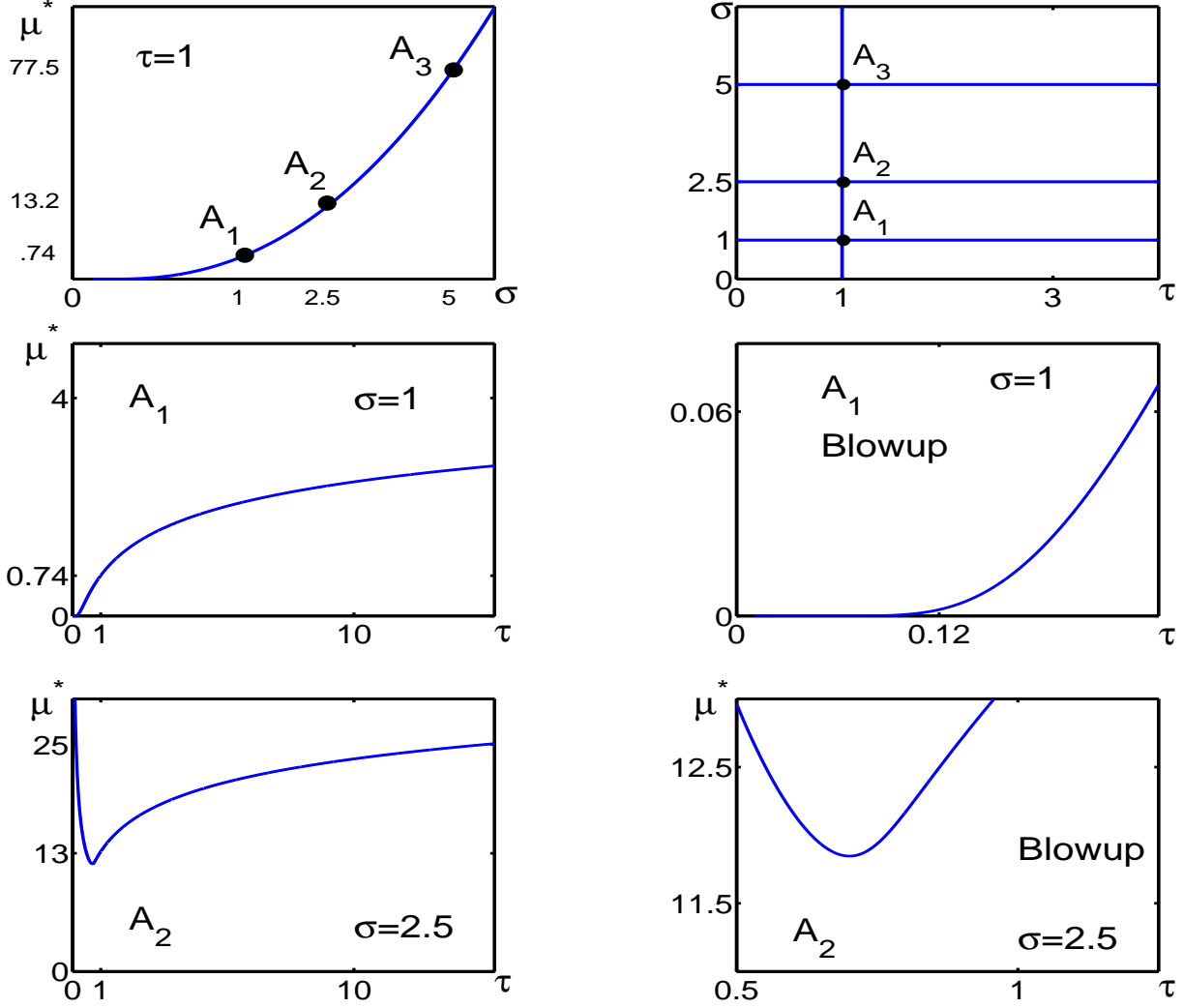


Figure 4: **Top Left:** With τ held at the constant value $\tau = 1$, the solid curve is the solution, $\mu^*(\sigma)$, of $\frac{d\mu^*}{d\sigma} = -\frac{F_\sigma}{F_\mu}$ through the point $A_1 = (1, .74)$, i.e. the initial value is $\mu^*(1) = .74$ **Top Right:** The first components of $A_1 = (1, .74)$, $A_2 = (2.5, 13.2)$ and $A_3 = (5, 77.5)$ are the σ values corresponding to $\tau = 1$. Thus, the (τ, σ) values $(1, 1)$, $(1, 2.5)$ and $(1, 5)$ are graphed on the vertical line $\tau = 1$ in the (τ, σ) plane. **Second Row, Left:** With σ held at the constant value $\sigma = 1$, the solid curve is the solution, $\mu^*(\tau)$, of $\frac{d\mu^*}{d\tau} = -\frac{F_\tau}{F_\mu}$ corresponding to $A_1 = (1, .74)$, i.e. the initial value is $\mu^*(1) = .74$ **Third Row, Left:** With σ held at the constant value $\sigma = 2.5$, the solid curve is the solution, $\mu^*(\tau)$, of $\frac{d\mu^*}{d\tau} = -\frac{F_\tau}{F_\mu}$ corresponding to $A_2 = (2.5, 13.2)$, i.e. the initial value is $\mu^*(1) = 13.2$ **Middle and Bottom Right:** The graphs are blowups of solutions in the left panels. See Listing .10 in the Section A.2 for the code.

2.4.3 We consider the eigenvalue problem in the case $-\infty < V_L < V_R$. In particular, we derive the eigenfunctions and the nonlinear algebra equations that describe the eigenvalues. Next, we set $V_R = 0$ and let $V_L \rightarrow V_R^-$, and show the resulting equation for the eigenvalues is in agreement with the results of Section 2.4.3. Lastly, we derive the stationary solution, i.e. the eigenfunction corresponding to the eigenvalue $\lambda = 0$ and plot this function for different parameter values (see Figure 6).

2.4.4 We show that a stationary solution for the IF can not be constructed when $\mu < 0$ and $V_L = -\infty$.

2.4.1 The ODE BVP for Eigenfunctions of the IF Model

Recall that the full FPE boundary value problem for the IF model is given by (2.26). Here $V(t)$ is constrained to lie in a finite interval $[V_L, V_T]$, where $-\infty < V_L \leq V_R \leq V_T$, and with a reflecting boundary condition when $V(t) = V_L$. Analogous to the Leaky case, i.e. LIF model, we search for solutions to (2.26) of the form

$$\rho(V, t) = \phi(V)e^{\lambda t}. \quad (2.62)$$

Place (2.62) into (2.26) and obtain the ODE

$$\phi''(V) - \frac{2\mu}{\sigma^2}\phi'(V) - \frac{2\lambda}{\sigma^2}\phi(V) = 0. \quad (2.63)$$

with boundary conditions

$$\begin{cases} \mu\phi(V_L) - \frac{\sigma^2}{2}\phi'(V_L) = 0 \\ \phi(V_T) = 0 \\ \phi'(V_T) = \phi'(V_R^+) - \phi'(V_R^-) \\ \phi(V_R^+) = \phi(V_R^-). \end{cases} \quad (2.64)$$

Remark: When $\tau = \infty$, equation (2.30) formally reduces to the eigenvalue ODE for the IF problem, namely

$$\phi''(V) - \frac{2\mu}{\sigma^2}\phi'(V) - \frac{2\lambda}{\sigma^2}\phi(V) = 0, \quad (2.65)$$

in agreement with (2.63).

2.4.2 ODE Eigenvalue Problem for the Case $V_L = V_R$

We first consider the special case where $V_L = V_R = 0 < V_T = \theta$. In this case the eigenvalue problem becomes

$$\begin{cases} \phi'' - \frac{2\mu}{\sigma^2}\phi' - \frac{2\lambda}{\sigma^2}\phi = 0 \\ \phi(\theta) = 0 \\ \phi'(\theta) = \phi'(0) - \frac{2\mu}{\sigma^2}\phi(0). \end{cases} \quad (2.66)$$

Remark: Notice that the jump condition $\phi'(V_T) = \phi'(V_R^+) - \phi'(V_R^-)$ has changed in this case.

We show why. For $V_L < V_R < V_T$ we recall that $\mu\phi(V_L) - \frac{\sigma^2}{2}\phi'(V_L) = 0$. Letting $V_L \rightarrow V_R^-$, it follows that

$$\mu\phi(V_R^-) - \frac{\sigma^2}{2}\phi'(V_R^-) = 0. \quad (2.67)$$

Under the assumption that ϕ is continuous it follows that

$$\phi'(V_R^-) = \frac{2\mu}{\sigma^2}\phi(V_R) = 0. \quad (2.68)$$

Combine this with the jump condition $\phi'(V_T) = \phi'(V_R^+) - \phi'(V_R^-)$ so that

$$\phi'(V_T) = \phi'(V_R^+) - \frac{2\mu}{\sigma^2}\phi(V_R). \quad (2.69)$$

Thus, in the special case $-\infty < V_L = V_R = 0 < V_T = \theta$, we have that

$$\phi'(\theta) = \phi'(0) - \frac{2\mu}{\sigma^2}\phi(0) \quad (2.70)$$

as claimed.

Goals: We prove the following properties:

I. The eigenvalues of (2.66) are given by the equation

$$\gamma e^z = \gamma \cosh(\gamma) + z \sinh(\gamma), \quad (2.71)$$

where

$$z = \frac{\mu\theta}{\sigma^2} \text{ and } \gamma = \frac{\theta}{\sigma^2} \sqrt{\mu^2 + 2\lambda\sigma^2} \quad (2.72)$$

as claimed by Mattia and Del Giudice [24]. We show (see Section 4.5) that the only real solutions of (2.71) are $\gamma = 0, \pm z$, and that these gamma values correspond to the trivial eigenfunction $\phi_n(V) = 0$.

II. In the special case, $\mu = 0$, the eigenfunction corresponding to the eigenvalue $\lambda = 0$ is given by

$$\phi_0(V) = \frac{2}{\theta^2} (\theta - V), \quad 0 \leq V \leq \theta. \quad (2.73)$$

III. The eigenfunction $\phi_0(V)$, corresponding to the eigenvalue $\lambda = 0$, is given by

$$\phi_0(V) = C_0 \left(1 - \exp \left[\frac{-2z(\theta - V)}{\theta} \right] \right), \quad (2.74)$$

where C_0 is a normalizing constant.

Proof of I: We derive (2.71). A standard approach is to look for solutions to (2.66) of the form

$$\phi(V) = e^{\frac{mV}{\theta}}. \quad (2.75)$$

Put (2.75) into (2.63) and obtain the algebra equation

$$m^2 - \frac{2\mu\theta}{\sigma^2} m - \frac{2\lambda\theta^2}{\sigma^2} = 0 \quad (2.76)$$

with solution

$$m = \frac{\mu\theta}{\sigma^2} \pm \frac{\theta}{\sigma^2} \sqrt{\mu^2 + 2\lambda\sigma^2}. \quad (2.77)$$

Set

$$z = \frac{\mu\theta}{\sigma^2} \text{ and } \gamma = \frac{\theta}{\sigma^2} \sqrt{\mu^2 + 2\lambda\sigma^2}. \quad (2.78)$$

It follows that the general solution to (2.63) is

$$\phi(V) = \exp \left[\frac{zV}{\theta} \right] \left(c_1 \exp \left[\frac{\gamma V}{\theta} \right] + c_2 \exp \left[-\frac{\gamma V}{\theta} \right] \right). \quad (2.79)$$

Next, apply the boundary condition $\phi(\theta) = 0$ to obtain

$$c_2 = -c_1 e^{2\gamma}. \quad (2.80)$$

Combining (2.79) with (2.80) yields

$$\begin{aligned}
\phi(V) &= \exp\left[\frac{zV}{\theta}\right] \left(c_1 \exp\left[\frac{\gamma V}{\theta}\right] + c_2 \exp\left[-\frac{\gamma V}{\theta}\right] \right) \\
&= c_1 \exp\left[\frac{zV}{\theta}\right] \exp[\gamma] \left[\exp\left[\frac{\gamma V}{\theta} - \gamma\right] - \exp\left[\gamma + \frac{\gamma V}{\theta}\right] \right] \\
&= c_\lambda \exp\left[\frac{zV}{\theta}\right] \sinh\left[\frac{\gamma(\theta - V)}{\theta}\right].
\end{aligned}$$

Note that

$$\phi'(\theta) = -c_\lambda \frac{\gamma}{\theta} e^z, \quad (2.81)$$

$$\phi'(0) = -c_\lambda \frac{z}{\theta} \sinh(\gamma) - c_\lambda \frac{\gamma}{\theta} \cosh(\gamma), \quad (2.82)$$

and

$$\phi'(0) = c_\lambda \sinh(\gamma) \frac{2\mu}{\sigma^2}. \quad (2.83)$$

The identities (2.81)-(2.82)-(2.83), combined with the boundary condition $\phi'(\theta) = \phi'(0) - \frac{2\mu}{\sigma^2}\phi(0)$ yield the desired result:

$$\gamma e^z = \gamma \cosh(\gamma) + z \sinh(\gamma). \quad (2.84)$$

This completes the proof of **I**.

Proof of II: Set $\mu = \lambda = 0$ so that the ODE boundary value problem (2.66) becomes

$$\begin{cases} \phi'' = 0 \\ \phi(\theta) = 0 \quad \text{and} \quad \int_0^\theta \phi(V) dV = 1 \\ \phi'(\theta) = \phi'(0). \end{cases} \quad (2.85)$$

The general solution of (2.85) is given by

$$\phi_0(V) = C_1 V + C_2, \quad 0 < V < \theta. \quad (2.86)$$

Apply the boundary condition $\phi'(\theta) = \phi'(0)$ and the normalizing condition $\int_0^\theta \phi(V) dV = 1$ to (2.85) and obtain

$$\phi_0(V) = \frac{2}{\theta^2} (\theta - V), \quad 0 \leq V \leq \theta. \quad (2.87)$$

This completes the proof of **II**.

Proof of III: To find $\phi_0(V)$ we set $\lambda = 0$ in (2.66) and obtain the appropriate ODE boundary boundary value problem

$$\begin{cases} \phi'' - \frac{2\mu}{\sigma^2}\phi' = 0 \\ \phi(\theta) = 0 \quad \text{and} \quad \int_0^\theta \phi(V) dV = 1 \\ \phi'(\theta) = \phi'(0) - \frac{2\mu}{\sigma^2}\phi(0). \end{cases} \quad (2.88)$$

The boundary condition $\phi(\theta) = 0$ implies that the $\phi'' - \frac{2\mu}{\sigma^2}\phi' = 0$ has the general solution

$$\phi_0(V) = C \exp \left[\frac{2\mu}{\sigma^2} V \right] \int_\theta^V \exp \left[-\frac{2\mu}{\sigma^2} x \right] dx. \quad (2.89)$$

Integrate (2.89) to obtain

$$\phi_0(V) = C_0 \left(1 - \exp \left[\frac{-2z(\theta - V)}{\theta} \right] \right). \quad (2.90)$$

The normality condition, $\int_0^\theta \phi_0 = 1$, implies that

$$C_0 = \left[\frac{\sigma^2}{2\mu} (2z - 1 + e^{-2z}) \right]^{-1}. \quad (2.91)$$

A routine calculation shows that all boundary conditions in (2.88) are satisfied by $\phi_0(V)$.

Remark: An application of L'Hospital's rule shows that

$$\lim_{\mu \rightarrow 0^+} \phi_0(V) = \frac{2}{\theta^2} (\theta - V), \quad 0 \leq V \leq \theta \quad (2.92)$$

in agreement with (2.87).

In Figure (5) below we plot $\phi_0(V)$ for different values of μ . In each case $\sigma = 1$ and $\theta = 1$.

This completes the proof of **III**.

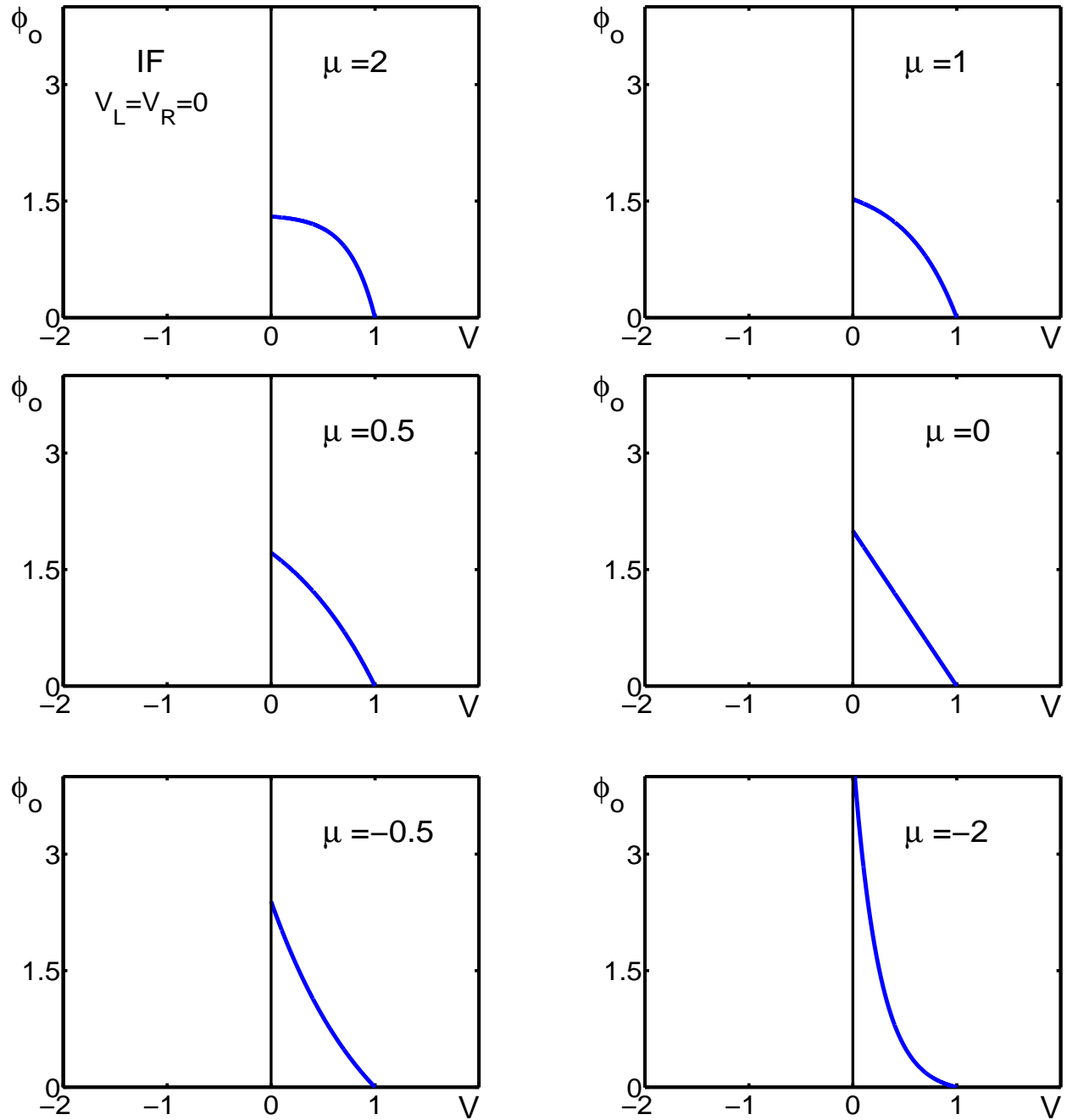


Figure 5: Stationary solutions for the IF model with parameters $V_L = V_R = 0$, $\theta = \sigma = 1$ and μ decreases from $\mu = 2$ (upper left) to $\mu = -2$ (lower right). As μ passes through 0 from above, the concavity changes because of the no flux boundary condition: $\mu\phi(V_L) - \frac{\sigma^2}{2}\phi'(V_L) = 0$. See Listing .8 in the Appendix for the Matlab code.

2.4.3 The Eigenvalue Problem for the IF in the General Case

We examine the IF eigenvalue problem for the case $-\infty < V_L < V_R < V_T = \theta$. In this case, the appropriate ODE boundary value problem is

$$\begin{cases} \phi'' - \frac{2\mu}{\sigma^2}\phi' - \frac{2\lambda}{\sigma^2}\phi = 0 \\ \mu\phi(V_L) - \frac{\sigma^2}{2}\phi'(V_L) = 0 \\ \phi(\theta) = 0 \\ \phi'(\theta) = \phi'(V_R^+) - \phi'(V_R^-) \\ \phi(V_R^+) = \phi(V_R^-). \end{cases} \quad (2.93)$$

Goals: Our goal is to prove the following properties:

I. The solution to (2.93) is given by

$$\phi_\lambda(V) = \begin{cases} D_\lambda e^{\frac{zV}{\theta}} \left[\frac{B}{A} e^{(V-V_L)\frac{\gamma}{\theta}} + e^{-(V-V_L)\frac{\gamma}{\theta}} \right], & V_L < V < V_R, \\ C_\lambda e^{\frac{zV}{\theta}} \sinh \left[\frac{\gamma(\theta-V)}{\theta} \right], & V_R < V < \theta, \end{cases} \quad (2.94)$$

where D_λ and C_λ are normalizing constants.

II. In the special case where $V_R = 0$, the algebra equations that determine the eigenvalues are

$$\begin{cases} C_\lambda \sinh(\gamma) = D_\lambda \left[\frac{B}{A} e^{-\frac{V_L\gamma}{\theta}} + e^{\frac{V_L\gamma}{\theta}} \right] \\ -C_\lambda \frac{\gamma}{\theta} e^z = \frac{C_\lambda}{\theta} [z \sinh(\gamma) - \gamma \cosh(\gamma)] \\ \quad - \frac{D_\lambda}{\theta} \left[z \left(\frac{B}{A} e^{-\frac{V_L\gamma}{\theta}} + e^{\frac{V_L\gamma}{\theta}} \right) + \gamma \left(\frac{B}{A} e^{-\frac{V_L\gamma}{\theta}} - e^{\frac{V_L\gamma}{\theta}} \right) \right] \\ D_\lambda I_3 + C_\lambda I_4 = 1 \end{cases} \quad (2.95)$$

where

$$I_3 = \int_{V_L}^0 e^{\frac{zV}{\theta}} \left[\frac{B}{A} e^{(V-V_L)\frac{\gamma}{\theta}} + e^{-(V-V_L)\frac{\gamma}{\theta}} \right] dV, \quad (2.96)$$

and

$$I_4 = \int_0^\theta e^{\frac{zV}{\theta}} \sinh \left[\frac{\gamma(\theta-V)}{\theta} \right] dV. \quad (2.97)$$

III. In the special case where $V_R = 0$, (2.95) reduces to

$$\gamma e^z = \gamma \cosh(\gamma) + z \sinh(\gamma). \quad (2.98)$$

as $V_L \rightarrow 0^-$.

IV. When $V_R = 0$, the stationary solution to (2.93) is

$$\phi_0(V) = \begin{cases} C \left(1 - e^{\frac{2\mu\theta}{\sigma^2}}\right) e^{\frac{2\mu}{\sigma^2}V}, & V_L \leq V \leq V_R \\ C \left(e^{\frac{2\mu}{\sigma^2}V} - e^{\frac{2\mu\theta}{\sigma^2}}\right), & V_R \leq V \leq \theta. \end{cases} \quad (2.99)$$

where C is a normalizing constant.

Proof of I: We prove (2.94). We consider $V_R < V < \theta$. Here, the argument is identical to that of Section (see Section 2.4.2). It follows that

$$\phi(V) = C_\lambda e^{\frac{zV}{\theta}} \sinh \left[\frac{\gamma(\theta - V)}{\theta} \right], \quad V_R < V < \theta. \quad (2.100)$$

Next, consider the interval $V_L < V < V_R$. We search for solutions of the form

$$\phi(V) = e^{\bar{M}\frac{V}{V_L}} \quad (2.101)$$

in which case we have the algebra problem

$$\bar{M}^2 - \frac{2\mu V_L}{\sigma^2} \bar{M} - \frac{2\lambda V_L^2}{\sigma^2} = 0. \quad (2.102)$$

It follows that

$$\begin{aligned} \bar{M} &= \frac{\mu V_L}{\sigma^2} \pm \frac{V_L}{\sigma^2} \sqrt{\mu^2 + 2\lambda\sigma^2} \\ &= \frac{V_L}{\theta} m \end{aligned}$$

where

$$\begin{aligned} m &= \frac{\mu\theta}{\sigma^2} \pm \frac{\theta}{\sigma^2} \sqrt{\mu^2 + 2\lambda\sigma^2} \\ &= z \pm \gamma \end{aligned}$$

as in Section 2.4.2. Thus, we have the relationship

$$e^{\bar{M}\frac{V}{V_L}} = e^{m\frac{V}{\theta}}, \quad (2.103)$$

implying that the algebra problem is precisely the same as the case $V_L = V_R$ in Section 2.4.2. Therefore,

$$\phi(V) = C_1 e^{(z+\gamma)\frac{V}{\theta}} + C_2 e^{(z-\gamma)\frac{V}{\theta}}, \quad V_L < V < V_R. \quad (2.104)$$

Apply the boundary condition $\mu\phi(V_L) - \frac{\sigma^2}{2}\phi'(V_L) = 0$ to obtain

$$C_1 = C_2 \frac{B}{A} e^{-2\gamma\frac{V_L}{\theta}}, \quad (2.105)$$

where

$$A = \mu - \frac{\sigma^2(z+\gamma)}{2\theta} \quad \text{and} \quad B = \frac{\sigma^2(z-\gamma)}{2\theta} - \mu. \quad (2.106)$$

Next, combine (2.104) and (2.105). It follows that

$$\phi(V) = D_\lambda e^{\frac{zV}{\theta}} \left[\frac{B}{A} e^{(V-V_L)\frac{\gamma}{\theta}} + e^{-(V-V_L)\frac{\gamma}{\theta}} \right], \quad V_L < V < V_R. \quad (2.107)$$

In summary, we combine (2.100) and (2.107) to obtain the desired result:

$$\phi_\lambda(V) = \begin{cases} D_\lambda e^{\frac{zV}{\theta}} \left[\frac{B}{A} e^{(V-V_L)\frac{\gamma}{\theta}} + e^{-(V-V_L)\frac{\gamma}{\theta}} \right], & V_L < V < V_R, \\ C_\lambda e^{\frac{zV}{\theta}} \sinh \left[\frac{\gamma(\theta-V)}{\theta} \right], & V_R < V < \theta. \end{cases} \quad (2.108)$$

This completes the proof of **I**.

Proof of II: We assume that $V_R = 0$. The continuity condition, $\phi(0^+) = \phi(0^-)$, applied to (2.108) implies that

$$C_\lambda \sinh(\gamma) = D_\lambda \left[\frac{B}{A} e^{-\frac{V_L\gamma}{\theta}} + e^{\frac{V_L\gamma}{\theta}} \right] \quad (2.109)$$

Combine the reset condition, $\phi'(\theta) = \phi'(0^+) - \phi'(0^-)$, with (2.108)

$$\begin{aligned} -C_\lambda \frac{\gamma}{\theta} e^z &= \frac{C_\lambda}{\theta} [z \sinh(\gamma) - \gamma \cosh(\gamma)] \\ &\quad - \frac{D_\lambda}{\theta} \left[z \left(\frac{B}{A} e^{-\frac{V_L\gamma}{\theta}} + e^{\frac{V_L\gamma}{\theta}} \right) + \gamma \left(\frac{B}{A} e^{-\frac{V_L\gamma}{\theta}} - e^{\frac{V_L\gamma}{\theta}} \right) \right] \end{aligned} \quad (2.110)$$

Equation (2.109), applied to (2.110), yields

$$\begin{aligned} -C_\lambda \frac{\gamma}{\theta} e^z &= \frac{C_\lambda}{\theta} [z \sinh(\gamma) - \gamma \cosh(\gamma)] \\ &\quad - \frac{z}{\theta} C_\lambda \sinh(\gamma) - \frac{D_\lambda \gamma}{\theta} \left(\frac{B}{A} e^{-\frac{V_L\gamma}{\theta}} - e^{\frac{V_L\gamma}{\theta}} \right), \end{aligned}$$

which simplifies to

$$C_\lambda e^z = C_\lambda \cosh(\gamma) + D_\lambda \left(\frac{B}{A} e^{-\frac{V_L \gamma}{\theta}} - e^{\frac{V_L \gamma}{\theta}} \right). \quad (2.111)$$

It remains to consider the constants C_λ and D_λ . The normality condition, $\int_{V_L}^\theta \phi = 1$, implies that

$$D_\lambda I_3 + C_\lambda I_4 = 1 \quad (2.112)$$

where

$$I_3 = \int_{V_L}^0 e^{\frac{zV}{\theta}} \left[\frac{B}{A} e^{(V-V_L)\frac{\gamma}{\theta}} + e^{-(V-V_L)\frac{\gamma}{\theta}} \right] dV, \quad (2.113)$$

and

$$I_4 = \int_0^\theta e^{\frac{zV}{\theta}} \sinh \left[\frac{\gamma(\theta - V)}{\theta} \right] dV. \quad (2.114)$$

Thus, the equations (2.109), (2.110) and (2.112) determine the eigenvalues, λ_n :

$$\begin{cases} C_\lambda \sinh(\gamma) = D_\lambda \left[\frac{B}{A} e^{-\frac{V_L \gamma}{\theta}} + e^{\frac{V_L \gamma}{\theta}} \right] \\ -C_\lambda \frac{\gamma}{\theta} e^z = \frac{C_\lambda}{\theta} [z \sinh(\gamma) - \gamma \cosh(\gamma)] \\ \quad - \frac{D_\lambda}{\theta} \left[z \left(\frac{B}{A} e^{-\frac{V_L \gamma}{\theta}} + e^{\frac{V_L \gamma}{\theta}} \right) + \gamma \left(\frac{B}{A} e^{-\frac{V_L \gamma}{\theta}} - e^{\frac{V_L \gamma}{\theta}} \right) \right] \\ D_\lambda I_3 + C_\lambda I_4 = 1. \end{cases} \quad (2.115)$$

This completes the proof of **II**.

Proof of III: Note that (2.115) reduces to

$$\begin{cases} C_\lambda \sinh(\gamma) = D_\lambda \left[\frac{B}{A} + 1 \right] \\ -C_\lambda \frac{\gamma}{\theta} e^z = \frac{C_\lambda}{\theta} [z \sinh(\gamma) - \gamma \cosh(\gamma)] \\ \quad - \frac{D_\lambda}{\theta} \left[z \left(\frac{B}{A} + 1 \right) + \gamma \left(\frac{B}{A} - 1 \right) \right] \\ C_\lambda I_4 = 1 \end{cases} \quad (2.116)$$

as $V_L \rightarrow 0^-$. Put the first equality in (2.116) into the second equality so that

$$\begin{aligned} -C_\lambda \frac{\gamma}{\theta} e^z &= \frac{C_\lambda}{\theta} [z \sinh(\gamma) - \gamma \cosh(\gamma)] \\ &\quad - \frac{C_\lambda \sinh(\gamma)}{\left(\frac{B}{A} + 1\right)\theta} \left[z \left(\frac{B}{A} + 1 \right) + \gamma \left(\frac{B}{A} - 1 \right) \right]. \end{aligned} \quad (2.117)$$

$$(2.118)$$

That is,

$$\begin{aligned}
\gamma e^z &= -z \sinh(\gamma) + \gamma \cosh(\gamma) + \sinh(\gamma) \left[z + \gamma \frac{B+A}{B-A} \right] \\
&= \gamma \cosh(\gamma) + \sinh(\gamma) \left[\gamma \frac{B+A}{B-A} \right] \\
&= \gamma \cosh(\gamma) + \sinh(\gamma) \left[\gamma \frac{\mu\theta}{\gamma\sigma^2} \right] \\
&= \gamma \cosh(\gamma) + z \sinh(\gamma),
\end{aligned}$$

since $z = \frac{\mu\theta}{\sigma^2}$. We remark that this is consistent with the previous case, $V_L = V_R = 0$. This completes the proof of **III**.

Proof of IV: We look for the stationary solutions corresponding, i.e. the eigenfunction corresponding to $\lambda = 0$:

$$\phi'' - \frac{2\mu}{\sigma^2}\phi = 0. \quad (2.119)$$

For $V_R < V \leq \theta$ the argument is identical to that of the previous section. It follows that

$$\phi_0^+(V) = Ae^{-\frac{2\mu}{\sigma^2}V} + B, \quad V_R < V \leq \theta \quad (2.120)$$

It remains to consider the regime of $V_L \leq V < V_R$. An integration of (2.119) from V_L to V along with the condition $\phi(V_L) - \frac{\sigma^2}{2\mu}\phi'(V_L) = 0$ yields the ODE

$$\left(\phi e^{-\frac{2\mu}{\sigma^2}V} \right)' = De^{-\frac{2\mu}{\sigma^2}V}. \quad (2.121)$$

Integration of (2.121) from V_L to V yields the solution

$$\phi_0^-(V) = D + Ne^{\frac{2\mu}{\sigma^2}V}. \quad (2.122)$$

The continuity condition at V_R gives $D=B$. The jump condition $\phi_0'(\theta) = \phi_0'(V_R^+) - \phi_0'(V_R^-)$ implies that

$$N = A \left(1 - e^{\frac{2\mu}{\sigma^2}\theta} \right). \quad (2.123)$$

It follows that the stationary solution of (2.93) when $V_R = 0$ is

$$\phi_0(V) = \begin{cases} C \left(1 - e^{\frac{2\mu\theta}{\sigma^2}} \right) e^{\frac{2\mu}{\sigma^2}V}, & V_L \leq V \leq V_R \\ C \left(e^{\frac{2\mu}{\sigma^2}V} - e^{\frac{2\mu\theta}{\sigma^2}} \right), & V_R \leq V \leq \theta \end{cases} \quad (2.124)$$

where C is a normalizing constant.

Figure (6) below plots (2.124) for different values of μ . This completes the proof of **IV**.

2.4.4 The Stationary Solution when $V_L = -\infty$

In this section we assume that $V_L = -\infty$, $\mu < 0$, and prove that a stationary solution of the FPE boundary value problem corresponding to the IF model does not exist. Thus, when investigating the IF model we require

$$-\infty < V_L \leq V_R < V_T. \quad (2.125)$$

Recall from Section 2.2.3 that the stationary solution of the FPE boundary value problem is a solution of

$$\left\{ \begin{array}{l} -\mu \frac{\partial}{\partial V} \rho + \frac{\sigma^2}{2} \frac{\partial^2}{\partial V^2} \rho = 0, \\ \rho(V_T) = 0, \quad \forall t > 0, \\ \int_{-\infty}^{V_T} \rho(V) dV = 1, \quad \forall t > 0 \\ \frac{\partial}{\partial V} \rho(V_T) = \frac{\partial}{\partial V} \rho(V_R^+) - \frac{\partial}{\partial V} \rho(V_R^-), \quad \forall t > 0, \\ (\rho(V), \rho'(V)) \rightarrow (0, 0) \text{ as } V \rightarrow -\infty. \end{array} \right. \quad (2.126)$$

First, notice that

$$-\mu \frac{\partial}{\partial V} \rho(V) + \frac{\sigma^2}{2} \frac{\partial^2}{\partial V^2} \rho(V) = 0 \quad (2.127)$$

is equivalent to

$$-\mu \rho(V) + \frac{\sigma^2}{2} \frac{\partial}{\partial V} \rho(V) = C_1, \quad (2.128)$$

for some real number C_1 . Suppose that $-\infty < V < V_R$, and let $V \rightarrow -\infty$ in (2.128) to find that $C_1 = 0$. Thus,

$$-\mu \rho(V) + \frac{\sigma^2}{2} \frac{\partial}{\partial V} \rho(V) = 0, \quad \forall V \in (-\infty, V_R). \quad (2.129)$$

The general solution of (2.129) is

$$\rho(V) = C_2 e^{\frac{2\mu}{\sigma^2} V}. \quad (2.130)$$

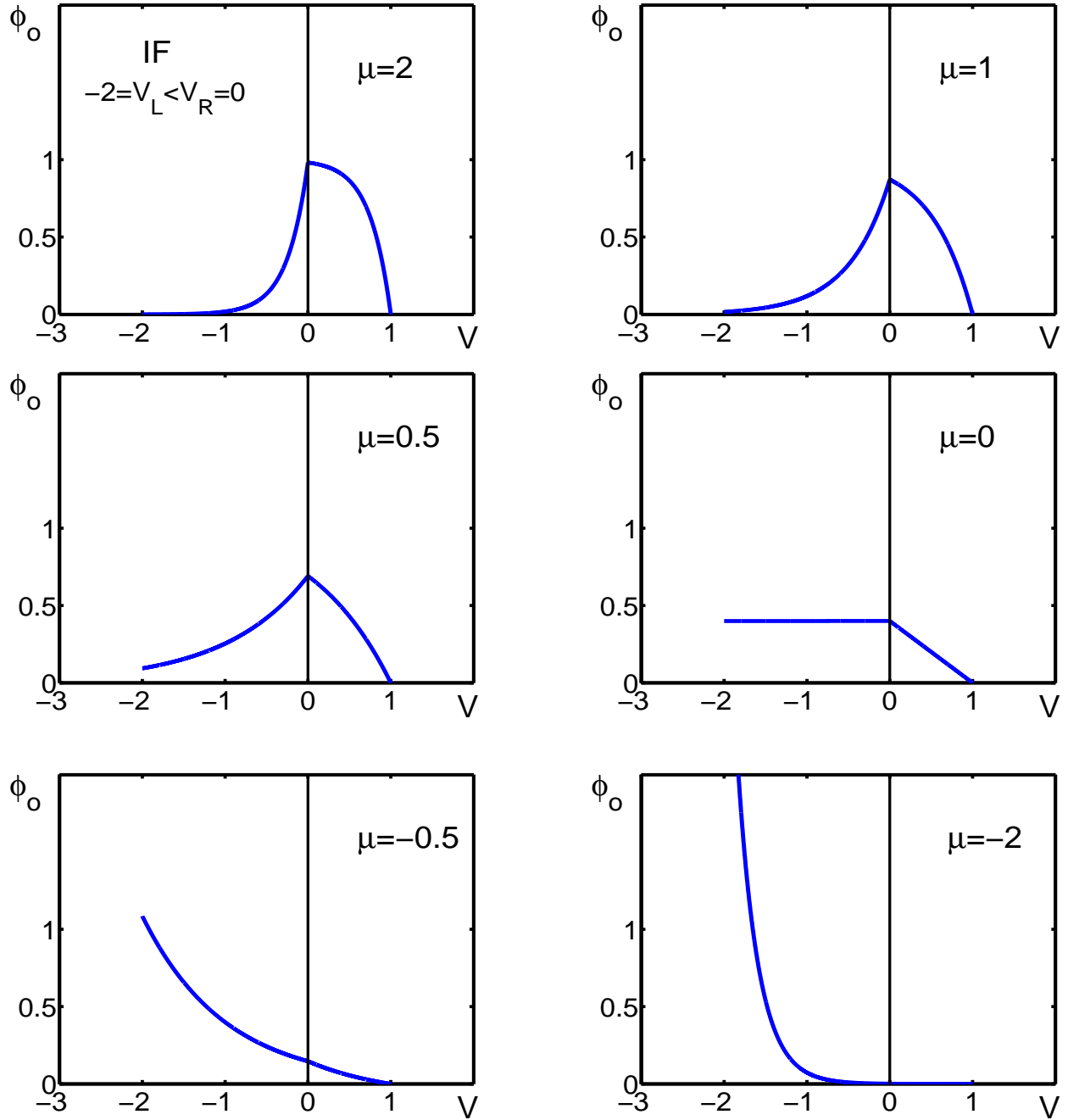


Figure 6: Stationary solutions for the IF with parameters: $V_L = -2, V_R = 0, \theta = \sigma = 1$ and μ decreases from $\mu = 2$ (upper left) to $\mu = -2$ (lower right). As μ passes through 0 from above, the concavity changes because of the no flux boundary condition: $\mu\phi(V_L) - \frac{\sigma^2}{2}\phi'(V_L) = 0$. See Listing .7 in the Appendix for the Matlab code.

Recall that $\mu < 0$. Thus

$$\lim_{V \rightarrow -\infty} \rho(V) = \infty, \quad (2.131)$$

contradicting the boundary condition

$$(\rho(V), \rho(V)) \rightarrow (0, 0) \text{ as } V \rightarrow -\infty. \quad (2.132)$$

We conclude that a stationary solution of the FPE corresponding to the IF model does not exist when $\mu < 0$ and $V_L = -\infty$.

2.5 CONCLUSION AND OPEN PROBLEM

As previously noted the LIF model is more biologically reasonable when compared to the IF model. However, the LIF model presents many challenges when attempting rigorous analysis. As we noted in Section (2.3.5) the primary analytic difficulty, due to the presence of the term $-\frac{V}{\tau}\phi'(V)$ in the ODE (2.30) makes analytic treatment very difficult. This term is present even when we assume that $\mu = 0$.

Open Problem: It remains an open problem to give a rigorous proof of the existence of branches of eigenvalues of the FPE corresponding to the LIF model. A first step is to prove the existence of the first eigenvalue (i.e. the ‘dominate’ eigenvalue), and corresponding eigenfunction for problem (2.30)-(2.31), for both $\mu > 0$ and $\mu < 0$. The resolution of this problem will allow us to begin the construction of an eigenfunction expansion for firing rate for the LIF model. To our knowledge there are no rigorous results for this challenging problem.

In this thesis, our focus is on the IF model, which is more analytically tractable than the LIF equation. In studying the IF model we have found that the general IF eigenvalue problem also presents significant challenges. As was shown in (2.95), the eigenvalues for the IF problem are given by three nonlinear algebra equations. In Chapter 4 we begin our analytic treatment of the IF model by assuming that $V_L = V_R = 0 < V_T$. As we will see in Chapter (4), proving the existence of eigenvalues under these particular assumptions is easier, but still highly non trivial.

3.0 BACKGROUND PROPERTIES OF THE IF MODEL WHEN $V_L = V_R$

In this chapter we follow [9],[24],[19] and develop appropriate mathematical properties that will be used in the remainder of this thesis to analyze the linear integrate and fire (IF) model. In particular, we focus on the case

$$V_L = V_R = 0, \quad V_T = \theta > 0 \quad (3.1)$$

and do the following:

3.1 We state the Fokker-Planck equation (FPE) partial differential equation (PDE) that is associated with the IF model when (3.1) holds:

$$\left\{ \begin{array}{l} \frac{\partial}{\partial t} \rho = -\mu \frac{\partial}{\partial V} \rho + \frac{\sigma^2}{2} \frac{\partial^2}{\partial V^2} \rho \\ \rho(V, 0|V_0, 0) = \delta(V - V_0) \\ \rho(\theta, t|V_0, 0) = 0, \text{ for all } t > 0 \\ -\mu \rho(0, t|V_0, 0) + \frac{\sigma^2}{2} \frac{\partial}{\partial V} \rho(0, t|V_0, 0) = 0, \text{ for all } t \geq 0 \\ \int_0^\theta \rho(V, t|V_0, 0) dV = 1, \text{ for all } t > 0 \\ \frac{\partial}{\partial V} \rho(\theta, t|V_0, 0) = \frac{\partial}{\partial V} \rho(0^+, t|V_0, 0) - \frac{2\mu}{\sigma^2} \rho(0, t|V_0, 0), \text{ for all } t > 0. \end{array} \right. \quad (3.2)$$

3.2 We define the operator L and its adjoint operator L^+ . We develop ODE eigenvalue boundary value problems associated with L and L^+ .

3.3 We construct an eigenfunction expansion solution for the ODE eigenvalue boundary value problems developed in Section 3.2. In particular, we make use of eigenfunctions $\{\phi_n\}$ and $\{\psi_n\}$ of the operators L and L^+ , respectively, to construct the probability density function

$$\rho(V, t|V_0, 0) = \sum_{-\infty}^{\infty} \psi_n(V_0) \phi_n(V) e^{\lambda_n t}. \quad (3.3)$$

3.4 We state a conjecture by Mattia and Guidice [24] regarding the eigenvalues of the operator L .

3.1 THE LINEAR INTEGRATE AND FIRE (IF) FPE BOUNDARY VALUE PROBLEM

We follow a two step procedure:

Step 1. We assume that $V_L < V_R = 0 < \theta$ and develop the FPE boundary value problem.

Step 2. We let $V_L \rightarrow V_R = 0$ in the FPE boundary value problem developed in **Step 1**, and derive the FPE boundary value problem when $V_L = V_R = 0$.

Step 1. The IF stochastic differential equation (SDE) [24],[19] is

$$dV = \mu dt + \sigma dW, \quad V_L \leq V(0) = V_0 \leq V_T \quad (3.4)$$

where $-\infty < V_L < V_T$, W is a Brownian motion, and $V(t)$ represents the membrane potential of a neuron. Throughout, we assume that the input μ , and the variation σ , are constant, independent of t . (see Mattia [24] for a discussion of the general case $\mu = \mu(t)$ and $\sigma = \sigma(t)$). If $V(t) = V_T$, the neuron is assumed to fire, and immediately thereafter the membrane potential is reset to a resting value $V_R \in (V_L, V_T)$ as follows:

$$\text{if } V(t^-) = V_T, \text{ then } V(t^+) = V_R. \quad (3.5)$$

The range of $V(t)$ is

$$V_L \leq V(t) \leq V_T, \text{ for all } t \geq 0. \quad (3.6)$$

Finally, it is assumed that $V(t)$ satisfies a reflective boundary condition when $V(t) = V_L$.

Remark: For convenience we adopt subscript notation for partial derivative, e.g.

$$\frac{\partial}{\partial t} \rho = \rho_t.$$

The corresponding FPE PDE [9] for the IF model is

$$\frac{\partial}{\partial t} \rho = -\mu \frac{\partial}{\partial V} \rho + \frac{\sigma^2}{2} \frac{\partial^2}{\partial V^2} \rho + \nu(t) \delta(V - V_R). \quad (3.7)$$

The function $\nu(t)$ in (3.7) is the firing rate, or emission rate function. The appropriate solution of the FPE PDE (3.7), which corresponds to the IF SDE model (3.4), is the conditional probability $\rho(V, t|V_0, 0)$. It satisfies the initial condition

$$\rho(V, 0|V_0, 0) = \delta(V - V_0), \quad (3.8)$$

the absorbing boundary condition

$$\rho(\theta, t|V_0, 0) = 0, \text{ for all } t > 0, \quad (3.9)$$

the normalizing condition

$$\int_{V_L}^{\theta} \rho(V, t|V_0, 0) dV = 1, \text{ for all } t > 0, \quad (3.10)$$

and the reflective boundary condition

$$-\mu\rho(V_L, t|V_0, 0) + \frac{\sigma^2}{2} \frac{\partial}{\partial V} \rho(V_L, t|V_0, 0) = 0, \text{ for all } t \geq 0. \quad (3.11)$$

We assume that $\rho(V, t|V_0, 0)$ is a continuous function of V , t and V_0 , and that $\frac{\partial}{\partial t}\rho(V, t|V_0, 0)$ and $\frac{\partial}{\partial V}\rho(V, t|V_0, 0)$ are piecewise continuous functions.

FPE Boundary Value Problem: To develop the FPE boundary value problem, the first step is to develop two identities involving the firing rate function $\nu(t)$.

First Firing Rate Identity: We begin by integrating (3.7) from $V = V_L$ to $V = V_T$ to obtain

$$\begin{aligned} \int_{V_L}^{\theta} \rho_t(V, t|V_0, 0) dV &= -\mu \int_{V_L}^{\theta} \rho_V(V, t|V_0, 0) dV + \frac{\sigma^2}{2} \int_{V_L}^{\theta} \rho_{VV}(V, t|V_0, 0) dV \\ &+ \nu(t) \int_{V_L}^{\theta} \delta(V - V_R) dV. \end{aligned} \quad (3.12)$$

Since $\rho(V, t|V_0, 0)$ is assumed to be continuous we can interchange the integral and derivative.

Thus, upon applying the normalizing condition (3.10) to (3.12), we have that

$$\begin{aligned} 0 &= -\mu \int_{V_L}^{\theta} \rho_V(V, t|V_0, 0) dV + \frac{\sigma^2}{2} \int_{V_L}^{\theta} \rho_{VV}(V, t|V_0, 0) dV \\ &+ \nu(t) \int_{V_L}^{\theta} \delta(V - V_R) dV. \end{aligned} \quad (3.13)$$

By the definition of $\delta(V)$ we have that $\int_{V_L}^{\theta} \delta(V - V_R) dV = 1$ and (3.13) becomes

$$0 = -\mu \int_{V_L}^{\theta} \rho_V(V, t|V_0, 0) dV + \frac{\sigma^2}{2} \int_{V_L}^{\theta} \rho_{VV}(V, t|V_0, 0) dV + \nu(t). \quad (3.14)$$

Evaluate the integrals in (3.14), and apply (3.9), (3.11), to obtain the firing rate formula

$$\nu(t) = -\frac{\sigma^2}{2} \frac{\partial}{\partial V} \rho(V_T, t|V_0, 0), \text{ for all } t \geq 0. \quad (3.15)$$

Second Firing Rate Identity: Integrate (3.7) from $V = V_R - \epsilon$ to $V = V_R + \epsilon$:

$$\begin{aligned} \int_{V_R - \epsilon}^{V_R + \epsilon} \rho_t(V, t|V_0, 0) dV &= -\mu \int_{V_R - \epsilon}^{V_R + \epsilon} \rho_V(V, t|V_0, 0) dV \\ &+ \frac{\sigma^2}{2} \int_{V_R - \epsilon}^{V_R + \epsilon} \rho_{VV}(V, t|V_0, 0) dV \\ &+ \nu(t) \int_{V_R - \epsilon}^{V_R + \epsilon} \delta(V - V_R) dV. \end{aligned} \quad (3.16)$$

Evaluating the three integrals in the right hand side of (3.16) gives

$$\begin{aligned} \int_{V_R - \epsilon}^{V_R + \epsilon} \rho_t(V, t|V_0, 0) dV &= -\mu (\rho(V_R + \epsilon, t|V_0, 0) - \rho(V_R - \epsilon, t|V_0, 0)) \\ &+ \frac{\sigma^2}{2} (\rho_V(\rho(V_R + \epsilon, t|V_0, 0) - \rho(V_R - \epsilon, t|V_0, 0))) \\ &+ \nu(t). \end{aligned} \quad (3.17)$$

Recall that ρ is assumed to be continuous while ρ_V is piecewise continuous. Interchange the integral with derivative, and let $\epsilon \rightarrow 0^+$ to obtain

$$\nu(t) = -\frac{\sigma^2}{2} \left(\frac{\partial}{\partial V} \rho(V_R^+, t|V_0, 0) - \frac{\partial}{\partial V} \rho(V_R^-, t|V_0, 0) \right) \text{ for all } t \geq 0. \quad (3.18)$$

Equating (3.15) and (3.18) gives the identity

$$\frac{\partial}{\partial V} \rho(\theta, t|V_0, 0) = \frac{\partial}{\partial V} \rho(V_R^+, t|V_0, 0) - \frac{\partial}{\partial V} \rho(V_R^-, t|V_0, 0), \text{ for all } t > 0. \quad (3.19)$$

We remove the term $\nu(t)\delta(V - V_0)$ in (3.7) and impose the condition (3.19). The FPE boundary value problem becomes

$$\left\{ \begin{array}{l} \frac{\partial}{\partial t}\rho = -\mu\frac{\partial}{\partial V}\rho + \frac{\sigma^2}{2}\frac{\partial^2}{\partial V^2}\rho \\ \rho(V, 0|V_0, 0) = \delta(V - V_0) \\ \rho(\theta, t|V_0, 0) = 0, \text{ for all } t > 0 \\ -\mu\rho(V_L, t|V_0, 0) + \frac{\sigma^2}{2}\frac{\partial}{\partial V}\rho(V_L, t|V_0, 0) = 0, \text{ for all } t \geq 0 \\ \int_{V_L}^{\theta} \rho(V, t|V_0, 0) dV = 1, \quad \forall t > 0 \\ \frac{\partial}{\partial V}\rho(\theta, t|V_0, 0) = \frac{\partial}{\partial V}\rho(V_R^+, t|V_0, 0) - \frac{\partial}{\partial V}\rho(V_R^-, t|V_0, 0), \text{ for all } t > 0. \end{array} \right. \quad (3.20)$$

Step 2. We now fix $V_R = 0$ and let $V_L \rightarrow V_R^-$, i.e. $V_L \rightarrow 0^-$. As ρ is assumed continuous, (3.11) reduces to

$$\mu\rho(0, t|V_0, 0) - \frac{\sigma^2}{2}\frac{\partial}{\partial V}\rho(0^-, t|V_0, 0) = 0, \text{ for all } t > 0, V_L = 0. \quad (3.21)$$

Next, combine (3.19) with (3.21) to obtain

$$\frac{\partial}{\partial V}\rho(\theta, t|V_0, 0) = \frac{\partial}{\partial V}\rho(0^+, t|V_0, 0) - \frac{2\mu}{\sigma^2}\rho(0, t|V_0, 0), \text{ for all } t > 0. \quad (3.22)$$

Thus, when $V_L = V_R = 0 < V_T = \theta$, the FPE boundary value problem for the IF model is

$$\left\{ \begin{array}{l} \frac{\partial}{\partial t}\rho = -\mu\frac{\partial}{\partial V}\rho + \frac{\sigma^2}{2}\frac{\partial^2}{\partial V^2}\rho \\ \rho(V, 0|V_0, 0) = \delta(V - V_0) \\ \rho(\theta, t|V_0, 0) = 0, \text{ for all } t > 0 \\ \int_0^{\theta} \rho(V, t|V_0, 0) dV = 1, \quad \forall t > 0 \\ \frac{\partial}{\partial V}\rho(\theta, t|V_0, 0) = \frac{\partial}{\partial V}\rho(0^+, t|V_0, 0) - \frac{2\mu}{\sigma^2}\rho(0^-, t|V_0, 0), \text{ for all } t > 0. \end{array} \right. \quad (3.23)$$

3.2 THE OPERATORS L AND L^+ WHEN $V_L = V_R = 0$.

A standard approach [9],[24],[19] to solve the FPE boundary value problem (3.23) is to assume that

$$\rho(V, t, |V_0, 0) = \sum A_n \rho_n(V, t), \quad (3.24)$$

where

$$\rho_n(V, t) = \phi_n(V) e^{\lambda_n t}. \quad (3.25)$$

Substitution of (3.25) into (3.23) gives the ODE boundary value problem

$$\begin{cases} \lambda \phi(V) = -\mu \phi'(V) + \frac{\sigma^2}{2} \phi''(V) \\ \phi(\theta) = 0 \\ \phi'(\theta) = \phi'(0^+) - \frac{2\mu}{\sigma^2} \phi(0). \end{cases} \quad (3.26)$$

The linear Operator L : Define the linear operator

$$L : \mathbf{C}^2([0, \theta]) \rightarrow \mathbf{C}((0, \theta)) \quad (3.27)$$

by

$$L = -\mu \frac{\partial}{\partial V} + \frac{\sigma^2}{2} \frac{\partial^2}{\partial V^2}. \quad (3.28)$$

Therefore

$$L(\phi) = -\mu \phi' + \frac{\sigma^2}{2} \phi'', \quad \phi \in \mathbf{C}^2([0, \theta]). \quad (3.29)$$

The appropriate solution of (3.26) is an eigenpair, (ϕ, λ) , of the operator L .

The Adjoint Operator L^+ : First, introduce the inner product

$$(\psi, \phi) = \int_0^\theta \psi(V) \phi(V) dV \in \mathbf{R}. \quad (3.30)$$

Define the linear operator

$$L^+ : \mathbf{C}^2([0, \theta]) \rightarrow \mathbf{C}((0, \theta)) \quad (3.31)$$

by

$$(L^+ \psi, \phi) = (\psi, L\phi). \quad (3.32)$$

For each eigenfunction ϕ , and associated eigenvalue λ , there exist corresponding eigenfunctions, ψ , and eigenvalues β of L^+ . The boundary value problem satisfied by $\psi(V)$ (see Mattia and Del Giudice [24], page 051917-3) is

$$\begin{cases} \beta\psi(V) = \mu\psi'(V) + \frac{\sigma^2}{2}\psi''(V) \\ \psi(0) = \psi(\theta) \\ \psi'(0) = 0. \end{cases} \quad (3.33)$$

It follows from (3.29), (3.32) and (3.33) (see Mattia and Del Giudice [24], page 051917-3) that

$$L^+ = \mu \frac{\partial}{\partial V} + \frac{\sigma^2}{2} \frac{\partial^2}{\partial V^2}. \quad (3.34)$$

Therefore

$$L^+(\psi) = \mu\psi' + \frac{\sigma^2}{2}\psi'', \quad \psi \in \mathbf{C}^2([0, \theta]). \quad (3.35)$$

Remark: Why L is not Hermitian. Mattia and Del Giudice [24] point out that L is not Hermitian. We give a brief explanation why this is so. First, it follows from (3.34) that

$$L^* = \overline{L^+} = \mu \frac{\partial}{\partial V} + \frac{\sigma^2}{2} \frac{\partial^2}{\partial V^2}. \quad (3.36)$$

This, together with (3.28), implies that $L^* \neq L$, i.e. L is not Hermitian. Since L is not Hermitian, Mattia and Del Giudice [24] also point out that one can not immediately claim that the eigenfunctions of L form a complete basis for the range of L . However, they conjecture that the eigenfunctions of L do form a complete basis. Much of their analysis assumes that this conjecture is true.

Orthonormal Properties: Mattia and Del Giudice [24] (see page 051917-4) show that, “under the completeness assumption of the eigenfunctions of the Fokker-Planck operator,”

- (i) the operators L and L^+ have the same eigenvalues, and
- (ii) eigenfunctions $\phi(V)$ and $\psi(V)$ corresponding to eigenvalues λ and β satisfy

$$(\psi(V), \phi(V)) = 0, \quad \text{if } \lambda \neq \beta, \quad (3.37)$$

$$(\psi(V), \phi(V)) = 1, \text{ if } \lambda = \beta. \quad (3.38)$$

Mattia and Del Giudice [24] (see page 051917-4) also show that “If λ_n is an eigenvalue, also λ_n^* is an eigenvalue, with eigenfunction $|\phi_n^* \rangle \langle \psi_n^*|$,” and that “we set $\lambda_{-n} = \lambda_n^*$ and consequently $|\phi_{-n} \rangle = |\phi_n^* \rangle$, so that the sums over the spectrum of the Fokker-Planck operator range over all the integer numbers.”

3.3 THE EIGENFUNCTION EXPANSION WHEN $V_L = V_R$

Assume that a solution of the FPE boundary value problem (3.23) is of the form (3.24), i.e.

$$\rho(V, t, |V_0, 0) = \sum_{-\infty}^{\infty} A_n \phi_n(V) e^{\lambda_n t}. \quad (3.39)$$

We need to prove that

$$A_n = \psi(V_0), \text{ for all } n. \quad (3.40)$$

The first step in proving (3.40) is to multiply (3.39) on both sides by $\psi_k(V)$ to obtain

$$\psi_k(V) \rho(V, t, |V_0, 0) = \psi_k(V) \sum A_n \phi_n(V) e^{\lambda_n t}. \quad (3.41)$$

Formally, upon an integration of (3.41), we have that

$$\int_0^\theta \psi_k(V) \rho(V, t, |V_0, 0) dV = \sum \left(A_n e^{\lambda_n t} \int_0^\theta \phi_n(V) \psi_k(V) dV \right). \quad (3.42)$$

Apply the orthonormal conditions (3.37) and (3.38) to (3.42):

$$\int_0^\theta \psi_k(V) \rho(V, t, |V_0, 0) dV = A_k e^{\lambda_k t}. \quad (3.43)$$

The identity (3.43) holds for all $t \geq 0$. In particular, it holds when $t = 0$:

$$\int_0^\theta \psi_k(V) \rho(V, 0, |V_0, 0) dV = A_k. \quad (3.44)$$

Apply the initial condition, $\rho(V, 0, |V_0, 0) = \delta(V - V_0)$, to (3.44) and obtain

$$\psi_k(V_0) = A_k. \tag{3.45}$$

This completes the proof of (3.40).

From (3.39) and (3.40) we conclude that

$$\rho(V, t|V_0, 0) = \sum_{-\infty}^{\infty} \psi_n(V_0)\phi_n(V)e^{\lambda_n t}. \tag{3.46}$$

This completes the derivation of (3.39)-(3.40).

3.4 THE MATTIA-DEL GIUDICE CONJECTURE

Mattia and Del Giudice [24] (see page) make the following conjecture describing the nature of the eigenvalues of L when $V_L = V_R$:

I. When $\mu > 0$ the eigenfunctions of L ‘form a complete set’, and the corresponding eigenvalues are complex with negative real parts.

II. When $\mu < 0$ the eigenfunctions of L ‘form a complete set’, and the corresponding eigenvalues are real and negative.

Mattia and Del Giudice [24] also claim that this conjecture is true when $V_L < V_R$.

For a partial proof of this conjecture when $V_L = V_R$ and $\mu > 0$ see Theorems 12 and 13 in Section 4.5. For a partial proof when $V_L = V_R$ and $\mu < 0$ see Section 4.6.

4.0 THE MAIN RESULTS: EXISTENCE OF EIGENVALUES WHEN

$$V_L = V_R$$

This chapter contains the main mathematical results of this thesis. In particular, we have the following:

4.1 We develop the eigenvalue problem associated with the Fokker Planck boundary value problem when $-\infty < V_L = V_R < V_T = \theta$. Next, we derive the nonlinear equation whose solutions are eigenvalues of the Fokker Planck boundary value problem when $-\infty < V_L = V_R < V_T = \theta$.

4.2 We investigate the FPE boundary value problem when $\mu = 0$ and $-\infty < V_L = V_R < V_T = \theta$. We prove that there infinitely many real, negative eigenvalues. We derive formulas for the eigenvalues and eigenfunctions and show that there is no eigenfunction expansion solution of the FPE boundary value.

4.3 We investigate the FPE boundary value problem when $\mu > 0$ and $-\infty < V_L = V_R < V_T = \theta$. A proof of the existence of infinitely many branches of eigenvalues is given. Asymptotic properties of these branches are derived as $\mu \rightarrow 0$.

4.4 We investigate the FPE boundary value problem when $\mu < 0$ and $-\infty < V_L = V_R < V_T = \theta$. A proof of the existence of infinitely many branches of eigenvalues is given. Asymptotic properties of these branches are derived as $\mu \rightarrow 0$ and $\mu \rightarrow -\infty$.

4.5 A partial proof of the Mattia-Del Giudice conjecture is given when $\mu > 0$.

4.6 A partial proof of the Mattia-Del Giudice conjecture is given when $\mu < 0$.

4.1 EIGENVALUE STRUCTURE OF THE IF WHEN $V_L = V_R$

The goal in this section is to develop the nonlinear equation whose solutions are eigenvalues of the Fokker Planck boundary value problem associated with the IF model. The resulting eigenvalue problem will be referred to in subsequent sections, namely Sections 4.2, 4.3 and 4.4. We develop this problem in three steps:

4.1.1 First, we recall the Fokker Planck boundary value problem in the case $-\infty < V_L < V_R < V_T = \theta$. Next, we let $V_L \rightarrow V_R^-$ and develop the Fokker Planck boundary value problem when $-\infty < V_L = V_R < V_T = \theta$.

4.1.2 Second, we develop the eigenvalue problem associated with the Fokker Planck boundary value problem when $-\infty < V_L = V_R < V_T = \theta$.

4.1.3 Third, we derive the nonlinear equation whose solutions are eigenvalues of the Fokker Planck boundary value problem when $-\infty < V_L = V_R < V_T = \theta$.

4.1.4 The eigenfunctions ϕ_n of L and ψ_n of L^+ are derived.

4.1.1 The Fokker Planck Problem When $-\infty < V_L = V_R < \theta$

In this section we develop the Fokker Planck equation (FPE) boundary value problem when $-\infty < V_L = V_R < \theta$. The first step is to recall from Chapter 2 that the complete FPE boundary value problem for the IF model when $-\infty < V_L < V_R < V_T = \theta$ is given by the partial differential equation

$$\frac{\partial}{\partial t} \rho(V, t|V_0, 0) = -\mu \frac{\partial}{\partial V} \rho(V, t|V_0, 0) + \frac{\sigma^2}{2} \frac{\partial^2}{\partial V^2} \rho(V, t|V_0, 0) \quad (4.1)$$

with initial condition

$$\rho(V, 0|V_0, 0) = \delta(V - V_0), \quad (4.2)$$

absorbing condition

$$\rho(V_T, t|V_0, 0) = 0, \quad \forall t > 0, \quad (4.3)$$

reflective boundary condition

$$\mu\rho(V_L, t) - \frac{\sigma^2}{2} \frac{\partial}{\partial V} \rho(V_L, t), \quad \forall t \geq 0, \quad (4.4)$$

normalizing condition

$$\int_{V_R}^{V_T} \rho(V, t|V_0, 0) dV = 1, \quad \forall t > 0, \quad (4.5)$$

and jump condition

$$\frac{\partial}{\partial V} \rho(V_T, t|V_0, 0) = \frac{\partial}{\partial V} \rho(V_R^+, t|V_0, 0) - \frac{\partial}{\partial V} \rho(V_R^-, t|V_0, 0), \quad \forall t > 0. \quad (4.6)$$

When $V_L \rightarrow V_R^-$ it was shown in Section 2.4.2 that the jump condition, i.e. equation (4.6), reduces to

$$\frac{\partial}{\partial V} \rho(V_T, t|V_0, 0) = \frac{\partial}{\partial V} \rho(V_R^+, t|V_0, 0) - \frac{\sigma^2}{2} \rho(V_R, t|V_0, 0), \quad \forall t > 0. \quad (4.7)$$

4.1.2 The Eigenvalue Problem When $V_L = V_R$

In this subsection we assume that $-\infty < V_L = V_R < V_T = \theta$. Our goal is to derive the eigenvalue boundary value problem corresponding to the Fokker Planck problem (4.1)-(4.2)-(4.3)-(4.4)-(4.5)-(4.7).

The first step in solving problem (4.1)-(4.2)-(4.3)-(4.4)-(4.5)-(4.7) is to investigate the existence of a solution $\rho(V, t|V_0, 0)$ of equation (4.1) of the form

$$\rho(V, t|V_0, 0) = \phi(V)e^{\lambda t}. \quad (4.8)$$

Substitution of (4.8) into (4.1), (4.3), (4.4) and (4.7) gives the ODE boundary value problem

$$\phi''(V) - \frac{2\mu}{\sigma^2} \phi'(V) - \frac{2\lambda}{\sigma^2} \phi(V) = 0, \quad (4.9)$$

with absorbing condition

$$\phi(\theta) = 0, \quad (4.10)$$

reflective boundary condition

$$\mu\phi(0) - \frac{\sigma^2}{2}\phi'(0) = 0, \quad (4.11)$$

and jump condition

$$\phi'(\theta) = \phi'(0) - \frac{2\mu}{\sigma^2}\phi(0). \quad (4.12)$$

4.1.3 The Nonlinear Eigenvalue Equation

In this section we analyze problem (4.9)-(4.10)-(4.11)-(4.12) and derive the nonlinear equation that determines the eigenvalues λ . Although the derivation was originally given by Mattia [24], here we give the details for completeness. In particular, we show that the eigenvalues are determined by

$$\lambda = \frac{\sigma^4(\gamma_1^2 - \gamma_2^2) - \mu^2\theta^2}{2\theta^2\sigma^2} + i\frac{\gamma_1\gamma_2\sigma^2}{\theta^2}, \quad (4.13)$$

where

$$\gamma e^z = \gamma \cosh(\gamma) + z \sinh(\gamma), \quad (4.14)$$

and

$$z = \frac{\mu\theta}{\sigma^2} \text{ and } \gamma = \frac{\theta}{\sigma^2} \sqrt{\mu^2 + 2\lambda\sigma^2}. \quad (4.15)$$

Derivation of (4.13)-(4.14)-(4.15).

We follow Mattia [24] and look for solutions to problem (4.9)-(4.12) of the form

$$\phi(V) = e^{\frac{mV}{\theta}}, \quad m \text{ real.} \quad (4.16)$$

Substitute (4.16) into (4.9) and obtain

$$m^2 - \frac{2\mu\theta}{\sigma^2}m - \frac{2\lambda\theta^2}{\sigma^2} = 0. \quad (4.17)$$

Solve (4.17) for m and obtain

$$m = \frac{\mu\theta}{\sigma^2} \pm \frac{\theta}{\sigma^2} \sqrt{\mu^2 + 2\lambda\sigma^2}. \quad (4.18)$$

Next, set

$$z = \frac{\mu\theta}{\sigma^2} \text{ and } \gamma = \frac{\theta}{\sigma^2} \sqrt{\mu^2 + 2\lambda\sigma^2}. \quad (4.19)$$

The general solution of (4.9) is

$$\phi(V) = \exp\left[\frac{zV}{\theta}\right] \left(c_1 \exp\left[\frac{\gamma V}{\theta}\right] + c_2 \exp\left[-\frac{\gamma V}{\theta}\right] \right). \quad (4.20)$$

Substituting (4.20) into the absorbing condition, $\phi(\theta) = 0$, gives

$$c_2 = -c_1 e^{2\gamma}. \quad (4.21)$$

Next, combine (4.21) and (4.20) and obtain

$$\phi(V) = c_1 \exp\left[\frac{zV}{\theta}\right] \exp[\gamma] \left[\exp\left[\frac{\gamma V}{\theta} - \gamma\right] - \exp\left[\gamma - \frac{\gamma V}{\theta}\right] \right]. \quad (4.22)$$

The identity (4.21) applied to (4.22) gives

$$\phi(V) = c_\lambda \exp\left[\frac{zV}{\theta}\right] \sinh\left[\frac{\gamma(\theta - V)}{\theta}\right], \quad (4.23)$$

where $c_\lambda = -2c_1 \exp(\gamma)$. It follows from (4.23) that

$$\phi(0) = c_\lambda \sinh(\gamma), \quad (4.24)$$

$$\phi'(\theta) = -c_\lambda \frac{\gamma}{\theta} e^z, \quad (4.25)$$

and

$$\phi'(0) = -c_\lambda \frac{z}{\theta} \sinh(\gamma) - c_\lambda \frac{\gamma}{\theta} \cosh(\gamma). \quad (4.26)$$

Lastly, combine (4.24), (4.25) and (4.26) with the jump condition $\phi'(\theta) = \phi'(0) - \frac{2\mu}{\sigma^2}\phi(0)$ to obtain the nonlinear eigenvalue equation

$$\gamma e^z = \gamma \cosh(\gamma) + z \sinh(\gamma). \quad (4.27)$$

4.1.4 The Eigenfunctions ϕ_n of L and ψ_n of L^+

The eigenfunctions $\phi_n(V)$ and adjoint eigenfunctions $\psi_n(V)$ are needed to construct the mean firing rate generated by an eigenfunction expansion. In this section we derive the eigenfunctions $\phi_n(V)$ and adjoint eigenfunctions $\psi_n(V)$ for $n \neq 0$. In particular, we show that

$$\phi_n(V) = C_n e^{\frac{z}{\theta}V} \sinh\left(\frac{\gamma(\theta - V)}{\theta}\right), \quad (4.28)$$

and

$$\psi_n(V) = e^{-\frac{z}{\theta}V} \left(\gamma \cosh\left(\frac{\gamma}{\theta}V\right) + z \sinh\left(\frac{\gamma}{\theta}V\right) \right), \quad (4.29)$$

where

$$C_n = \frac{2z}{\theta(z\gamma \cosh(\gamma) + (\gamma^2 - z) \sinh(\gamma))}. \quad (4.30)$$

Derivation of (4.28)-(4.29)-(4.30): The eigenfunctions (4.28) were derived in Section 2.4. Therefore, it remains to derive the eigenfunctions corresponding to the boundary value problem 4.31. Recall from Section 3.2 the appropriate boundary value problem is

$$\begin{cases} \lambda\psi(V) = \mu\psi'(V) + \frac{\sigma^2}{2}\psi''(V) \\ \psi(0) = \psi(\theta) \\ \psi'(0) = 0. \end{cases} \quad (4.31)$$

We follow Mattia and Del Giudice [24] and assume that

$$\psi_n(V) = e^{\frac{m}{\theta}V}. \quad (4.32)$$

Thus, the general solution of $\beta\psi(V) = \mu\psi'(V) + \frac{\sigma^2}{2}\psi''(V)$ is

$$\psi_n(V) = e^{\frac{-z}{\theta}V} \left(C_1 e^{\frac{\gamma}{\theta}V} + C_2 e^{\frac{-\gamma}{\theta}V} \right). \quad (4.33)$$

where

$$\gamma e^z = \gamma \cosh(\gamma) + z \sinh(\gamma), \quad (4.34)$$

and

$$z = \frac{\mu\theta}{\sigma^2} \text{ and } \gamma = \frac{\theta}{\sigma^2} \sqrt{\mu^2 + 2\lambda\sigma^2}. \quad (4.35)$$

The boundary condition $\psi(0) = \psi(\theta)$ implies that

$$C_1 = \frac{z + \gamma}{\gamma - z}. \quad (4.36)$$

Thus, equation (4.33) may be expressed as

$$\psi_n(V) = \frac{2C_2}{\gamma - z} e^{\frac{-z}{\theta}V} \left(\frac{1}{2}(z + \gamma)e^{\frac{\gamma}{\theta}V} + \frac{1}{2}(\gamma - z)e^{\frac{-\gamma}{\theta}V} \right). \quad (4.37)$$

A rearrangement of the terms in (4.37), combined with standard identities for cosh and sinh, gives

$$\psi_n(V) = \frac{2C_2}{\gamma - z} e^{\frac{-z}{\theta}V} \left(\gamma \cosh\left(\frac{\gamma}{\theta}V\right) + z \sinh\left(\frac{\gamma}{\theta}V\right) \right). \quad (4.38)$$

It remains to determine the constant C_2 . To this end recall the orthonormal properties from Chapter 3:

$$(\psi_n, \phi_m) = \delta_{nm}. \quad (4.39)$$

Suppress C_2 in C_n and note that, since $(\psi_n, \phi_n) = 1$, it follows after an integration that

$$C_n = \frac{2z}{\theta(z\gamma \cosh(\gamma) + (\gamma^2 - z) \sinh(\gamma))}. \quad (4.40)$$

4.2 EIGENVALUES FOR THE IF MODEL WHEN $\mu = 0$

In this chapter we set $\mu = 0$ in the IF model and compute the associated eigenvalues and eigenfunctions. We then investigate whether the associated Fokker Planck solution exists as a series expansion of eigenfunctions and eigenvalues. In particular we do the following

4.2.1 First, we recall the eigenvalue problem developed in Chapter 3.

4.2.2 We state and prove our main result, namely, that the Fokker-Planck boundary value problem does not have an eigenfunction expansion solution when $\mu = 0$.

4.2.1 The ODE Boundary Value Problem

Recall from Chapter 3 that the ODE boundary value problem for the eigenvalues is given by

$$\begin{cases} L(\phi) = \lambda\phi \\ \phi(\theta) = 0 \\ \phi'(\theta) = \phi'(0) - \frac{2\mu}{\sigma^2}\phi(0) \end{cases} \quad (4.41)$$

where

$$L(\phi) = -\mu\phi'(V) + \frac{\sigma^2}{2}\phi''(V). \quad (4.42)$$

Set $\mu = 0$ and obtain the ODE boundary value problem

$$\frac{\sigma^2}{2}\phi''(V) = \lambda\phi(V), \quad 0 < V < \theta, \quad (4.43)$$

$$\phi(\theta) = 0, \quad (4.44)$$

and

$$\phi'(\theta) = \phi'(0). \quad (4.45)$$

Similarly, the associated adjoint ODE boundary value problem is given by (see Chapter 3 for details) is given by

$$\frac{\sigma^2}{2}\psi''(V) = \tilde{\lambda}\psi(V), \quad 0 < V < \theta, \quad (4.46)$$

$$\psi(\theta) = \psi(0) \quad (4.47)$$

and

$$\text{and } \psi'(0) = 0. \quad (4.48)$$

We follow Mattia [24] (see Chapter 3) and impose the orthogonality condition

$$(\phi_n, \psi_m) = \delta_{nm}. \quad (4.49)$$

Remark: Below, we show that property (4.49) fails to hold when we assume that problem (4.43)-(4.44)-(4.45) has an eigenfunction expansion type solution.

4.2.2 The Main Theoretical Result

We investigate the existence of a solution of problem (4.43)-(4.44)-(4.45) which can be written as a series of eigenfunctions ϕ_n and eigenvalues λ_n :

$$\rho(V, t|V_0, 0) = \sum_{n=0}^{\infty} A_n e^{\lambda_n t} \phi_n(V). \quad (4.50)$$

In Theorem 2 we investigate key properties of the eigenvalues and eigenfunctions associated with problem (4.43)-(4.44)-(4.45) and the adjoint problem (4.46)-(4.47)-(4.48). In particular, we show how these properties lead to the non existence of a solution of the form (4.50).

Theorem 2. *Let $\theta > 0$ and $\sigma > 0$. The following are true:*

(A.) *Suppose that when $\lambda = 0$. Then $\phi_0(V) = \frac{2}{\theta^2}(\theta - V)$ and $\psi_0(V) = 1$.*

(B.) *For $n \geq 1$, the eigenvalues of (4.43)-(4.44)-(4.45) are $\lambda_n = -\frac{2\sigma^2 n^2 \pi^2}{\theta^2}$ with eigenfunctions*

$$\phi_n(V) = \sin\left(\frac{2n\pi}{\theta}V\right). \quad (4.51)$$

(C.) *For $n \geq 1$, the eigenvalues of (4.46)-(4.47)-(4.48) are $\tilde{\lambda}_n = -\frac{2\sigma^2 n^2 \pi^2}{\theta^2}$ with eigenfunctions*

$$\psi_n(V) = \cos\left(\frac{2n\pi}{\theta}V\right). \quad (4.52)$$

(D.) When $n \geq 1$:

$$\int_0^\theta \phi_n dV = 0, \quad \int_0^\theta \psi_n dV = 0, \quad \text{and} \quad \int_0^\theta \phi_n \psi_n dV = 0. \quad (4.53)$$

(E.) For $n \geq 0$, $A_n = \psi_n(V_0) = \cos\left(\frac{2n\pi}{\theta}V_0\right)$.

(F.) A solution to problem (4.43)-(4.44)-(4.45), of the form (4.50), does not exist.

Proof of A. When $\lambda = 0$ equation (4.43) reduces to

$$\phi'' = 0, \quad (4.54)$$

with general solution

$$\phi_0(V) = C_1V + C_2. \quad (4.55)$$

The boundary conditions (4.44) and (4.45), combined with (4.55) give

$$\phi_0(V) = \frac{2}{\theta^2}(\theta - V), \quad 0 \leq V \leq \theta. \quad (4.56)$$

Next, let $\tilde{\lambda} = 0$ and note that equation (4.46) reduces to

$$\psi'' = 0, \quad (4.57)$$

with general solution is

$$\psi_0(V) = D_1V + D_2. \quad (4.58)$$

Substitute the boundary conditions (4.47) and (4.48) and obtain

$$\psi_0(V) = 1, \quad 0 \leq V \leq \theta. \quad (4.59)$$

This completes the proof of **Part A**.

Proof of B. We assume that $\lambda \neq 0$ and show that the eigenvalues of the ODE problem (4.43)-(4.44)-(4.45) are real and negative. The proof of this requires three Lemmas.

Lemma 7. *Suppose that ϕ is a solution of the ODE problem (4.43)-(4.44)-(4.45). Then*

$$\phi(0) = 0. \quad (4.60)$$

Proof. First, multiply (4.43) by ϕ' :

$$\phi' \phi'' - \frac{2\lambda}{\sigma^2} \phi' \phi = 0. \quad (4.61)$$

Integration of (4.61) shows that there is a real constant C such that

$$\frac{[\phi']^2}{2} - \frac{\lambda}{\sigma^2} \phi^2 = C, \quad 0 < V < \theta. \quad (4.62)$$

It follows from (4.44) that $\phi(\theta) = 0$. This fact, combined with (4.62) gives

$$\frac{[\phi'(\theta)]^2}{2} = C. \quad (4.63)$$

Thus, (4.62) may be rewritten as

$$\frac{[\phi']^2}{2} - \frac{\lambda}{\sigma^2} \phi^2 = \frac{[\phi'(\theta)]^2}{2}, \quad 0 < V < \theta. \quad (4.64)$$

Lastly, combine boundary condition (4.45), i.e. $\phi'(0) = \phi'(\theta)$, with (4.64) and obtain

$$-\frac{\lambda}{\sigma^2} \phi^2(0) = 0. \quad (4.65)$$

Since $\lambda \neq 0$ it follows that $\phi(0) = 0$, as claimed. This completes the proof of Lemma 7. \square

We now show that λ is real.

Lemma 8. *The eigenvalues of the ODE problem (4.43)-(4.44)-(4.45) are real.*

Proof. For contradiction assume that $\lambda = x + iy$ is complex. Then

$$\phi'' - \frac{2\lambda}{\sigma^2}\phi = 0 \quad (4.66)$$

and

$$\bar{\phi}'' - \frac{2\bar{\lambda}}{\sigma^2}\bar{\phi} = 0. \quad (4.67)$$

Next, multiply (4.66) by $\bar{\phi}$ and multiply (4.67) by ϕ . Thus,

$$\bar{\phi}\phi'' - \frac{2\lambda}{\sigma^2}\bar{\phi}\phi = 0 \quad (4.68)$$

and

$$\phi\bar{\phi}'' - \frac{2\bar{\lambda}}{\sigma^2}\phi\bar{\phi} = 0. \quad (4.69)$$

Subtracting (4.69) from (4.68) yields

$$(\bar{\phi}\phi' - \bar{\phi}'\phi)' = \frac{2(\lambda - \bar{\lambda})}{\sigma^2}\phi\bar{\phi}. \quad (4.70)$$

An integration of (4.70) from 0 to θ , combined with equation (4.44) and Lemma 7, imply that

$$\frac{2(\lambda - \bar{\lambda})}{\sigma^2} \int_0^\theta \phi\bar{\phi} = 0. \quad (4.71)$$

A non trivial eigenfunction, ϕ , is not identically zero. Thus, $\int_0^\theta \phi\bar{\phi} > 0$. It follows that $\lambda = \bar{\lambda}$, i.e. λ is real. This completes the proof of Lemma 8. \square

Next, we prove that the eigenvalues are negative.

Lemma 9. *The non zero eigenvalues of the ODE problem (4.43)-(4.44)-(4.45) are negative.*

Proof. For contradiction suppose that $\lambda > 0$ and that ϕ is an associated non trivial eigenfunction. Then (4.43) is equivalent to

$$\phi'' - r^2\phi = 0, \quad 0 < V < \theta, \quad (4.72)$$

where $r = \sqrt{\frac{2\lambda}{\sigma^2}} > 0$.

The general solution of (4.72) is

$$\phi(V) = E_1 e^{rV} + E_2 e^{-rV}. \quad (4.73)$$

The boundary condition (4.44), i.e. $\phi(0) = 0$, implies that $E_1 = -E_2$ and thus

$$\phi(V) = E_1 e^{rV} - E_1 e^{-rV}. \quad (4.74)$$

The boundary condition $\phi(\theta) = 0$ implies that

$$E_1 (e^{r\theta} - e^{-r\theta}) = 0. \quad (4.75)$$

Since $(e^{r\theta} - e^{-r\theta}) > 0$ when $r > 0$, it follows from (4.75) that $E_1 = 0$. In turn, this implies that $\phi = 0$ for all V , a contradiction of our assumption that ϕ is a non trivial eigenfunction. \square

Summary: Lemmas 7-8-9 imply that the non zero eigenvalues of the ODE problem (4.43)-(4.44)-(4.45) are real and negative. It remains to find their exact values.

Suppose that $B > 0$ and $\frac{2\lambda}{\sigma^2} = -B^2$. Then the general solution of

$$\phi'' + B^2\phi = 0 \quad (4.76)$$

is

$$\phi(V) = C_1 \cos(BV) + C_2 \sin(BV). \quad (4.77)$$

The condition $\phi(0) = 0$ implies that $C_1 = 0$ so that (4.77) becomes

$$\phi(V) = C_2 \sin(BV). \quad (4.78)$$

The condition $\phi'(\theta) = \phi'(0)$ implies that

$$\cos(B\theta) = 1. \quad (4.79)$$

It follows from (4.79), and the fact that $B > 0$, that $B = \frac{2n\pi}{\theta}$, $n \geq 1$. Therefore, the eigenvalues are

$$\lambda_n = -\frac{2n^2\pi^2\sigma^2}{\theta^2}, \quad n \geq 1, \quad (4.80)$$

with corresponding eigenfunctions

$$\phi_n = \sin\left(\frac{2n\pi}{\theta}V\right). \quad (4.81)$$

Proof of C. First, we consider (4.46) when $\tilde{\lambda} \neq 0$ and show that the eigenvalues of the ODE problem (4.46)-(4.47)-(4.47) are real and negative. The proof of this requires three Lemmas.

Remark: For notational convenience we set $\alpha = \tilde{\lambda}$ for the remainder of this proof.

Lemma 10. *Let ψ solve the ODE problem (4.46)-(4.47)-(4.47). Then*

$$\psi'(\theta) = 0. \quad (4.82)$$

Proof. First, multiply (4.46) by ψ' :

$$\psi'\psi'' - \frac{2\alpha}{\sigma^2}\psi'\psi = 0. \quad (4.83)$$

Integration of (4.83) shows that there is a real constant C such that

$$\frac{[\psi']^2}{2} - \frac{\alpha}{\sigma^2}\psi^2 = C, \quad 0 < V < \theta. \quad (4.84)$$

Recall from (4.48) that $\psi'(0) = 0$. This, combined with (4.84) gives

$$-\frac{\alpha}{\sigma^2}\psi^2(0) = C. \quad (4.85)$$

Thus, (4.84) becomes

$$\frac{[\psi']^2}{2} - \frac{\alpha}{\sigma^2}\psi^2 = -\frac{\alpha}{\sigma^2}\psi^2(0), \quad 0 < V < \theta. \quad (4.86)$$

Lastly, apply the boundary condition (4.47), i.e. $\psi(0) = \psi(\theta)$, to (4.86) and obtain

$$\frac{[\psi'(\theta)]^2}{2} = 0. \quad (4.87)$$

It follows that $\psi'(\theta) = 0$, as claimed. This completes the proof of Lemma 10. \square

Next, we show that the eigenvalues of (4.46)-(4.47)-(4.47) are real.

Lemma 11. *The eigenvalues of the ODE problem (4.46)-(4.47)-(4.47) are real.*

Proof. For contradiction assume that $\alpha = x + iy$ is complex. Then

$$\psi'' - \frac{2\alpha}{\sigma^2}\psi = 0 \quad (4.88)$$

and

$$\bar{\psi}'' - \frac{2\bar{\alpha}}{\sigma^2}\bar{\psi} = 0. \quad (4.89)$$

Multiply (4.88) by $\bar{\psi}$ and multiply (4.89) by ψ . Thus,

$$\bar{\psi}\psi'' - \frac{2\alpha}{\sigma^2}\bar{\psi}\psi = 0 \quad (4.90)$$

and

$$\psi\bar{\psi}'' - \frac{2\bar{\alpha}}{\sigma^2}\psi\bar{\psi} = 0. \quad (4.91)$$

Subtracting (4.91) from (4.90) yields

$$(\bar{\psi}\psi' - \bar{\psi}'\psi)' = \frac{2(\alpha - \bar{\alpha})}{\sigma^2}\psi\bar{\psi}. \quad (4.92)$$

An integration of (4.92) from 0 to θ , combined with (4.48) and (4.82), gives

$$\frac{2(\alpha - \bar{\alpha})}{\sigma^2} \int_0^\theta \psi\bar{\psi} = 0. \quad (4.93)$$

A non trivial eigenfunction, ψ , is not identically zero. Thus, $\int_0^\theta \psi\bar{\psi} > 0$. It follows that $\alpha = \bar{\alpha}$, i.e. α is real. This completes the proof of Lemma 11. \square

Lastly, we prove the following Lemma:

Lemma 12. *The non zero eigenvalues of the ODE problem (4.46)-(4.47)-(4.47) are negative.*

Proof. For contradiction suppose that $\alpha > 0$ and that ψ is an associated non trivial eigenfunction. Then (4.46) is equivalent to

$$\psi'' - r^2\psi = 0, \quad 0 < V < \theta, \quad (4.94)$$

where $r = \sqrt{\frac{2\alpha}{\sigma^2}} > 0$. The general solution of (4.94) has the form $\psi(V) = F_1e^{rV} + F_2e^{-rV}$. The boundary condition $\psi'(0) = 0$ implies that $F_1 = F_2$ so that

$$\psi(V) = F_1e^{rV} + F_1e^{-rV}. \quad (4.95)$$

The boundary condition $\psi'(\theta) = 0$ implies that

$$F_1r(e^{r\theta} - e^{-r\theta}) = 0. \quad (4.96)$$

Since $(e^{r\theta} - e^{-r\theta}) > 0$ when $r > 0$, it follows from (4.96) that $F_1 = 0$. In turn, this implies that $\psi = 0$ for all V , a contradiction of our assumption that ψ is a non trivial eigenfunction. \square

The previous three Lemmas imply that the non zero eigenvalues of the ODE problem (4.46)-(4.47)-(4.47) are real and negative. It remains to find their exact values.

Suppose that $B > 0$ and $\frac{2\alpha}{\sigma^2} = -B^2$. Then the general solution of

$$\psi'' + B^2\psi = 0 \quad (4.97)$$

has the form

$$\psi(V) = G_1 \cos(BV) + G_2 \sin(BV). \quad (4.98)$$

The condition $\psi'(0) = 0$ implies that $G_2 = 0$ so that (4.98) becomes

$$\psi(V) = G_1 \cos(BV). \quad (4.99)$$

The condition $\psi(\theta) = \psi(0)$ implies that

$$\cos(B\theta) = 1. \quad (4.100)$$

It follows from (4.100), and the fact that $B > 0$, that $B = \frac{2n\pi}{\theta}$, $n \geq 1$. Therefore, the eigenvalues are

$$\tilde{\lambda}_n = \alpha_n = -\frac{2n^2\pi^2\sigma^2}{\theta^2}, \quad n \geq 1, \quad (4.101)$$

with corresponding eigenfunctions

$$\psi_n = \cos\left(\frac{2n\pi}{\theta}V\right). \quad (4.102)$$

Proof of D. Let $n \geq 1$ and notice that a straight forward calculation gives

$$\int_0^\theta \phi_n(V) dV = \int_0^\theta \sin\left(\frac{2n\pi}{\theta}V\right) dV = 0,$$

and

$$\int_0^\theta \psi_n(V) dV = \int_0^\theta \cos\left(\frac{2n\pi}{\theta}V\right) dV = 0.$$

Finally,

$$\int_0^\theta \phi_n(V)\psi_n(V) dV = \int_0^\theta \sin\left(\frac{2n\pi}{\theta}V\right) \cos\left(\frac{2n\pi}{\theta}V\right) dV = 0.$$

Proof of E. Recall that we are assuming that a solution to problem (4.43)-(4.44)-(4.45) exists, and has the form

$$\rho(V, t|V_0, 0) = \sum_{n=0}^{\infty} A_n e^{\lambda_n t} \phi_n(V), \quad \text{for all } t \geq 0, 0 \leq V \leq \theta. \quad (4.103)$$

To prove property **V.**, we need to find the values of the coefficients on the right side of (4.103). For this, a standard approach is to multiply (4.103) by ψ_m :

$$\psi_m(V)\rho(V, t|V_0, 0) = \sum_{n=0}^{\infty} A_n e^{\lambda_n t} \psi_m(V)\phi_n(V), \quad \text{for all } t \geq 0. \quad (4.104)$$

A formal integration of (4.104) yields

$$\int_0^\theta \psi_m(V)\rho(V, t|V_0, 0) dV = A_m e^{\lambda_m t}, \quad \text{for all } t \geq 0. \quad (4.105)$$

Let $t = 0$ and recall the requirement that $\rho(V, 0|V_0, 0) = \delta(V - V_0)$. Then (4.105) reduces to

$$\int_0^\theta \psi(V) \delta(V - V_0) dV = A_m, \quad m \geq 0. \quad (4.106)$$

Combining (4.106) with (4.52) gives

$$A_m = \psi_m(V_0) = \cos\left(\frac{2m\pi}{\theta} V_0\right), \quad m \geq 0. \quad (4.107)$$

This completes the proof of **Part E**.

Proof of F. We show that a solution to problem (4.43)-(4.44)-(4.45) of the form (4.50) does not exist. By **Part A** and **Part E**, (4.50) becomes

$$\rho(V, t|V_0, 0) = \frac{2}{\theta^2}(\theta - V) + \sum_{n=1}^{\infty} e^{\lambda_n t} \cos\left(\frac{2n\pi}{\theta} V_0\right) \sin\left(\frac{2n\pi}{\theta} V\right) \quad \text{for all } t \geq 0. \quad (4.108)$$

When $t = 0$, equation (4.108) reduces to

$$\rho(V, 0|V_0, 0) = \frac{2}{\theta^2}(\theta - V) + \sum_{n=1}^{\infty} \cos\left(\frac{2n\pi}{\theta} V_0\right) \sin\left(\frac{2n\pi}{\theta} V\right) \quad 0 \leq V \leq \theta. \quad (4.109)$$

Substituting the requirement that $\rho(V, 0|V_0, 0) = \delta(V - V_0)$ into (4.109) gives

$$\delta(V - V_0) = \frac{2}{\theta^2}(\theta - V) + \sum_{n=1}^{\infty} \cos\left(\frac{2n\pi}{\theta} V_0\right) \sin\left(\frac{2n\pi}{\theta} V\right), \quad 0 \leq V \leq \theta. \quad (4.110)$$

Now, let $V = 0$. Then (4.110) reduces to

$$\delta(-V_0) = \frac{2}{\theta}. \quad (4.111)$$

Alternatively, let $V = \frac{\theta}{2}$. Then (4.110) reduces to

$$\delta\left(\frac{\theta}{2} - V_0\right) = \frac{1}{\theta}. \quad (4.112)$$

Properties (4.111) and (4.112) contradict the fact that the delta function can have at most one non zero value. Thus, we conclude that problem (4.43)-(4.44)-(4.45) does not have an eigenfunction expansion solution of the form (4.50). This completes the proof of **Part F**

The proof of Theorem 2 is now complete.

4.3 EIGENVALUES FOR THE IF MODEL WHEN $Z = \frac{\mu\theta}{\sigma^2} > 0$

In this section we fix $\mu > 0$ in the IF model and analytically investigate properties of the eigenvalues of the associated Fokker Planck equation (FPE). Recall from Section 4.1 that, to compute the eigenvalues, λ , we set $z = \frac{\mu\theta}{\sigma^2}$, where $\theta > 0$ and $\sigma > 0$ are fixed, and solve the nonlinear algebraic equation

$$\gamma e^z = \gamma \cosh(\gamma) + z \sinh(\gamma), \quad (4.113)$$

where

$$z = \frac{\mu\theta}{\sigma^2} > 0 \quad \text{and} \quad \gamma = \gamma_1 + i\gamma_2 = \frac{\theta}{\sigma^2} \sqrt{\mu^2 + 2\lambda\sigma^2}. \quad (4.114)$$

It follows from (4.114) that the eigenvalues are given by

$$\lambda = \frac{\sigma^4(\gamma_1^2 - \gamma_2^2) - \mu^2\theta^2}{2\theta^2\sigma^2} + i\frac{\gamma_1\gamma_2\sigma^2}{\theta^2}. \quad (4.115)$$

The remainder of this section consists of Subsections 4.3.1-4.3.5, which focus on the following issues:

4.3.1 We develop non linear algebraic equations for γ_1 and γ_2 .

4.3.2 Using the non linear algebra equations derived in Subsection 4.3.1, we develop ODEs for γ_1 and γ_2 . The solutions of these ODEs will, because of equation (4.115), generate corresponding branches of eigenvalues.

4.3.3 For small, fixed $z > 0$, we prove the existence of infinitely many initial values for the (γ_1, γ_2) ODEs developed in Subsection 4.3.2.

4.3.4 We prove that, corresponding to the infinitely many initial values proved in Subsection 4.3.3, there are infinitely many distinct solutions, $(\gamma_1^n(z), \gamma_2^n(z))$, $n \geq 1$, of the ODEs developed in Subsection 4.3.2. In turn, these solutions generate infinitely many branches of eigenvalues, $\lambda^n(z) = \lambda_1^n(z) + i\lambda_2^n(z)$, $n \geq 1$, of the form given in (4.115).

4.3.5 We analyze the asymptotic behavior, as $z \rightarrow 0^+$, of the eigenvalues $\lambda^n(z)$.

4.3.1 The Nonlinear Algebraic Equations for γ_1 and γ_2

Assume that $\gamma = \gamma_1 + i\gamma_2$. Then (4.113) becomes

$$\begin{aligned} (\gamma_1 + i\gamma_2)e^z &= \gamma_1 [\cosh(\gamma_1) \cosh(i\gamma_2) + \sinh(\gamma_1) \sinh(i\gamma_2)] \\ &+ i\gamma_2 [\cosh(\gamma_1) \cosh(i\gamma_2) + \sinh(\gamma_1) \sinh(i\gamma_2)] \\ &+ z [\sinh(\gamma_1) \cosh(i\gamma_2) + \cosh(\gamma_1) \sinh(i\gamma_2)]. \end{aligned} \quad (4.116)$$

Note that $\cosh(ix) = \cos(x)$ and $\sinh(ix) = i \sin(x)$. Separating real and imaginary parts in (4.116) and obtain the two algebraic equations

$$\gamma_1 e^z - \gamma_1 \cosh(\gamma_1) \cos(\gamma_2) + \gamma_2 \sinh(\gamma_1) \sin(\gamma_2) - z \sinh(\gamma_1) \cos(\gamma_2) = 0, \quad (4.117)$$

$$\gamma_2 e^z - \gamma_1 \sinh(\gamma_1) \sin(\gamma_2) - \gamma_2 \cosh(\gamma_1) \cos(\gamma_2) - z \cosh(\gamma_1) \sin(\gamma_2) = 0. \quad (4.118)$$

We keep $\sigma > 0$ and $\theta > 0$ fixed, and vary $\mu > 0$. Thus, we assume that $z = \frac{\mu\theta}{\sigma^2} > 0$ varies only with $\mu > 0$. Our goal is to make use of the implicit function theorem to solve (4.117)-(4.118) for real functions $\gamma_1(z)$ and $\gamma_2(z)$. The first step is to define functions $f(\gamma_1, \gamma_2, z)$ and $g(\gamma_1, \gamma_2, z)$ by

$$f = \gamma_1 e^z - \gamma_1 \cosh(\gamma_1) \cos(\gamma_2) + \gamma_2 \sinh(\gamma_1) \sin(\gamma_2) - z \sinh(\gamma_1) \cos(\gamma_2), \quad (4.119)$$

$$g = \gamma_2 e^z - \gamma_1 \sinh(\gamma_1) \sin(\gamma_2) - \gamma_2 \cosh(\gamma_1) \cos(\gamma_2) - z \cosh(\gamma_1) \sin(\gamma_2). \quad (4.120)$$

To use the implicit function theorem we must find a solution $(\bar{\gamma}_1, \bar{\gamma}_2, \bar{z})$, which satisfies

$$f(\bar{\gamma}_1, \bar{\gamma}_2, \bar{z}) = 0, \quad (4.121)$$

$$g(\bar{\gamma}_1, \bar{\gamma}_2, \bar{z}) = 0. \quad (4.122)$$

4.3.2 ODEs for γ_1 and γ_2

Our approach to proving the existence of infinitely many branches of solutions of the non-linear algebra problem

$$f(\gamma_1, \gamma_2, z) = 0, \quad (4.123)$$

$$g(\gamma_1, \gamma_2, z) = 0, \quad (4.124)$$

is to develop ODEs for $\gamma_1(z)$ and $\gamma_2(z)$. The first step is to differentiate (4.123) and (4.124) with respect to z :

$$\frac{\partial f}{\partial \gamma_1} \frac{d\gamma_1}{dz} + \frac{\partial f}{\partial \gamma_2} \frac{d\gamma_2}{dz} + \frac{\partial f}{\partial z} = 0, \quad (4.125)$$

$$\frac{\partial g}{\partial \gamma_1} \frac{d\gamma_1}{dz} + \frac{\partial g}{\partial \gamma_2} \frac{d\gamma_2}{dz} + \frac{\partial g}{\partial z} = 0. \quad (4.126)$$

Solving for $\gamma_1'(z)$ and $\gamma_2'(z)$ gives the system

$$\frac{d\gamma_1}{dz} = \frac{1}{J} \left(\frac{\partial f}{\partial \gamma_1} \frac{\partial f}{\partial z} - \frac{\partial g}{\partial \gamma_2} \frac{\partial g}{\partial z} \right), \quad (4.127)$$

$$\frac{d\gamma_2}{dz} = \frac{1}{J} \left(\frac{\partial g}{\partial \gamma_1} \frac{\partial f}{\partial z} - \frac{\partial f}{\partial \gamma_2} \frac{\partial g}{\partial z} \right), \quad (4.128)$$

with initial values

$$\gamma_1(\bar{z}) = \bar{\gamma}_1 \text{ and } \gamma_2(\bar{z}) = \bar{\gamma}_2, \quad (4.129)$$

where

$$J = \left(\frac{\partial f}{\partial \gamma_1} \right)^2 + \left(\frac{\partial f}{\partial \gamma_2} \right)^2, \quad (4.130)$$

$$\frac{\partial f}{\partial z} = \gamma_1 e^z - \sinh(\gamma_1) \cos(\gamma_2), \quad (4.131)$$

$$\frac{\partial g}{\partial z} = \gamma_2 e^z - \cosh(\gamma_1) \sin(\gamma_2), \quad (4.132)$$

$$\frac{\partial f}{\partial \gamma_1} = e^z + \gamma_2 \cosh(\gamma_1) \sin(\gamma_2) - (1+z) \cosh(\gamma_1) \cos(\gamma_2) - \gamma_1 \sinh(\gamma_1) \cos(\gamma_2), \quad (4.133)$$

$$\frac{\partial f}{\partial \gamma_2} = \gamma_1 \cosh(\gamma_1) \sin(\gamma_2) + (1+z) \sinh(\gamma_1) \sin(\gamma_2) + \gamma_2 \sinh(\gamma_1) \cos(\gamma_2), \quad (4.134)$$

$$\frac{\partial g}{\partial \gamma_1} = -\gamma_1 \cosh(\gamma_1) \sin(\gamma_2) - (1+z) \sinh(\gamma_1) \sin(\gamma_2) - \gamma_2 \sinh(\gamma_1) \cos(\gamma_2), \quad (4.135)$$

and

$$\frac{\partial g}{\partial \gamma_2} = e^z + \gamma_1 \sinh(\gamma_1) \cos(\gamma_2) - (1+z) \cosh(\gamma_1) \cos(\gamma_2) + \gamma_2 \cosh(\gamma_1) \sin(\gamma_2). \quad (4.136)$$

Below, in Theorem 3, we show that there are infinitely many solutions of the algebra problem (4.123)-(4.124), each of which provides the initial values, at an appropriately chosen \bar{z} , for the ODE initial value problem (4.127)-(4.128)-(4.129). We will prove below, see subsection 4.3.4, that equations (4.125)-(4.126) can be solved for $\gamma'_1(z)$ and $\gamma'_2(z)$.

4.3.3 Infinitely Many Initial Values for the (γ_1, γ_2) ODEs.

This entire subsection is devoted to proving the existence of infinitely many solutions of (4.123)-(4.124), each of which is an initial value for the ODE initial value problem (4.127)-(4.128)-(4.129). We do this in

Theorem 3. *Let $\bar{z} > 0$ and $n \geq 1$, and define*

$$\gamma_1^*(\bar{z}) = \ln \left(e^{\bar{z}} + \sqrt{e^{2\bar{z}} - 1} \right). \quad (4.137)$$

For sufficiently small $\bar{z} > 0$ and $\epsilon > 0$, there is at least one solution $(\bar{\gamma}_1, \bar{\gamma}_2, \bar{z})$ of (4.123)-(4.124), where $(\bar{\gamma}_1, \bar{\gamma}_2)$ lies in a rectangle

$$B_n \subset (\epsilon\sqrt{\bar{z}}, \gamma_1^*(\bar{z})) \times \left(2n\pi, 2n\pi + \frac{\pi}{2} \right). \quad (4.138)$$

Remarks: (i) The specific definition of B_n is given below in equation (4.142) in the proof of Theorem 3. (ii) Each solution $(\bar{\gamma}_1, \bar{\gamma}_2)$ is an initial value, at $z = \bar{z}$, for the ODE problem (4.127)-(4.128)-(4.129).

4.3.3.1 Outline of the Proof of Theorem 3 Step I. Let $\bar{z} > 0$ and $n \geq 1$ be fixed, and define the rectangle B_n (see Figure 7).

Step II. Use the implicit function theorem to show that there is a C^1 function $\gamma_2 = \gamma_2(\gamma_1)$ such that $(\gamma_1, \gamma_2(\gamma_1))$ defines a continuous curve $C_n \subset B_n$ with the property that $f(\gamma_1, \gamma_2(\gamma_1), \bar{z}) = 0$ everywhere on C_n . We prove that C_n begins on the right edge of B_n , enters the interior of B_n , and exits along a point $(\hat{\gamma}_1, \hat{\gamma}_2) \in \Gamma_{1,n} \cup \Gamma_{4,n}$. (see Figure 7).

Step III. Evaluate $g(\gamma_1, \gamma_2(\gamma_1), \bar{z})$ along the curve C_n . Show that $g(\gamma_1, \gamma_2(\gamma_1), \bar{z})$ changes sign along C_n . This implies that $g(\gamma_1, \gamma_2(\gamma_1), \bar{z}) = 0$ at some point $(\gamma_1, \gamma_2(\gamma_1)) \in C_n$. In particular, we prove that $g(\gamma_1, \gamma_2(\gamma_1), \bar{z}) < 0$ at the point where C_n intersects the right edge of B_n , and that $g(\gamma_1, \gamma_2(\gamma_1), \bar{z}) > 0$ along $\Gamma_{1,n} \cup \Gamma_{4,n}$. Thus, $g(\gamma_1, \gamma_2(\gamma_1), \bar{z}) > 0$ at the first point where C_n leaves B_n . An application of the intermediate value theorem shows that $g(\gamma_1, \gamma_2(\gamma_1), \bar{z}) = 0$ at some point $(\bar{\gamma}_1, \gamma_2(\bar{\gamma}_1)) \in C_n$ (see Figure 7).

4.3.3.2 Proof of Theorem 3. We begin **Step I** with the construction of the rectangle B_n . Assume throughout that $\bar{z} > 0$ and $n \geq 1$ are fixed. Recall from equation (4.120) that

$$g(\gamma_1, 2n\pi, \bar{z}) = 0 \Leftrightarrow \cosh(\gamma_1) = e^{\bar{z}}.$$

Taking the inverse hyperbolic cosine yields

$$\gamma_1^* := \gamma_1 = \ln \left(e^{\bar{z}} + \sqrt{e^{2\bar{z}} - 1} \right). \quad (4.139)$$

Next, consider the function $l_n(x) = \tan(x) - \frac{\bar{z}}{2n\pi + x}$.

Lemma 13. *Let $\bar{z} > 0$ and $n \geq 1$ be fixed. Then $l_n(x) = 0$ has a unique solution in $(0, \pi/2)$.*

Proof. A calculation shows that

$$l'_n(x) = \sec^2(x) + \frac{\bar{z}}{(2n\pi + x)^2}. \quad (4.140)$$

It follows that l_n is strictly increasing. Since $\lim_{x \rightarrow \pi/2^-} l_n(x) = \infty$ there exists $\delta > 0$ such that $l_n(x) > 0$ for $x \in (\pi/2 - \delta, \pi/2)$. Since $l_n(0) < 0$, the intermediate value theorem guarantees a unique root of $l_n(x) = 0$ in $(0, \pi/2)$. \square

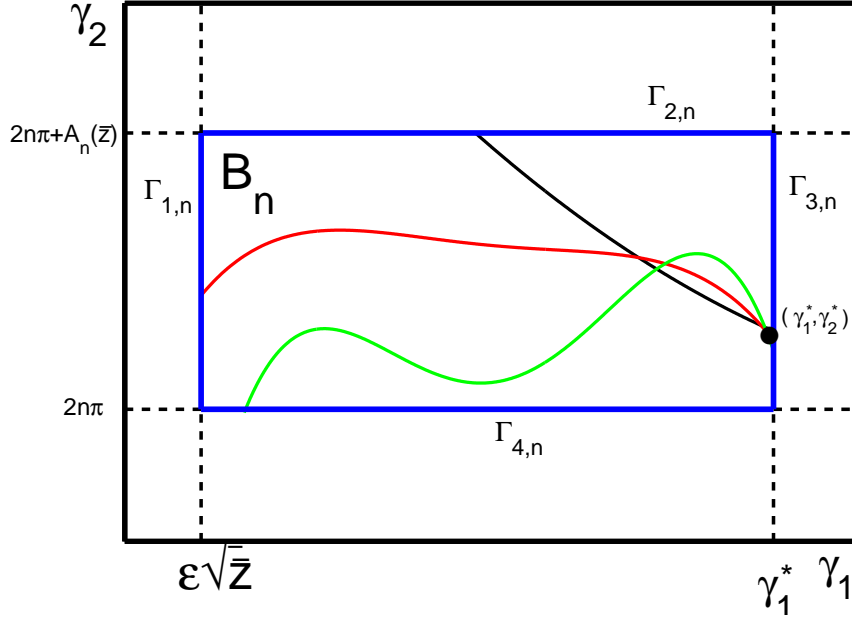


Figure 7: The rectangle $B_n = (\epsilon\sqrt{\bar{z}}, \gamma_1^*) \times (2n\pi, 2n\pi + A_n(\bar{z}))$ in the (γ_1, γ_2) plane. Here, $\bar{z} = \frac{\mu\theta}{\sigma^2} > 0$ is fixed, ϵ is small, and $\gamma_1^* = \ln(e^{\bar{z}} + \sqrt{e^{2\bar{z}} - 1})$. The three curves represent the possible behavior of the curve C_n generated by the \mathbf{C}^1 function $\gamma_2(\gamma_1)$ that passes through the point (γ_1^*, γ_2^*) . By the implicit function theorem C_n enters B_n at the point (γ_1^*, γ_2^*) and continues through B_n , exiting along one of the other three sides. Along each of the three curves we prove that $f(\gamma_1, \gamma_2(\gamma_1), \bar{z}) = 0$. Secondly, at the right endpoint of each curve we show that $g(\gamma_1^*, \gamma_2^*, \bar{z}) < 0$. Finally, we prove that $g(\gamma_1, \gamma_2(\gamma_1), \bar{z}) > 0$ at the point where each of the three curves exit B_n . Thus, there is an interior point, $(\bar{\gamma}_1, \gamma_2(\bar{\gamma}_1), \bar{z})$, on C_n where $f(\bar{\gamma}_1, \gamma_2(\bar{\gamma}_1), \bar{z}) = g(\bar{\gamma}_1, \gamma_2(\bar{\gamma}_1), \bar{z}) = 0$.

To define B_n we need

Definition 1. *Let $\bar{z} > 0$ and $n \geq 1$ be fixed. Then $A_n(\bar{z})$ is the unique number in $(0, \pi/2)$ such that*

$$\tan(A_n(\bar{z})) = \frac{\bar{z}}{2\pi n + A_n(\bar{z})}. \quad (4.141)$$

We are now ready to define the sets B_n .

Definition 2. *Let $\bar{z} > 0$ and $n \geq 1$ be fixed, and let $0 < \epsilon < \sqrt{1/2}$. We define*

$$B_n = B_{\epsilon, \bar{z}, n} = (\epsilon\sqrt{\bar{z}}, \gamma_1^*) \times (2n\pi, 2n\pi + A_n(\bar{z})). \quad (4.142)$$

The boundary of B_n consists of four sides (see Figure 7):

$$\begin{aligned} \Gamma_{1,n} &= \{(\gamma_1, \gamma_2) \in \mathbf{R}^2 \mid \gamma_1 = \epsilon\sqrt{\bar{z}}, 2n\pi \leq \gamma_2 \leq 2n\pi + A_n(\bar{z})\} \\ \Gamma_{2,n} &= \{(\gamma_1, \gamma_2) \in \mathbf{R}^2 \mid 0 < \gamma_1 < \gamma_1^*, \gamma_2 = 2n\pi + A_n(\bar{z})\} \\ \Gamma_{3,n} &= \{(\gamma_1, \gamma_2) \in \mathbf{R}^2 \mid \gamma_1 = \gamma_1^*, 2n\pi \leq \gamma_2 \leq 2n\pi + A_n(\bar{z})\} \\ \Gamma_{4,n} &= \{(\gamma_1, \gamma_2) \in \mathbf{R}^2 \mid 0 < \gamma_1 < \gamma_1^*, \gamma_2 = 2n\pi\} \end{aligned}$$

This completes the construction of B_n .

Existence of a C^1 function $\gamma_2(\gamma_1)$.

The next step is to show the existence of a C^1 function $\gamma_2(\gamma_1)$ that generates a curve $C_n \subset B_n$. We do this in Lemma 14.

Lemma 14. *Fix $\bar{z} > 0$ and $n \geq 1$. For sufficiently small $\beta > 0$, there exists a C^1 function $\gamma_2(\gamma_1)$ such that $f(\gamma_1, \gamma_2(\gamma_1), \bar{z}) = 0$ for all $\gamma_1 \in [\gamma_1^* - \beta, \gamma_1^*]$. Furthermore, $\gamma_2(\gamma_1)$ continues to exist for $\gamma_1 \leq \gamma_1^* - \beta$ until $(\gamma_1, \gamma_2(\gamma_1))$ exits B_n at a point $(\hat{\gamma}_1, \hat{\gamma}_2) \in \Gamma_{1,n} \cup \Gamma_{4,n}$.*

Proof. Notice that $f(\gamma_1, \gamma_2, \bar{z})$ is C^1 by definition. Also, recall that $\Gamma_{3,n}$ forms the right side of B_n . We need to show that there exists $(\gamma_1^*, \gamma_2^*) \in \Gamma_{3,n}$ such that $f(\gamma_1^*, \gamma_2^*, \bar{z}) = 0$. A calculation shows that

$$f(\gamma_1^*, 2n\pi, \bar{z}) = \gamma_1^* (e^{\bar{z}} - \cosh(\gamma_1^*)) - \bar{z} \sinh(\gamma_1^*) = -\bar{z} \sinh(\gamma_1^*) < 0. \quad (4.143)$$

Similarly,

$$f(\gamma_1^*, 2n\pi + A_n(\bar{z}), \bar{z}) = \gamma_1^* e^{\bar{z}} (1 - \cos(A_n(\bar{z}))) \quad (4.144)$$

$$+ \sinh(\gamma_1^*) [(2n\pi + A_n(\bar{z})) \sin(A_n(\bar{z})) - \bar{z} \cos(A_n(\bar{z}))].$$

Applying the definition of $A_n(z)$, (see Definition 1 above), it follows that

$$f(\gamma_1^*, 2n\pi + A_n(\bar{z}), \bar{z}) = \gamma_1^* e^{\bar{z}} (1 - \cos(A_n(\bar{z}))) > 0. \quad (4.145)$$

By the intermediate value theorem there exists $\gamma_2^* \in (2n\pi, 2n\pi + A_n(\bar{z}))$ such that $(\gamma_1^*, \gamma_2^*) \in \Gamma_{3,n}$ and $f(\gamma_1^*, \gamma_2^*, \bar{z}) = 0$. To use the implicit function theorem we need only show that $f_{\gamma_2}(\gamma_1^*, \gamma_2^*, \bar{z}) \neq 0$. A differentiation of (4.119) with respect to γ_2 shows that

$$f_{\gamma_2}(\gamma_1^*, \gamma_2^*, \bar{z}) = \gamma_1^* \cosh(\gamma_1^*) \sin(\gamma_2^*) \quad (4.146)$$

$$+ \sinh(\gamma_1^*) [\sin(\gamma_2^*) + \gamma_2^* \cos(\gamma_2^*) + \bar{z} \sin(\gamma_2^*)]$$

Since $\gamma_2^* \in (2n\pi, 2n\pi + A_n(\bar{z})) \subset (2n\pi, 2n\pi + \pi/2)$, both terms in (4.146) are positive and therefore the implicit function theorem guarantees a neighborhood $(\gamma_1^* - \beta, \gamma_1^* + \beta)$ where $\gamma_2(\gamma_1)$ exists as a \mathbf{C}^1 function.

Next, we show that $f_{\gamma_2}(\gamma_1, \gamma_2, \bar{z}) > 0$ for all $(\gamma_1, \gamma_2) \in \bar{B}_n$. A calculation shows that

$$f_{\gamma_2}(\gamma_1, \gamma_2, z) = \gamma_1 \cosh(\gamma_1) \sin(\gamma_2) + (1 + \bar{z}) \sinh(\gamma_1) \sin(\gamma_2) + \gamma_2 \sinh(\gamma_1) \cos(\gamma_2). \quad (4.147)$$

Since all three terms are positive for $(\gamma_1, \gamma_2) \in [\epsilon\sqrt{\bar{z}}, \gamma_1^*] \times [2n\pi, 2n\pi + A_n(\bar{z})]$ we conclude that

$$f_{\gamma_2}(\gamma_1, \gamma_2, \bar{z}) > 0$$

on the closure of B_n . This property, together with the implicit function theorem, guarantees that $\gamma_2(\gamma_1)$ continues to exist for $\gamma_1 \leq \gamma_1^* - \beta$ until $(\gamma_1, \gamma_2(\gamma_1))$ exits B_n at a point $(\hat{\gamma}_1, \hat{\gamma}_2) \in$

$\Gamma_{1,n} \cup \Gamma_{2,n} \cup \Gamma_{4,n}$. Finally, we eliminate the possibility that $(\hat{\gamma}_1, \hat{\gamma}_2) \in \Gamma_{2,n}$. For this, it suffices to prove that

$$f(\gamma_1, \gamma_2, \bar{z}) > 0 \text{ for all } (\gamma_1, \gamma_2) \in \Gamma_{2,n}. \quad (4.148)$$

Let $(\gamma_1, \gamma_2) \in \Gamma_{2,n}$. Then

$$\begin{aligned} f(\gamma_1, \gamma_2, \bar{z}) &= \gamma_1 e^{\bar{z}} - \gamma_1 \cosh(\gamma_1) \cos(A_n(\bar{z})) + (2n\pi + A_n(\bar{z})) \sinh(\gamma_1) \sin(A_n(\bar{z})) \\ &\quad - \bar{z} \sinh(\gamma_1) \cos(A_n(\bar{z})) \end{aligned} \quad (4.149)$$

By the definition of $A_n(z)$ we have that

$$\begin{aligned} f(\gamma_1, \gamma_2, \bar{z}) &= \gamma_1 e^{\bar{z}} - \gamma_1 \cosh(\gamma_1) \cos(A_n(\bar{z})) \\ &> \gamma_1 e^{\bar{z}} - \gamma_1 \cosh(\gamma_1). \end{aligned}$$

Since \cosh is an increasing function, we apply the definition of γ_1^* and obtain

$$f(\gamma_1, \gamma_2, \bar{z}) > \gamma_1 (\cosh(\gamma_1^*) - \cosh(\gamma_1)) > 0 \text{ for all } (\gamma_1, \gamma_2) \in \Gamma_{2,n} \quad (4.150)$$

as claimed. This completes the proof of Lemma 14. \square

Summary: We have now completed **Step II**. That is, we have shown how to use the implicit function theorem to prove that there is a C^1 function $\gamma_2 = \gamma_2(\gamma_1)$ such that $(\gamma_1, \gamma_2(\gamma_1))$ defines a continuous curve $C_n \subset B_n$ with the property that $f(\gamma_1, \gamma_2(\gamma_1), \bar{z}) = 0$ everywhere on C_n . We have proved that C_n begins on the right edge of B_n , enters the interior of B_n , and exits along one of the edges, $\Gamma_{1,n}$, or $\Gamma_{4,n}$, of B_n (see Figure 7).

We now proceed with **Step III** of the proof of Theorem 3 and show that $g(\gamma_1, \gamma_2, \bar{z}) = 0$ at a point $(\bar{\gamma}_1, \gamma_2(\bar{\gamma}_1)) \in C_n$. We first evaluate $g(\gamma_1, \gamma_2, \bar{z})$ along the boundary of B_n .

Analysis of $g(\gamma_1, \gamma_2, \bar{z})$ on the boundary of B_n .

We need the following two technical lemmas:

Lemma 15. Let $\bar{z} > 0$ and $n \geq 1$ be fixed, and let $(\gamma_1, \gamma_2) \in B_n$. Then

$$\gamma_1 e^{\bar{z}} - \gamma_1 \cosh(\gamma_1) \cos(\gamma_2) > 0. \quad (4.151)$$

Proof. Recall that \cosh is an increasing function. Thus,

$$\cosh(\gamma_1) \cos(\gamma_2) < \cosh(\gamma_1) < \cosh(\gamma_1^*) = e^{\bar{z}}. \quad (4.152)$$

Multiply (4.152) by γ_1 and obtain (4.151). \square

Lemma 16. Let $\bar{z} > 0$ and $n \geq 1$ be fixed, and let $(\gamma_1, \gamma_2) \in B_n$. Suppose that $f(\gamma_1, \gamma_2, \bar{z}) = 0$. Then

$$\gamma_2 \sin(\gamma_2) - \bar{z} \cos(\gamma_2) < 0. \quad (4.153)$$

Proof. For contradiction assume that

$$\gamma_2 \sin(\gamma_2) - \bar{z} \cos(\gamma_2) \geq 0. \quad (4.154)$$

A rearrangement of equation (4.119) gives

$$f(\gamma_1, \gamma_2, \bar{z}) = \gamma_1 e^{\bar{z}} - \gamma_1 \cosh(\gamma_1) \cos(\gamma_2) + \sinh(\gamma_1) [\gamma_2 \sin(\gamma_2) - \bar{z} \cos(\gamma_2)]. \quad (4.155)$$

Set $f = 0$ and note that $\sinh(\gamma_1) > 0$ on $(\epsilon\sqrt{\bar{z}}, \gamma_1^*)$. Lemma 15, together with (4.154) gives

$$\begin{aligned} 0 &= \gamma_1 e^{\bar{z}} - \gamma_1 \cosh(\gamma_1) \cos(\gamma_2) + \sinh(\gamma_1) [\gamma_2 \sin(\gamma_2) - \bar{z} \cos(\gamma_2)] \\ &\geq \gamma_1 e^{\bar{z}} - \gamma_1 \cosh(\gamma_1) \cos(\gamma_2) > 0, \end{aligned}$$

which is a contradiction. This completes the proof of Lemma 16. \square

We now determine the sign of $g(\gamma_1, \gamma_2(\gamma_1), \bar{z})$ on the right boundary of B_n .

Analysis of $g(\gamma_1, \gamma_2(\gamma_1), \bar{z})$ on $\Gamma_{3,n}$.

Below, in Lemma 17 we prove that $g(\gamma_1, \gamma_2, \bar{z}) < 0$ for each $(\gamma_1, \gamma_2) \in \Gamma_{3,n}$ provided $f(\gamma_1, \gamma_2, \bar{z}) = 0$ and $\bar{z} > 0$ is sufficiently small.

Lemma 17. *Let $n \geq 1$. There exists a value $\delta_1 > 0$ such that, if $0 < \bar{z} < \delta_1$, then the following property holds:*

$$\text{if } (\gamma_1, \gamma_2) \in \Gamma_{3,n} \text{ and } f(\gamma_1, \gamma_2, \bar{z}) = 0 \text{ then } g(\gamma_1, \gamma_2, \bar{z}) < 0. \quad (4.156)$$

In particular, $g(\gamma_1^, \gamma_2(\gamma_1^*), \bar{z}) < 0$.*

The proof of Lemma 17 requires four lemmas, Lemmas 18-21.

Lemma 18. *Fix $\bar{z} > 0$ and $n \geq 1$. If $(\gamma_1, \gamma_2) \in B_n$, then*

$$g_{\gamma_2\gamma_2}(\gamma_1, \gamma_2, \bar{z}) > 0. \quad (4.157)$$

Proof. A differentiation of (4.120) gives

$$g_{\gamma_2\gamma_2} = e^{\bar{z}} + \sinh(\gamma_1) \sin(\gamma_2) + \cosh(\gamma_1) [(2 + \bar{z}) \sin(\gamma_2) + \gamma_2 \cos(\gamma_2)]. \quad (4.158)$$

Note that $\sin(\gamma_2) \geq 0$ and $\cos(\gamma_2) \geq 0$ when $\gamma_2 \in [2n\pi, 2n\pi + A_n(\bar{z})]$. Thus, the last two terms in (4.158) are nonnegative on B_n . From this, and the fact that $e^{\bar{z}} > 0$, it follows that (4.158) reduces to $g_{\gamma_2\gamma_2} > 0$, as claimed. \square

Remark: Recall that to prove Theorem 3 we must show the existence of only one solution $(\bar{\gamma}_1, \bar{\gamma}_2, \bar{z})$ to (4.123)-(4.124). As we mentioned at the beginning of this section, to find this solution we must put restrictions on the size of z . That is, some proofs hold only when z is sufficiently small.

The next goal is to show that $g_{\gamma_2}(\gamma_1^*, \gamma_2, \bar{z}) < 0$ on $\Gamma_{3,n}$. This is done in Lemma 17. Both the statement and proof of Lemma 17 require the next three technical lemmas which place a restriction on the size of z .

Lemma 19. *There exists $\delta_1 > 0$ such that*

$$e^z + \sqrt{e^{2z} - 1} - e^{\sqrt{z}} > 0 \text{ for all } 0 < z < \delta_1. \quad (4.159)$$

Proof. Let $z > 0$ and consider the \mathbf{C}^1 function $H(z) = e^z + \sqrt{e^{2z} - 1} - e^{\sqrt{z}}$. By Taylor's theorem, there exist functions $q_1(z), q_2(z), q_3(z)$ such that

$$\frac{q_1(z)}{\sqrt{z}} \rightarrow 0, \quad \frac{q_2(z)}{z} \rightarrow 0 \text{ and } \frac{q_3(z)}{\sqrt{z}} \rightarrow 0, \text{ as } z \rightarrow 0, \quad (4.160)$$

and

$$\begin{aligned} H(z) &= 1 + z + q_1(z) + \sqrt{1 + 2z - q_2(z) - 1} - \left[1 + \sqrt{z} + \frac{z}{2} + q_3(z)\right] \\ &= \frac{z}{2} + q_1(z) + \sqrt{2z - q_2(z)} - \sqrt{z} - q_3(z). \end{aligned} \quad (4.161)$$

It follows from (4.161) that there is $\delta_1 > 0$ such that, if $0 < z < \delta$, then

$$H(z) = \sqrt{z} \left\{ \frac{\sqrt{z}}{2} + \frac{q_1(z)}{\sqrt{z}} + \sqrt{2 - \frac{q_2(z)}{z}} - 1 - \frac{q_3(z)}{\sqrt{z}} \right\} > 0. \quad (4.162)$$

□

Lemma 20. *Let $0 < \bar{z} < \delta_1$ where δ_1 satisfies Lemma 19. Then*

$$\sqrt{\bar{z}} < \gamma_1^* = \ln(e^{\bar{z}} + \sqrt{e^{2\bar{z}} - 1}). \quad (4.163)$$

Proof. By the definition of γ_1^* , the inequality $\sqrt{\bar{z}} < \gamma_1^*$ is equivalent to

$$\sqrt{\bar{z}} < \ln(e^{\bar{z}} + \sqrt{e^{2\bar{z}} - 1}). \quad (4.164)$$

Recall that e^x is an increasing function. Thus, (4.164) is equivalent to

$$e^{\sqrt{\bar{z}}} < e^{\bar{z}} + \sqrt{e^{2\bar{z}} - 1}. \quad (4.165)$$

Let $0 < \bar{z} < \delta_1$. Then, (4.165) is a true statement by Lemma 19. Thus, $\sqrt{\bar{z}} < \gamma_1^*$, as claimed. □

We can now prove

Lemma 21. *Let $0 < \bar{z} < \delta_1$ where δ_1 satisfies Lemma 19 and let $n \geq 1$. If $(\gamma_1^*, \gamma_2) \in \Gamma_{3,n}$ and $f(\gamma_1^*, \gamma_2, \bar{z}) = 0$, then*

$$g_{\gamma_2}(\gamma_1^*, \gamma_2, \bar{z}) < 0. \quad (4.166)$$

Proof. First notice that $f(\gamma_1^*, \gamma_2, \bar{z}) = 0$ implies that

$$\gamma_1 e^{\bar{z}} - \gamma_1^* \cosh(\gamma_1^*) \cos(\gamma_2) = \bar{z} \sinh(\gamma_1^*) \cos(\gamma_2) - \gamma_2 \sinh(\gamma_1^*) \sin(\gamma_2). \quad (4.167)$$

Multiply g_{γ_2} by γ_1^* , and combine with (4.167), to obtain

$$\begin{aligned} g_{\gamma_2}(\gamma_1^*, \gamma_2, \bar{z}) &= (\bar{z} - (\gamma_1^*)^2) \sinh(\gamma_1^*) \cos(\gamma_2) - \gamma_2 \sinh(\gamma_1^*) \sin(\gamma_2) \\ &\quad + \gamma_1^* \cosh(\gamma_1^*) [\gamma_2 \sin(\gamma_2) - \bar{z} \cos(\gamma_2)]. \end{aligned} \quad (4.168)$$

By Lemma 20, $\gamma_1^* > \sqrt{\bar{z}}$ so that the first term of (4.168) is negative. The third term of (4.168) is also negative because of Lemma 16. Since the second term of (4.168) is always negative on B_n , we have that $g_{\gamma_2}(\gamma_1^*, \gamma_2, \bar{z}) < 0$. \square

Lemma 21 implies the desired result regarding the sign of $g(\gamma_1, \gamma_2, \bar{z})$ on $\Gamma_{3,n}$.

Proof of Lemma 17

Let $0 < \bar{z} < \delta_1$ where δ_1 satisfies Lemma 19. Observe that

$$g_{\gamma_2}(\gamma_1^*, 2n\pi, \bar{z}) = -\gamma_1^* \sinh(\gamma_1^*) - \bar{z} \cosh(\gamma_1^*) < 0. \quad (4.169)$$

By Lemma 21, $g(\gamma_1^*, \gamma_2, \bar{z})$ is decreasing. This completes the proof of Lemma 17.

We now continue with the completion of **Step III** of the proof of Theorem 3. In Lemma 17 we proved that

$$g(\gamma_1^*, \gamma_2(\gamma_1^*), \bar{z}) < 0. \quad (4.170)$$

By Lemma 14, the curve C_n , generated by $\gamma_2(\gamma_1)$ exits B_n at some point $(\hat{\gamma}_1, \hat{\gamma}_2) \in \Gamma_{1,n} \cup \Gamma_{4,n}$. It remains to show that $g(\hat{\gamma}_1, \hat{\gamma}_2, \bar{z}) > 0$. First, we consider the case where $(\hat{\gamma}_1, \hat{\gamma}_2) \in \Gamma_{4,n}$.

Analysis of $g(\gamma_1, \gamma_2, \bar{z})$ on $\Gamma_{4,n}$.

We consider the case where C_n exits B_n along $\Gamma_{4,n}$. We prove the following

Lemma 22. *Let $\bar{z} > 0$ and $n \geq 1$. If $(\gamma_1, \gamma_2) \in \Gamma_{4,n}$ then*

$$g(\gamma_1, \gamma_2, \bar{z}) > 0. \quad (4.171)$$

In particular, if C_n exits B_n at a point $(\hat{\gamma}_1, \hat{\gamma}_2) = (\hat{\gamma}_1, \gamma_2(\hat{\gamma}_1)) \in \Gamma_{4,n}$, then $\hat{\gamma}_2 = 2n\pi$ and

$$g(\hat{\gamma}_1, 2n\pi, \bar{z}) > 0. \quad (4.172)$$

Proof. By definition, $e^{\bar{z}} = \cosh(\gamma_1^*) > \cosh(\gamma_1)$. Therefore,

$$g(\gamma_1, 2n\pi, \bar{z}) = 2n\pi (e^{\bar{z}} - \cosh(\gamma_1)) > 0. \quad (4.173)$$

From this, and the definition of B_n , it follows that if C_n exits B_n at a point $(\hat{\gamma}_1, \hat{\gamma}_2) \in \Gamma_{4,n}$, then $\hat{\gamma}_2 = \gamma_2(\hat{\gamma}_1) = 2n\pi$ and

$$g(\hat{\gamma}_1, \gamma_2(\hat{\gamma}_1), \bar{z}) > 0. \quad (4.174)$$

This completes the proof of Lemma 22. □

Lastly, we consider the possibility that C_n exits B_n at a point $(\hat{\gamma}_1, \hat{\gamma}_2) \in \Gamma_{1,n}$.

Analysis of $g(\gamma_1, \gamma_2, \bar{z})$ on $\Gamma_{1,n}$

We consider the case that C_n exits B_n at a point $(\hat{\gamma}_1, \hat{\gamma}_2) \in \Gamma_{1,n}$. We prove

Lemma 23. Let $\bar{z} > 0$ and $n \geq 1$. There exists a value $\delta_4 > 0$ such that, if $0 < \bar{z} < \delta_4$ and $(\gamma_1, \gamma_2) \in \Gamma_{1,n}$, then

$$g(\gamma_1, \gamma_2, \bar{z}) > 0. \quad (4.175)$$

In particular, if C_n exits B_n at a point $(\hat{\gamma}_1, \hat{\gamma}_2) = (\hat{\gamma}_1, \gamma_2(\hat{\gamma}_1)) \in \Gamma_{1,n}$, then

$$g(\hat{\gamma}_1, \hat{\gamma}_2, \bar{z}) > 0. \quad (4.176)$$

The proof of Lemma 23 requires the following technical result:

Lemma 24. Fix $\bar{z} > 0$ and $n \geq 1$. There exists a value $\delta_2 > 0$ such that, if $0 < \bar{z} < \delta_2$, then

$$\frac{e^{\bar{z}} - \frac{1}{2} \left(e^{\epsilon\sqrt{\bar{z}}} + e^{-\epsilon\sqrt{\bar{z}}} \right)}{\bar{z}} > \frac{1}{2}. \quad (4.177)$$

Proof. Let

$$m(\bar{z}) = \frac{e^{\bar{z}} - \frac{1}{2} \left(e^{\epsilon\sqrt{\bar{z}}} + e^{-\epsilon\sqrt{\bar{z}}} \right)}{\bar{z}}. \quad (4.178)$$

By Taylor's theorem there exist functions $q_1(\bar{z})$ and $q_2(\bar{z})$ such that

$$\frac{q_i(\bar{z})}{\bar{z}} \rightarrow 0 \text{ as } \bar{z} \rightarrow 0, \quad i = 1, 2. \quad (4.179)$$

and

$$m(\bar{z}) = \frac{1}{\bar{z}} \left[1 + \bar{z} + q_1(\bar{z}) - \frac{1}{2} \left(1 + \epsilon\sqrt{\bar{z}} + \frac{\epsilon^2\bar{z}}{2} + 1 - \epsilon\sqrt{\bar{z}} + \frac{\epsilon^2\bar{z}}{2} + q_2(\bar{z}) \right) \right]. \quad (4.180)$$

By (4.179), there exists a value $\delta_2 > 0$ such that when $0 < \bar{z} < \delta_2$, we have

$$-\frac{\epsilon^2}{4} < \frac{q_1(\bar{z})}{\bar{z}} < \frac{\epsilon^2}{4} \quad \text{and} \quad -\frac{\epsilon^2}{4} < \frac{q_2(\bar{z})}{\bar{z}} < \frac{\epsilon^2}{4}.$$

Thus, if $0 < \bar{z} < \delta_2$,

$$\begin{aligned} m(\bar{z}) &= 1 + \frac{q_1(\bar{z})}{\bar{z}} - \frac{\epsilon^2}{2} - \frac{q_2(\bar{z})}{\bar{z}} \\ &> 1 - \frac{\epsilon^2}{4} - \frac{\epsilon^2}{2} - \frac{\epsilon^2}{4} \\ &= 1 - \epsilon^2 > 0. \end{aligned} \quad (4.181)$$

□

Proof of Lemma 23.

Fix $0 < \bar{z} < \delta_2$ where δ_2 satisfies Lemma 24 and suppose that $(\gamma_1, \gamma_2) \in \Gamma_{1,n}$. It follows that

$$\begin{aligned} g(\gamma_1, \gamma_2, \bar{z}) &= \gamma_2 e^{\bar{z}} - \epsilon \sqrt{\bar{z}} \sinh(\epsilon \sqrt{\bar{z}}) \sin(\gamma_2) \\ &\quad - \gamma_2 \cosh(\epsilon \sqrt{\bar{z}}) \cos(\gamma_2) - \bar{z} \cosh(\epsilon \sqrt{\bar{z}}) \sin(\gamma_2) \end{aligned}$$

Note that $-\sin(x) \geq -1$ and $-\cos(x) \geq -1$. Thus,

$$g(\gamma_1, \gamma_2, \bar{z}) \geq \gamma_2 e^{\bar{z}} - \epsilon \sqrt{\bar{z}} \sinh(\epsilon \sqrt{\bar{z}}) - \gamma_2 \cosh(\epsilon \sqrt{\bar{z}}) - \bar{z} \cosh(\epsilon \sqrt{\bar{z}}). \quad (4.182)$$

The definition of the hyperbolic cosine, and a rearrangement of terms, yields

$$g(\gamma_1, \gamma_2, \bar{z}) \geq \gamma_2 \left[e^{\bar{z}} - \frac{1}{2} \left(e^{\epsilon \sqrt{\bar{z}}} + e^{-\epsilon \sqrt{\bar{z}}} \right) \right] - \epsilon^2 \bar{z} \frac{\sinh(\epsilon \sqrt{\bar{z}})}{\epsilon \sqrt{\bar{z}}} - \bar{z} \cosh(\epsilon \sqrt{\bar{z}}). \quad (4.183)$$

Factor out \bar{z} and obtain

$$g(\gamma_1, \gamma_2, \bar{z}) \geq \bar{z} \left[\gamma_2 \frac{e^{\bar{z}} - \frac{1}{2} \left(e^{\epsilon \sqrt{\bar{z}}} + e^{-\epsilon \sqrt{\bar{z}}} \right)}{\bar{z}} - \epsilon^2 \frac{\sinh(\epsilon \sqrt{\bar{z}})}{\epsilon \sqrt{\bar{z}}} - \cosh(\epsilon \sqrt{\bar{z}}) \right]. \quad (4.184)$$

By Lemma 24, it follows that

$$g(\gamma_1, \gamma_2, \bar{z}) > \bar{z} \left[\gamma_2 \frac{1}{2} - \epsilon^2 \frac{\sinh(\epsilon \sqrt{\bar{z}})}{\epsilon \sqrt{\bar{z}}} - \cosh(\epsilon \sqrt{\bar{z}}) \right]. \quad (4.185)$$

Since $2\pi \leq 2n\pi \leq \gamma_2$ it follows that

$$g(\gamma_1, \gamma_2, \bar{z}) > \bar{z} \left[\pi - \epsilon^2 \frac{\sinh(\epsilon \sqrt{\bar{z}})}{\epsilon \sqrt{\bar{z}}} - \cosh(\epsilon \sqrt{\bar{z}}) \right]. \quad (4.186)$$

Note that

$$\frac{\sinh(\epsilon \sqrt{\bar{z}})}{\epsilon \sqrt{\bar{z}}} \rightarrow 1 \text{ and } \cosh(\epsilon \sqrt{\bar{z}}) \rightarrow 1 \text{ as } \bar{z} \rightarrow 0. \quad (4.187)$$

Thus, there is a $\delta_3 > 0$ such that $0 < \epsilon \sqrt{\bar{z}} < \delta_3$ implies

$$\pi - \epsilon^2 \frac{\sinh(\epsilon \sqrt{\bar{z}})}{\epsilon \sqrt{\bar{z}}} - \cosh(\epsilon \sqrt{\bar{z}}) > 0. \quad (4.188)$$

Let $\delta_4 = \min(\delta_2, \frac{\delta_3^2}{\epsilon^2})$ and suppose that $0 < \bar{z} < \delta_4$. Then,

$$g(\gamma_1, \gamma_2, \bar{z}) > 0 \tag{4.189}$$

as desired. This completes the proof of Lemma 23.

Summary and Conclusion

Let $\delta = \min(\delta_1, \delta_4)$. Let $0 < \bar{z} < \delta$, $n \geq 1$ and $0 < \epsilon < \sqrt{1/2}$. By Lemma 14 there exists $\gamma_2(\gamma_1) \in \mathbf{C}^1([\epsilon\sqrt{\bar{z}}, \gamma_1^*])$ such that $\gamma_2(\gamma_1) \in [2n\pi, 2n\pi + A_n(\bar{z})]$ and

$$f(\gamma_1, \gamma_2(\gamma_1), \bar{z}) = 0. \tag{4.190}$$

An important consequence of Lemma 14 is that $\gamma_2(\gamma_1)$ generates a curve $C_n \subset B_n$ that enters B_n at $(\gamma_1^*, \gamma_2^*) \in \Gamma_{3,n}$ and exists B_n at a point $(\hat{\gamma}_1, \hat{\gamma}_2) \in \Gamma_{1,n} \cup \Gamma_{4,n}$. In Lemmas 17,22,23 we showed that $g(\gamma_1^*, \gamma_2^*) < 0$ while $g(\hat{\gamma}_1, \hat{\gamma}_2, \bar{z}) > 0$. Since $g(\gamma_1, \gamma_2, \bar{z})$ is continuous in each variable, the intermediate value theorem guarantees a point $(\bar{\gamma}_1, \bar{\gamma}_2) = (\bar{\gamma}_1, \gamma_2(\bar{\gamma}_1)) \in B_n$ with the property that

$$f(\bar{\gamma}_1, \bar{\gamma}_2, \bar{z}) = 0 \quad \text{and} \quad g(\bar{\gamma}_1, \bar{\gamma}_2, \bar{z}) = 0. \tag{4.191}$$

Furthermore, for each $n \geq 1$, the solution $(\bar{\gamma}_1, \bar{\gamma}_2)$, at $z = \bar{z}$, of the non linear algebra problem (4.123)-(4.124) is an initial value for the ODE problem (4.127)-(4.128)-(4.129). This completes the proof of Theorem 3.

4.3.4 Infinitely many $\mathbf{C}^1((0, \infty))$ solutions of the ODEs.

In this section we address the issue raised at the beginning of Section 4.3.2. That is, we prove the existence of infinitely many branches of functions, $\gamma_1^n(z)$ and $\gamma_2^n(z)$, which satisfy, for each $n \geq 1$,

$$f(\gamma_1^n(z), \gamma_2^n(z), z) = 0 \quad \text{and} \quad g(\gamma_1^n(z), \gamma_2^n(z), z) = 0, \quad \text{for all } z > 0. \tag{4.192}$$

Remark: For the remainder of this section the superscript n denotes the solution corresponding to the natural number $n \geq 1$.

We prove the following result:

Theorem 4. Fix $0 < \bar{z} < \delta$, where δ satisfies Theorem 3, and $n \geq 1$. Let J denote the Jacobian matrix of $F = (f, g)$. There are functions

$$\gamma_1^n(z) \in \mathbf{C}^1((0, \infty)) \text{ and } \gamma_2^n(z) \in \mathbf{C}^1((0, \infty)) \quad (4.193)$$

with initial values

$$(\gamma_1^n(\bar{z}), \gamma_2^n(\bar{z})) = (\bar{\gamma}_1^n, \bar{\gamma}_2^n) \in B_n, \quad (4.194)$$

such that

$$f(\gamma_1^n(z), \gamma_2^n(z), z) = 0 \text{ and } g(\gamma_1^n(z), \gamma_2^n(z), z) = 0, \text{ for all } z > 0, \quad (4.195)$$

and

$$(\gamma_1^n(z), \gamma_2^n(z)) \in D_n(z) \text{ for all } z > 0, \quad (4.196)$$

where (see Figure 8)

$$D_n(z) = (0, \gamma_1^*(z)) \times (2n\pi, 2n\pi + A_n(z)). \quad (4.197)$$

Furthermore,

$$\text{Det}(J) = \left(\frac{\partial f}{\partial \gamma_1^n} \right)^2 + \left(\frac{\partial g}{\partial \gamma_1^n} \right)^2 > 0, \text{ for all } z > 0, \quad (4.198)$$

$$\frac{d\gamma_1^n}{dz} = \frac{1}{\text{Det}(J)} \left(\frac{\partial f}{\partial \gamma_1^n} \frac{\partial f}{\partial z} - \frac{\partial g}{\partial \gamma_2^n} \frac{\partial g}{\partial z} \right), \text{ for all } z > 0, \quad (4.199)$$

and

$$\frac{d\gamma_2^n}{dz} = \frac{1}{\text{Det}(J)} \left(\frac{\partial g}{\partial \gamma_1^n} \frac{\partial f}{\partial z} - \frac{\partial f}{\partial \gamma_1^n} \frac{\partial g}{\partial z} \right), \text{ for all } z > 0. \quad (4.200)$$

A direct, and important, consequence of Theorem 4 is the existence of infinitely many branches of eigenvalues:

Theorem 5. For each $n \geq 1$, let $(\gamma_1^n(z), \gamma_2^n(z))$ solve Theorem 4. The corresponding eigenvalues are given by

$$\lambda^n(z) = \lambda_1^n(z) + i\lambda_2^n(z) = \frac{\sigma^4 ((\gamma_1^n)^2 - (\gamma_2^n)^2) - \mu^2 \theta^2}{2\theta^2 \sigma^2} + i \frac{\gamma_1^n \gamma_2^n \sigma^2}{\theta^2}, \quad (4.201)$$

and are continuously differentiable for $z \in (0, \infty)$.

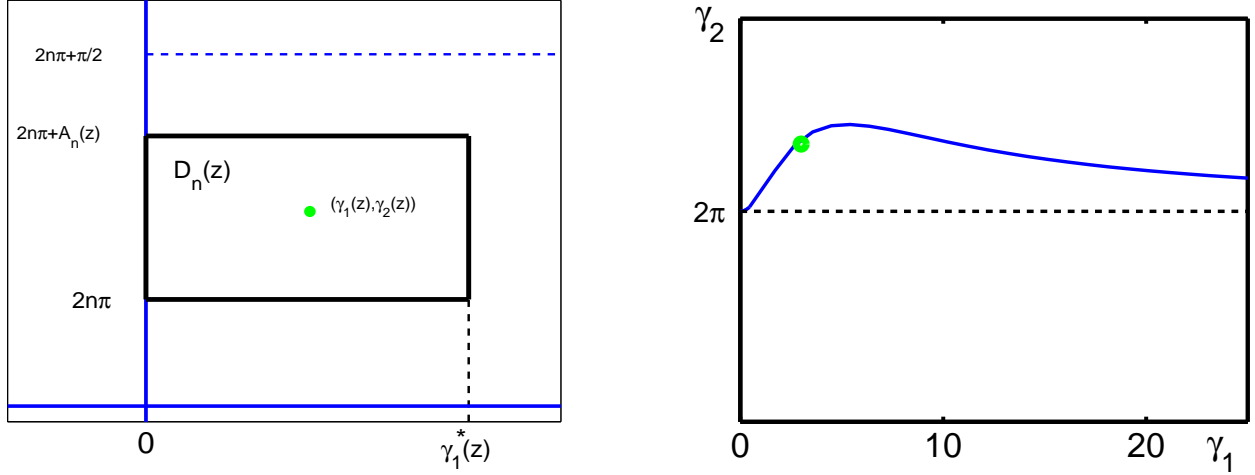


Figure 8: **Left Panel:** $D_n(z)$ is the rectangle defined in (4.197). As z increases or decreases, the size of $D_n(z)$ increases or decreases. Lemma 27 proves that the large dot, which represents $(\gamma_1^n(z), \gamma_2^n(z))$, is contained in the interior of $D_n(z)$ for all $z > 0$. **Right Panel:** As z increases and decreases the green dot generates the curve in the (γ_1^n, γ_2^n) plane.

The proof of Theorem 5 follows directly from formula (4.115) and Theorem 4. The proof of Theorem 4 requires Lemmas 25, 26 and 27, together with an application of the implicit function theorem. We prove Theorem 4 immediately following the proof of Lemma 27.

The first step is to let J denote the Jacobian matrix in the statement of Theorem 4. In Lemma 25 we prove that the determinant of J is nonzero at the point $(\bar{\gamma}_1^n, \bar{\gamma}_2^n, \bar{z})$.

Lemma 25. *Let $0 < z < \delta$, where δ satisfies Theorem 3, and $n \geq 1$. Suppose that $(\gamma_1^n, \gamma_2^n) \in B_n$, then*

$$\text{Det}(J) = \left(\frac{\partial f}{\partial \gamma_1^n} \right)^2 + \left(\frac{\partial g}{\partial \gamma_1^n} \right)^2 > 0, \text{ for all } z \in (0, \delta). \quad (4.202)$$

Proof. Note that

$$J = \begin{pmatrix} \frac{\partial f}{\partial \gamma_1^n} & \frac{\partial f}{\partial \gamma_2^n} \\ \frac{\partial g}{\partial \gamma_1^n} & \frac{\partial g}{\partial \gamma_2^n} \end{pmatrix}. \quad (4.203)$$

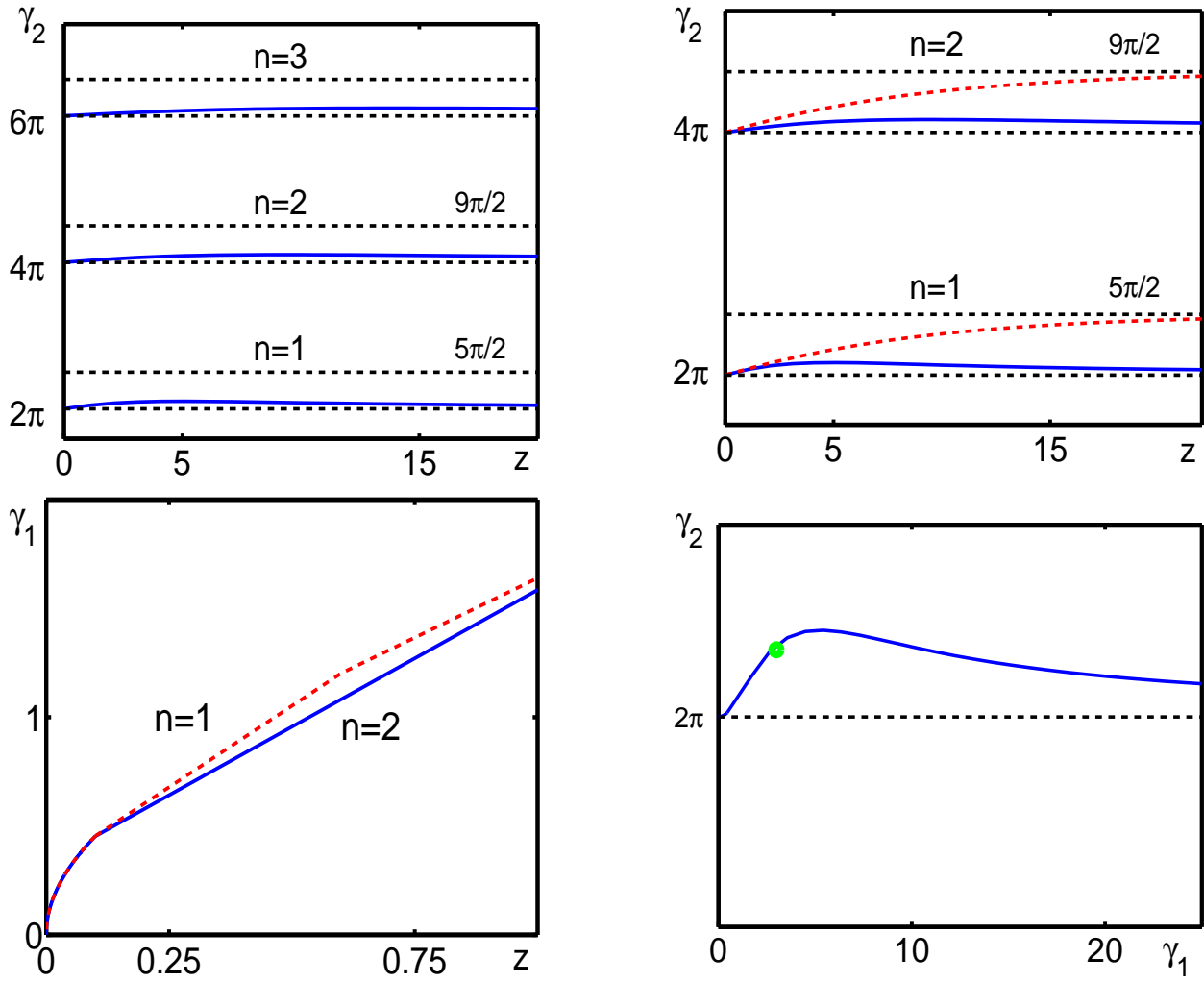


Figure 9: **Top Left:** The function $\gamma_2^n(z)$ for $n = 1$, $n = 2$ and $n = 3$ (solid blue curves). **Top Right:** The function $\gamma_2^n(z)$ for $n = 1$ and $n = 2$ (solid blue curves). The functions $A_1(z)$ and $A_2(z)$ are represented by the dotted red lines. **Bottom Left:** The function $\gamma_1^n(z)$ for $n = 1$ and $n = 2$. **Bottom Right:** The function $\gamma_2^n(z)$ plotted against $\gamma_1^n(z)$ when $n = 1$. To reproduce the figures see Section [A.3](#)

A calculation shows that

$$\frac{\partial f}{\partial \gamma_1^n} = \frac{\partial g}{\partial \gamma_2^n} \quad \text{and} \quad \frac{\partial f}{\partial \gamma_2^n} = -\frac{\partial g}{\partial \gamma_1^n}. \quad (4.204)$$

Thus, $\text{Det}(J) = \left(\frac{\partial f}{\partial \gamma_1^n}\right)^2 + \left(\frac{\partial g}{\partial \gamma_1^n}\right)^2$ where

$$\frac{\partial f}{\partial \gamma_1^n} = -(1+z) \cosh(\gamma_1^n) \cos(\gamma_2^n) - \gamma_1^n \sinh(\gamma_1^n) \cos(\gamma_2^n) + \gamma_2^n \cosh(\gamma_1^n) \sin(\gamma_2^n) + e^z \quad (4.205)$$

and

$$\frac{\partial g}{\partial \gamma_1^n} = (1+z) \sinh(\gamma_1^n) \sin(\gamma_2^n) + \gamma_1^n \cosh(\gamma_1^n) \sin(\gamma_2^n) + \gamma_2^n \sinh(\gamma_1^n) \cos(\gamma_2^n). \quad (4.206)$$

Notice that all three terms in (4.206) are nonnegative since $\gamma_2^n \in (2n\pi, 2n\pi + A_n(z))$. Since all three can not be 0 for the same γ_1^n and γ_2^n we conclude that $\frac{\partial g}{\partial \gamma_1^n} > 0$. Furthermore, $\text{Det}(J) > 0$. \square

An important consequence of Lemma 25 is the following

Lemma 26. *Fix $0 < \bar{z} < \delta$, where δ satisfies Theorem 3, and $n \geq 1$. Then, there exists $\rho > 0$ and functions $\gamma_1^n(z) \in \mathbf{C}^1((\bar{z} - \rho, \bar{z} + \rho))$ and $\gamma_2^n(z) \in \mathbf{C}^1((\bar{z} - \rho, \bar{z} + \rho))$ where*

$$f(\gamma_1^n(z), \gamma_2^n(z), z) = g(\gamma_1^n(z), \gamma_2^n(z), z) = 0, \quad \text{for all } z \in (\bar{z} - \rho, \bar{z} + \rho). \quad (4.207)$$

Furthermore, the functions $\gamma_1^n(z)$ and $\gamma_2^n(z)$ are determined by the equations

$$\frac{d\gamma_1^n}{dz} = \frac{1}{\text{Det}(J)} \left(\frac{\partial f}{\partial \gamma_1^n} \frac{\partial g}{\partial z} - \frac{\partial g}{\partial \gamma_2^n} \frac{\partial f}{\partial z} \right) \quad (4.208)$$

and

$$\frac{d\gamma_2^n}{dz} = \frac{1}{\text{Det}(J)} \left(\frac{\partial g}{\partial \gamma_1^n} \frac{\partial f}{\partial z} - \frac{\partial f}{\partial \gamma_1^n} \frac{\partial g}{\partial z} \right). \quad (4.209)$$

Proof. By Theorem 3 there exist $(\bar{\gamma}_1^n, \bar{\gamma}_2^n) \in B_n$ such that (4.191) holds. A differentiation of (4.191) with respect to z yields

$$\frac{\partial f}{\partial \gamma_1^n} \frac{d\gamma_1^n}{dz} + \frac{\partial f}{\partial \gamma_2^n} \frac{d\gamma_2^n}{dz} + \frac{\partial f}{\partial z} = 0 \quad (4.210)$$

$$\frac{\partial g}{\partial \gamma_1^n} \frac{d\gamma_1^n}{dz} + \frac{\partial g}{\partial \gamma_2^n} \frac{d\gamma_2^n}{dz} + \frac{\partial g}{\partial z} = 0. \quad (4.211)$$

By Lemma 25, we can solve (4.210) and (4.211) for $\frac{d\gamma_1^n}{dz}$ and $\frac{d\gamma_2^n}{dz}$ and obtain equations (4.208)-(4.208). By the implicit function theorem, there exists $\rho > 0$ such that

$$\gamma_1^n(z) \in \mathbf{C}^1((\bar{z} - \rho, \bar{z} + \rho)) \text{ and } \gamma_2^n(z) \in \mathbf{C}^1((\bar{z} - \rho, \bar{z} + \rho)).$$

□

It remains to prove that $\gamma_1^n(z) \in \mathbf{C}^1((0, \infty))$ and $\gamma_2^n(z) \in \mathbf{C}^1((0, \infty))$. We need the following

Lemma 27. *Let $0 < \bar{z} < \delta$, where δ satisfies Theorem 3, and $n \geq 1$. Then*

$$0 < \gamma_1^n(z) < \gamma_1^*(z) \text{ for all } z \in (0, \infty), \quad (4.212)$$

and

$$2n\pi < \gamma_2^n(z) < 2n\pi + A_n(z) \text{ for all } z \in (0, \infty). \quad (4.213)$$

Proof. By Theorem 3, $(\gamma_1^n(\bar{z}), \gamma_2^n(\bar{z})) \in (0, \gamma_1^*(\bar{z})) \times (2n\pi, 2n\pi + A_n(\bar{z}))$. Recall that

$$D_n(z) = (0, \gamma_1^*(z)) \times (2n\pi, 2n\pi + A_n(z)). \quad (4.214)$$

For contradiction, assume that there exists $\beta > 0$ such that

$$(\gamma_1^n(\beta), \gamma_2^n(\beta)) \in \partial D_n(\beta) \quad (4.215)$$

and

$$f(\gamma_1^n(\beta), \gamma_2^n(\beta), \beta) = 0 = g(\gamma_1^n(\beta), \gamma_2^n(\beta), \beta). \quad (4.216)$$

There are sixteen cases to consider:

Case 1a: There exists $0 < \beta < \bar{z}$ such that

$$(\gamma_1^n(z), \gamma_2^n(z)) \in D_n \text{ for all } z \in (\beta, \bar{z}), \quad (4.217)$$

and (4.215) is given by

$$(\gamma_1^n(\beta), \gamma_2^n(\beta)) = (0, 2n\pi + A_n(\beta)). \quad (4.218)$$

Notice that

$$\begin{aligned} g(\gamma_1^n(\beta), \gamma_2^n(\beta), \beta) &= (2n\pi + A_n(\beta))e^\beta - (2n\pi + A_n(\beta)) \cos(A_n(\beta)) - \beta \sin(A_n(\beta)) \\ &> (2n\pi + A_n(\beta))e^\beta - (2n\pi + A_n(\beta)) - \beta A_n(\beta) \\ &> A_n(\beta) (e^\beta - (1 + \beta)) > 0, \end{aligned}$$

contradicting (4.216). We conclude that (4.217) and (4.218) cannot hold.

Case 1b: There exists $0 < \bar{z} < \beta$ such that

$$(\gamma_1^n(z), \gamma_2^n(z)) \in D_n \text{ for all } z \in (\bar{z}, \beta), \quad (4.219)$$

and (4.215) is given by

$$(\gamma_1^n(\beta), \gamma_2^n(\beta)) = (0, 2n\pi + A_n(\beta)). \quad (4.220)$$

Notice that

$$\begin{aligned} g(\gamma_1^n(\beta), \gamma_2^n(\beta), \beta) &= (2n\pi + A_n(\beta))e^\beta - (2n\pi + A_n(\beta)) \cos(A_n(\beta)) - \beta \sin(A_n(\beta)) \\ &> (2n\pi + A_n(\beta))e^\beta - (2n\pi + A_n(\beta)) - \beta A_n(\beta) \\ &> A_n(\beta) (e^\beta - (1 + \beta)) > 0, \end{aligned}$$

contradicting (4.216). We conclude that (4.219) and (4.220) cannot hold.

Case 2a: There exists $0 < \beta < \bar{z}$ such that

$$(\gamma_1^n(z), \gamma_2^n(z)) \in D_n \text{ for all } z \in (\beta, \bar{z}) \quad (4.221)$$

and (4.215) is given by

$$(\gamma_1^n(\beta), \gamma_2^n(\beta)) = (0, \gamma_2^n(\beta)), \quad \gamma_2^n(\beta) \in (2n\pi, 2n\pi + A_n(\beta)). \quad (4.222)$$

Notice that

$$\begin{aligned}
g(\gamma_1^n(\beta), \gamma_2^n(\beta), \beta) &= \gamma_2^n(\beta)e^\beta - \gamma_2^n(\beta) \cos(\gamma_2^n(\beta)) - \beta \sin(\gamma_2^n(\beta)) \\
&> \gamma_2^n(\beta)e^\beta - \gamma_2^n(\beta) - \beta\gamma_2^n(\beta) \\
&> \gamma_2^n(\beta) (e^\beta - (1 + \beta)) > 0,
\end{aligned}$$

contradicting (4.216). We conclude that (4.221) and (4.222) cannot hold.

Case 2b: There exists $0 < \beta < \bar{z}$ such that

$$(\gamma_1^n(z), \gamma_2^n(z)) \in D_n \text{ for all } z \in (\beta, \bar{z}) \quad (4.223)$$

and (4.215) is given by

$$(\gamma_1^n(\beta), \gamma_2^n(\beta)) = (0, \gamma_2^n(\beta)), \quad \gamma_2^n(\beta) \in (2n\pi, 2n\pi + A_n(\beta)). \quad (4.224)$$

Notice that

$$\begin{aligned}
g(\gamma_1^n(\beta), \gamma_2^n(\beta), \beta) &= \gamma_2^n(\beta)e^\beta - \gamma_2^n(\beta) \cos(\gamma_2^n(\beta)) - \beta \sin(\gamma_2^n(\beta)) \\
&> \gamma_2^n(\beta)e^\beta - \gamma_2^n(\beta) - \beta\gamma_2^n(\beta) \\
&> \gamma_2^n(\beta) (e^\beta - (1 + \beta)) > 0,
\end{aligned}$$

contradicting (4.216). We conclude that (4.223) and (4.224) cannot hold.

Case 3a: There exists $0 < \beta < \bar{z}$ such that

$$(\gamma_1^n(z), \gamma_2^n(z)) \in D_n \text{ for all } z \in (\beta, \bar{z}) \quad (4.225)$$

and (4.215) is given by

$$(\gamma_1^n(\beta), \gamma_2^n(\beta)) = (0, 2n\pi). \quad (4.226)$$

Notice that

$$\begin{aligned}
g(\gamma_1^n(\beta), \gamma_2^n(\beta), \beta) &= 2n\pi e^\beta - 2n\pi \\
&= 2n\pi (e^\beta - 1) > 0,
\end{aligned}$$

contradicting (4.216). We conclude that (4.225) and (4.226) cannot hold.

Case 2b: There exists $0 < \beta < \bar{z}$ such that

$$(\gamma_1^n(z), \gamma_2^n(z)) \in D_n \text{ for all } z \in (\beta, \bar{z}) \quad (4.227)$$

and (4.215) is given by

$$(\gamma_1^n(\beta), \gamma_2^n(\beta)) = (0, 2n\pi). \quad (4.228)$$

Notice that

$$\begin{aligned} g(\gamma_1^n(\beta), \gamma_2^n(\beta), \beta) &= 2n\pi e^\beta - 2n\pi \\ &= 2n\pi (e^\beta - 1) > 0, \end{aligned}$$

contradicting (4.216). We conclude that (4.227) and (4.228) cannot hold.

Case 4a: There exists $0 < \beta < \bar{z}$ such that

$$(\gamma_1^n(z), \gamma_2^n(z)) \in D_n \text{ for all } z \in (\beta, \bar{z}) \quad (4.229)$$

and (4.215) is given by

$$(\gamma_1^n(\beta), \gamma_2^n(\beta)) = (\gamma_1^n(\beta), 2n\pi), \quad \gamma_1^n(\beta) \in (0, \gamma_1^*(\beta)). \quad (4.230)$$

Recall that

$$e^\beta - \cosh(\gamma_1^*(\beta)) > 0 \text{ since } \gamma_1^n(\beta) \in (0, \gamma_1^*(\beta)). \quad (4.231)$$

Therefore,

$$\begin{aligned} g(\gamma_1^n(\beta), \gamma_2^n(\beta), \beta) &= 2n\pi e^\beta - 2n\pi \cosh(\gamma_1^*(\beta)) \\ &= 2n\pi (e^\beta - \cosh(\gamma_1^*(\beta))) > 0, \end{aligned}$$

contradicting (4.216). We conclude that (4.229) and (4.230) cannot hold.

Case 4b: There exists $0 < \beta < \bar{z}$ such that

$$(\gamma_1^n(z), \gamma_2^n(z)) \in D_n \text{ for all } z \in (\beta, \bar{z}) \quad (4.232)$$

and (4.215) is given by

$$(\gamma_1^n(\beta), \gamma_2^n(\beta)) = (0, 2n\pi). \quad (4.233)$$

Recall that

$$e^\beta - \cosh(\gamma_1^*(\beta)) > 0 \text{ since } \gamma_1^n(\beta) \in (0, \gamma_1^*(\beta)). \quad (4.234)$$

Therefore,

$$\begin{aligned} g(\gamma_1^n(\beta), \gamma_2^n(\beta), \beta) &= 2n\pi e^\beta - 2n\pi \cosh(\gamma_1^*(\beta)) \\ &= 2n\pi (e^\beta - \cosh(\gamma_1^*(\beta))) > 0, \end{aligned}$$

contradicting (4.216). We conclude that (4.232) and (4.233) cannot hold.

Case 5a: There exists $0 < \beta < \bar{z}$ such that

$$(\gamma_1^n(z), \gamma_2^n(z)) \in D_n \text{ for all } z \in (\beta, \bar{z}) \quad (4.235)$$

and (4.215) is given by

$$(\gamma_1^n(\beta), \gamma_2^n(\beta)) = (\gamma_1^*(\beta), 2n\pi). \quad (4.236)$$

Recall from Lemma 17 that $g(\gamma_1^*(z), \gamma_2^n(z), z) < 0$ for all $z > 0$ and $\gamma_2^n(z) \in [2n\pi, 2n\pi + A_n(z)]$, contradicting (4.216). We conclude that (4.235) and (4.236) cannot hold.

Case 5b: There exists $0 < \beta < \bar{z}$ such that

$$(\gamma_1^n(z), \gamma_2^n(z)) \in D_n \text{ for all } z \in (\beta, \bar{z}) \quad (4.237)$$

and (4.215) is given by

$$(\gamma_1^n(\beta), \gamma_2^n(\beta)) = (\gamma_1^*(\beta), 2n\pi). \quad (4.238)$$

Recall from Lemma 17 that $g(\gamma_1^*(z), \gamma_2^n(z), z) < 0$ for all $z > 0$ and $\gamma_2^n(z) \in [2n\pi, 2n\pi + A_n(z)]$, contradicting (4.216). We conclude that (4.237) and (4.238) cannot hold.

Case 6a: There exists $0 < \beta < \bar{z}$ such that

$$(\gamma_1^n(z), \gamma_2^n(z)) \in D_n \text{ for all } z \in (\beta, \bar{z}) \quad (4.239)$$

and (4.215) is given by

$$(\gamma_1^n(\beta), \gamma_2^n(\beta)) = (\gamma_1^*(\beta), \gamma_2^n(\beta)) \quad \gamma_2^n(\beta) \in (2n\pi, 2n\pi + A_n(\bar{z})). \quad (4.240)$$

Recall from Lemma 17 that $g(\gamma_1^*(z), \gamma_2^n(z), z) < 0$ for all $z > 0$ and $\gamma_2^n(z) \in [2n\pi, 2n\pi + A_n(z)]$, contradicting (4.216). We conclude that (4.239) and (4.240) cannot hold.

Case 6b: There exists $0 < \beta < \bar{z}$ such that

$$(\gamma_1^n(z), \gamma_2^n(z)) \in D_n \text{ for all } z \in (\beta, \bar{z}) \quad (4.241)$$

and (4.215) is given by

$$(\gamma_1^n(\beta), \gamma_2^n(\beta)) = (\gamma_1^*(\beta), \gamma_2^n(\beta)) \quad \gamma_2^n(\beta) \in (2n\pi, 2n\pi + A_n(\bar{z})). \quad (4.242)$$

Recall from Lemma 17 that $g(\gamma_1^*(z), \gamma_2^n(z), z) < 0$ for all $z > 0$ and $\gamma_2^n(z) \in [2n\pi, 2n\pi + A_n(z)]$, contradicting (4.216). We conclude that (4.241) and (4.242) cannot hold.

Case 7a: There exists $0 < \beta < \bar{z}$ such that

$$(\gamma_1^n(z), \gamma_2^n(z)) \in D_n \text{ for all } z \in (\beta, \bar{z}) \quad (4.243)$$

and (4.215) is given by

$$(\gamma_1^n(\beta), \gamma_2^n(\beta)) = (\gamma_1^*(\beta), 2n\pi + A_n(\bar{z})) \quad (4.244)$$

Recall from Lemma 17 that $g(\gamma_1^*(z), \gamma_2^n(z), z) < 0$ for all $z > 0$ and $\gamma_2^n(z) \in [2n\pi, 2n\pi + A_n(z)]$, contradicting (4.216). We conclude that (4.243) and (4.244) cannot hold.

Case 7b: There exists $0 < \beta < \bar{z}$ such that

$$(\gamma_1^n(z), \gamma_2^n(z)) \in D_n \text{ for all } z \in (\beta, \bar{z}) \quad (4.245)$$

and (4.215) is given by

$$(\gamma_1^n(\beta), \gamma_2^n(\beta)) = (\gamma_1^*(\beta), 2n\pi + A_n(\bar{z})). \quad (4.246)$$

Recall from Lemma 17 that $g(\gamma_1^*(z), \gamma_2^n(z), z) < 0$ for all $z > 0$ and $\gamma_2^n(z) \in [2n\pi, 2n\pi + A_n(z)]$, contradicting (4.216). We conclude that (4.245) and (4.246) cannot hold.

Case 8a: There exists $0 < \beta < \bar{z}$ such that

$$(\gamma_1^n(z), \gamma_2^n(z)) \in D_n \text{ for all } z \in (\beta, \bar{z}), \quad (4.247)$$

and (4.215) is given by

$$(\gamma_1^n(\beta), \gamma_2^n(\beta)) = (\gamma_1^n(\beta), 2n\pi + A_n(\beta)), \quad \gamma_1^n(\beta) \in (0, \gamma_1^*(\beta)). \quad (4.248)$$

Recall from the definition of $A_n(z)$ that

$$(2n\pi + A_n(z)) \sin(A_n(z)) - \beta \cos(A_n(z)) = 0. \quad (4.249)$$

Therefore,

$$\begin{aligned} f(\gamma_1^n(\beta), \gamma_2^n(\beta), \beta) &= \gamma_1^n(\beta) e^\beta - \gamma_1^n(\beta) \cosh(\gamma_1^n(\beta)) \cos(A_n(\beta)) \\ &\quad + \sinh(\gamma_1^n(\beta)) [(2n\pi + A_n(z)) \sin(A_n(z)) - \beta \cos(A_n(z))] \\ &= \gamma_1^n(\beta) [e^\beta - \cosh(\gamma_1^n(\beta)) \cos(A_n(z))] \\ &> \gamma_1^n(\beta) (e^\beta - \cosh(\gamma_1^n(\beta))) > 0, \end{aligned}$$

contradicting (4.216). We conclude that (4.247) and (4.248) cannot hold.

Case 8b: There exists $0 < \bar{z} < \beta$ such that

$$(\gamma_1^n(z), \gamma_2^n(z)) \in D_n \text{ for all } z \in (\bar{z}, \beta), \quad (4.250)$$

and (4.215) is given by

$$(\gamma_1^n(\beta), \gamma_2^n(\beta)) = (0, 2n\pi + A_n(\beta)). \quad (4.251)$$

Recall from the definition of $A_n(z)$ that

$$(2n\pi + A_n(z)) \sin(A_n(z)) - \beta \cos(A_n(z)) = 0. \quad (4.252)$$

Therefore,

$$\begin{aligned} f(\gamma_1^n(\beta), \gamma_2^n(\beta), \beta) &= \gamma_1^n(\beta) e^\beta - \gamma_1^n(\beta) \cosh(\gamma_1^n(\beta)) \cos(A_n(\beta)) \\ &\quad + \sinh(\gamma_1^n(\beta)) [(2n\pi + A_n(z)) \sin(A_n(z)) - \beta \cos(A_n(z))] \\ &= \gamma_1^n(\beta) [e^\beta - \cosh(\gamma_1^n(\beta)) \cos(A_n(z))] \\ &> \gamma_1^n(\beta) (e^\beta - \cosh(\gamma_1^n(\beta))) > 0, \end{aligned}$$

contradicting (4.216). We conclude that (4.250) and (4.251) cannot hold. \square

We can now complete the proof of Theorem 4.

Proof of Theorem 4. First, note that the Jacobian of $F = (f, g)$ is

$$J = \begin{pmatrix} \frac{\partial f}{\partial \gamma_1^n} & \frac{\partial f}{\partial \gamma_2^n} \\ \frac{\partial g}{\partial \gamma_1^n} & \frac{\partial g}{\partial \gamma_2^n} \end{pmatrix}. \quad (4.253)$$

A calculation shows that

$$\frac{\partial f}{\partial \gamma_1^n} = \frac{\partial g}{\partial \gamma_2^n} \quad \text{and} \quad \frac{\partial f}{\partial \gamma_2^n} = -\frac{\partial g}{\partial \gamma_1^n}. \quad (4.254)$$

Thus, $\text{Det}(J) = \left(\frac{\partial f}{\partial \gamma_1^n}\right)^2 + \left(\frac{\partial g}{\partial \gamma_1^n}\right)^2$ where

$$\frac{\partial f}{\partial \gamma_1^n} = -(1+z) \cosh(\gamma_1^n) \cos(\gamma_2^n) - \gamma_1^n \sinh(\gamma_1^n) \cos(\gamma_2^n) + \gamma_2^n \cosh(\gamma_1^n) \sin(\gamma_2^n) + e^z \quad (4.255)$$

and

$$\frac{\partial g}{\partial \gamma_1^n} = (1+z) \sinh(\gamma_1^n) \sin(\gamma_2^n) + \gamma_1^n \cosh(\gamma_1^n) \sin(\gamma_2^n) + \gamma_2^n \sinh(\gamma_1^n) \cos(\gamma_2^n). \quad (4.256)$$

By Lemma 27, $\gamma_1^n \in (0, \gamma_1^*)$ and $\gamma_2^n \in (2n\pi, 2n\pi + A_n(z))$. It follows that all three terms in (4.256) are positive and furthermore, $\text{Det}(J) > 0$. An application of the implicit function theorem shows that

$$\gamma_1^n(z) \in \mathbf{C}^1((0, \infty)) \quad \text{and} \quad \gamma_2^n(z) \in \mathbf{C}^1((0, \infty)) \quad (4.257)$$

with (4.199) and (4.200) holding for all $z > 0$. (See Section 4.3.2 for the derivation.) This completes the proof of Theorem 4.

Next, we study the functions $\gamma_1^n(z)$ and $\gamma_2^n(z)$ when $z > 0$ is near zero.

4.3.5 Properties of $\lambda_1^n(z)$ and $\lambda_2^n(z)$ as $z = \frac{\mu\theta}{\sigma^2} \rightarrow 0^+$

In this section we investigate the behavior of the eigenvalues, $\lambda_1^n(z)$ and $\lambda_2^n(z)$, as $z = \frac{\mu\theta}{\sigma^2} \rightarrow 0^+$, where

$$\lambda(z) = \lambda_1^n(z) + i\lambda_2^n(z) = \frac{\sigma^4((\gamma_1^n)^2 - (\gamma_2^n)^2) - \mu^2\theta^2}{2\theta^2\sigma^2} + i\frac{\gamma_1^n\gamma_2^n\sigma^2}{\theta^2}. \quad (4.258)$$

Therefore, we first study the functions $\gamma_1^n(z)$ and $\gamma_2^n(z)$ as $z \rightarrow 0^+$. Our first of two results in this subsection is

Theorem 6. (Behavior of $\gamma_1^n(z)$ and $\gamma_2^n(z)$ as $z \rightarrow 0^+$.) *Let $z > 0$ and $n \geq 1$. Let $\gamma_1^n(z)$ and $\gamma_2^n(z)$ satisfy Theorem 4. Then (see Figures 8-9)*

$$\lim_{z \rightarrow 0^+} (\gamma_1^n(z), \gamma_2^n(z)) = (0, 2n\pi), \quad (4.259)$$

and

$$0 \leq \gamma_2^n'(0^+) \leq A_n'(0^+) = \frac{1}{2n\pi}. \quad (4.260)$$

Theorem 7. (Behavior of $\lambda^n(z) = \lambda_1^n(z) + i\lambda_2^n(z)$ as $z \rightarrow 0^+$.) *Let $z > 0$ and $n \geq 1$. Let $\gamma_1^n(z)$ and $\gamma_2^n(z)$ satisfy Theorem 4. Then (see Figures 8-9-10) the eigenvalues*

$$\lambda(z) = \lambda_1^n(z) + i\lambda_2^n(z) = \frac{\sigma^4((\gamma_1^n)^2 - (\gamma_2^n)^2) - \mu^2\theta^2}{2\theta^2\sigma^2} + i\frac{\gamma_1^n\gamma_2^n\sigma^2}{\theta^2} \quad (4.261)$$

satisfy

$$\lim_{z \rightarrow 0^+} (\lambda_1^n(z), \lambda_2^n(z)) = \left(-\frac{2\sigma^2 n^2 \pi^2}{\theta^2}, 0 \right). \quad (4.262)$$

Let $\epsilon > 0$ satisfy Theorem 3. If $z > 0$ is sufficiently small, then

$$C_1 n \sqrt{z} < \lambda_2^n(z) < C_2 n \sqrt{z} \quad \text{and} \quad (\lambda_2^n)'(0^+) = \infty, \quad (4.263)$$

where

$$C_1 = \frac{2\epsilon\pi\sigma^2}{\theta^2} \quad \text{and} \quad C_2 = \frac{3\sigma^2}{4\theta^2}(4\pi + \pi/n). \quad (4.264)$$

Remark: Note that inequality (4.263) explains the gap between each branch of $\lambda_2^n(z)$ (see Figure 10, right panel).

The proofs of Theorems 6 and 7 make use of the following three technical results:

Lemma 28. *Let $z > 0$ and $n \geq 1$. Then $0 < A_n(z) < \sqrt{z}$.*

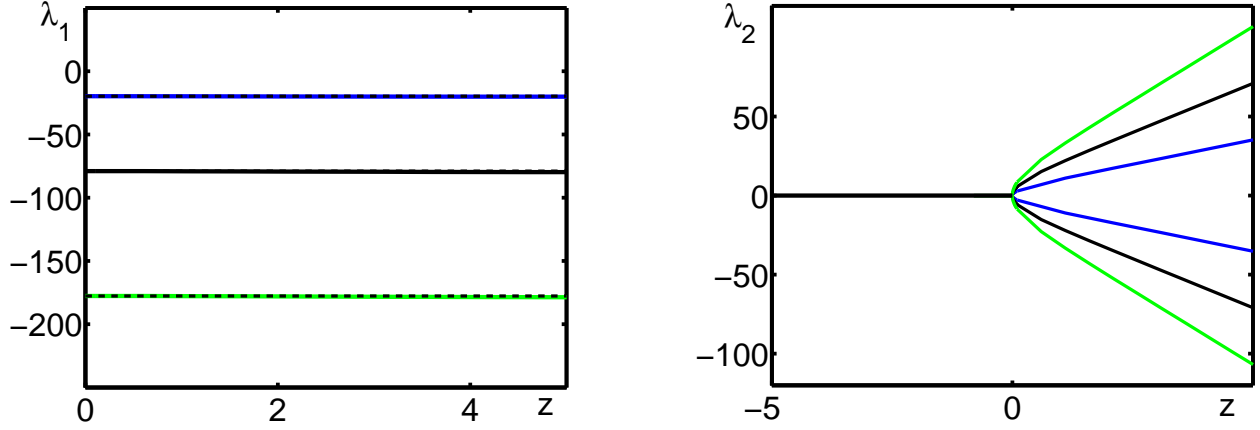


Figure 10: **Left:** The function $\lambda_1^n(z)$ for $n = 1, n = 2$ and $n = 3$. The dotted lines represent the values $-2n^2\pi^2$. **Right:** The function $\lambda_2^n(z)$ for $n = \pm 1, \pm 2$ and $n = \pm 3$. To reproduce the figures see Section A.3.

Proof. For contradiction, assume that $A_n(z) \geq \sqrt{z}$ and consider the function $G(x) = \sin(x)(2n\pi + x) - z \cos(x)$. By the definition of $A_n(z)$ it follows that

$$G(A_n(z)) = 0. \tag{4.265}$$

However,

$$\begin{aligned} G(A_n(z)) &= \sin(A_n(z))(2n\pi + A_n(z)) - z \cos(A_n(z)) \\ &= \cos(A_n(z)) [\tan(A_n(z))(2n\pi + A_n(z)) - z]. \end{aligned}$$

Recall that $\tan(x) > x$ when $x > 0$. Thus, $\tan(A_n(z)) > A_n(z)$ and

$$G(A_n(z)) > \cos(A_n(z)) [A_n(z)2n\pi + A_n(z)z - z]. \tag{4.266}$$

If $A_n(z) \geq \sqrt{z}$ and $2n\pi > 2\pi$ we have that

$$G(A_n(z)) > 2\pi\sqrt{z} \cos(a_n(z)) > 0, \tag{4.267}$$

contradicting (4.265). We conclude that $0 < A_n(z) < \sqrt{z}$. □

Next, we prove a result regarding the derivative of $A_n(z)$.

Lemma 29. *Let $z > 0$ and $n \geq 1$. Then*

$$\lim_{z \rightarrow 0^+} A'_n(z) = \frac{1}{2n\pi}. \quad (4.268)$$

Proof. By definition, $A_n(z)$ satisfies

$$\tan(A_n(z)) = \frac{z}{2n\pi + A_n(z)}. \quad (4.269)$$

Differentiate (4.269) with respect to z and solve for $A'_n(z)$ to obtain

$$A'_n(z) = \frac{2n\pi + A_n(z)}{(2n\pi + A_n(z))^2 \sec^2(A_n(z)) + z}. \quad (4.270)$$

Notice that $\lim_{z \rightarrow 0^+} A_n(z) = 0$ by Lemma 28. Therefore, upon taking limits, equation (4.270) reduces to

$$\lim_{z \rightarrow 0^+} A'_n(z) = \frac{1}{2n\pi} \quad (4.271)$$

as claimed. □

Lemma 30. *There exists $\alpha > 0$ such that*

$$\frac{\gamma_1^*(z)}{\sqrt{z}} < \frac{3}{2} \text{ for all } 0 < z < \alpha. \quad (4.272)$$

Proof. Recall that $\gamma_1^*(z) = \ln(e^z + \sqrt{e^{2z} - 1})$. An application of L'Hospital's rule shows that

$$\lim_{z \rightarrow 0^+} \frac{\gamma_1^*(z)}{\sqrt{z}} = \sqrt{2}. \quad (4.273)$$

Note that $\sqrt{z} < \frac{3}{2}$. Thus, there exists $\alpha > 0$ such that

$$\left| \frac{\gamma_1^*(z)}{\sqrt{z}} - \sqrt{2} \right| < \frac{3}{2} - \sqrt{2}, \text{ for all } 0 < z < \alpha. \quad (4.274)$$

Rearranging the terms in (4.274) gives the desired result. □

Proof of Theorem 6.

First, we prove (4.259). Recall from Lemma 27 that

$$0 < \gamma_1^n(z) < \gamma_1^*(z) \text{ and } 2n\pi < \gamma_2^n(z) < 2n\pi + A_n(z), \text{ for all } z > 0. \quad (4.275)$$

Combine the first part of (4.275) with the definition of $\gamma_1^*(z)$ and obtain

$$0 < \gamma_1^n(z) < \gamma_1^*(z) = \ln(e^z + \sqrt{e^{2z} - 1}), \text{ for all } z > 0. \quad (4.276)$$

Combine the second part of (4.275) with Lemma 28 to get

$$2n\pi < \gamma_2^n(z) < 2n\pi + A_n(z) < 2n\pi + \sqrt{z}, \text{ for all } z > 0. \quad (4.277)$$

Let $z \rightarrow 0^+$ in both (4.276) and (4.277) to obtain (4.259), namely

$$(\gamma_1^n(0^+), \gamma_2^n(0^+)) = \lim_{z \rightarrow 0^+} (\gamma_1^n(z), \gamma_2^n(z)) = (0, 2n\pi). \quad (4.278)$$

Next, we prove (4.260). Let $z > 0$. It then follows from (4.275) and (4.278) that

$$0 < \frac{\gamma_2^n(z) - \gamma_2^n(0^+)}{z} = \frac{\gamma_2^n(z) - 2n\pi}{z} < \frac{A_n(z)}{z}. \quad (4.279)$$

Letting $z \rightarrow 0^+$ in (4.279) gives

$$0 \leq \lim_{z \rightarrow 0^+} \frac{\gamma_2^n(z) - \gamma_2^n(0)}{z} \leq \lim_{z \rightarrow 0^+} \frac{A_n(z)}{z}. \quad (4.280)$$

By Lemma 28, $A_n(0^+) = 0$. This, combined with Lemma 29 and (4.280) gives

$$0 \leq \gamma_2^n'(0^+) \leq A_n'(0^+) = \frac{1}{2n\pi}, \quad (4.281)$$

as claimed. This completes the proof of Theorem 6.

Proof of Theorem 7. First, we prove (4.262). Recall from (4.261) that

$$\lambda = \lambda_1^n(z) + i\lambda_2^n(z) = \frac{\sigma^4((\gamma_1^n)^2 - (\gamma_2^n)^2) - \mu^2\theta^2}{2\theta^2\sigma^2} + i\frac{\gamma_1^n\gamma_2^n\sigma^2}{\theta^2}. \quad (4.282)$$

Let $z \rightarrow 0^+$ in (4.282) and apply (4.259) to obtain (4.262). To prove 4.263 recall from (4.282) that

$$\lambda_2^n(z) = \frac{\gamma_1^n\gamma_2^n\sigma^2}{\theta^2}. \quad (4.283)$$

Combine (4.283) with Lemma 27 and obtain

$$\frac{\epsilon\sigma^2 2n\pi}{\theta^2} \sqrt{z} < \lambda_2^n(z) < \frac{2n\pi + A_n(z)}{\theta^2} \gamma_1^*(z), \text{ for all } z > 0. \quad (4.284)$$

By Lemma 30 there exists $\alpha > 0$ such that

$$\frac{\epsilon\sigma^2 2n\pi}{\theta^2} < \frac{\lambda_2^n(z)}{\sqrt{z}} < \frac{5(2n\pi + A_n(z))}{2\theta^2}, \text{ for all } 0 < z < \alpha. \quad (4.285)$$

By Lemma 28, $A_n(z) < \sqrt{z}$. This, combined with (4.285), gives

$$\frac{\epsilon\sigma^2 2n\pi}{\theta^2} \sqrt{z} < \lambda_2^n(z) < \frac{5(2n\pi + \sqrt{z})}{2\theta^2}, \text{ for all } 0 < z < \alpha. \quad (4.286)$$

This completes the proof of Theorem 7.

4.4 EIGENVALUES FOR THE IF MODEL WHEN $Z = \frac{\mu\theta}{\sigma^2} < 0$

In this chapter we fix $z = \frac{\mu\theta}{\sigma^2} < 0$ in the IF model and analytically investigate properties of the associated eigenvalues. Recall from Section 4.1 that, to compute the eigenvalues, we need to solve the system

$$\gamma e^z = \gamma \cosh(\gamma) + z \sinh(\gamma), \quad (4.287)$$

where

$$z = \frac{\mu\theta}{\sigma^2} < 0 \quad \text{and} \quad \gamma = \gamma_1 + i\gamma_2 = \frac{\theta}{\sigma^2} \sqrt{\mu^2 + 2\lambda\sigma^2}. \quad (4.288)$$

We assume that $\theta > 0$ and $\sigma > 0$. It follows from (4.288) that the eigenvalues λ have the form

$$\lambda = \frac{\sigma^4 (\gamma_1^2 - \gamma_2^2) - \mu^2 \theta^2}{2\theta^2 \sigma^2} + i \frac{\gamma_1 \gamma_2 \sigma^2}{\theta^2}. \quad (4.289)$$

In Section 4.4.1 below we state and prove four theorems which describe the existence and asymptotic behavior of the eigenvalues. In Theorem 8 we assume that γ is real (i.e. $\gamma_2 = 0$ in (4.288)) and prove that there are precisely two eigenvalues, $\lambda = 0$ and $\lambda = -\frac{\mu^2}{2\sigma^2}$. In Theorem 9 we assume that γ is purely imaginary (i.e. $\gamma_1 = 0$ in (4.288)) and prove that there are infinitely many branches of real, negative eigenvalues. Theorems 10 and 11 are

devoted to proving the asymptotic behavior of the eigenvalues as $z \rightarrow 0^-$ and $z \rightarrow \infty$, respectively

Remark: The Open Problem When $z = \frac{\mu\theta}{\sigma^2} < 0$.

It remains a challenging open problem to prove whether complex eigenvalues

$$\lambda = \lambda_1 + i\lambda_2 \tag{4.290}$$

exist when $z = \frac{\mu\theta}{\sigma^2} < 0$. Numerical evidence (Mattia [24]) suggests that the eigenvalues are real and non positive, i.e. $\lambda_1 \leq 0$ and $\lambda_2 = 0$, when $z = \frac{\mu\theta}{\sigma^2} < 0$.

4.4.1 Existence and Asymptotic Behavior When $z = \frac{\mu\theta}{\sigma^2} < 0$

Here, our goal is to consider the general setting, and give a rigorous proof of the existence of infinitely many branches of eigenvalues of the form (4.289) when $\mu < 0$ (see Figure 11, left column). Below, in Theorems 8-11, we analyze the existence and behavior of γ , and the associated eigenvalues, as $z = \frac{\mu\theta}{\sigma^2} < 0$ varies, and prove the following:

Theorem 8. (Existence When $z = \frac{\mu\theta}{\sigma^2} < 0$ and γ is Real)

Let $\gamma = \gamma_1 + i\gamma_2$ be real, i.e. $\gamma_2 = 0$. For each fixed $z < 0$, (4.287) has precisely three real solutions, $\gamma_1 = \pm z$ and $\gamma_1 = 0$. That is, there are three real eigenvalues of the form

$$\lambda = \frac{\sigma^4\gamma_1^2 - \mu^2\theta^2}{2\theta^2\sigma^2} \tag{4.291}$$

and are given by

$$\lambda = 0 \quad \text{and} \quad \lambda = -\frac{\mu^2}{2\sigma^2}. \tag{4.292}$$

Theorem 9. (Existence When $z = \frac{\mu\theta}{\sigma^2} < 0$ and γ is Imaginary) *Let $\gamma = \gamma_1 + i\gamma_2$ be purely imaginary, i.e. $\gamma_1 = 0$. Then, for each fixed $z < 0$, equation (4.287) has infinitely many solutions of the form*

$$\gamma = i\gamma_2^{n1}(z) \quad \text{and} \quad \gamma = i\gamma_2^{n2}(z) \quad \text{for } n \geq 1, \tag{4.293}$$

where

$$\gamma_2^{n1}(z), \gamma_2^{n2}(z) \in \mathbf{C}^1((-\infty, 0)), \quad (4.294)$$

with

$$\gamma_2^{n1} \in ((2n - 1)\pi, 2n\pi), \quad (4.295)$$

and

$$\gamma_2^{n2} \in (2n\pi, (2n + 1/2)\pi). \quad (4.296)$$

The eigenvalues corresponding to $\gamma_2^{n1}(z)$ and $\gamma_2^{n2}(z)$ are real and have the forms

$$\lambda^{n1}(z) = -\frac{\sigma^2}{2\theta^2}((\gamma_2^{n1}(z))^2 + z^2) \quad \text{and} \quad \lambda^{n2}(z) = -\frac{\sigma^2}{2\theta^2}((\gamma_2^{n2}(z))^2 + z^2). \quad (4.297)$$

Equation (4.287) has no solution in the interval $[(2n + 1/2)\pi, (2n + 1)\pi]$.

Theorem 10. (Asymptotic Behavior of $\gamma_2^{n2}(z)$ and $\lambda^{n2}(z)$)

For each $z < 0$, the \mathbf{C}^1 function $\gamma_2^{n2}(z)$ satisfies

$$\gamma_2^{n2}(z) \rightarrow 2n\pi \quad \text{as} \quad z \rightarrow 0^-, \quad (4.298)$$

$$\gamma_2^{n2}(z) \rightarrow 2n\pi \quad \text{as} \quad z \rightarrow -\infty. \quad (4.299)$$

The corresponding eigenvalues $\lambda^{n2}(z) = -\frac{(\gamma_2^{n2}(z))^2 + z^2}{2} \in \mathbf{C}^1$ satisfy

$$\lambda^{n2}(z) \rightarrow -2(n\pi)^2 \quad \text{as} \quad z \rightarrow 0^-, \quad (4.300)$$

and

$$\lambda^{n2}(z) \rightarrow -\infty \quad \text{as} \quad z \rightarrow -\infty. \quad (4.301)$$

Theorem 11. (Asymptotic Behavior of $\gamma_2^{n1}(z)$ and $\lambda^{n1}(z)$)

For each $z < 0$, the \mathbf{C}^1 function $\gamma_2^{n1}(z)$ satisfies

$$\gamma_2^{n1}(z) \rightarrow 2n\pi \quad \text{as } z \rightarrow 0^-, \quad (4.302)$$

$$\gamma_2^{n1}(z) \rightarrow (2n - 1)\pi \quad \text{as } z \rightarrow -\infty. \quad (4.303)$$

The corresponding eigenvalues $\lambda^{n1}(z) = -\frac{(\gamma_2^{n1}(z))^2 + z^2}{2} \in \mathbf{C}^1$ satisfy

$$\lambda^{n1}(z) \rightarrow -2(n\pi)^2 \quad \text{as } z \rightarrow 0^-, \quad (4.304)$$

and

$$\lambda^{n1}(z) \rightarrow -\infty \quad \text{as } z \rightarrow -\infty. \quad (4.305)$$

Remark: The above asymptotic properties of $\gamma_2^{n1}(z)$, $\gamma_2^{n2}(z)$, $\lambda^{n1}(z)$ and $\lambda^{n2}(z)$ are illustrated in the left column of Figure 11.

4.4.1.1 Proof of Theorem 8. We assume that $\gamma = \gamma_1 + i\gamma_2$ is real, hence $\gamma_2 = 0$, and (4.287) reduces to

$$\gamma_1 e^z = \gamma_1 \cosh(\gamma_1) + z \sinh(\gamma_1). \quad (4.306)$$

To prove Theorem 8 we study the function

$$H(z, \gamma_1) = \gamma_1 e^z - \gamma_1 \cosh(\gamma_1) - z \sinh(\gamma_1). \quad (4.307)$$

A direct evaluation shows that $H(z, -z) = H(z, 0) = H(z, z) = 0$. We claim that $\gamma_1 = \pm z$ or $\gamma_1 = 0$ are the only real solutions of $H(z, \gamma_1) = 0$. To prove this, first note that for each fixed z , $H(z, \gamma_1)$ is an odd function of γ_1 . Therefore, we concentrate on the positive γ_1 axis and show that there is exactly one real zero of $H(z, \gamma_1) = 0$ other than $\gamma_1 = 0$.

To prove that $H(z, \gamma_1)$ has a unique positive zero, namely $\gamma_1 = -z$, we make use of four technical results, Lemmas 31-34.

Lemma 31. *The function $f(x) = e^x - (1 + x)$ is positive for all $x \neq 0$.*

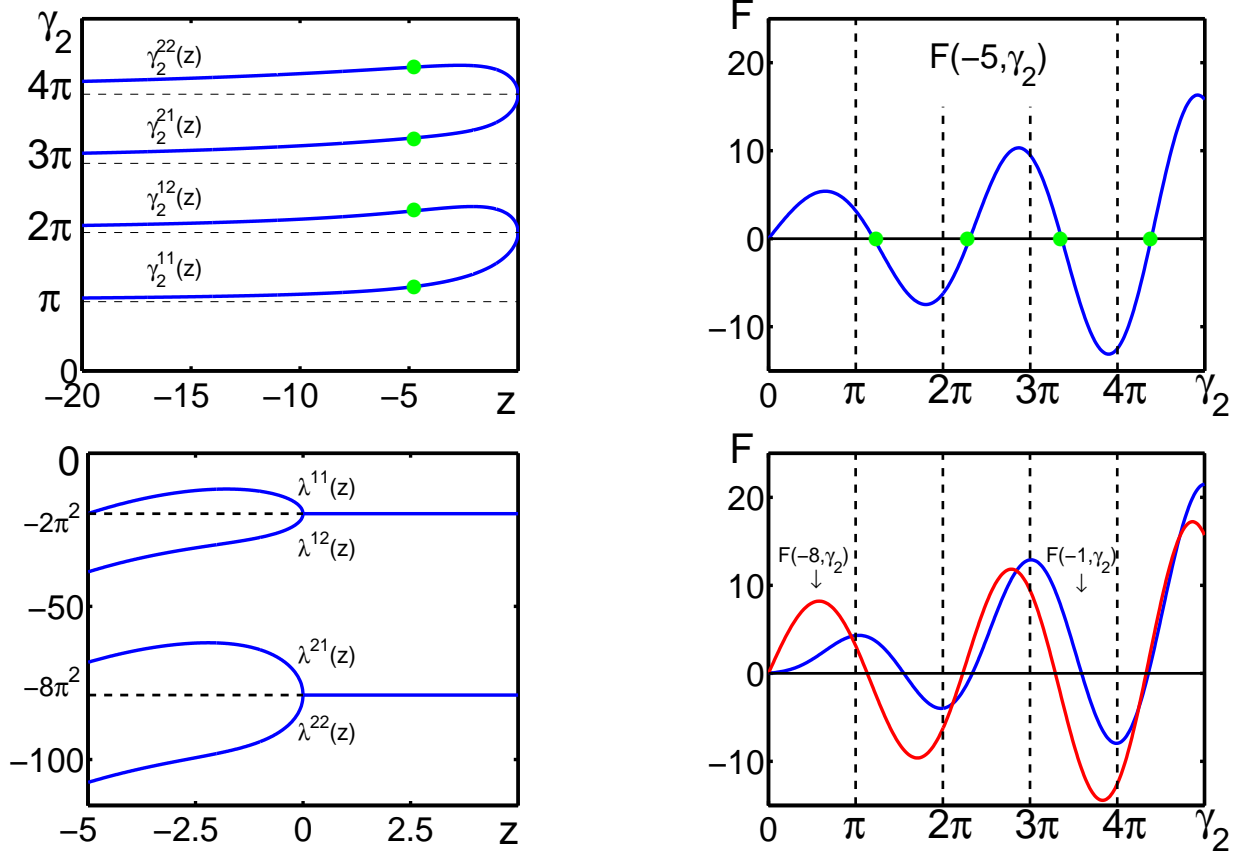


Figure 11: In all plots the parameter values are $\sigma = \theta = 1$ and $V_L = V_R = 0$. **Top Left:** The functions $\gamma_2^{11}(z)$, $\gamma_2^{12}(z)$, $\gamma_2^{21}(z)$, and $\gamma_2^{22}(z)$. The dotted lines represent integer multiples of π . **Top Right:** The function $F(-5, \gamma_2)$. The four green dots in both left and right figures represent the first four solutions of $F(-5, \gamma_2) = 0$. **Bottom Left:** The functions $\lambda^{11}(z)$, $\lambda^{12}(z)$, $\lambda^{21}(z)$ and $\lambda^{22}(z)$. This plot precisely matches the results of Mattia [24], page 66, figure 2. **Bottom Right:** The functions $F(-1, \gamma_2)$ and $F(-8, \gamma_2)$.

Proof. Notice that $f'(x) = e^x - 1$ so that f has a minimum at $x = 0$. Since $f' > 0$ for $x > 0$ and $f' < 0$ for $x < 0$ it follows that $f > 0$ for each $x \neq 0$. \square

Lemma 32. *For each fixed z , $H_{\gamma_1}(z, 0) > 0$.*

Proof. Since $H_{\gamma_1}(z, \gamma_1) = e^z - \cosh(\gamma_1) - \gamma_1 \sinh(\gamma_1) - z \cosh(\gamma_1)$ it follows from Lemma 31 that

$$H_{\gamma_1}(z, 0) = e^z - (1 + z) > 0, \quad (4.308)$$

as desired. \square

Remarks: (i) It follows from Lemma 32 and the fact that $H(z, 0) = 0$ that $H(z, \gamma_1) > 0$ for small $\gamma_1 > 0$.

(ii) Below we let $H_{\gamma_1}(z, \gamma_1) = \frac{\partial H}{\partial \gamma_1}(z, \gamma_1)$ and $H_{\gamma_1 \gamma_1}(z, \gamma_1) = \frac{\partial^2 H}{\partial \gamma_1^2}(z, \gamma_1)$.

Next, fix $z < 0$ and suppose that there is more than one $\gamma_1 > 0$ such that $H(z, \gamma_1) = 0$. Denote the smallest non zero positive root of $H(z, \gamma_1) = 0$ by $\bar{\gamma}$. We claim that $\bar{\gamma}$ is in fact the only root. Since $H(z, \gamma_1) > 0 \forall \gamma_1 \in (0, \bar{\gamma})$, it follows that $H_{\gamma_1}(z, \bar{\gamma}) \leq 0$. We first show that $H_{\gamma_1}(z, \bar{\gamma}) < 0$.

Lemma 33. *For each fixed $z < 0$, $H_{\gamma_1}(z, \bar{\gamma}) < 0$.*

Proof. For contradiction, suppose that $H_{\gamma_1}(z, \bar{\gamma}) = H(z, \bar{\gamma}) = 0$. A calculation shows that

$$H_{\gamma_1 \gamma_1}(z, \bar{\gamma}) = -\sinh(\bar{\gamma})(2 + z) - \bar{\gamma} \cosh(\bar{\gamma}) < 0 \quad (4.309)$$

since $\bar{\gamma} > 0$. This implies that there exists a $\delta > 0$ such that $H_{\gamma_1}(z, \gamma_1) > 0$ for all $\gamma_1 \in [\bar{\gamma} - \delta, \bar{\gamma})$. Therefore,

$$H(z, \gamma_1) = - \int_{\gamma_1}^{\bar{\gamma}} H_{\gamma_1}(z, x) dx < 0 \forall \gamma_1 \in [\bar{\gamma} - \delta, \bar{\gamma}), \quad (4.310)$$

contradicting the fact that $H(z, \gamma_1) > 0 \forall \gamma_1 \in [\bar{\gamma} - \delta, \bar{\gamma})$. We conclude that $H_{\gamma_1}(z, \bar{\gamma}) < 0$. \square

To show that this root is unique we assume that there exists a positive root larger than $\bar{\gamma}$. We show that this is impossible.

Lemma 34. *For each fixed $z < 0$, $\bar{\gamma}$ is the largest positive root.*

Proof. Because of Lemma 33, there exists an $\epsilon > 0$ such that $H(z, \gamma_1) < 0$ for each $\gamma_1 \in (\bar{\gamma}_1, \bar{\gamma}_1 + \epsilon]$. Thus, if there is a root of $H(z, \gamma_1) = 0$ that is larger than $\bar{\gamma}$, then there is a $\gamma^* > \bar{\gamma}$ such that

$$H(z, \gamma^*) < 0, \quad H_{\gamma_1}(z, \gamma^*) = 0 \text{ and } H_{\gamma_1 \gamma_1}(z, \gamma^*) > 0. \quad (4.311)$$

As in the proof of Lemma (33), it follows that $H_{\gamma_1 \gamma_1}(z, \gamma^*) < 0$. This contradicts (4.311), hence there is no root of $H(z, \gamma_1) = 0$ larger than $\bar{\gamma}$. \square

We conclude from Lemmas 31-34 that there is at most one positive root of $H(z, \gamma_1) = 0$ provided $z < 0$. Since $H(z, -z) = 0$, we conclude that $\gamma_1 = -z$ is the only positive root of $H(z, \gamma_1) = 0$. This completes the proof of Theorem (8).

4.4.1.2 Proof of Theorem 9. We assume that $\gamma = i\gamma_2$. Then (4.287) reduces to

$$\gamma_2 e^z = \gamma_2 \cos(\gamma_2) + z \sin(\gamma_2). \quad (4.312)$$

We study the function

$$F(z, \gamma_2) = \gamma_2 e^z - \gamma_2 \cos(\gamma_2) - z \sin(\gamma_2). \quad (4.313)$$

Let $n \geq 1$ and consider the interval $(2n\pi, (2n + 1/2)\pi)$. The first result (see Lemma 35) we prove is that $F(z, \gamma_2) = 0$ has a unique solution in $(2n\pi, (2n + \frac{1}{2})\pi)$ for each fixed $z < 0$.

Lemma 35. *Let $z < 0$ and $n \geq 1$. Then $F(z, \gamma_2) = 0$ has a unique solution in $(2n\pi, (2n + \frac{1}{2})\pi)$. We denote this root by $\gamma_2 = \gamma_2^{n2}(z)$. Furthermore,*

$$\gamma_2^{n2}(z) \in \mathbf{C}^1((-\infty, 0)) \quad (4.314)$$

and

$$2n\pi < \gamma_2^{n2}(z) < (2n + 1/2)\pi. \quad (4.315)$$

The corresponding eigenvalues $\lambda^{n2}(z)$ satisfy

$$\lambda^{n2}(z) = -\frac{(\gamma_2^{n2}(z))^2 + z^2}{2} \in \mathbf{C}^1((-\infty, 0)). \quad (4.316)$$

Proof. The first step is to show that the solution exists. As in the previous section, we note that $F(z, \gamma_2)$ is an odd function of γ_2 for each fixed $z < 0$. We complete the proof of Lemma 35 with the aide of two technical results, Lemmas 36-37.

Lemma 36. *Let $z < 0$ and $n \geq 1$. Then there exists a $c \in (2n\pi, (2n + 1/2)\pi)$ such that $F(z, c) = 0$.*

Proof. A calculation shows that

$$F(z, 2n\pi) = 2n\pi(e^z - 1) < 0 \quad (4.317)$$

and

$$F(z, (2n + 1/2)\pi) = (2n + 1/2)\pi e^z - z > 0. \quad (4.318)$$

Since $F(z, \gamma_2)$ is continuous the intermediate value theorem guarantees a root $c \in (2n\pi, 2n\pi + \frac{\pi}{2})$. \square

We now show that this solution is unique.

Lemma 37. *For each $z < 0$ the c_n satisfying $F(z, c_n) = 0$ is unique on $[2n\pi, (2n + 1/2)\pi]$.*

Proof. It is enough to show that $F_{\gamma_2}(z, \gamma_2) > 0$ on $[2n\pi, (2n + 1/2)\pi]$. Observe that $\cos(\gamma_2) > 0$ and $\sin(\gamma_2) > 0$ on $(2n\pi, (2n + \frac{1}{2})\pi)$. We first let $\gamma_2 \in (2n\pi, (2n + 1/2)\pi)$ and consider three cases.

1. $z + 1 < 0$: Thus,

$$F_{\gamma_2}(z, \gamma_2) = e^z - \cos(\gamma_2)(1 + z) + \gamma_2 \sin(\gamma_2) > 0 \quad (4.319)$$

as desired.

2. $z + 1 > 0$: Then $-\cos(\gamma_2)(1 + z) > -(1 + z)$. Thus,

$$\begin{aligned} F_{\gamma_2}(z, \gamma_2) &= e^z - \cos(\gamma_2)(1 + z) + \gamma_2 \sin(\gamma_2) \\ &> e^z - (1 + z) + \gamma_2 \sin(\gamma_2). \end{aligned}$$

This, together with Lemma (31), imply that $F_{\gamma_2}(z, \gamma_2) > 0$.

3. $z = -1$: When $z = -1$ it follows that

$$F_{\gamma_2} = e^z + \gamma_2 \sin(\gamma_2) > 0. \quad (4.320)$$

Since $F_{\gamma_2} > 0$ on $(2n\pi, (2n + \frac{1}{2})\pi)$ we conclude that the root is unique. \square

We let $\gamma_2^{n2}(z)$ denote the unique root of $F(z, \gamma_2) = 0$ in $(2n\pi, (2n + \frac{1}{2})\pi)$.

This completes the proof of Lemma 35. \square

Next, we show that there is no root in the interval $[(2n + \frac{1}{2})\pi, (2n + 1)\pi]$. This property follows immediately from the following lemma.

Lemma 38. *For each fixed $z < 0$, $F(z, \gamma_2) > 0$ on $[(2n + \frac{1}{2})\pi, (2n + 1)\pi]$.*

Proof. Let $z < 0$. At the left and right endpoints of $[(2n + \frac{1}{2})\pi, (2n + 1)\pi]$, observe that

$$F\left(z, \left(2n + \frac{1}{2}\right)\pi\right) = \left(2n + \frac{1}{2}\right)\pi e^z - z > 0, \quad (4.321)$$

and

$$F(z, (2n + 1)\pi) = (2n + 1)\pi(e^z + 1) > 0. \quad (4.322)$$

Next, recall that $\cos(\gamma_2) < 0$ and $\sin(\gamma_2) > 0$ on $((2n + \frac{1}{2})\pi, (2n + 1)\pi)$. Therefore,

$$F(z, \gamma_2) = \gamma_2 e^z - \gamma_2 \cos(\gamma_2) - z \sin(\gamma_2) > 0 \quad (4.323)$$

when $z < 0$ and $\gamma_2 \in ((2n + \frac{1}{2})\pi, (2n + 1)\pi)$. \square

This completes the proof that there is no solution of $F(z, \gamma_2) = 0$ when $z < 0$, $n \geq 1$ and $\gamma_2 \in [(2n + \frac{1}{2})\pi, (2n + 1)\pi]$.

We now turn our attention to proving the existence and uniqueness properties of γ_2^{n1} . For this, we fix $z < 0$ and $n \geq 1$, and analyze properties of the function $F(z, \gamma_2)$ when $\gamma_2 \in ((2n - 1)\pi, 2n\pi)$. First, we observe that, if $z < 0$ and $n \geq 1$, then

$$F(z, (2n - 1)\pi) = (2n - 1)\pi(e^z + 1) > 0, \quad (4.324)$$

and

$$F(z, 2n\pi) = 2n\pi(e^z - 1) < 0. \quad (4.325)$$

From (4.324)-(4.325) and the intermediate value theorem we immediately obtain the following result:

Lemma 39. *Let $z < 0$ and $n \geq 1$. Then there exists at least one solution of $F(z, \gamma_2) = 0$ in $((2n - 1)\pi, 2n\pi)$.*

Our goal is to prove the following lemma:

Lemma 40. *Let $z < 0$ and $n \geq 1$. Then $F(z, \gamma_2) = 0$ has a unique solution in $((2n - 1)\pi, 2n\pi)$. We denoted this solution by $\gamma_2^{n1}(z)$. Furthermore,*

$$\gamma_2^{n1}(z) \in \mathbf{C}^1((-\infty, 0)) \quad (4.326)$$

and

$$(2n - 1)\pi < \gamma_2^{n1}(z) < 2n\pi. \quad (4.327)$$

The corresponding eigenvalues $\lambda^{n1}(z)$ satisfy

$$\lambda^{n1}(z) = -\frac{(\gamma_2^{n1}(z))^2 + z^2}{2} \in \mathbf{C}^1((-\infty, 0)). \quad (4.328)$$

Proof. We consider two regimes of z values:

Regime I. $-\infty < z \leq -2$.

Regime II. $-2 < z < 0$.

Regime I. We assume that $z \leq -2$ is fixed, and that $n \geq 1$. We prove three technical results. First, a direct calculation leads to

Lemma 41. *Let $z \leq -2$ and $n \geq 1$. Then*

$$F(z, (2n - 1)\pi) = (2n - 1)\pi(e^z + 1) > 0 \quad \text{and} \quad F_{\gamma_2}(z, (2n - 1)\pi) = e^z + 1 + z < 0. \quad (4.329)$$

Next, we focus on the interval $\gamma_2 \in [(2n - 1/2)\pi, 2n\pi]$ when $n \geq 1$. Again, a direct calculation gives

Lemma 42. *Let $z \leq -2$ and $n \geq 1$. Then*

$$F_{\gamma_2\gamma_2}(z, \gamma_2) = \sin(\gamma_2)(2 + z) + \gamma_2 \cos(\gamma_2) > 0 \quad (4.330)$$

when $\gamma_2 \in [(2n - 1/2)\pi, 2n\pi]$.

Lemma 43. *Let $z \leq -2$ and $n \geq 1$. Then $F_{\gamma_2}(z, \gamma_2) < 0$ on $[(2n - 1)\pi, (2n - 1/2)\pi]$.*

Proof. A calculation shows that

$$\begin{aligned} F_{\gamma_2}(z, \gamma_2) &= e^z - \cos(\gamma_2)(1 + z) + \gamma_2 \sin(\gamma_2) \\ &< 1 + \cos(\gamma_2) + \gamma_2 \sin(\gamma_2). \end{aligned} \quad (4.331)$$

The function $h(\gamma_2) = 1 + \cos(\gamma_2) + \gamma_2 \sin(\gamma_2)$ satisfies $h((2n - 1)\pi) = 0$ and $h'(\gamma_2) < 0$ for $\gamma_2 \in ((2n - 1)\pi, (2n - 1/2)\pi)$. Thus,

$$F_{\gamma_2}(z, \gamma_2) < 0 \quad \text{for all } \gamma_2 \in [(2n - 1)\pi, (2n - 1/2)\pi]. \quad (4.332)$$

□

Below, in Lemma 44 we make use of Lemmas 41-43 to show that there is a unique value $\gamma^* \in ((2n - 1)\pi, 2n\pi)$ where $F_{\gamma_2}(z, \gamma^*) = 0$. Lemma 43 implies that $F(z, \gamma_2)$ is strictly decreasing on $[(2n - 1)\pi, (2n - 1/2)\pi]$ when $z \leq -2$.

Lemma 44. *Let $z \leq -2$ and $n \geq 1$. Then there exists a unique $\gamma^* \in ((2n - 1/2)\pi, 2n\pi)$ such that $F_{\gamma_2}(z, \gamma^*) = 0$. In particular,*

$$F_{\gamma_2}(z, \gamma_2) < 0 \quad \text{for } \gamma_2 \in [(2n - 1)\pi, \gamma^*), \quad (4.333)$$

and

$$F_{\gamma_2}(z, \gamma_2) > 0 \quad \text{for } \gamma_2 \in (\gamma^*, 2n\pi]. \quad (4.334)$$

Proof. Recall, from Lemma 41 that

$$F_{\gamma_2}(z, (2n - 1)\pi) = e^z + 1 + z < 0. \quad (4.335)$$

At the right endpoint a calculation shows that

$$F_{\gamma_2}(z, 2n\pi) = e^z - (1 + z) > 0. \quad (4.336)$$

It follows from (4.335)-(4.336) and the intermediate value theorem that there is at least one solution of $F_{\gamma_2}(z, \gamma_2) = 0$ on the interval $((2n - 1)\pi, 2n\pi)$. We claim that there is exactly one such solution, and that it lies in $((2n - 1/2)\pi, 2n\pi)$. These properties follow immediately from Lemmas 42-43. This completes the proof of Lemma 44. □

We are now ready to prove our main result for **Regime 1**.

Lemma 45. *Let $z \leq -2$ and $n \geq 1$, and let $\gamma^* \in ((2n - 1/2)\pi, 2n\pi)$ denote the unique value such that $F_{\gamma_2}(z, \gamma^*) = 0$. Then there is a unique $\gamma_2^{n1}(z) \in ((2n - 1)\pi, 2n\pi)$ such that $F(z, \gamma_2^{n1}(z)) = 0$. Furthermore, $\gamma_2^{n1}(z) \in \mathbf{C}^1((-\infty, -2])$,*

$$\gamma_2^{n1}(z) \in ((2n - 1)\pi, \gamma^*) \quad \text{and} \quad \frac{d}{dz}\gamma_2^{n1}(z) > 0. \quad (4.337)$$

Proof. Lemma 44 implies that

$$F(z, \gamma_2) < F(z, 2n\pi) < 0 \quad \text{for} \quad \gamma_2 \in [\gamma^*, 2n\pi]. \quad (4.338)$$

Thus, the unique solution $\gamma_2^{n1}(z)$ of $F(z, \gamma_2) = 0$ must satisfy

$$\gamma_2^{n1}(z) \in ((2n - 1)\pi, \gamma^*) \quad \text{for all} \quad z \leq -2. \quad (4.339)$$

Lemma 44 guarantees that $\gamma_2^{n1}(z)$ is unique because

$$F_{\gamma_2}(z, \gamma_2) < 0 \quad \text{for all} \quad \gamma_2 \in ((2n - 1)\pi, \gamma^*). \quad (4.340)$$

Thus,

$$F_{\gamma_2}(z, \gamma_2^{n1}(z)) < 0 \quad \text{for all} \quad z \leq -2. \quad (4.341)$$

It follows from (4.341) and the implicit function theorem that

$$\gamma_2^{n1}(z) \in \mathbf{C}^1((-\infty, -2]). \quad (4.342)$$

Next, a direct calculation shows that

$$F_z(z, \gamma_2^{n1}(z)) = \gamma_2^{n1}(z)e^z - \sin(\gamma_2^{n1}(z)) > 0 \quad \text{for all} \quad z \leq -2. \quad (4.343)$$

Finally, a differentiation of $F(z, \gamma_2^{n1}(z)) = 0$ shows that

$$F_z(z, \gamma_2^{n1}(z)) + F_{\gamma_2}(z, \gamma_2^{n1}(z))\frac{d}{dz}\gamma_2^{n1}(z) = 0 \quad \text{for all} \quad z \leq -2. \quad (4.344)$$

Combining (4.341), (4.343) and (4.344) gives

$$\frac{d}{dz}\gamma_2^{n1}(z) = \frac{-F_z(z, \gamma_2^{n1}(z))}{F_{\gamma_2}(z, \gamma_2^{n1}(z))} > 0 \quad \text{for all} \quad z \leq -2. \quad (4.345)$$

□

This concludes the analysis of $\gamma_2^{n1}(z)$ in **Regime 1**: $z \in (-\infty, -2]$.

Regime II: $z \in (-2, 0)$. We assume that $z \in (-2, 0)$ is fixed, and that $n \geq 1$. Our goal is to complete the proof of Lemma 40 in this regime. That is, it remains to be proved that there is exactly one solution of $F(z, \gamma_2) = 0$, denoted by $\gamma_2^{n1}(z)$, in $((2n - 1)\pi, 2n\pi)$ when $z \in (-2, 0)$, and $\gamma_2^{n1}(z) \in \mathbf{C}^1((-2, 0))$.

The first step is to consider $n \geq 3$ and show that there is no solution of $F(z, \gamma_2) = 0$ on the interval $((2n - 1)\pi, (2n - 1/2)\pi)$. The proof of this requires Lemmas 46 and 47

In the following Lemma we determine the values of $F(z, \gamma_2)$ at the left and right endpoints of the γ_2 interval $[(2n - 1)\pi, (2n - 1/2)\pi]$.

Lemma 46. *Let $z \in (-2, 0)$ and $n \geq 3$. Then*

$$F(z, (2n - 1)\pi) = (2n - 1)\pi(e^z + 1) > 0, \quad (4.346)$$

and

$$F(z, (2n - 1/2)\pi) > 0. \quad (4.347)$$

Proof. Property (4.346) follows immediately from (4.313). To verify (4.347) we combine the assumption that $n \geq 3$ with (4.313). Then,

$$\begin{aligned} F(z, (2n - 1/2)\pi) &= (2n - 1/2)\pi e^z + z & (4.348) \\ &\geq \frac{11\pi}{2} e^z + z \\ &\geq \frac{11\pi}{2} e^{-2} - 2 > 0. \end{aligned}$$

□

Next, we show that $F(z, \gamma_2)$ is concave down when $\gamma_2 \in [(2n - 1)\pi, (2n - 1/2)\pi]$. It should be noted that this property holds for each $n \geq 1$.

Lemma 47. *Let $z \in (-2, 0)$ and $n \geq 1$. Then*

$$F_{\gamma_2\gamma_2}(z, \gamma_2) < 0 \quad \text{for all } \gamma_2 \in [(2n - 1)\pi, (2n - 1/2)\pi]. \quad (4.349)$$

Proof. Two differentiations of equation (4.313) give

$$F_{\gamma_2\gamma_2}(z, \gamma_2) = \sin(\gamma_2)(2 + z) + \gamma_2 \cos(\gamma_2). \quad (4.350)$$

Since $\sin(x) \leq 0$ and $\cos(x) \leq 0$ on $[(2n - 1)\pi, (2n - 1/2)\pi]$ the result follows. \square

In the next Lemma we make use of Lemmas 46 and 47 to prove that $F(z, \gamma_2) > 0$ on the entire interval $[(2n - 1)\pi, (2n - 1/2)\pi]$ when $z \in (-2, 0)$ and $n \geq 3$:

Lemma 48. *Let $z \in (-2, 0)$ and $n \geq 3$. Then $F(z, \gamma_2) > 0$ on $[(2n - 1)\pi, (2n - 1/2)\pi]$.*

Proof. Suppose for contradiction that $F(z, \hat{\gamma}) \leq 0$ at some $\hat{\gamma} \in ((2n - 1)\pi, (2n - 1/2)\pi)$. This, and Lemma 46 imply that there exists a point $\gamma_2 = \beta \in ((2n - 1)\pi, (2n - 1/2)\pi)$ where $F(z, \gamma_2)$ attains a minimum. As $F(z, \gamma_2)$ is C^∞ it follows that

$$F_{\gamma_2\gamma_2}(z, \beta) \geq 0. \quad (4.351)$$

However, Lemma 47 implies that

$$F_{\gamma_2\gamma_2}(z, \beta) < 0, \quad (4.352)$$

which contradicts (4.351). This completes the proof of Lemma 48. \square

We have now proved the following: $F(z, \gamma_2) = 0$ does not have a solution on the interval $[(2n - 1)\pi, (2n - 1/2)\pi]$ when $z \in (-2, 0)$ and $n \geq 3$. Below, in Lemma 52, we prove that $F(z, \gamma_2) = 0$ has a unique solution in $[(2n - 1/2)\pi, 2n\pi]$ for each $z \in (-2, 0)$ when $n \geq 3$.

The proof of Lemma 52 requires three Lemmas. First, recall from (4.324) that

$$F(z, 2n\pi) = 2n\pi(e^z - 1) < 0 \quad \text{for all } z \in (-2, 0). \quad (4.353)$$

This fact, along with Lemma 46 and the intermediate value theorem, yield the following result:

Lemma 49. *Let $z \in (-2, 0)$ and $n \geq 3$. Then there exists at least one solution of $F(z, \gamma_2) = 0$ in $((2n - 1/2)\pi, 2n\pi)$.*

It remains to show that there is exactly one such root. We prove this claim in the next three Lemmas.

Lemma 50. *Let $z \in (-2, 0)$ and $n \geq 3$. Then*

$$F_{\gamma_2\gamma_2\gamma_2}(z, \gamma_2) > 0 \quad \text{for all } \gamma_2 \in [(2n - 1/2)\pi, 2n\pi]. \quad (4.354)$$

Proof. Three differentiations of equation (4.313) give

$$F_{\gamma_2\gamma_2\gamma_2}(z, \gamma_2) = \cos(\gamma_2)(3 + z) - \gamma_2 \sin(\gamma_2). \quad (4.355)$$

Property (4.354) follows from (4.355) together with the observations that $\cos(x) \geq 0$ and $\sin(x) \leq 0$ on $[(2n - 1/2)\pi, 2n\pi]$. \square

Lemma 51. *Let $z \in (-2, 0)$ and $n \geq 3$. Then there is a unique solution to $F_{\gamma_2\gamma_2}(z, \gamma_2) = 0$ on $((2n - 1/2)\pi, 2n\pi)$.*

Proof. Recall from Lemma 47 that

$$F_{\gamma_2\gamma_2}(z, \gamma_2) = \sin(\gamma_2)(2 + z) + \gamma_2 \cos(\gamma_2) \quad (4.356)$$

so that

$$F_{\gamma_2\gamma_2}(z, (2n - 1/2)\pi) = -(2 + z) < 0 \quad (4.357)$$

and

$$F_{\gamma_2\gamma_2}(z, 2n\pi) = 3 + z > 0. \quad (4.358)$$

Existence is guaranteed by the intermediate value theorem. To prove uniqueness we appeal to the third derivative. By Lemma 50 it follows that $F_{\gamma_2\gamma_2}(z, \gamma_2)$ is increasing in γ_2 . We conclude that there is a unique solution of $F_{\gamma_2\gamma_2}(z, \gamma_2) = 0$ on $((2n - 1/2)\pi, 2n\pi)$. \square

We are now ready to show that $F(z, \gamma_2) = 0$ has a unique root in $((2n - 1/2)\pi, 2n\pi)$.

Lemma 52. *Let $z \in (-2, 0)$ and $n \geq 3$. Then there is a unique $\alpha \in ((2n - 1/2)\pi, 2n\pi)$ such that*

$$F(z, \alpha) = 0. \quad (4.359)$$

Proof. We have already shown that a root $\gamma_2 = \alpha$ of $F(z, \gamma_2) = 0$ exists. Recall that

$$F(z, (2n - 1/2)\pi) > 0, \quad F_{\gamma_2}(z, (2n - 1/2)\pi) < 0 \quad (4.360)$$

and

$$F(z, 2n\pi) < 0, \quad F_{\gamma_2}(z, 2n\pi) > 0. \quad (4.361)$$

Now suppose that there exist two distinct roots $\gamma_2 = \alpha_1$ and $\gamma_2 = \alpha_2$ with

$$(2n - 1/2)\pi < \alpha_1 < \alpha_2 < 2n\pi. \quad (4.362)$$

From this supposition and (4.360)-(4.361) we may conclude that

$$F(z, \alpha_1) = 0, \quad F_{\gamma_2}(z, \alpha_1) \leq 0, \quad (4.363)$$

and

$$F(z, \alpha_2) = 0, \quad F_{\gamma_2}(z, \alpha_2) \geq 0. \quad (4.364)$$

Furthermore, we conclude from Lemmas 50 and 51 that $F_{\gamma_2\gamma_2}(z, \gamma_2)$ has at most one zero on $[(2n - 1/2)\pi, 2n\pi]$. In turn, this property implies that $F_{\gamma_2}(z, \gamma_2)$ has at most one zero on $[(2n - 1/2)\pi, 2n\pi]$. Therefore, we conclude that

$$F_{\gamma_2}(z, \alpha_1) < 0 \quad \text{or} \quad F_{\gamma_2}(z, \alpha_2) > 0. \quad (4.365)$$

It follows from (4.360) and (4.361), and (4.363)-(4.364)-(4.365), that $F(z, \gamma_2)$ has at least two distinct minima and one maximum on $((2n - 1/2)\pi, 2n\pi)$. Hence there would exist two points β_1 and β_2 where

$$F_{\gamma_2\gamma_2}(z, \beta_i) = 0, \quad i = 1, 2. \quad (4.366)$$

As this contradicts Lemma 51 the proof is complete. \square

Remark: It follows from Lemma 52 that for each $z \in (-2, 0)$ and $n \geq 3$ there is a unique solution, $\gamma_2^{n1}(z)$, of the equation $F(z, \gamma_2) = 0$.

It remains to show that $\gamma_2^{n1}(z) \in \mathbf{C}^1((-2, 0))$ for $n \geq 3$. This property follows immediately from the implicit function theorem if we prove that

$$F_{\gamma_2}(z, \gamma_2^{n1}(z)) \neq 0 \quad z \in (-2, 0), \quad n \geq 3. \quad (4.367)$$

Lemma 53. *Let $z \in (-2, 0)$ and $n \geq 3$. Then*

$$F_{\gamma_2}(z, \gamma_2^{n_1}(z)) < 0 \quad (4.368)$$

Proof. Recall that

$$F(z, (2n - 1/2)\pi) > 0 \quad \text{and} \quad F(z, 2n\pi) < 0. \quad (4.369)$$

From (4.369) and the uniqueness of $\gamma_2^{n_1}(z)$ we conclude that

$$F(z, \gamma_2) > 0 \quad \forall \gamma_2 \in [(2n - 1/2)\pi, \gamma_2^{n_1}(z)] \quad \text{and} \quad F(z, \gamma_2^{n_1}(z)) = 0. \quad (4.370)$$

Therefore

$$F_{\gamma_2}(z, \gamma_2) \leq 0. \quad (4.371)$$

For contradiction suppose that there exists a $z \in (-2, 0)$ such that

$$F_{\gamma_2}(z, \gamma_2^{n_1}(z)) = 0. \quad (4.372)$$

Then it must be true that

$$F_{\gamma_2\gamma_2}(z, \gamma_2^{n_1}(z)) \geq 0. \quad (4.373)$$

It follows from Lemma 50 that

$$F_{\gamma_2\gamma_2\gamma_2}(z, \gamma_2) > 0 \quad \text{for all } \gamma_2 \in [\gamma_2^{n_1}(z), 2n\pi]. \quad (4.374)$$

Combining (4.373) and (4.374) gives

$$F_{\gamma_2\gamma_2}(z, \gamma_2) > 0 \quad \text{for all } \gamma_2 \in [\gamma_2^{n_1}(z), 2n\pi]. \quad (4.375)$$

It follows from (4.372) and (4.375) that

$$F_{\gamma_2}(z, \gamma_2) > 0 \quad \text{for all } \gamma_2 \in [\gamma_2^{n_1}(z), 2n\pi]. \quad (4.376)$$

It follows from (4.370) and (4.376) that $F(z, 2n\pi) > 0$, contradicting (4.369). We conclude that $F_{\gamma_2}(z, \gamma_2^{n_1}(z)) < 0$. This completes the proof of the Lemma. \square

Summary: To this point we have proven the following about **Regime 2:** For $z \in (-2, 0)$ and $n \geq 3$ we have proved that there exists $\gamma_2^{n1}(z) \in \mathbf{C}^1((-2, 0))$ such that

$$F(z, \gamma_2^{n1}(z)) = 0, \quad (4.377)$$

and

$$\gamma_2^{n1}(z) \in ((2n - 1/2)\pi, 2n\pi). \quad (4.378)$$

To finish the analysis of $\gamma_2^{n1}(z)$, it remains to consider the cases $n = 1$ and $n = 2$, and show that $\gamma_2^{n1}(z)$ is unique, and that $\gamma_2^{n1}(z) \in \mathbf{C}^1((-2, 0))$. Thus, in the remainder of this proof we keep $z \in (-2, 0)$ fixed, and vary γ_2 .

The first step is to recall from Lemma 39 that at least one solution of $F(z, \gamma_2) = 0$ exists in the interval $((2n - 1)\pi, 2n\pi)$ for each $n \geq 1$. We denote the smallest root by $\gamma_2 = \gamma_2^*$. Note that

$$F(z, (2n - 1/2)\pi) = (2n - 1/2)\pi e^z + z. \quad (4.379)$$

When $n = 1, 2$ the sign of $F(z, (2n - 1/2)\pi)$ can be positive or negative, depending on the value of z . Lemma 47 shows that $F(z, \gamma_2)$ is positive at $\gamma_2 = (2n - 1)\pi$, and concave down on $[(2n - 1)\pi, (2n - 1/2)\pi]$. This property, together with (4.379), allow us to determine the location of the smallest solution of $F(z, \gamma_2) = 0$ on $((2n - 1)\pi, 2n\pi)$:

- (i) If $F(z, (2n - 1/2)\pi) > 0$, then $\gamma_2^* \in ((2n - 1/2)\pi, 2n\pi)$.
- (ii) If $F(z, (2n - 1/2)\pi) = 0$, then $\gamma_2^* = (2n - 1/2)\pi$.
- (iii) If $F(z, (2n - 1/2)\pi) < 0$, then $\gamma_2^* \in ((2n - 1)\pi, (2n - 1/2)\pi)$.

We now prove that γ_2^* is the only solution in $((2n - 1)\pi, 2n\pi)$.

Lemma 54. *Let $z \in (-2, 0)$ and $n = 1, 2$. Then the equation $F(z, \gamma_2) = 0$ has a unique solution, $\gamma_2^{n1}(z)$, in $((2n - 1)\pi, 2n\pi)$.*

Proof. In cases (i) and (ii), where $F(z, (2n - 1/2)\pi) \geq 0$, the proofs are identical to the proof of Lemma 52. We thus focus on case (iii). This and Lemma 41 imply that

$$F(z, (2n - 1/2)\pi) < 0 \quad \text{and} \quad F_{\gamma_2}(z, (2n - 1/2)\pi) < 0. \quad (4.380)$$

For contradiction, suppose that there is a second value, $\gamma_2 = \alpha \in ((2n - 1)\pi, 2n\pi)$, such that $F(z, \alpha) = 0$. By choosing α to be the first such value greater than γ_2^* , we conclude that

$$F(z, \alpha) = 0 \quad \text{and} \quad F_{\gamma_2}(z, \alpha) \geq 0. \quad (4.381)$$

It follows from (4.380) and the fact that $F(z, \gamma_2)$ is concave down on $[(2n - 1)\pi, (2n - 1/2)\pi]$ that

$$\gamma_2^* < (2n - 1/2)\pi < \alpha. \quad (4.382)$$

The definition of α , together with (4.380), imply that $F(z, \gamma_2)$ attains a relative minimum at some point in $((2n - 1/2)\pi, \alpha)$. Thus, there exists a point $\beta \in ((2n - 1/2)\pi, \alpha)$ such that

$$F_{\gamma_2\gamma_2}(z, \beta) \geq 0. \quad (4.383)$$

It follows from equation (4.383) and Lemma (50) that

$$F_{\gamma_2\gamma_2}(z, \gamma_2) > 0 \quad \text{for all} \quad \gamma_2 \in (\beta, 2n\pi]. \quad (4.384)$$

Finally, from (4.381) and (4.384) we conclude that

$$F(z, 2n\pi) > 0, \quad (4.385)$$

which contradicts the fact that $F(z, 2n\pi) < 0$. This completes the proof. \square

It remains to prove that

$$\gamma_2^{n1}(z) \in \mathbf{C}^1((-2, 0)) \quad (4.386)$$

when $n = 1, 2$. We consider two cases:

1. $\gamma_2^{n1}(z) \geq (2n - 1/2)\pi$.
2. $\gamma_2^{n1}(z) < (2n - 1/2)\pi$.

The details for case 1 are exactly the same as those given in the proof of Lemma 53. For case 2 we note that the definition of $\gamma_2^{n1}(z)$ implies that

$$F(z, \gamma_2) > 0 \quad \forall \gamma_2 \in [(2n-1)\pi, \gamma_2^{n1}(z)), \quad F(z, \gamma_2^{n1}(z)) = 0 \quad (4.387)$$

and

$$F_{\gamma_2}(z, \gamma_2^{n1}(z)) \leq 0. \quad (4.388)$$

Suppose that $F_{\gamma_2}(z, \gamma_2^{n1}(z)) = 0$. Then the fact that $F_{\gamma_2\gamma_2}(z, \gamma_2^{n1}(z)) < 0$ implies that $F(z, \gamma_2) < 0$ on an interval of the form $(\gamma_2^{n1}(z) - \epsilon, \gamma_2^{n1}(z))$, contradicting (4.387).

This concludes the analysis of $\gamma_2^{n1}(z)$ in **Regime II**: $z \in (-2, 0)$. The proof of Lemma 40 is now complete. \square

Theorem 9 follows from Lemmas 35, 40

4.4.1.3 Proof of Theorem 10. Recall from Lemma 35 in **Part II** that $\gamma_2^{n2}(z) \in \mathbf{C}^1((-\infty, 0))$ for each $n \geq 1$ and

$$2n\pi < \gamma_2^{n2}(z) < (2n+1/2)\pi \quad \forall z < 0. \quad (4.389)$$

The proofs of (4.298)-(4.299) require the next three technical Lemmas.

Lemma 55. *There exists $z^* < 0$ such that*

$$1 + z - \cos\left(2\sqrt{|z|}\right) > 0 \quad \text{when } z^* < z < 0. \quad (4.390)$$

Proof. First, notice that (4.390) is equivalent to proving $g(x) > 0$ where

$$g(x) = 1 - x - \cos\left(2\sqrt{x}\right), \quad x \geq 0. \quad (4.391)$$

We claim that there exists $\delta > 0$ such that $g(x) > 0$ for $x \in (0, \delta)$. Indeed,

$$g'(x) = -1 + \frac{\sin(2\sqrt{x})}{\sqrt{x}}, \quad x > 0, \quad (4.392)$$

so that

$$g'(0) = \lim_{x \rightarrow 0} g'(x) = 1. \quad (4.393)$$

As $g(0) = 0$ it follows that $g(x) > 0$ on $(0, \delta)$. Therefore, there exists $z^* < 0$ such that $1 + z - \cos\left(2\sqrt{|z|}\right) > 0$ for $z^* < z < 0$. \square

Lemma 56. *There exists $z_1 < 0$ such that*

$$\left(2n\pi + \frac{3\pi^2}{|z|}\right) \left[e^z - \cos\left(\frac{3\pi^2}{|z|}\right)\right] > -2n\pi - \frac{\pi}{2} \quad \text{when } z < z_1. \quad (4.394)$$

Proof. Elementary calculus shows that

$$\lim_{z \rightarrow -\infty} \left(2n\pi + \frac{3\pi^2}{|z|}\right) \left[e^z - \cos\left(\frac{3\pi^2}{|z|}\right)\right] = -2n\pi. \quad (4.395)$$

It follows that there exists $z_1 < 0$ such that

$$\left| \left(2n\pi + \frac{3\pi^2}{|z|}\right) \left[e^z - \cos\left(\frac{3\pi^2}{|z|}\right)\right] + 2n\pi \right| < \frac{\pi}{2} \quad (4.396)$$

for $z < z_1$. Rearranging the terms completes the proof of the lemma. \square

Lemma 57. *There exists $z_2 < 0$ such that*

$$\sin\left(\frac{3\pi^2}{|z|}\right) > \frac{6\pi}{|z|} \quad \text{when } z < z_2. \quad (4.397)$$

Proof. Recall that $\sin(x) > \frac{2}{\pi}x$ for $x \in (0, \frac{\pi}{2})$. Since $\lim_{x \rightarrow \infty} \frac{3\pi^2}{x} = 0$, there exists a $z_2 < 0$ such that $\frac{3\pi^2}{|z|} \in (0, \frac{\pi}{2})$ when $z < z_2$. Therefore,

$$\sin\left(\frac{3\pi^2}{|z|}\right) > \frac{2}{\pi} \left(\frac{3\pi^2}{|z|}\right) = \frac{6\pi}{|z|} \quad \text{when } z < z_2 < 0. \quad (4.398)$$

\square

We now have the necessary tools to prove Theorem 10.

Proof of Theorem 10. First, we prove (4.298). Recall that

$$F(z, 2n\pi) < 0 \quad \text{when } z < 0 \quad \text{and } n \geq 1. \quad (4.399)$$

Next, we claim that there exists a $z^* < 0$ such that

$$F(z, 2n\pi + 2\sqrt{|z|}) > 0 \quad \text{when } z^* < z < 0 \quad \text{and } n \geq 1. \quad (4.400)$$

A calculation shows that

$$\begin{aligned} F(z, 2n\pi + 2\sqrt{|z|}) &= (2n\pi + 2\sqrt{|z|}) \left[e^z - \cos(2\sqrt{|z|}) \right] - z \sin(2\sqrt{|z|}) \\ &> (2n\pi + 2\sqrt{|z|}) \left[e^z - \cos(2\sqrt{|z|}) \right] \\ &> (2n\pi + 2\sqrt{|z|}) \left[1 + z - \cos(2\sqrt{|z|}) \right] \end{aligned}$$

where the last inequality follows from Lemma 31. By Lemma 55 it follows that $F(z, 2n\pi + 2\sqrt{|z|}) > 0$ for $z^* < z < 0$. Since $\gamma_2^{n^2}(z)$ is continuous and unique, it follows from (4.399) and (4.400) that

$$2n\pi < \gamma_2^{n^2}(z) < 2n\pi + 2\sqrt{|z|} \quad \text{when } z^* < z < 0. \quad (4.401)$$

Property (4.298) follows immediately from (4.401).

It remains to prove (4.299). First, we claim that there exists $z^* < 0$ such that

$$F\left(z, 2n\pi + \frac{3\pi^2}{|z|}\right) > 0 \quad \text{when } z < z^* \quad \text{and } n \geq 1. \quad (4.402)$$

By Lemmas 56 and 57 there exists a $\bar{z} < 0$ such that

$$\begin{aligned} F\left(z, 2n\pi + \frac{3\pi^2}{|z|}\right) &= \left(2n\pi + \frac{3\pi^2}{|z|}\right) \left[e^z - \cos\left(\frac{3\pi^2}{|z|}\right) \right] - z \sin\left(\frac{3\pi^2}{|z|}\right) \\ &= \left(2n\pi + \frac{3\pi^2}{|z|}\right) \left[e^z - \cos\left(\frac{3\pi^2}{|z|}\right) \right] + |z| \sin\left(\frac{3\pi^2}{|z|}\right) \\ &> -2\pi - \frac{\pi}{2} + |z| \frac{6\pi}{|z|} = \frac{7\pi}{2} > 0 \quad \forall z < \bar{z}. \end{aligned} \quad (4.403)$$

Since $\gamma_2^{n2}(z)$ is continuous and unique, it follows from (4.399) and (4.403) that

$$2n\pi + \frac{3\pi^2}{|z|} < \gamma_2^{n2}(z) < 2n\pi \quad \text{when } z < \bar{z} \text{ and } n \geq 1. \quad (4.404)$$

Property (4.299) follows from (4.404). This completes the proof of properties (4.298) and (4.299) in Theorem 10.

A fundamentally important consequence of property (4.298) in Theorem 10 is that we can now prove the limiting asymptotic result given in (4.300) regarding the eigenvalues $\lambda^{n2}(z)$:

$$\lambda^{n2}(z) \rightarrow -\frac{(2n\pi)^2}{2} \quad \text{as } z \rightarrow 0^-. \quad (4.405)$$

It follows from (4.297) that

$$\lambda^{n2}(z) = -\frac{(\gamma_2^{n2}(z))^2 + z^2}{2} \quad \text{when } z < 0 \text{ and } n \geq 1. \quad (4.406)$$

Applying property (4.298) in Theorem 10 to (4.406) gives (4.405). Lastly, property (4.301) follows from (4.299) and (4.406).

This completes the proof of Theorem 8.

4.4.1.4 Proof of Theorem 11. Recall from Lemma 40 in **Part II** above that $\gamma_2^{n1}(z) \in \mathbf{C}^1((-\infty, 0))$ for each $n \geq 1$ and

$$(2n - 1)\pi < \gamma_2^{n1}(z) < 2n\pi \quad \forall z < 0. \quad (4.407)$$

We begin with the proof of (4.302). Recall that

$$F(z, 2n\pi) < 0 \quad \text{when } z < 0 \text{ and } n \geq 1. \quad (4.408)$$

Next, we claim that there exists a $z^* < 0$ such that

$$F(z, 2n\pi - 2\sqrt{|z|}) > 0 \quad \text{when } z^* < z < 0 \text{ and } n \geq 1. \quad (4.409)$$

A calculation shows that

$$\begin{aligned}
F(z, 2n\pi - 2\sqrt{|z|}) &= (2n\pi - 2\sqrt{|z|}) \left[e^z - \cos(2\sqrt{|z|}) \right] - z \sin(2\sqrt{|z|}) \\
&> (2n\pi - 2\sqrt{|z|}) \left[e^z - \cos(2\sqrt{|z|}) \right] \\
&> (2n\pi - 2\sqrt{|z|}) \left[1 + z - \cos(2\sqrt{|z|}) \right]
\end{aligned}$$

where the last inequality follows from Lemma 31. Notice that $(2n\pi - 2\sqrt{|z|}) \rightarrow 2n\pi$ as $z \rightarrow 0^-$. Therefore, there exists $\hat{z} < 0$ such that

$$2n\pi - 2\sqrt{|z|} > 0 \quad \text{when } \hat{z} < z < 0. \quad (4.410)$$

By Lemma 55 there exists $z^\# < 0$ such that

$$1 + z - \cos(2\sqrt{|z|}) > 0 \quad \text{when } z^\# < z < 0. \quad (4.411)$$

Then, if $z^* = \text{Min}(|\hat{z}|, |z^\#|)$, it follows from (4.410) and (4.411) that

$$F(z, 2n\pi - 2\sqrt{|z|}) > 0 \quad \text{when } z^* < z < 0 \quad \text{and } n \geq 1. \quad (4.412)$$

Since $\gamma_2^{n1}(z)$ is continuous and unique, it follows from (4.408) and (4.412) that

$$2n\pi - 2\sqrt{|z|} < \gamma_2^{n1}(z) < 2n\pi \quad \text{when } z^* < z < 0. \quad (4.413)$$

Property (4.302) follows immediately from (4.413).

It remains to prove (4.303). We first prove two technical Lemmas.

Lemma 58. *Fix $n \geq 1$. Then there exists $z_3 < 0$ such that*

$$-\sin\left(\frac{2n\pi^2}{|z|}\right) < -\frac{4n\pi}{|z|} \quad \text{when } z < z_3. \quad (4.414)$$

Proof. Fix $n \geq 1$. Recall that $-\sin(x) < -\frac{2}{\pi}x$ for $x \in (0, \frac{\pi}{2})$. Since $\lim_{x \rightarrow \infty} \frac{2n\pi^2}{x} = 0$, there exists a $z_3 < 0$ such that $\frac{2n\pi^2}{|z|} \in (0, \frac{\pi}{2})$ when $z < z_3$. Therefore,

$$-\sin\left(\frac{2n\pi^2}{|z|}\right) < -\frac{2}{\pi}\left(\frac{2n\pi^2}{|z|}\right) = -\frac{4n\pi}{|z|} \quad \text{when } z < z_3 < 0. \quad (4.415)$$

□

Lemma 59. Fix $n \geq 1$. Then there exists a $z_4 < 0$ such that

$$\left((2n-1)\pi + \frac{2n\pi^2}{|z|} \right) \left[e^z + \cos \left(\frac{2n\pi^2}{|z|} \right) \right] < \frac{8n\pi - 3\pi}{2} \quad \text{when } z < z_4. \quad (4.416)$$

Proof. Elementary calculus shows that

$$\lim_{z \rightarrow -\infty} \left((2n-1)\pi + \frac{2n\pi^2}{|z|} \right) \left[e^z + \cos \left(\frac{2n\pi^2}{|z|} \right) \right] = 2(2n-1)\pi. \quad (4.417)$$

It follows that there exists $z_4 < 0$ such that

$$\left| \left((2n-1)\pi + \frac{2n\pi^2}{|z|} \right) \left[e^z + \cos \left(\frac{2n\pi^2}{|z|} \right) \right] - 2(2n-1)\pi \right| < \frac{\pi}{2} \quad (4.418)$$

for $z < z_4$.

Rearranging the terms we have that

$$\left((2n-1)\pi + \frac{2n\pi^2}{|z|} \right) \left[e^z + \cos \left(\frac{2n\pi^2}{|z|} \right) \right] < \frac{\pi}{2} + 4n\pi - 2\pi = \frac{8n\pi - 3\pi}{2} \quad (4.419)$$

when $z < z_4$. □

We now prove (4.303). Recall that

$$F(z, (2n-1)\pi) > 0 \quad \text{when } z < 0 \quad \text{and } n \geq 1. \quad (4.420)$$

Next, we claim that there exists a $z^* < 0$ such that

$$F \left(z, (2n-1)\pi + \frac{2n\pi^2}{|z|} \right) < 0 \quad \text{when } z < z^* < 0 \quad \text{and } n \geq 1. \quad (4.421)$$

A calculation shows that

$$\begin{aligned} F \left(z, (2n-1)\pi + \frac{2n\pi^2}{|z|} \right) &= \left((2n-1)\pi + \frac{2n\pi^2}{|z|} \right) \left[e^z + \cos \left(\frac{2n\pi^2}{|z|} \right) \right] + z \sin \left(\frac{2n\pi^2}{|z|} \right) \\ &= \left((2n-1)\pi + \frac{2n\pi^2}{|z|} \right) \left[e^z + \cos \left(\frac{2n\pi^2}{|z|} \right) \right] - |z| \sin \left(\frac{2n\pi^2}{|z|} \right) \end{aligned}$$

By Lemmas 58 and 59 there exists $z^* < 0$ such that

$$F \left(z, (2n-1)\pi + \frac{2n\pi^2}{|z|} \right) < \frac{8n\pi - 3\pi}{2} - |z| \frac{4n\pi}{|z|} = -\frac{3\pi}{2} \quad \text{when } z < z^* \quad (4.422)$$

and (4.421) follows.

Since $\gamma_2^{n1}(z)$ is continuous and unique, it follows from (4.420) and (4.421) that

$$(2n - 1)\pi < \gamma_2^{n1}(z) < (2n - 1)\pi + \frac{2n\pi^2}{|z|} \quad \text{when } z < z^* < 0 \quad (4.423)$$

Property (4.303) follows immediately from (4.423).

A fundamentally important consequence of property (4.302) in Theorem 11 is that we can now prove the limiting asymptotic result given in (4.304) regarding the eigenvalues $\lambda^{n1}(z)$:

$$\lambda^{n1}(z) \rightarrow -2(n\pi)^2 \quad \text{as } z \rightarrow 0^-. \quad (4.424)$$

It follows from (4.297) that

$$\lambda^{n1}(z) = -\frac{(\gamma_2^{n1}(z))^2 + z^2}{2} \quad \text{when } z < 0 \quad \text{and } n \geq 1. \quad (4.425)$$

Applying property (4.302) in Theorem 11 to (4.425) gives (4.424). Lastly, property (4.305) follows from (4.303) and (4.425).

This completes the proof of Theorem 11.

4.5 PARTIAL PROOF OF THE MATTIA-DEL GIUDICE CONJECTURE WHEN $\mu > 0$

In this section we provide a partial proof of the Mattia-Del Giudice Conjecture (see 3.4) when $\mu > 0$ and $V_L = V_R$ in the IF model. First, recall from Section 4.1 that the eigenvalues associated with the FPE for the IF model are given by

$$\lambda = \frac{\sigma^4(\gamma_1^2 - \gamma_2^2) - \mu^2\theta^2}{2\theta^2\sigma^2} + i\frac{\gamma_1\gamma_2\sigma^2}{\theta^2}, \quad (4.426)$$

where γ_1 and γ_2 satisfy

$$\gamma = \gamma_1 + i\gamma_2 = \frac{\theta}{\sigma^2}\sqrt{\mu^2 + 2\lambda\sigma^2}, \quad (4.427)$$

and $\gamma = \gamma_1 + i\gamma_2$ satisfies the algebraic equation

$$\gamma e^z = \gamma \cosh(\gamma) + z \sinh(\gamma), \quad z = \frac{\mu\theta}{\sigma^2} > 0. \quad (4.428)$$

The remainder of this section addresses the following:

4.5.1 In Theorem 12 we prove that all eigenvalues satisfying problem (4.426)-(4.427)-(4.428) must be complex.

4.5.2 We consider the branches of eigenvalues, $\lambda^n(\mu)$, whose existence was proved in Theorem 5 (see Section 4.3). In Theorem 13 we prove that

$$\operatorname{Re}(\lambda^n(\mu)) < 0 \text{ when } 0 < \mu < \frac{4\theta\pi^2}{\ln(2)}n^2 - \frac{\sigma^2}{2\theta}, \quad n \neq 0. \quad (4.429)$$

4.5.3 We state open problems that remain regarding the Mattia-Del Giudice conjecture.

4.5.1 All Eigenvalues are Complex When $\mu > 0$

In this section we investigate solutions of problem (4.426)-(4.427)-(4.428) describing the eigenvalues of the FPE corresponding to the IF model when $\mu > 0$, $\sigma > 0$, $V_L = V_R$ and $V_T = \theta > 0$.

Our goal is to prove

Theorem 12. *Let λ satisfy (4.426)-(4.427)-(4.428). Then each λ is complex.*

Proof. Assume that λ is given by (4.426) and is real, i.e.

$$i \frac{\gamma_1 \gamma_2 \sigma^2}{\theta^2} = 0. \quad (4.430)$$

There are three cases to consider:

Case I: $\gamma_1 = \gamma_2 = 0$.

Case II: $\gamma_1 = 0, \gamma_2 \neq 0$.

Case III: $\gamma_2 = 0, \gamma_1 \neq 0$.

Case I. Assume that $\gamma_1 = \gamma_2 = 0$. Then $\gamma = 0$ is a solution of equation (4.428). Set $\gamma_1 = \gamma_2 = 0$ in (4.426), and therefore

$$\lambda = -\frac{\mu^2}{2\sigma^2}. \quad (4.431)$$

We claim that the eigenfunction corresponding to $\lambda = -\frac{\mu^2}{2\sigma^2}$ is identically zero. The first step in proving this claim is to recall from Chapter 3 (see Section 3.2) that the corresponding eigenvalue problem is

$$\begin{cases} \lambda\phi(V) = -\mu\phi'(V) + \frac{\sigma^2}{2}\phi''(V) \\ \phi(\theta) = 0 \\ \phi'(\theta) = \phi'(0) - \frac{2\mu}{\sigma^2}\phi(0). \end{cases} \quad (4.432)$$

Assume that $\lambda = -\frac{\mu^2}{2\sigma^2}$ and obtain the boundary value problem

$$\begin{cases} -\frac{\mu^2}{2\sigma^2}\phi(V) = -\mu\phi'(V) + \frac{\sigma^2}{2}\phi''(V) \\ \phi(\theta) = 0 \\ \phi'(\theta) = \phi'(0) - \frac{2\mu}{\sigma^2}\phi(0). \end{cases} \quad (4.433)$$

To show that the only solution of the boundary value problem (4.433) is the trivial solution $\phi \equiv 0$ first note that

$$-\frac{\mu^2}{2\sigma^2}\phi(V) = -\mu\phi'(V) + \frac{\sigma^2}{2}\phi''(V) \quad (4.434)$$

is equivalent to

$$\phi''(V) - \frac{2\mu}{\sigma^2}\phi'(V) + \frac{\mu^2}{\sigma^4}\phi(V) = 0. \quad (4.435)$$

The general solution of equation (4.435) is

$$\phi(V) = C_1 e^{\frac{\mu}{\sigma^2}V} + C_2 V e^{\frac{\mu}{\sigma^2}V}. \quad (4.436)$$

The condition $\phi(\theta) = 0$ implies that

$$C_1 = -C_2\theta. \quad (4.437)$$

Thus, $C_1 = 0 \Leftrightarrow C_2 = 0$, in which case $\phi(V) = 0$ for all V . Assume that $C_1 \neq 0$ and $C_2 \neq 0$. Next, a differentiation of (4.436) gives

$$\phi'(V) = C_1 \frac{\mu}{\sigma^2} e^{\frac{\mu}{\sigma^2} V} + C_2 e^{\frac{\mu}{\sigma^2} V} + C_2 \frac{\mu}{\sigma^2} V e^{\frac{\mu}{\sigma^2} V}. \quad (4.438)$$

Combine (4.436)-(4.437)-(4.438) with the boundary condition $\phi'(\theta) = \phi'(0) - \frac{2\mu}{\sigma^2} \phi(0)$, and obtain

$$e^z = z + 1, \quad z = \frac{\mu\theta}{\sigma^2} > 0. \quad (4.439)$$

However, a routine calculation shows that

$$e^z = z + 1 \Leftrightarrow z = 0. \quad (4.440)$$

Under the assumption that $z > 0$, we conclude that $C_1 = C_2 = 0$, and therefore $\phi(V) = 0$ for all V . To summarize, if $\gamma_1 = \gamma_2 = 0$, there exist no non zero eigenvalues satisfying (4.426)-(4.427)-(4.428). This completes the analysis of **Case I**.

Case II. Assume that $\gamma_1 = 0$ and $\gamma_2 \neq 0$. Then $\gamma = i\gamma_2$, and (4.428) reduces to

$$\begin{aligned} i\gamma_2 e^z &= i\gamma_2 \cosh(i\gamma_2) + z \sinh(i\gamma_2) \\ &= i\gamma_2 \cos(\gamma_2) + iz \sin(\gamma_2) \end{aligned} \quad (4.441)$$

Consider the function

$$F(z, \gamma_2) = \gamma_2 e^z - \gamma_2 \cos(\gamma_2) - z \sin(\gamma_2), \quad z \geq 0, \quad \gamma_2 \neq 0. \quad (4.442)$$

Our goal is to show that $F(z, \gamma_2) \neq 0$ when $z > 0$ and $\gamma_2 \neq 0$. The following two lemmas will play a key role in proving this claim.

Lemma 60. *Let $F(z, \gamma_2)$ be given by (4.442). Then*

$$F(0, \gamma_2) = \begin{cases} \gamma_2(1 - \cos(\gamma_2)) \geq 0, & \gamma_2 > 0 \\ \gamma_2(1 - \cos(\gamma_2)) \leq 0, & \gamma_2 < 0. \end{cases} \quad (4.443)$$

Proof. The result follows from a direct calculation of $F(0, \gamma_2)$ and the inequality $-1 \leq \cos(\gamma_2) \leq 1$. □

Lemma 61. Let $F(z, \gamma_2)$ be given by (4.442). Then

$$F_z(0, \gamma_2) = \begin{cases} \gamma_2 - \sin(\gamma_2) > 0, & \gamma_2 > 0 \\ \gamma_2 - \sin(\gamma_2) < 0, & \gamma_2 < 0. \end{cases} \quad (4.444)$$

Furthermore, for $z > 0$,

$$F_z(z, \gamma_2) = \begin{cases} \gamma_2 e^z - \sin(\gamma_2) > 0, & \gamma_2 > 0 \\ \gamma_2 e^z - \sin(\gamma_2) < 0, & \gamma_2 < 0. \end{cases} \quad (4.445)$$

Proof. Property (4.444) follows from the well-known fact that

$$x - \sin(x) > 0, \quad x > 0 \quad (4.446)$$

and

$$x - \sin(x) < 0, \quad x < 0. \quad (4.447)$$

To prove (4.445) first consider the case $\gamma_2 > 0$ and note by (4.446) that $\gamma_2 > \sin(\gamma_2)$. It follows that

$$F_z(z, \gamma_2) = \gamma_2 e^z - \sin(\gamma_2) > \gamma_2(e^z - 1) > 0. \quad (4.448)$$

Next, assume that $\gamma_2 < 0$ and apply (4.447), i.e. $\gamma_2 < \sin(\gamma_2)$. Then

$$F_z(z, \gamma_2) = \gamma_2 e^z - \sin(\gamma_2) < \gamma_2(e^z - 1) < 0 \quad (4.449)$$

as desired. This completes the proof of Lemma 61. □

We now show that $\gamma_2 = 0$ is the only solution of $F(z, \gamma_2) = 0$ for $z = \frac{\mu\theta}{\sigma^2} > 0$. Fix $\bar{\gamma}_2 > 0$. By the fundamental theorem of calculus we have that

$$F(z, \bar{\gamma}_2) = F(0, \bar{\gamma}_2) + \int_0^z F_z(t, \bar{\gamma}_2) dt, \quad z \geq 0. \quad (4.450)$$

By Lemma 60 it follows that

$$F(z, \bar{\gamma}_2) \geq \int_0^z F_z(t, \bar{\gamma}_2) dt, \quad z \geq 0. \quad (4.451)$$

Combine Lemma 61 with (4.451) and conclude that

$$F(z, \bar{\gamma}_2) \geq \int_0^z F_z(t, \bar{\gamma}_2) dt > 0, \quad z > 0. \quad (4.452)$$

A similar argument shows that $F(z, \gamma_2) < 0$ for each $z > 0$ and $\gamma_2 < 0$. This concludes the proof that $F(z, \gamma_2) \neq 0$ when $z > 0$ and $\gamma_2 \neq 0$.

It follows that, if $\gamma_1 = 0$ and $\gamma_2 \neq 0$, there are no non zero eigenvalues satisfying (4.426)-(4.427)-(4.428). This completes **Case II**.

Case III. Assume that $\gamma_2 = 0$ and $\gamma_1 \neq 0$. Then $\gamma = \gamma_1$, and (4.428) reduces to

$$\gamma_1 e^z = \gamma_1 \cosh(\gamma_1) - z \sinh(\gamma_1). \quad (4.453)$$

We look for (z, γ_1) satisfying (4.453) by studying the function

$$H(z, \gamma_1) = \gamma_1 e^z - \gamma_1 \cosh(\gamma_1) - z \sinh(\gamma_1). \quad (4.454)$$

A direct evaluation of (4.454) shows that

$$H(z, \pm z) = 0. \quad (4.455)$$

We prove that $\gamma_1 = \pm z$ are the **only** solutions when $z > 0$. The proof of this requires two lemmas:

Lemma 62. Let $H(z, \gamma_1)$ be given by (4.454). Then,

$$H(0, \gamma_1) < 0 \text{ and } H_z(0, \gamma_1) < 0 \text{ for all } \gamma_1 > 0, \quad (4.456)$$

and

$$H(0, \gamma_1) > 0 \text{ and } H_z(0, \gamma_1) > 0 \text{ for all } \gamma_1 < 0. \quad (4.457)$$

Proof. A straightforward calculation gives

$$H(0, \gamma_1) = \begin{cases} \gamma_1(1 - \cosh(\gamma_1)) < 0, & \gamma_1 > 0 \\ \gamma_1(1 - \cosh(\gamma_1)) > 0, & \gamma_1 < 0. \end{cases} \quad (4.458)$$

□

Lemma 63. Let $H(z, \gamma_1)$ be given by (4.454). Then

$$H_{zz}(z, \gamma_1) = \begin{cases} \gamma_1 e^z < 0, & \gamma_1 < 0 \\ \gamma_1 e^z > 0, & \gamma_1 > 0. \end{cases} \quad (4.459)$$

Proof. The result follows from a direct calculation. □

We now complete the proof that $\gamma_1 = \pm z$ are the only solutions of $H(z, \gamma_1) = 0$ when $\gamma_1 \neq 0$.

Assume that $\gamma_1 = \bar{\gamma} > 0$. Lemma 4.457 implies that

$$H(0, \bar{\gamma}) < 0. \quad (4.460)$$

Define

$$z^* = \sup \{ \hat{z} \mid H(z, \bar{\gamma}) < 0, \text{ for all } z \in [0, \hat{z}] \} \quad (4.461)$$

Because $H(\bar{\gamma}, \bar{\gamma}) = 0$ we conclude that $0 < z^* \leq \bar{\gamma}$. From (4.461) it follows that

$$H(z^*, \bar{\gamma}) = 0 \text{ and } H_z(z^*, \bar{\gamma}) \geq 0. \quad (4.462)$$

By the fundamental theorem of calculus

$$H_z(z, \bar{\gamma}) = H_z(z^*, \bar{\gamma}) + \int_{z^*}^z H_{zz}(t, \bar{\gamma}) dt, \text{ for all } z \geq z^*. \quad (4.463)$$

By (4.462),

$$H_z(z, \bar{\gamma}) \geq \int_{z^*}^z H_{zz}(t, \bar{\gamma}) dt \text{ for all } z \geq z^*. \quad (4.464)$$

Lemma 63, along with (4.464) gives

$$H_z(z, \bar{\gamma}) \geq \int_{z^*}^z H_{zz}(t, \bar{\gamma}) dt > 0, \text{ for all } z \geq z^*. \quad (4.465)$$

We conclude that $H(z, \bar{\gamma}) > 0$ for all $z > z^*$. Therefore, z^* is the only solution of $H(z, \bar{\gamma}) = 0$. Since $H(\bar{\gamma}, \bar{\gamma}) = 0$ it must be the case that $z^* = \bar{\gamma}$ and the proof of **Case III** when $\gamma_1 > 0$ is complete. A similar argument shows that the only negative solution of $H(z, \gamma_1) = 0$ is $\gamma_1 = -z$.

Remark: The eigenvalues corresponding to $\gamma_2 = 0$, $\gamma_1 = \pm z$.

Assume that $\gamma_2 = 0$ and $\gamma_1 = \pm z$. Then equation (4.426) reduces to

$$\lambda = 0. \quad (4.466)$$

Therefore, there is no nonzero eigenvalue, λ , satisfying (4.426)-(4.427)-(4.428). This completes **Case III** and the proof of Theorem 12. \square

4.5.2 The Real Parts of the Eigenvalues are Negative

In this section we consider the branches of eigenvalues proved in Theorem 5 and prove the following:

Theorem 13. *Let $n \neq 0$ be an integer, and let $\lambda^n(\mu)$ satisfy Theorem 5. Then*

$$\text{Re}(\lambda^n) < 0 \text{ when } 0 < \mu < \frac{4\theta\pi^2}{\ln(2)}n^2 - \frac{\sigma^2}{2\theta}. \quad (4.467)$$

Proof. Recall from Lemma 27 (see Section 4.3) that $\gamma^n(z) = \gamma_1^n(z) + i\gamma_2^n(z)$ satisfies

$$0 < \gamma_1^n < \gamma_1^* = \ln(e^z + \sqrt{e^{2z} - 1}), \quad z > 0, \quad (4.468)$$

and

$$2n\pi < \gamma_2^n < 2n\pi + \pi/2. \quad (4.469)$$

Next, recall from (4.426) that

$$\operatorname{Re}(\lambda^n) = \frac{\sigma^4(\gamma_1^2 - \gamma_2^2) - \mu^2\theta^2}{2\theta^2\sigma^2}. \quad (4.470)$$

Applying the inequalities (4.468) and (4.469) to (4.470) gives

$$\frac{\sigma^4(\gamma_1^2 - \gamma_2^2) - \mu^2\theta^2}{2\theta^2\sigma^2} < \frac{\sigma^4((\ln(e^z + \sqrt{e^{2z} - 1}))^2 - 4n^2\pi^2) - \mu^2\theta^2}{2\theta^2\sigma^2}. \quad (4.471)$$

Note that $\sqrt{e^{2z} - 1} < e^z$ when $z > 0$. Therefore, by (4.470) and (4.471), we have

$$\operatorname{Re}(\lambda^n) < \frac{\sigma^4([\ln(2e^z)]^2 - 4n^2\pi^2) - \mu^2\theta^2}{2\theta^2\sigma^2}. \quad (4.472)$$

Expand the term $[\ln(2e^z)]^2$ and obtain

$$\operatorname{Re}(\lambda^n) < \frac{\sigma^4(\ln(2)^2 + 2\ln(2)z + z^2 - 4n^2\pi^2) - \mu^2\theta^2}{2\theta^2\sigma^2}. \quad (4.473)$$

Set $z = \frac{\mu\theta}{\sigma^2}$ in (4.473) to obtain

$$\operatorname{Re}(\lambda^n) < \frac{\sigma^2 \ln(2)^2}{2\theta^2} + \ln(2)\frac{\mu}{\theta} - \frac{2n^2\pi^2\sigma^2}{\theta^2}. \quad (4.474)$$

The right hand side of (4.474) is negative when

$$0 < \mu < \frac{4\theta\pi^2}{\ln(2)}n^2 - \frac{\sigma^2}{2\theta}. \quad (4.475)$$

This completes the proof of Theorem 13. □

4.5.3 Open Problem: Real parts of the Eigenvalues are Negative

Suppose that $\lambda = \lambda_1 + i\lambda_2$ is an eigenvalue satisfying (4.426)-(4.427)-(4.428). Prove that the corresponding eigenfunctions form a complete set, and that

$$\operatorname{Re}(\lambda) < 0 \text{ for all } z = \frac{\mu\theta}{\sigma^2} > 0. \quad (4.476)$$

4.6 PARTIAL PROOF OF THE MATTIA-DEL GIUDICE CONJECTURE WHEN $\mu < 0$

In this section we give a partial proof of the Mattia-Del Giudice Conjecture (see 3.4) when $\mu < 0$ and $V_L = V_R$ in the IF model. Recall from Section 4.1 that the eigenvalues associated with the FPE for the IF model are given by

$$\lambda = \frac{\sigma^4(\gamma_1^2 - \gamma_2^2) - \mu^2\theta^2}{2\theta^2\sigma^2} + i\frac{\gamma_1\gamma_2\sigma^2}{\theta^2}, \quad (4.477)$$

where γ_1 and γ_2 satisfy

$$\gamma = \gamma_1 + i\gamma_2 = \frac{\theta}{\sigma^2}\sqrt{\mu^2 + 2\lambda\sigma^2}, \quad (4.478)$$

and $\gamma = \gamma_1 + i\gamma_2$ satisfies the algebraic equation

$$\gamma e^z = \gamma \cosh(\gamma) + z \sinh(\gamma), \quad z = \frac{\mu\theta}{\sigma^2} > 0. \quad (4.479)$$

In this section we address the following:

4.6.1 We consider the branches of eigenvalues proved in Theorem 9 and give a partial proof of the Mattia-Del Giudice Conjecture (see 3.4) when $\mu < 0$ and $V_L = V_R$ in the IF model.

4.6.2 We state an open problem regarding the Mattia-Del Giudice Conjecture.

4.6.1 Eigenvalues are Negative when $\gamma_1 = 0$

We consider the branches of eigenvalues proved in Theorem 9 and prove the following

Theorem 14. *Let $n \neq 0$ be an integer, and let $\lambda^{n1}(\mu)$ and $\lambda^{n2}(\mu)$ satisfy Theorem 9. Then*

$$\lambda^{n1}(\mu) < 0 \text{ and } \lambda^{n2}(\mu) < 0, \quad \mu < 0, \quad n \neq 0. \quad (4.480)$$

Proof. Recall that in Theorem 9 we assume λ^{n1} and λ^{n2} are real and set $\gamma_1 = 0$. Thus, (4.477) reduces to

$$\lambda^{n1} = -\frac{\sigma^4}{2\theta^2\sigma^2}(\gamma_2^2 + \mu^2\theta^2) < 0, \quad \mu < 0. \quad (4.481)$$

A similar argument shows that $\lambda^{n2} < 0$, $\mu < 0$. This completes the proof of Theorem 14. \square

4.6.2 Open Problem: The Eigenvalues are Real and Negative

Suppose that $\lambda = \lambda_1 + i\lambda_2$ is an eigenvalue satisfying (4.477)-(4.478)-(4.479). Prove that the corresponding eigenfunctions form a complete set, and that λ is real with

$$\lambda < 0 \text{ for all } z = \frac{\mu\theta}{\sigma^2} < 0. \quad (4.482)$$

5.0 THE FIRING RATE

In this chapter we make use of the eigenvalues and eigenfunctions whose existence was proved in Chapter 4 to study the firing rate function corresponding to the IF model when $V_L = V_R = 0$ and $V_T = \theta > 0$. In particular, we set $\mu > 0$ and do the following:

5.1 The eigenvalues are explicitly calculated and the theoretical firing rate function is generated by an eigenfunction expansion. Next, a numerical simulation of the population firing rate is performed. Upon comparison, one sees that the numerical simulation is in agreement with theoretical results of Chapter 4.

5.2 Asymptotic properties of the firing rate function are developed. Relative error is introduced and a numerical experiment is performed to illustrate the relative error.

5.1 NUMERICAL SIMULATIONS FOR IF WHEN $\mu > 0$

In this section our primary goal is to compute the firing rate function $\nu(t)$ when $\mu > 0$. For this computation we make use of the eigenvalue structure of the IF model to generate the eigenfunction expansion representation for the Fokker Planck PDE. This will give us confidence in our theoretical predictions. Throughout, we follow Mattia [24], and keep θ and σ fixed at the values $\theta = \sigma = 1$. In particular, we do the following:

5.1.1 We numerically compute the eigenvalues, denoted by λ_i , when $\mu > 0$. In Tables 2, 4, 6, 8 below we list the first ten eigenvalues when $\mu = 20, 5, 1$ and $.1$

5.1.2 We use the computed values to determine, and plot (see Figure 12), the corresponding neuronal firing rate functions, $\nu(t)$. Next (see Figure 14), we simulate a population of

$N = 10000$ IF neurons and plot the population firing rate. In Figure 14 we compare the population (i.e. N is finite) firing rate with the theoretical (i.e. $N = \infty$) firing rate.

5.1.1 Numerical Computation of the Eigenvalues.

Recall from Section 4.1.3 that the eigenvalues λ satisfy

$$\gamma e^z = \gamma \cosh(\gamma) + z \sinh(\gamma), \quad (5.1)$$

where

$$z = \frac{\mu\theta}{\sigma^2} < 0 \quad \text{and} \quad \gamma = \gamma_1 + i\gamma_2 = \frac{\theta}{\sigma^2} \sqrt{\mu^2 + 2\lambda\sigma^2}. \quad (5.2)$$

We use Matlab (see Section A.4 for details) to do the following computations: First, we compute γ_1 and γ_2 . Then, using (5.2), we compute the eigenvalues

$$\lambda = \text{Re}(\lambda) + i \text{Im}(\lambda) = \frac{\gamma_1^2 - \gamma_2^2 - \mu^2}{2} + i\gamma_1\gamma_2. \quad (5.3)$$

To compute γ_1 and γ_2 replace γ with $\gamma_1 + i\gamma_2$ in (5.1). Separating real and imaginary parts, we have two non linear functions

$$F(\gamma_1, \gamma_2, z) = \gamma_1 e^z - \gamma_1 \cosh(\gamma_1) \cos(\gamma_2) + \gamma_2 \sinh(\gamma_1) \sin(\gamma_2) - z \sinh(\gamma_1) \cos(\gamma_2)$$

and

$$G(\gamma_1, \gamma_2, z) = \gamma_2 e^z - \gamma_1 \sinh(\gamma_1) \sin(\gamma_2) - \gamma_2 \cosh(\gamma_1) \cos(\gamma_2) - z \cosh(\gamma_1) \sin(\gamma_2).$$

Thus, to find γ_1 and γ_2 , we solve the system

$$F(\gamma_1, \gamma_2, z) = 0$$

$$G(\gamma_1, \gamma_2, z) = 0.$$

To solve this system we use Matlab solver `fsolve`. Tables 2, 4, 6 and 8 below give the γ and λ values when $\mu = 20, 5, 1, 0.1$ For a discussion of these tables see Section 5.1.1.1.

5.1.1.1 Remarks About the Eigenvalue Tables

- The left two columns of Table 1 represent the first 10 values of $\gamma = \gamma_1 + i\gamma_2$, where γ_1 and γ_2 are the simulated solutions of the equations $F(\gamma_1, \gamma_2) = 0$, $G(\gamma_1, \gamma_2) = 0$. The right two columns of Table 1 are the values of $F(\gamma_1, \gamma_2)$ and $G(\gamma_1, \gamma_2)$. The number of zeros to the right of the decimal point in the F and G evaluations increases as μ decreases to zero (see Tables 3,5,7 below). This suggests an improvement in numerical error as μ decreases. Table 2 gives the real and imaginary parts of the eigenvalues corresponding to the γ values in Table 1.
- The left two columns of Table 3 represent the first 10 values of $\gamma = \gamma_1 + i\gamma_2$, where γ_1 and γ_2 are the simulated solutions of the equations $F(\gamma_1, \gamma_2) = 0$, $G(\gamma_1, \gamma_2) = 0$. The right two columns of Table 3 are the values of $F(\gamma_1, \gamma_2)$ and $G(\gamma_1, \gamma_2)$. The number of zeros to the right of the decimal point in the F and G evaluations increases as μ decreases to zero (see Tables 1, 5, 7). Again, this suggests an improvement in numerical error as μ decreases. Table 4 gives the real and imaginary parts of the eigenvalues corresponding to the γ values in Table 3. These results match the results of Mattia [24] (Fig. 1, p. 12).
- The left two columns of Table 5 represent the first 10 values of $\gamma = \gamma_1 + i\gamma_2$, where γ_1 and γ_2 are the simulated solutions of the equations $F(\gamma_1, \gamma_2) = 0$, $G(\gamma_1, \gamma_2) = 0$. The right two columns of Table 5 are the values of $F(\gamma_1, \gamma_2)$ and $G(\gamma_1, \gamma_2)$. The number of zeros to the right of the decimal point in the F and G evaluations increases as μ decreases to zero (see Tables 1,3,7). This suggests an improvement in numerical error as μ decreases. Table 6 gives the real and imaginary parts of the eigenvalues corresponding to the γ values in Table 5. These results match the results of Mattia [24] (Fig. 1, p. 12).
- The left two columns of Table 7 represent the first 10 values of $\gamma = \gamma_1 + i\gamma_2$, where γ_1 and γ_2 are the simulated solutions of the equations $F(\gamma_1, \gamma_2) = 0$, $G(\gamma_1, \gamma_2) = 0$. The right two columns of Table 7 are the values of $F(\gamma_1, \gamma_2)$ and $G(\gamma_1, \gamma_2)$. The number of zeros to the right of the decimal point in the F and G evaluations increases as μ decreases to zero (see Tables 1,3,5 above). This suggests an improvement in numerical error as μ decreases. Table 8 gives the real and imaginary parts of the eigenvalues corresponding to the γ values in Table 7. These results match the results of Mattia [24] (Fig. 1, p. 12).

5.1.2 The Firing Rate Function

In this section we use the first four eigenvalues computed in Section 5.1.1 to approximate the theoretical firing rate function (see Figures 12 and 14). For this, recall from Section 2.2.2 that the theoretical firing rate (see Mattia [24] pp. 051917-3, equation 2.6) is given by

$$\nu(t) = -\frac{\sigma^2}{2}\rho_V(\theta, t|V_0, 0), \quad (5.4)$$

where

$$\rho(V, t|V_0, 0) = \sum_{-\infty}^{\infty} \psi_n(V_0)e^{\lambda_n t}\phi_n(V). \quad (5.5)$$

The eigenfunctions $\phi_n(V)$ and $\psi_n(V)$ above were developed in Chapter 4.1.4. Below, in Figure 12, we plot $\nu(t)$ for four different values of μ . For instructions on reproducing these plots see Section A.5.

5.1.2.1 Numerical Simulation of a Population of IF neurons To perform a numerical simulation first recall that an IF neuron is modeled by the SDE

$$dV = \mu dt + \sigma dW, \quad V_L \leq V(0) = V_0 \leq V_T. \quad (5.6)$$

where $\infty < V_L < V_T$. There exists a reset value $V_R \in (V_L, V_T)$ when the neuron fires:

$$\text{if } V(t^-) = V_T, \text{ then } V(t^+) = V_R. \quad (5.7)$$

The range of $V(t)$ is

$$V_L \leq V(t) \leq V_T, \quad \forall t \geq 0, \quad (5.8)$$

and we assume reflective boundary conditions when $V(t) = V_L$.

Computation of the Firing Rate

For a finite number N of IF neurons, we follow Mattia [24], and define the population firing rate $\nu_N(t)$ by

$$\nu_N(t) = \lim_{\Delta t \rightarrow 0} \frac{N(t, t + \Delta t)}{N\Delta t} \quad (5.9)$$

where $N(t, t + \Delta t)$ is the number of times the neurons fire in the time interval $(t, t + \Delta t)$.

The precise instructions to duplicate the simulation and Figure 14 can be found in Section A.5.2 in the Appendix .

5.2 FIRING RATE ANALYSIS WHEN $\mu > 0$

In this chapter we investigate asymptotic properties of the firing rate function generated by an eigenfunction expansion of solutions of the FPE (i.e. the Fokker Planck equation), when $\mu > 0$. In particular we do the following:

5.2.1 We develop the theoretical firing rate function $\nu(t)$ generated by an eigenfunction expansion of solutions of the FPE problem when $\mu > 0$, $\sigma > 0$ and $V_T = \theta > 0$. Using the resultant formula for $\nu(t)$, we show that

$$\nu(\infty) = \lim_{t \rightarrow \infty} \nu(t) = C = \left[\frac{\sigma^2}{2\mu^2} \left(\frac{2\mu\theta}{\sigma^2} - 1 + e^{-2\frac{\mu\theta}{\sigma^2}} \right) \right]^{-1}. \quad (5.10)$$

5.2.2 We prove Theorem 15, which describes asymptotic formulas for the following:

- (i) $\nu(\infty)$ when $\mu > 0$ is fixed and $\sigma \rightarrow 0^+$.
- (ii) $\nu(\infty)$ when $\sigma > 0$ is fixed and $\mu \rightarrow 0^+$.

5.2.3 We provide a numerical calculation to illustrate the relative error between C and the formulas provided in Theorem 15.

5.2.1 The Firing Rate function generated by the FPE.

Recall from Chapter 2 that the theoretical firing rate (see Mattia [24] pp. 051917-3, equation 2.6) is given by

$$\nu(t) = -\frac{\sigma^2}{2} \rho_V(\theta, t|V_0, 0), \quad (5.11)$$

where $\rho(V, t|V_0, 0)$ is assumed to have the eigenfunction expansion

$$\rho(V, t|V_0, 0) = \phi_0(v) + \sum_{n \neq 0} \psi_n(V_0) e^{\lambda^n t} \phi_n(V). \quad (5.12)$$

A differentiation of (5.12) gives

$$\rho_V(\theta, t|V_0, 0) = \phi'_0(\theta) + \sum_{n \neq 0} \psi_n(V_0) e^{\lambda_n t} \phi'_n(\theta). \quad (5.13)$$

Thus, combining (5.11) and (5.13) gives

$$\nu(t) = -\frac{\sigma^2}{2} \left(\phi'_0(\theta) + \sum_{n \neq 0} \psi_n(V_0) e^{\lambda_n t} \phi'_n(\theta) \right). \quad (5.14)$$

In Section 4.3 we proved that the n^{th} eigenvalue, λ^n , is complex and of the form

$$\lambda^n = \lambda_1^n + i\lambda_2^n, \quad n \geq 1 \quad (5.15)$$

where $\lambda_1^n < 0$ and $\lambda_2^n \neq 0$. We also proved that

$$\lambda^{-n} = \lambda^n, \quad n \geq 1. \quad (5.16)$$

These properties, combined with (5.14), imply that

$$\nu(\infty) = \lim_{t \rightarrow \infty} \nu(t) = -\frac{\sigma^2}{2} \phi'_0(\theta). \quad (5.17)$$

It was shown in Chapter 2 that

$$\phi_0(V) = \frac{C}{\mu} \left[1 - e^{-2\frac{z(\theta-V)}{\theta}} \right] \quad (5.18)$$

where

$$C = \left[\frac{\sigma^2}{2\mu^2} \left(\frac{2\mu\theta}{\sigma^2} - 1 + e^{-2\frac{\mu\theta}{\sigma^2}} \right) \right]^{-1}. \quad (5.19)$$

Remark: This formula for C was previously developed by Mattia [24].

Next, a differentiation of 5.18 yields

$$\phi'_0(V) = -2\frac{zC}{\mu\theta} e^{-2\frac{z(\theta-V)}{\theta}} \quad (5.20)$$

Thus, since $z = \frac{\mu\theta}{\sigma^2}$, it follows that

$$\phi'_0(\theta) = -2\frac{zC}{\mu\theta} = -\frac{2}{\sigma^2} C \quad (5.21)$$

This, together with (5.17) and (5.19), give

$$\nu(\infty) = -\frac{\sigma^2}{2} \phi'_0(\theta) = C = \left[\frac{\sigma^2}{2\mu^2} \left(\frac{2\mu\theta}{\sigma^2} - 1 + e^{-2\frac{\mu\theta}{\sigma^2}} \right) \right]^{-1}. \quad (5.22)$$

5.2.2 Asymptotic Results for the Firing Rate Function

Below, in Theorem 15 we prove asymptotic formulae for $\nu(\infty)$. The statement of Theorem 15 requires the following definition for asymptotic limit:

$$f(x) \sim g(x) \text{ as } x \rightarrow a \iff \lim_{x \rightarrow a} \frac{f(x)}{g(x)} = 1. \quad (5.23)$$

Theorem 15. *Let C be defined as in (5.22), i.e.*

$$\nu(\infty) = C = \left[\frac{\sigma^2}{2\mu^2} \left(\frac{2\mu\theta}{\sigma^2} - 1 + e^{-2\frac{\mu\theta}{\sigma^2}} \right) \right]^{-1}. \quad (5.24)$$

(i) *Let $\mu > 0$. Then*

$$C \sim \frac{\mu}{\theta} \left(1 + \frac{\sigma^2}{2\mu\theta} \right) \text{ as } \sigma \rightarrow 0^+. \quad (5.25)$$

(ii) *Let $\sigma > 0$. Then*

$$C \sim \frac{\sigma^2}{\theta^2} \left(1 + \frac{2\mu\theta}{3\sigma^2} \right) \text{ as } \mu \rightarrow 0^+. \quad (5.26)$$

Proof. We begin by proving (5.25). A direct computation shows that

$$\begin{aligned} \lim_{\sigma \rightarrow 0^+} \frac{\theta}{\mu} \frac{C}{1 + \frac{\sigma^2}{2\mu\theta}} &= \lim_{\sigma \rightarrow 0^+} \frac{2\mu\theta}{\sigma^2} \left(\frac{1}{1 + \frac{\sigma^2}{2\mu\theta}} \right) \left(\frac{1}{\frac{2\mu\theta}{\sigma^2} - 1 + e^{-2\mu\theta/\sigma^2}} \right) \\ &= \lim_{\sigma \rightarrow 0^+} \left(\frac{2\mu\theta}{1 + \frac{\sigma^2}{2\mu\theta}} \right) \left(\frac{1}{2\mu\theta - \sigma^2 + \sigma^2 e^{-2\mu\theta/\sigma^2}} \right). \\ &= 1 \end{aligned}$$

This completes the proof of (5.25).

To prove (5.26) first apply L'Hospital's rule twice and obtain

$$\begin{aligned} \lim_{\mu \rightarrow 0^+} \frac{\mu^2}{\frac{2\mu\theta}{\sigma^2} - 1 + e^{-2\mu\theta/\sigma^2}} &= \lim_{\mu \rightarrow 0^+} \frac{2\mu}{\frac{2\theta}{\sigma^2} - \frac{2\theta}{\sigma^2} e^{-2\mu\theta/\sigma^2}} \\ &= \lim_{\mu \rightarrow 0^+} \frac{2}{\frac{4\theta^2}{\sigma^4} e^{-2\mu\theta/\sigma^2}} \\ &= \frac{\sigma^4}{2\theta^2}. \end{aligned} \quad (5.27)$$

Note that

$$\frac{C\theta^2}{\sigma^2} \frac{1}{1 + \frac{2\mu\theta}{3\sigma^2}} = \frac{2\theta^2}{\sigma^4} \left(\frac{1}{1 + \frac{2\mu\theta}{3\sigma^2}} \right) \left(\frac{\mu^2}{\frac{2\mu\theta}{\sigma^2} - 1 + e^{-2\mu\theta/\sigma^2}} \right). \quad (5.28)$$

Finally, combine (5.27) and (5.28), and obtain

$$\lim_{\mu \rightarrow 0^+} \frac{C\theta^2}{\sigma^2} \frac{1}{1 + \frac{2\mu\theta}{3\sigma^2}} = \frac{2\theta^2}{\sigma^4} \cdot 1 \cdot \frac{\sigma^4}{2\theta^2} = 1. \quad (5.29)$$

This completes the proof of Theorem 15. \square

5.2.3 Relative Error Between Theoretical and Numerical Values of $\nu(\infty)$

In this section we investigate the relative error between C and the approximations described in Theorem 15. The relative error between C and the approximation $\frac{\mu}{\theta} \left(1 + \frac{\sigma^2}{2\mu\theta}\right)$ is given by

$$\text{Relative Error} = \frac{\left|C - \frac{\mu}{\theta} \left(1 + \frac{\sigma^2}{2\mu\theta}\right)\right|}{|C|}. \quad (5.30)$$

Similarly, the relative error between C and the approximation $\frac{\sigma^2}{\theta^2} \left(1 + \frac{2\mu\theta}{3\sigma^2}\right)$ is given by

$$\text{Relative Error} = \frac{\left|C - \frac{\sigma^2}{\theta^2} \left(1 + \frac{2\mu\theta}{3\sigma^2}\right)\right|}{|C|}. \quad (5.31)$$

Below, in Table 5.2.3 we compute the relative errors, (5.30) and (5.31), for the numerical results in Figure 12, that was completed in Section 5.1.

5.3 FIRING RATE WHEN $\mu(T)$ IS A STEP FUNCTION

In real nervous systems neurons react to inputs from dynamic environments (e.g. sensory, memory recall). The input statistics for a given neuron change during the course of a task. Thus, in the context of the stochastic IF SDE

$$dV = \mu dt + \sigma dW, \quad (5.32)$$

$\mu(t)$ and/or $\sigma(t)$ are time dependent quantities. A simple example illustrating this property is when the neuron input $\mu(t)$ is a step function, e.g.

$$\mu(t) = \begin{cases} 0 & 0 \leq t < T^* = 1000 \text{ msec.}, \\ 25 & t \geq T^*, \end{cases} \quad (5.33)$$

and $\sigma(t)$ is constant, e.g.

$$\sigma(t) = 1 \quad \forall t \geq 0. \quad (5.34)$$

In this section we assume that $\mu(t)$ is of the form (5.33) and $\sigma(t) \equiv 1$ and perform two tasks.

I. Determine the theoretical firing rate in terms of an eigenfunction expansion solution of the corresponding FPE.

II. Next, we simulate a population of 10000 IF neurons and determine the population mean firing rate, and we see that the theory and simulation are in agreement.

5.3.1 Theoretical Firing rate

Recall that $V_L = V_R = 0$ and $V_T = \theta$. Since $\mu(t)$ is constant on the intervals $[0, 1000]$ and $(1000, \infty)$ we apply the results of Chapter 4. Thus, on the interval $(1000, \infty)$, $\mu = 25$ and it follows that

$$\rho(V, t|V_0, 0) = \sum_{n=-\infty}^{\infty} A_n e^{\lambda_n t} \phi_n(V), \quad t > 1000. \quad (5.35)$$

It was shown in Section 4.2 that there is no eigenfunction expansion solution for $\rho(V, t|V_0, 0)$ when $\mu = 0$. Under the assumption that $\rho(V, t|V_0, 0)$ relaxes to its stationary solution for large t we set

$$\rho(V, t|V_0, 0) = \frac{2}{\theta^2}(\theta - V), \quad 0 \leq t \leq 1000. \quad (5.36)$$

Therefore,

$$\rho(V, t|V_0, 0) = \begin{cases} \frac{2}{\theta^2}(\theta - V), & 0 \leq t \leq 1000, \\ \sum_{n=-\infty}^{\infty} A_n e^{\lambda_n(t-1000)} \phi_n(V), & t > 1000. \end{cases} \quad (5.37)$$

The constants A_n are determined so that $\rho(V, t|V_0, 0)$ is continuous at $t = 1000$:

$$\frac{2}{\theta^2}(\theta - V) = \sum_{n=-\infty}^{\infty} A_n \phi_n(V). \quad (5.38)$$

Recall that the functions $\psi_n(V)$ satisfy the orthonormal condition

$$\int_0^\theta \phi_n(V) \psi_m(V) dV = \begin{cases} 1, & m = n, \\ 0, & m \neq n. \end{cases} \quad (5.39)$$

Multiply each side of (5.38) by $\psi_m(V)$, integrate, and apply (5.39) to obtain

$$A_n = \int_0^\theta \frac{2}{\theta^2}(\theta - V) \psi_n(V) dV. \quad (5.40)$$

5.3.2 Population Firing Rate

The left panel of Figure 15 illustrates a simulation of population mean firing rate, $\nu_N(t)$, for $N = 10,000$ neurons. Here, we assume that each neuron satisfies the initial condition $V(0) = V_R = 0$. Over the subinterval $0 \leq t < T^* = 1000$ the neurons receive constant input $\mu = 0$, and the population mean firing rate quickly relaxes to the equilibrium level $\nu_N(\infty) \approx 1$. When $t \geq 1000$ the input discontinuously jumps to the new constant level $\mu = 25$. In response to this discontinuous change of input, the population mean firing rate initially undergoes oscillations (i.e. ringing) with peaks that decrease in amplitude during a transition period of length approximately 200 *msecs*. By the end of this transition interval, the firing rate has relaxed to its equilibrium level, $\nu_N \approx 25$. The right panel shows the theoretical mean firing rate, $\nu(t)$, resulting from the eigenfunction expansion method. During the transition interval, $[1000, 1200)$, the theoretical firing rate $\nu(t)$ also undergoes oscillations, with peaks that decrease to zero in amplitude as the $\nu(t)$ relaxes to its equilibrium level, $\nu \approx 25$ (see Section 5.2.2). A major thrust of this thesis is to give a firm foundation to the use of the eigenfunction expansion to understand non equilibrium behavior of firing rate when μ and σ are constant during the two subintervals $[0, T^*)$ and $[T^*, \infty)$. Our study includes the parameter regime $\mu > 0$ and $\sigma > 0$, and also the regime $\mu < 0$ and $\sigma > 0$.

5.4 PROOF THAT $E([\nu_N(T) - \nu(T)]^2) \approx \frac{\nu(T)}{N\Delta T}$, $N \gg 1$.

In this section our goal is to obtain, under reasonable assumptions on a population of neurons, the following approximation:

$$E([\nu_N(t) - \nu(t)]^2) \approx \frac{\nu(t)}{N\Delta t}, \quad N \gg 1. \quad (5.41)$$

Proof of (5.41): Fix $N \gg 1$ and consider a population of N neurons with uncorrelated input. For each $i \in [1, N]$, define

$$X_i(t) = \text{the number of spikes emitted by the } i\text{th cell in } (0, t). \quad (5.42)$$

Set

$$\Delta X_i(t) = X_i(t + \Delta t) - X_i(t), \quad (5.43)$$

and note that

$$\Delta X_i(t) = \text{the number of spikes emitted by the } i\text{th cell in the interval } (t, t + \Delta t). \quad (5.44)$$

Fix $t > 0$, and let $\Delta t > 0$ be small. Assume that each $\Delta X_i(t)$ is a Poisson random variable with parameter $\nu(t)$, which is essentially constant for large t . Then

$$E(\Delta X_i(t)) = \nu(t)\Delta t = \text{Var}(\Delta X_i(t)), \quad 1 \leq i \leq N. \quad (5.45)$$

An application of the Central Limit Theorem gives

$$\sum_{i=1}^N (\Delta X_i(t)) - N\nu(t)\Delta t \approx \sqrt{\nu(t)N\Delta t}N(0, 1), \quad N \gg 1. \quad (5.46)$$

Multiply (5.46) by $\frac{1}{N\Delta t}$ to obtain

$$\frac{1}{N\Delta t} \sum_{i=1}^N (\Delta X_i(t)) - \nu(t) \approx \sqrt{\frac{\nu(t)}{N\Delta t}}N(0, 1), \quad N \gg 1. \quad (5.47)$$

Recall that

$$\nu_N(t) \approx \frac{N(t, t + \Delta t)}{N\Delta t} = \frac{\sum_{i=1}^N (\Delta X_i(t))}{N\Delta t}. \quad (5.48)$$

It follows from (5.47) and (5.48) that

$$\nu_N(t) - \nu(t) \approx \sqrt{\frac{\nu(t)}{N\Delta t}} N(0, 1), \quad N \gg 1. \quad (5.49)$$

Recall that $E(N(0, 1)) = 0$. Therefore,

$$\begin{aligned} E([\nu_N(t) - \nu(t)]^2) &= \text{Var}(\nu_N(t) - \nu(t)) \\ &= \text{Var}\left(\sqrt{\frac{\nu(t)}{N\Delta t}} N(0, 1)\right) \\ &= \frac{\nu(t)}{N\Delta t} \text{Var}(N(0, 1)) \\ &= \frac{\nu(t)}{N\Delta t}. \end{aligned}$$

Table 1: $\gamma = \gamma_1 + i\gamma_2$ when $\mu = 20, \theta = \sigma = 1$.

γ_1	γ_2	$F(\gamma_1, \gamma_2)$	$G(\gamma_1, \gamma_2)$
20.0472	6.4344	0.000003814697	0.000004291534
20.1347	12.8242	-0.000008583064	-0.000003814697
20.2334	19.1633	-0.000029563903	-0.000001907348
20.3219	25.4668	0.000004291534	-0.000026702880
20.3943	31.7497	-0.000032424926	0.000005722045
20.4515	38.0220	-0.000048637390	0.000026702880
20.4962	44.2896	-0.000061988830	0.000003814697
20.5311	50.5556	0.000030517578	-0.000049591064
20.5586	56.8215,	0.000031471252	0.000034332275
20.5805	63.0882,	0.000064849853	-0.000045776367

Table 2: $\lambda = \text{Re}(\lambda) + i\text{Im}(\lambda)$ when $\mu = 20, \theta = \sigma = 1$.

$\text{Re}(\lambda)$	$\text{Im}(\lambda)$
-19.755	128.993
-79.526	258.214
-178.920	387.742
-317.788	517.535
-496.057	647.515
-713.706	777.611
-970.739	907.772
-1267.170	1037.967
-1603.014	1168.176
-1978.283	1298.388

Table 3: $\gamma = \gamma_1 + i\gamma_2$ when $\mu = 5, \theta = \sigma = 1$.

γ_1	γ_2	$F(\gamma_1, \gamma_2)$	$G(\gamma_1, \gamma_2)$
5.3346	6.6063	-0.000000000000	-0.000000000000
5.5307	12.8469	0.000000000078	0.000000000077
5.6095	19.0715	0.000000000000	-0.000000000007
5.6458	25.3117	-0.000000000005	-0.000000000001
5.6648	31.5644	0.000000000001	-0.000000000002
5.6758	37.8254	0.000000000009	0
5.6827	44.0920	0.000000000003	-0.000000000003
5.6874	50.3623	0.000000000005	0.000000000002
5.6906	56.6352	-0.000000000025	0.000000000003
5.6929	62.9101	-0.000000000007	0

Table 4: $\lambda = \text{Re}(\lambda) + i\text{Im}(\lambda)$ when $\mu = 5, \theta = \sigma = 1$.

$\text{Re}(\lambda)$	$\text{Im}(\lambda)$
-20.092	35.242
-79.727	71.053
-178.628	106.983
-316.904	142.905
-494.612	178.807
-711.776	214.692
-968.406	250.566
-1264.508	286.431
-1600.084	322.289
-1975.136	358.144

Table 5: $\gamma = \gamma_1 + i\gamma_2$ when $\mu = 1, \theta = \sigma = 1$.

γ_1	γ_2	$F(\gamma_1, \gamma_2)$	$G(\gamma_1, \gamma_2)$
1.6207	6.4243	0.000000016769	0.000000033862
1.6547	12.6438	0.000000000000	0
1.6620	18.9022	-0.000000000000	0.000000000000
1.6647	25.1725	0.000000000000	0.000000000000
1.6659	31.4478	-0.000000000000	0.000000000000
1.6666	37.7257	-0.000000000000	-0.000000000000
1.6670	44.0051	0.000000000000	0.000000000000
1.6673	50.2855	0.000000000000	-0.000000000000
1.6675	56.5664	0.000000000000	0.000000000000
1.6676	62.8479	0.000000000000	-0.000000000000

Table 6: $\lambda = \text{Re}(\lambda) + i\text{Im}(\lambda)$ when $\mu = 1, \theta = \sigma = 1$.

$\text{Re}(\lambda)$	$\text{Im}(\lambda)$
-19.822	10.412
-79.064	20.922
-177.766	31.416
-315.943	41.905
-493.597	52.390
-710.728	62.875
-967.338	73.358
-1263.427	83.842
-1598.993	94.324
-1974.038	104.807

Table 7: $\gamma = \gamma_1 + i\gamma_2$ when $\mu = 0.1, \theta = \sigma = 1$.

γ_1	γ_2	$F(\gamma_1, \gamma_2)$	$G(\gamma_1, \gamma_2)$
0.4532	6.2989	0.000000000000	0.000000000000
0.4543	12.5743	0.000000000000	0.000000000000
0.4545	18.8548	0.000000000000	0.000000000000
0.4546	25.1367	0.000000000000	0.000000000000
0.4546	31.4191	0.000000000000	0.000000000000
0.4546	37.7017	0.000000000000	0.000000000000
0.4546	43.9845	0.000000000000	0.000000000001
0.4546	50.2674	0.000000000000	0.000000000001
0.4546	56.5504	0.000000000000	0.000000000002
0.4546	62.8334	0.000000000000	0.000000000002

Table 8: $\lambda = \text{Re}(\lambda) + i\text{Im}(\lambda)$ when $\mu = 0.1, \theta = \sigma = 1$.

$\text{Re}(\lambda)$	$\text{Im}(\lambda)$
-0.019	0.002
-0.078	0.005
-0.177	0.008
-0.315	0.011
-0.493	0.014
-0.710	0.017
-0.967	0.019
-1.263	0.022
-1.598	0.025
-1.973	0.028

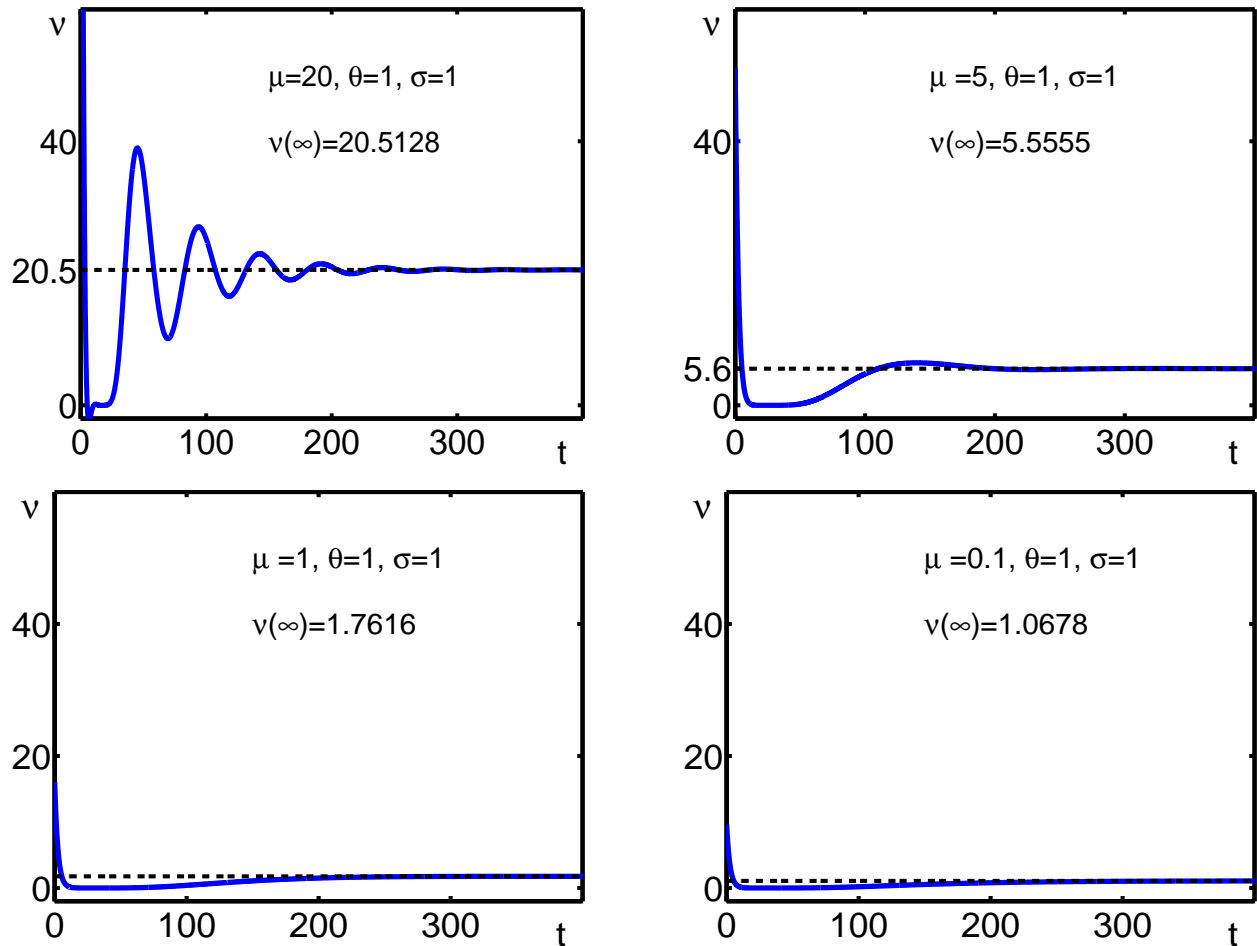


Figure 12: Graphs of the firing rate function $\nu(t)$ generated by the Fokker Planck eigenfunction expansion method when $\theta = \sigma = 1$, and μ decreases from $\mu = 20$ (upper left) to $\mu = 0.1$ (lower right). Theory (see Section 5.2) shows that $\nu(t) \rightarrow C$ as $t \rightarrow \infty$, where the formula for C , the normalizing constant for the eigenfunction $\phi_0(V)$, is given in (see Section 5.2). When μ is large relative to σ , e.g. when $\mu = 20$ and $\sigma = 1$, note that $\nu(\infty) = C \approx \frac{\mu}{\theta} \left(1 + \frac{\sigma^2}{2\mu\theta}\right) = 20.5$ This reflects the fact that, when μ is large relative to σ , the main contribution to $\nu(\infty)$ is the input μ , while a much lesser contribution is due to the noise term, σ . When μ is small relative to σ , e.g. when $\mu = 0.1$ and $\sigma = 1$, we find that $C \approx \frac{\sigma^2}{\theta^2} \left(1 + \frac{2\mu\theta}{3}\right) = 1.06$ This reflects the fact that, when μ is small relative to σ , the main contribution to $\nu(\infty)$ is σ , while the input plays a lesser role.

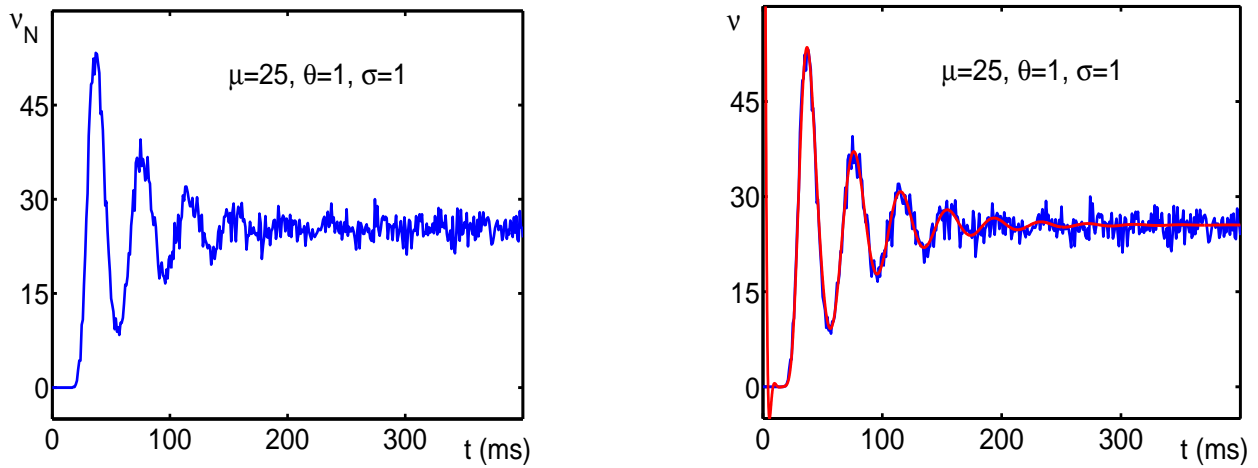


Figure 13: **Left Panel:** Plot of the population firing rate $\nu_N(t)$ with $N = 10000$ simulated IF neurons all with parameters $\mu = 25$ and $\sigma = 1$, where $V(0) = 0$, $V_L = V_R = 0$ and $V_T = \theta = 1$. **Right Panel:** The theoretical (i.e. $N = \infty$) firing rate $\nu(t)$ (red) plotted together with the population (i.e. $N = 10000$) firing rate $\nu_N(t)$ (blue). Again, the parameters are $\mu = 25$ and $\sigma = 1 = \theta$. Listing .23 in Section A.5 provides the Matlab code to produce both figures.

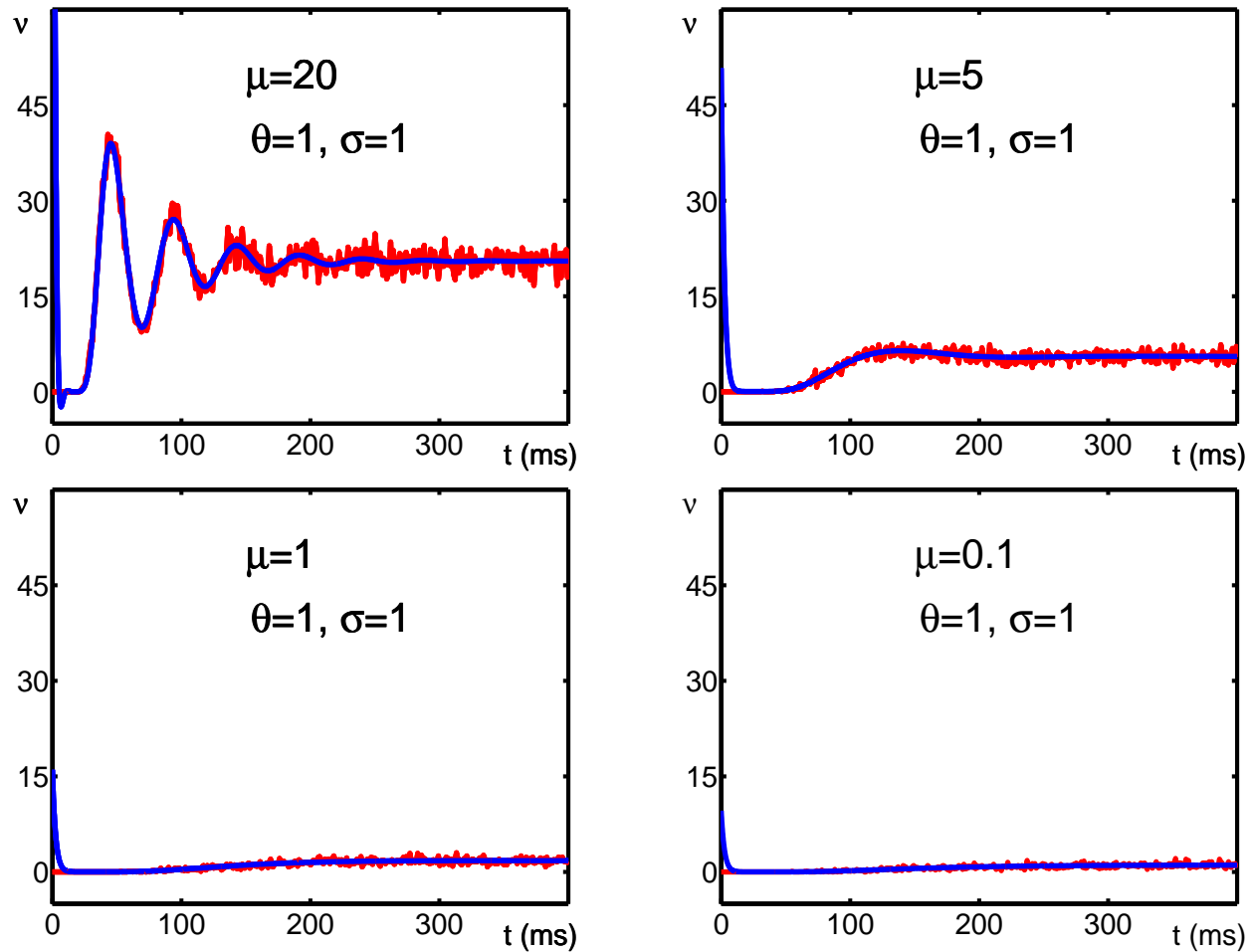


Figure 14: Graphs of the theoretical firing rate function $\nu(t)$ generated by the Fokker Planck eigenfunction expansion method (blue) and the population firing rate function $\nu_N(t)$ (red) when $N = 10000$, $\theta = \sigma = 1$, and μ decreases from $\mu = 20$ (upper left) to $\mu = 0.1$ (lower right). Listing .23 in Section A.5 provides the Matlab code to produce the figures.

Table 9: Parameters: $\sigma = \theta = 1$. The **Left Panel** shows the relative error given by equation (5.30). The error becomes worse as μ decreases and gets closer to σ . The **Right Panel** shows the relative error given by equation (5.31). The error becomes smaller as μ decreases below, and away from, σ .

C	μ	Relative Error
20.513	20	0.0006
5.556	5	0.0101

C	μ	Relative Error
1.762	1	0.0541
1.067	0.1	0.0003

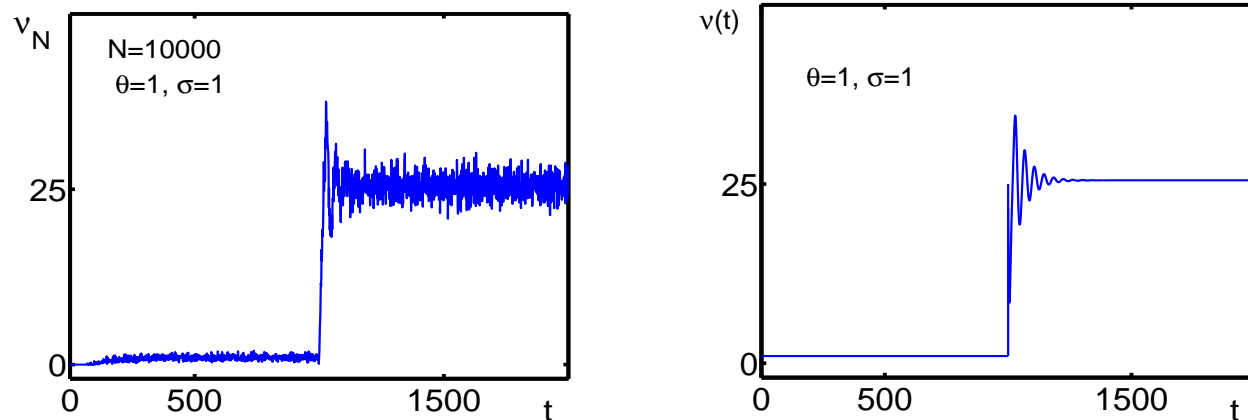


Figure 15: **Left Panel:** population mean firing rate, $\nu_N(t)$, (see formula (5.9)) for $N = 10,000$ neurons when $\sigma(t) \equiv 1$, and $\mu(t)$ is the step function defined in (1.8), i.e $\mu(t) = 0 \forall t \in [0, 1000)$, and $\mu(t) = 25 \forall t \in [1000, \infty)$. **Right Panel:** Theoretical mean firing rate, $\nu(t)$, of the FPE (1.5) constructed using the eigenfunction expansion method. See text.

6.0 OPEN PROBLEMS AND FUTURE RESEARCH

In this thesis we investigated the Mattia-Del Giudice conjecture for the IF firing rate model. We proved the existence of infinitely many branches of eigenvalues when $\mu > 0$ and $\mu < 0$. These results allowed us to derive eigenfunction expansions which give reasonable approximations for the firing rate. However, there were fundamentally important components of the Mattia-Del Giudice conjecture that we were unable to prove. These will provide a starting point for future research, both for the IF and LIF models. Below, we state open problems for both models.

6.1 OPEN PROBLEM 1: EXTREMUM PROPERTIES OF THE STATIONARY SOLUTION FOR THE LIF FPE

In Theorem 1 it was proved that there exists an open neighborhood $U \subset \mathbb{R} \times \mathbb{R}$ such that $(1, 1) \in U$, and a function $\mu^*(\tau, \sigma)$ such that

$$\mu^*(\tau, \sigma) \in \mathbb{C}^1(U, \mathbb{R}). \quad (6.1)$$

Furthermore, for each $(\tau, \sigma) \in U$, there is a unique value, $\mu^*(\tau, \sigma)$, such that $\phi'_0(0^+) = 0$ when $\mu = \mu^*$. The importance of this result is as follows: To our knowledge, it is an open problem to give a rigorous proof establishing extremum properties of the stationary solution. I believe the key to locating the critical points where $\phi_0(V)$ achieves a maximum value is understanding the sign of $\phi'_0(0^+)$ as a function of μ , τ , and σ . Since $\rho(V, t|V_0, 0) \rightarrow C\phi_0(V)$ as $t \rightarrow \infty$, for some constant C , the results of Theorem 1 provide a starting point for locating

the most probable value of $V(t)$ as $t \rightarrow \infty$, and also the behavior of the firing rate, $\nu(t)$, as $t \rightarrow \infty$.

Numerical experiments suggest that $U = \mathbb{R} \times \mathbb{R}$. Proving this conjecture may provide insight towards a complete analysis of the stationary solution for the LIF model.

6.2 OPEN PROBLEM 2: EXISTENCE OF EIGENVALUES AND EIGENFUNCTIONS FOR THE LIF FPE

It remains an open problem to give a rigorous proof of the existence of branches of eigenvalues of the FPE corresponding to the LIF model. A first step is to prove the existence of the first eigenvalue (i.e. the ‘dominate’ eigenvalue), and corresponding eigenfunction, for both $\mu > 0$ and $\mu < 0$. The resolution of this problem will allow us to begin the construction of an eigenfunction expansion for firing rate for the LIF model. To our knowledge there are no rigorous results for this challenging problem.

6.3 OPEN PROBLEM 3: RESOLUTION OF THE MATTIA-DEL GIUDICE CONJECTURE FOR THE IF MODEL

In Sections 4.5 and 4.6 partial proofs of the Mattia-Del Giudice conjecture were given. Recall that the eigenvalues are given by

$$\lambda = \frac{\sigma^4 (\gamma_1^2 - \gamma_2^2) - \mu^2 \theta^2}{2\theta^2 \sigma^2} + i \frac{\gamma_1 \gamma_2 \sigma^2}{\theta^2}, \quad (6.2)$$

where γ_1 and γ_2 satisfy

$$\gamma = \gamma_1 + i\gamma_2 = \frac{\theta}{\sigma^2} \sqrt{\mu^2 + 2\lambda\sigma^2}, \quad (6.3)$$

and $\gamma = \gamma_1 + i\gamma_2$ satisfies the algebraic equation

$$\gamma e^z = \gamma \cosh(\gamma) + z \sinh(\gamma), \quad z = \frac{\mu\theta}{\sigma^2} > 0. \quad (6.4)$$

To our knowledge it is an open problem to give a rigorous proof of the following:

Suppose that $\lambda = \lambda_1 + i\lambda_2$ is an eigenvalue satisfying (6.2)-(6.3)-(6.4). Prove that the corresponding eigenfunctions form a complete set, and that

$$\operatorname{Re}(\lambda) < 0 \text{ for all } z = \frac{\mu\theta}{\sigma^2} > 0. \quad (6.5)$$

Suppose that $\lambda = \lambda_1 + i\lambda_2$ is an eigenvalue satisfying (6.2)-(6.3)-(6.4). Prove that the corresponding eigenfunctions form a complete set, and that λ is real with

$$\lambda < 0 \text{ for all } z = \frac{\mu\theta}{\sigma^2} < 0. \quad (6.6)$$

APPENDIX

NUMERICAL CODES

In this chapter we provide the Matlab code that was used to compute all the figures and numerical experiments in this thesis. For ease of use, the code is ready to be copied and pasted.

A.1 REPRODUCING THE PLOTS OF THE STATIONARY SOLUTIONS FOR THE LIF AND IF

How to reproduce Figures 2 and 3

To reproduce Figures 2 and 3 recall that the stationary solution, $\phi_0(V)$, of the FPE corresponding to the LIF is given by (see equation 2.38 in Chapter 2)

$$\phi_0(V) = \begin{cases} Ae^{-\frac{\tau}{\sigma^2}(\mu-\frac{V}{\tau})^2}, & V < V_R \\ \frac{A}{B}e^{-\frac{\tau}{\sigma^2}(\mu-\frac{V}{\tau})^2} \int_V^{V_T} e^{\frac{\tau}{\sigma^2}(\mu-\frac{x}{\tau})^2} dx, & V_R < V \leq V_T. \end{cases} \quad (.1)$$

where A and B are constants. The first step is to define the function files *statsol_fun1.m*, *statsol_fun2.m* and *statsol_fun3.m* in Matlab.

Listing .1: Function file for Figures 2 and 3

```
% statsol_fun1.m
% Goal: Define one of the three functions for the LIF stationary solution
function B=statsol_fun1 (var ,mu,tau ,sigma)
B=exp (tau ./ (sigma .^ 2) .* (mu-(var ./ tau) ) .^ 2);
```

Listing .2: Function file for Figures 2 and 3

```
% statsol_fun2.m
% Goal: Define one of the three functions for the LIF stationary solution
function y=statsol_fun2(v,x,mu,tau,sigma)
y=exp(-tau./(sigma.^2).*(mu-(v./tau)).^2).*...
    exp(tau./(sigma.^2).*(mu-(x./tau)).^2);
```

Listing .3: Function file for Figures 2 and 3

```
% statsol_fun3.m
% Goal: Define one of the three functions for the LIF stationary solution
function B=statsol_fun3(v,mu,tau,sigma)
B=exp(-tau./(sigma.^2).*(mu-(v./tau)).^2);
```

Secondly, calculate the constants A and B with *Statsol_LIF_constants.m* and save the data.

Listing .4: File for calculating the constants

```
% Statsol_lif_constants.m
% Goal: Find Constants A and B for the stationary solution of the LIF.
% This file calls the functions statsol_fun1.m, statsol_fun2.m and
% statsol_fun3.m The Vectors A and B are called by the file
% Statsol_LIF.m
format long
% Set the parameters
mu=[2,1,0.50,0,-.5,-2];
sigma=1; theta=1; tau=1; VR=0;
z=mu.*theta./(sigma.^2); inf=-100;
% Set the solution vectors
A=zeros(1,6); B=zeros(1,6);
I1=zeros(1,6); I2=zeros(1,6);
% Set the lower bound of integration
bounds=@(s) s;
% Compute the constants A and B
for k=1:6
    B(k)=quad('statsol_fun1',VR,theta,[],[],mu(k),tau,sigma);
    I1(k)=quad('statsol_fun3',inf,VR,[],[],mu(k),tau,sigma);
    I2(k)=quad2d(@(v,x) statsol_fun2(v,x,mu(k),tau...
        ,sigma),VR,theta,bounds,theta);
end
CheckB=B;
CheckA=1./(I1+(1./B).*I2);
% Save the data
save Statsol_constant_A.dat -ascii CheckA
save Statsol_constant_B.dat -ascii CheckB
```

Thirdly, define the ode file *Statsol_LIF_ode.m* and solver *phi_plus_LIF.m*

Listing .5: ODE for Figures 2 and 3

```
% Statsol_LIF_ode.m
% Goal: Compute phi_0 when V>VR for LIF stat sol
function phiprime = Statsol_LIF_ode(v, phi, mu, sigma, tau, A, B);
phiprime = (2./(sigma.^2)).*phi.*(mu-v./tau)-A./B;
```

Listing .6: Function to solve the ODE and save the data

```
% phi_plus_LIF.m
% Goal: Solve the the right hand side of the LIF stat sol, phi_0^+
tic
% Set the parameters
mu=[2,1,0.50,0,-.5,-2];
sigma=1; theta=1; tau=1; VR=0; inf=-10;
% Load the constants from Statsol_lif_constants.m
load Statsol_constant_A.dat
load Statsol_constant_B.dat
A=Statsol_constant_A;
B=Statsol_constant_B;
span=theta:-0.01:VR;
SS=size(span);
t=linspace(theta,VR,SS(2));
sol=zeros(SS(2),7);
sol(:,1)=t;
for k=1:6
[v,phi]=ode45(@(v,phi)Statsol_LIF_ode(v,phi,mu(k),sigma,...
    tau,A(k),B(k)),span,0);
    for m=1:SS(2)
        sol(m,k+1)=phi(m);
    end
end
end
soldata=sol;
% Save the data for export to Statsol_LIF.m
save Statsol_phi_right.dat -ascii soldata

toc
```

Lastly, run the file *Statsol_LIF.m* to reproduce Figures 2 and 3:

Listing .7: Master file for Figures 2 and 3

```
% Statsol_LIF.m
% 3-15-11
%+-----+
% Goal: plot stationary solution for the LIF
%+-----+
% This file calls the functions statsol_fun1.m, statsol_fun2.m and
% statsol_fun3.m, the files Statsol_LIF_constants.m and phi_plus_LIF.m
% It also uses the ode file Statsol_LIF_ode.m
tic
```

```

% Set the parameters
mu=[2,1,0.50,0,-.5,-2];
% -----REMARK-----
% If you change a mu value in this file you must also change
% mu in the files phi_plus_LIF.m and Statsol_LIF_constants.m
% -----
sigma=1; theta=1; tau=1; VR=0; inf=-5;
z=mu.*theta./(sigma.^2);
% Load the normalizing constants from Statsol_lif_constants_test.m
load Statsol_constant_A.dat
load Statsol_constant_B.dat
A=Statsol_constant_A;
B=Statsol_constant_B;
% Load the values of phi_o^+ from phi_plus_LIF.m
load Statsol_phi_right.dat
sol=Statsol_phi_right; clf
% Set the vector to check normality
checkint=zeros(1,6);
% Plot the Solutions phi_0
t1=linspace(inf,VR,1000);
phi_1=zeros(6,length(t1));
for n=1:6
phi_1(n,:)=A(n).*statsol_fun3(t1,mu(n),tau,sigma);
figure(n)
plot(t1,phi_1(n,:), 'linewidth',4.5);
hold on
plot(sol(:,1),sol(:,n+1), 'linewidth',4.5);
hold on
plot([0,0],[0,2], '-k', 'linewidth',3);
hold off
set(gca, 'XTick', -4:2:0, 'fontsize',30);
set(gca, 'YTick', 0:1:1, 'fontsize',30);
set(gca, 'linewidth',3.5, 'fontsize',30);
text(-4.8,1.2, '\phi_o', 'fontsize',35);
text(1.75,-.1, 'V', 'fontsize',35);
if n==2
text(.75,1.1, ['\mu=', num2str(mu(n))], 'fontsize',30);
text(.75,.94, '\tau=1', 'fontsize',30)
elseif n==1
text(-3.3,1.05, 'LIF', 'fontsize',35);
text(-3.5,.89, 'V_R=0', 'fontsize',30);
text(.75,1.1, ['\mu=', num2str(mu(n))], 'fontsize',30);
text(.75,.94, '\tau=1', 'fontsize',30)
else
text(.25,1.1, ['\mu=', num2str(mu(n))], 'fontsize',30);
text(.25,.94, '\tau=1', 'fontsize',30)
end
end
axis([-4 2 0 1.2]);
grid off;
checkint(n)=trapz(fliplr(sol(:,1)')), fliplr(sol(:,n+1)'))+...
trapz(t1,phi_1(n,:));
end
check=checkint'
% Save the plots

```

```

% print -f1 -depsec2 stat_sol_leaky_mu2_tau1.eps
% print -f2 -depsec2 stat_sol_leaky_mu1_tau1.eps
% print -f3 -depsec2 stat_sol_leaky_muhalf_tau1.eps
% print -f4 -depsec2 stat_sol_leaky_mu0_tau1.eps
% print -f5 -depsec2 stat_sol_leaky_muneghalf_tau1.eps
% print -f6 -depsec2 stat_sol_leaky_muneg2_tau1.eps
toc

```

How to reproduce Figure 5

Figure 5 corresponds to the stationary solution of the FPE corresponding to the IF model when $-\infty < V_L = V_R < V_T$ given by

$$\phi_0(V) = C_0 \left(1 - \exp \left[\frac{-2z(\theta - V)}{\theta} \right] \right), \quad (.2)$$

where C_0 is a normalizing constant. To reproduce Figure 5 refer to the Matlab code in Listing .8 below.

Listing .8: Matlab code for Figure 5

```

% Statsol_VLeqVR_IF.m
% 3-27-11
%+++++
%Goal: Plot stationary solution for IF when V_L=V_R
%+++++
clf
% Set the parameters
mu=[-2, -.5, 0.0001, .5, 1, 2];
sigma=1; theta=1; %V_T=theta
VL=0; VR=0; z=mu.*theta./(sigma.^2);
% Set the normalizing constant
term1=2.*(mu.*theta./(sigma.^2))-1+exp(-2.*(mu.*theta./(sigma.^2)));
term2=((sigma.*sigma)./(2.*mu)).*term1;
C=1./term2;
% Set the domains
V = VR:.001:theta;
phi=zeros(length(V),6);
% Set the vector to check normality
checkint=zeros(1,6);
for k=1:6
% Define the functions
phi(:,k) =C(k).*(1-exp(-2.*z(k).*(theta-V)./theta));
% Plot the solution
if k==3
figure(k);
plot(V,phi(:,k),'linewidth',4.5);
hold on

```

```

    plot([0,0],[-.5,4.5], 'k', 'linewidth', 3);
    hold off
    axis([-2 2 0 4]);
    grid off;
    set(gca, 'XTick', -2:1:1, 'fontsize', 30);
    set(gca, 'YTick', 0:1.5:4, 'fontsize', 30);
    set(gca, 'linewidth', 3.5, 'fontsize', 30);
    text(.7, 3.3, '\mu=0', 'fontsize', 35);
    text(-2.5, 3.8, '\phi_0', 'fontsize', 35);
    text(1.8, -.26, 'V', 'fontsize', 35);
else
figure(k);
plot(V, phi(:, k), 'linewidth', 4.5);
hold on
plot([0,0],[-.5,4.5], 'k', 'linewidth', 3);
hold off
axis([-2 2 0 4]);
grid off;
set(gca, 'XTick', -2:1:1, 'fontsize', 30);
set(gca, 'YTick', 0:1.5:4, 'fontsize', 30);
set(gca, 'linewidth', 3.5, 'fontsize', 30);
text(.5, 3.3, ['\mu=', num2str(mu(k))], 'fontsize', 35);
text(-2.5, 3.8, '\phi_0', 'fontsize', 35);
text(1.8, -.26, 'V', 'fontsize', 35);
    if k==6
        text(-1.3, 3.3, 'IF', 'fontsize', 35);
        text(-1.7, 2.7, 'V_L=V_R=0', 'fontsize', 30);
    end
end
% check that the functions integrate to 1
checkint(k)=trapz(V, phi(:, k));
end
check=checkint'
% Save the plots
% print -f1 -depsc2 statsol_VLeqVR_mu_neg2.eps
% print -f2 -depsc2 statsol_VLeqVR_mu_neghalf.eps
% print -f3 -depsc2 statsol_VLeqVR_mu_0.eps
% print -f4 -depsc2 statsol_VLeqVR_mu_half.eps
% print -f5 -depsc2 statsol_VLeqVR_mu_1.eps
% print -f6 -depsc2 statsol_VLeqVR_mu_2.eps

```

How to reproduce Figure 6

Figure 6 corresponds to the stationary solution of the FPE corresponding to the IF model when $-\infty < V_L < V_R < V_T$ given by

$$\phi_0(V) = \begin{cases} C \left(1 - e^{\frac{2\mu\theta}{\sigma^2}}\right) e^{\frac{2\mu}{\sigma^2}V}, & V_L \leq V \leq V_R \\ C \left(e^{\frac{2\mu}{\sigma^2}V} - e^{\frac{2\mu\theta}{\sigma^2}}\right), & V_R \leq V \leq \theta \end{cases} \quad (.3)$$

where C is a normalizing constant. To reproduce Figure 6 refer to the Matlab code in Listing .9 below.

Listing .9: Matlab code for Figure 6

```

%Statsol_VLlessVR_IF.m
%3-27-11
%+++++
%Goal: Plot stationary solution for IF when VL<VR
%+++++
clf
% Set the parameters
mu=[-2,-.5,0.00001,.5,1,2];
sigma=1; theta=1; %V_T=theta=1
VL=-2; VR=0; z=mu.*theta./(sigma.^2);
% Compute the normalizing constant
term1=(1-exp(2.*z)).*((sigma.^2)./(2.*mu));
term2=exp((2.*mu.*VR)./(sigma.^2))-exp((2.*mu.*VL)./(sigma.^2));
term3=exp(2.*z)-exp((2.*mu.*VR)./(sigma.^2));
term4=exp(2.*z).*(theta-VR);
Ctest1=term1.*term2+term3.*(sigma.^2)./(2.*mu)-term4;
C=(1./Ctest1);
%-----The normalizing constant found via-----
%----- Mathematica solve command-----
C2=[0.00136692,0.232402,-20000.1,-0.402295,-0.136415,-0.0183171];
% Check the two methods agree
C_Check=C-C2;
% Set the domains
V1 = VL:.001:VR; V2 = VR:.001:theta;
y1=zeros(length(V1),6); y2=zeros(length(V2),6);
% Set the vector to check normality
checkint=zeros(1,6);
for k=1:6
% Define the functions
y1(:,k) =C(k).*(1-exp(2.*mu(k)./...
(sigma.^2).*theta)).*exp(2.*mu(k)./(sigma.^2).*V1);
y2(:,k) =C(k).*(exp(2.*mu(k).*V2./...
(sigma.^2))-exp(2.*mu(k).*theta./(sigma.^2)));
figure(k)
plot(V1,y1(:,k),'linewidth',4.5);
hold on
plot(V2,y2(:,k),'linewidth',4.5);
hold on
plot([0,0],[0,2],'-k','linewidth',3);
hold off
set(gca,'XTick',-4:2:0,'fontsize',30);
set(gca,'YTick',0:1:1,'fontsize',30);
set(gca,'linewidth',3.5,'fontsize',30);
text(-3.6,1.9,'\phi_o','fontsize',35);
text(1.8,-.15,'V','fontsize',35);
if k==3
text(.6,1.6,'\mu_0','fontsize',30);
elseif k==6

```

```

    text(-2.,1.7,'IF','fontsize',35);
    text(-2.7,1.4,'-2=V_L<V_R=0','fontsize',30);
    text(.4,1.6,['\mu_=' , num2str(mu(k))], 'fontsize',30);
else
    text(.4,1.6,['\mu_=' , num2str(mu(k))], 'fontsize',30);
end
axis([-3 2 0 2]);
grid off;
% check that the function integrates to 1
checkint(k)=trapz(V1,y1(:,k))+trapz(V2,y2(:,k));
end
check=checkint'
% Save the plots
% print -f1 -depsc2 statsol_VLlessVR_mu_neg2.eps
% print -f2 -depsc2 statsol_VLlessVR_mu_neghalf.eps
% print -f3 -depsc2 statsol_VLlessVR_mu_0.eps
% print -f4 -depsc2 statsol_VLlessVR_mu_half.eps
% print -f5 -depsc2 statsol_VLlessVR_mu_1.eps
% print -f6 -depsc2 statsol_VLlessVR_mu_2.eps

```

A.2 NUMERICAL INVESTIGATION OF THE NEIGHBORHOOD U

In this section we provide the code to reproduce Figure 4. First, Run the ODE file $\mu_star.ode$ in XXP and save the data. Next, export the data to Matlab and plot the simulated solution.

Listing .10: XPP code to Investigate the Neighborhood U

```

#Ryan O'Grady 3-6-2010
#This ode file is used to investigate the solution mu^*
#when sigma=1 and tau is positive.
#we wish to know if this solution fails to exist.
#Here tau is the variable and hence tau=t.
#Use numeric solver to find init.
#we use init U=.743622, start =1, dt =-0.001 and .0001, total 1
#we use init U=13.20207, for sigma=2.5
#Run the ode and save the data for export to matlab.
p sigma=2.5
#init U=0.743622
init U=13.20207
#Term1 is F_tau
term1=1/(2*t)-(U/(sigma*sigma))*exp(1/(sigma*sigma)*(1/t-2*U))*(U+1/t)
#term2 is F_mu
term2=1/U-2*t*U/(sigma*sigma)-...
      2*t*U/(sigma*sigma)*(exp(1/(sigma*sigma)*(1/t-2*U))-1)
U= -(term1)/(term2)
#aux fun=t*U
d

```

A.3 THE FUNCTIONS $\gamma(Z)$ AND $\lambda(Z)$

In this section we provide the instructions for reproducing Figures 9 and 10.

How to reproduce Figure 9

First, write the the function file *if_fandg_2.m* and the file *if_gammaofz_startingpoint.m* to find initial values for the ODEs.

Listing .11: Function file for Figure 9

```
% if_fandg_2.m
% The functions f and g used to calculate the values of the IF
function FF=if_fandg_2(gamma,z);
T1=gamma(1).*exp(z)-gamma(1).*cosh(gamma(1)).*cos(gamma(2));
T2=gamma(2).*sinh(gamma(1)).*sin(gamma(2));
T3=z*sinh(gamma(1)).*cos(gamma(2));
T4=gamma(2).*exp(z)-gamma(1).*sinh(gamma(1)).*sin(gamma(2));
T5=gamma(2).*cosh(gamma(1)).*cos(gamma(2));
T6=z*cosh(gamma(1)).*sin(gamma(2));
FF=[T1+T2-T3; T4-T5-T6];
```

Listing .12: Initial value solver

```
% if_gammaofz_startingpoint.m
% Goal: To find a starting point for odes gamma1(z)
% and gamma2(z) when z is small. This file requires the
% function file if_fandg_2.m
% This starting is used in the ode file
% if_gamma1_and_gamma2.ode in XPP
format long
z=.1;
g1=log(exp(z)+sqrt(exp(2*z)-1));
% Make sure to check the n!!!!!!!!!!!!!!!!!!!!!!
n=1;
% Make a starting guess at the solution
x0 = [g1; 2*n*pi];
% Option to display output
options=optimset('Display','off');
% Use the built in Newton solver
[x,fval] = fsolve(@if_fandg_2,x0,options,z);
% DEfine the solution vector
solution=x
% Check the solution is a solution
matlabscheck=fval
% Double Check the solution is a solution
mycheck=if_fandg_2(solution,z)
```

Next, write the ode files *if_g1_g2_zpos.ode* and *An_ofz.ode* to be used in XPP.

Listing .13: ODE file for A_n

```

# if_g1_g2_zpos.ode
# Goal: to plot the functions gamma1(z) and gamma2(z)
# when z>0.
# Define the ODES
Fterm1=exp(t)+gamma2*cosh(gamma1)*sin(gamma2)
Fterm2=cos(gamma2)
Fterm3=(1+t)*cosh(gamma1)+gamma1*sinh(gamma1)
F_gamma1=Fterm1-Fterm2*Fterm3
Fterm4=gamma1*cosh(gamma1)*sin(gamma2)
Fterm5=sinh(gamma1)
Fterm6=gamma2*cos(gamma2)+(1+t)*sin(gamma2)
F_gamma2=Fterm4+Fterm5*Fterm6
F3=-sinh(gamma1)*cos(gamma2)+exp(t)*gamma1
G_gamma1=-F_gamma2
G_gamma2=F_gamma1
G3=-cosh(gamma1)*sin(gamma2)+exp(t)*gamma2
Jac=F_gamma1*F_gamma1+F_gamma1+F_gamma2*F_gamma2
gamma1'=(F_gamma2*G3-G_gamma2*F3)/Jac
gamma2'=(G_gamma1*F3-F_gamma1*G3)/Jac
# Get the starting point from if_gammaofz_startingpoint.m
# Run the solver both forward and backward. Save the data
# for export to Matlab.
#####
#####
# I used z=.1
# =====
# n=1
# =====
#gamma1(0)=.4532754622
#gamma2(0)=6.298935755
# =====
# n=2
# =====
#gamma1(0)=.45434214488
#gamma2(0)=12.574307449
# =====
# n=3
# =====
# gamma1(0)=.454542329200
# gamma2(0)=18.8548548743
# =====
# For a small starting point
# =====
# This time I used n=1 and starting point z=0.0000001
#gamma1(0)=.000447213603066
#gamma2(0)=6.283185307179586
# =====
# n=-1 starting point z=0.1
# =====

```

```

gamma1(0)=.4532754622
gamma2(0)=-6.298935755
done

```

Listing .14: ODE file for A_n

```

# An_ofz.ode
# Goal: numerically solve the ode for A_n(z)
# which is used when studying the eigenvalues
# of the FPE of IF.
par n=1
term1=2*n*pi+An
term2=term1*term1*(1/cos(An))+t
An'=term1/term2
An(0)=0
done

```

Upon solving the two ODEs in XPP save and export the data to Matlab. Run the file *if_gamma1_and_gamma2_ofz_plots.m* to reproduce Figure 9

Listing .15: Master file for Figure 9

```

% if_gamma1_and_gamma2_ofz_plots.m
% ++++++
% Goal: plot the functions gamma_1(z) and gamma_2(z) for z>0
% ++++++
% This file calls the data simulated with the XPP files
% An_ofz.ode and if_gamma1_and_gamma2.ode
clf
% Load the data for n=1
load if_gammaofz_f.dat; load if_gammaofz_b.dat
% Load the data for n=2
load if_gammaofz_f_n2.dat; load if_gammaofz_b_n2.dat
% Load the data for n=3
load if_gammaofz_f_n3.dat; load if_gammaofz_b_n3.dat
% Load the data for A_1(z)
load if_A_nofz.dat
% Rename the data for clarity
sol1_f=if_gammaofz_f; sol2_b=if_gammaofz_b; sol1_f_n2=if_gammaofz_f_n2;
sol2_b_n2=if_gammaofz_b_n2; sol1_f_n3=if_gammaofz_f_n3;
sol2_b_n3=if_gammaofz_b_n3; A_n=if_A_nofz;
% Plot the function gamma_2(z) for n=1,2,3
figure(1)
plot(sol1_f(:,1),sol1_f(:,3),'b','linewidth',3); hold on
plot(sol2_b(:,1),sol2_b(:,3),'b','linewidth',3); hold on
plot(sol1_f_n2(:,1),sol1_f_n2(:,3),'b','linewidth',3); hold on
plot(sol2_b_n2(:,1),sol2_b_n2(:,3),'b','linewidth',3); hold on
plot(sol1_f_n3(:,1),sol1_f_n3(:,3),'b','linewidth',3); hold on
plot(sol2_b_n3(:,1),sol2_b_n3(:,3),'b','linewidth',3); hold on
plot([0 120],[2*1*pi 2*1*pi],'—k','linewidth',3); hold on

```

```

plot([0 120],[2*2*pi 2*2*pi], '—k', 'linewidth',3); hold on
plot([0 120],[2*1*pi+pi/2 2*1*pi+pi/2], '—k', 'linewidth',3); hold on
plot([0 120],[2*2*pi+pi/2 2*2*pi+pi/2], '—k', 'linewidth',3); hold on
plot([0 120],[2*3*pi 2*3*pi], '—k', 'linewidth',3); hold on
plot([0 120],[2*3*pi+pi/2 2*3*pi+pi/2], '—k', 'linewidth',3); hold on
axis([0 20 5 7*pi+.8]); hold on
set(gca, 'xtick',[0 5 15], 'fontsize',25); hold on
text(-1.9,23, '\gamma_2', 'fontsize',30); hold on
set(gca, 'ytick',[0 25], 'fontsize',25); hold on
text(19,4.2, 'z', 'fontsize',30); hold on
text(16.5,2*pi+2.6, '5\pi/2', 'fontsize',25); hold on
text(16.5,4*pi+2.6, '9\pi/2', 'fontsize',25); hold on
text(-2.3,2*pi-.2, '2\pi', 'fontsize',30); hold on
text(-2.3,2*2*pi-.2, '4\pi', 'fontsize',30); hold on
text(-2.3,2*3*pi-.2, '6\pi', 'fontsize',30); hold on
text(8,2*pi+2.6, 'n=1', 'fontsize',30); hold on
text(8,4*pi+2.6, 'n=2', 'fontsize',30); hold on
text(8,6*pi+2.6, 'n=3', 'fontsize',30); hold on
set(gca, 'linewidth',3.5, 'fontsize',30); hold off
% Plot the function gamma_2(z) for n=1 and A_1(z)
figure(2)
plot(sol1_f(:,1), sol1_f(:,3), 'b', 'linewidth',3); hold on
plot(sol2_b(:,1), sol2_b(:,3), 'b', 'linewidth',3); hold on
plot(sol1_f_n2(:,1), sol1_f_n2(:,3), 'b', 'linewidth',3); hold on
plot(sol2_b_n2(:,1), sol2_b_n2(:,3), 'b', 'linewidth',3); hold on
plot(sol1_f_n3(:,1), sol1_f_n3(:,3), 'b', 'linewidth',3); hold on
plot(sol2_b_n3(:,1), sol2_b_n3(:,3), 'b', 'linewidth',3); hold on
plot(A_n(:,1), A_n(:,2)+2*pi, '—r', 'linewidth',3); hold on
plot(A_n(:,1), A_n(:,2)+2*2*pi, '—r', 'linewidth',3); hold on
plot([0 120],[2*1*pi 2*1*pi], '—k', 'linewidth',3); hold on
plot([0 120],[2*2*pi 2*2*pi], '—k', 'linewidth',3); hold on
plot([0 120],[2*1*pi+pi/2 2*1*pi+pi/2], '—k', 'linewidth',3); hold on
plot([0 120],[2*2*pi+pi/2 2*2*pi+pi/2], '—k', 'linewidth',3); hold on
plot([0 120],[2*3*pi 2*3*pi], '—k', 'linewidth',3); hold on
plot([0 120],[2*3*pi+pi/2 2*3*pi+pi/2], '—k', 'linewidth',3); hold on
axis([0 22 5 5*pi]); hold on
set(gca, 'xtick',[0 5 15], 'fontsize',25); hold on
set(gca, 'ytick',[0 25], 'fontsize',25); hold on
text(-2.4,2*pi+.1, '2\pi', 'fontsize',30); hold on
text(-2.4,2*2*pi+.1, '4\pi', 'fontsize',30); hold on
text(-1.8,pi+.1, '\pi', 'fontsize',30); hold on
text(17.7,2*pi+2.3, '5\pi/2', 'fontsize',25); hold on
text(17.7,4*pi+2.3, '9\pi/2', 'fontsize',25); hold on
text(-2.3,15.5, '\gamma_2', 'fontsize',30); hold on
text(21,4.35, 'z', 'fontsize',30); hold on
text(8.5,2*pi+2.3, 'n=1', 'fontsize',30); hold on
text(8.5,4*pi+2.3, 'n=2', 'fontsize',30); hold on
set(gca, 'linewidth',3.5, 'fontsize',30); hold off
% Plot the function gamma_1(z) for n=1,2
figure(3)
plot(sol2_b(:,1), sol2_b(:,2), 'linewidth',3); hold on
plot(sol1_f(:,1), sol1_f(:,2), 'linewidth',3); hold on
plot(sol1_f_n2(:,1), sol1_f_n2(:,2), '—r', 'linewidth',3); hold on
plot(sol2_b_n2(:,1), sol2_b_n2(:,2), '—r', 'linewidth',3); hold on

```

```

axis([0 1 0 2]); hold on
text(.95,-.1,'z','fontsize',30); hold on
text(.22,1,'n=1','fontsize',32); hold on
text(.6,.96,'n=2','fontsize',32); hold on
text(-.074,1.9,'\gamma_1','fontsize',30); hold on
set(gca,'xtick',[0 .25 .75],'fontsize',25); hold on
set(gca,'ytick',[0 1],'fontsize',25); hold on
set(gca,'linewidth',3.5,'fontsize',30); hold off
% Plot gamma_1(z) against gamma_2(z)
figure(4)
plot(sol2_b(:,2),sol2_b(:,3),'linewidth',3); hold on
plot(sol1_f(:,2),sol1_f(:,3),'linewidth',3); hold on
plot([0 120],[2*1*pi 2*1*pi],'—k','linewidth',3); hold on
axis([0 25 5.5 7]); hold on
set(gca,'xtick',[0 10 20],'fontsize',25); hold on
set(gca,'ytick',[0 10],'fontsize',25); hold on
text(23,5.4,'\gamma_1','fontsize',30); hold on
text(-2.2,7,'\gamma_2','fontsize',30); hold on
text(-2.3,2*pi,'2\pi','fontsize',25); hold on
text(17.5,2*pi+1.1,'A_1(z)','fontsize',25); hold on
text(10,2*pi+1.8,'n=1','fontsize',35); hold on
set(gca,'linewidth',3.5,'fontsize',30); hold on
plot([3 3],[2*pi+.25 2*pi+.25],'og','linewidth',9); hold on
set(gca,'linewidth',3.5,'fontsize',30); hold off
% Save the plots
% print -f1 -depsc2 g2_ofz.eps
% print -f2 -depsc2 g2_ofz_andA_n.eps
% print -f3 -depsc2 g1_ofz.eps
% print -f4 -depsc2 g1-v-g2_ofz.eps

```

How to reproduce Figure 10

Run the ode file *if_g1_g2_zpos.ode* (see Listing .13) in XPP and export the saved data to the Matlab file *if_lambda1_and_lambda2_ofz_plots.m* found below in Listing .16.

Listing .16: Master file for Figure 10

```

% if_lambda1_and_lambda2_ofz_plots.m
% Goal: Use the gamma data simulated
% with the xpp file if_g1_g2_zpos.ode
% to plot the functions lambda_1(z)
% and lambda_2(z)
% Clear any current figures
clf
% Load the data for n=1
load if_gammaofz_f.dat; load if_gammaofz_b.dat
% Load the data for n=2
load if_gammaofz_f_n2.dat; load if_gammaofz_b_n2.dat
% Load the data for n=3
load if_gammaofz_f_n3.dat; load if_gammaofz_b_n3.dat

```

```

% Load the data for A_1(z)
load if_A_nofz.dat
% Rename the data for clarity
gamma_f_n1=if_gammaofz_f; gamma_b_n1=if_gammaofz_b;
gamma_f_n2=if_gammaofz_f_n2; gamma_b_n2=if_gammaofz_b_n2;
gamma_f_n3=if_gammaofz_f_n3; gamma_b_n3=if_gammaofz_b_n3;
A_n=if_A_nofz;
% Define the parameters
theta=1; sigma=1; mu=1; z=mu*theta/(sigma^2);
% Define the function lambda(z)
term1=sigma^4*(gamma_f_n1(:,2).^2 - gamma_f_n1(:,3).^2) - ...
      sigma^4.*gamma_f_n1(:,1).^2;
lambda_f_n1_r=term1/(2*theta^2*sigma^2);

term2=sigma^4*(gamma_b_n1(:,2).^2 - gamma_b_n1(:,3).^2) - ...
      sigma^4.*gamma_b_n1(:,1).^2;
lambda_b_n1_r=term2/(2*theta^2*sigma^2);

term3=sigma^4*(gamma_f_n2(:,2).^2 - gamma_f_n2(:,3).^2) - ...
      sigma^4.*gamma_f_n2(:,1).^2;
lambda_f_n2_r=term3/(2*theta^2*sigma^2);

term4=sigma^4*(gamma_b_n2(:,2).^2 - gamma_b_n2(:,3).^2) - ...
      sigma^4.*gamma_b_n2(:,1).^2;
lambda_b_n2_r=term4/(2*theta^2*sigma^2);

term5=sigma^4*(gamma_f_n3(:,2).^2 - gamma_f_n3(:,3).^2) - ...
      sigma^4.*gamma_f_n3(:,1).^2;
lambda_f_n3_r=term5/(2*theta^2*sigma^2);

term6=sigma^4*(gamma_b_n3(:,2).^2 - gamma_b_n3(:,3).^2) - ...
      sigma^4.*gamma_b_n3(:,1).^2;
lambda_b_n3_r=term6/(2*theta^2*sigma^2);
% Plot the functions Re (lambda(z))
figure(1)
plot(gamma_f_n1(:,1), lambda_f_n1_r, 'b', 'linewidth', 4); hold on
plot(gamma_b_n1(:,1), lambda_b_n1_r, 'b', 'linewidth', 4); hold on
plot(gamma_f_n2(:,1), lambda_f_n2_r, 'k', 'linewidth', 4); hold on
plot(gamma_b_n2(:,1), lambda_b_n2_r, 'k', 'linewidth', 4); hold on
plot(gamma_f_n3(:,1), lambda_f_n3_r, 'g', 'linewidth', 4); hold on
plot(gamma_b_n3(:,1), lambda_b_n3_r, 'g', 'linewidth', 4); hold on
plot([-5 5], [-2*1*pi^2 -2*1*pi^2], '--k', 'linewidth', 3); hold on
plot([-5 5], [-2*2^2*pi^2 -2*2^2*pi^2], '--k', 'linewidth', 3); hold on
plot([-5 5], [-2*3^2*pi^2 -2*3^2*pi^2], '--k', 'linewidth', 3); hold on
set(gca, 'xtick', [0 2 4], 'fontsize', 20); hold on
set(gca, 'ytick', [-200 -150 -100 -50 0], 'fontsize', 20); hold on
text(4.7, -263, 'z', 'fontsize', 30); hold on
text(-.47, 41, '\lambda_1', 'fontsize', 30); hold on
set(gca, 'linewidth', 3.5, 'fontsize', 30); hold on
axis([0 5 -250 50]); hold off
% Define the function IM lambda(z)
lambda_f_n1_im=gamma_f_n1(:,2).*gamma_f_n1(:,3);
lambda_b_n1_im=gamma_b_n1(:,2).*gamma_b_n1(:,3);
lambda_f_n2_im=gamma_f_n2(:,2).*gamma_f_n2(:,3);

```

```

lambda_b_n2_im=gamma_b_n2(:,2).*gamma_b_n2(:,3);
lambda_f_n3_im=gamma_f_n3(:,2).*gamma_f_n3(:,3);
lambda_b_n3_im=gamma_b_n3(:,2).*gamma_b_n3(:,3);
% plot the Im (lambda(z))
figure(2)
plot(gamma_f_n1(:,1),lambda_f_n1_im,'b','linewidth',3); hold on
plot(gamma_b_n1(:,1),lambda_b_n1_im,'b','linewidth',3);
plot(gamma_f_n2(:,1),lambda_f_n2_im,'k','linewidth',3);
plot(gamma_b_n2(:,1),lambda_b_n2_im,'k','linewidth',3);
plot(gamma_f_n3(:,1),lambda_f_n3_im,'g','linewidth',3);
plot(gamma_b_n3(:,1),lambda_b_n3_im,'g','linewidth',3);
plot(gamma_f_n1(:,1),-lambda_f_n1_im,'b','linewidth',3);
plot(gamma_b_n1(:,1),-lambda_b_n1_im,'b','linewidth',3);
plot(gamma_f_n2(:,1),-lambda_f_n2_im,'k','linewidth',3);
plot(gamma_b_n2(:,1),-lambda_b_n2_im,'k','linewidth',3);
plot(gamma_f_n3(:,1),-lambda_f_n3_im,'g','linewidth',3);
plot(gamma_b_n3(:,1),-lambda_b_n3_im,'g','linewidth',3);
plot([-5 0],[0 0],'k','linewidth',4);
text(3.7,-132,'z','fontsize',30);
%text(-6,110,'\lambda_2','fontsize',30);
set(gca,'xtick',[-5 0 5],'fontsize',20);
set(gca,'ytick',[-100 -50 0 50 100],'fontsize',15);
set(gca,'linewidth',3.5,'fontsize',30);
title('Im(\lambda(z))');
axis([-5 5 -120 120]); hold off
%
% Load the XPP data
load IF_muneg_gamma1.dat; load IF_muneg_gamma1_.dat
load IF_muneg_gamma2.dat; load IF_muneg_gamma2_.dat
load IF_muneg_gamma3.dat; load IF_muneg_gamma3_.dat
load IF_muneg_gamma4.dat; load IF_muneg_gamma4_.dat
% Rename the data for convenience
p=IF_muneg_gamma1; n=IF_muneg_gamma1_;
q=IF_muneg_gamma2; r=IF_muneg_gamma2_;
s=IF_muneg_gamma3; t=IF_muneg_gamma3_;
u=IF_muneg_gamma4; v=IF_muneg_gamma4_;
% Check the size of the matrix p.
size(p);
% Define the functions lambda(z)
y1=-(p(:,2).*p(:,2)+p(:,1).*p(:,1))./2;
y2=-(n(:,2).*n(:,2)+n(:,1).*n(:,1))./2;
y3=-(q(:,2).*q(:,2)+q(:,1).*q(:,1))./2;
y4=-(r(:,2).*r(:,2)+r(:,1).*r(:,1))./2;
y5=-(s(:,2).*s(:,2)+s(:,1).*s(:,1))./2;
y6=-(t(:,2).*t(:,2)+t(:,1).*t(:,1))./2;
y7=-(u(:,2).*u(:,2)+u(:,1).*u(:,1))./2;
y8=-(v(:,2).*v(:,2)+v(:,1).*v(:,1))./2;
figure(3)
plot(gamma_f_n1(:,1),lambda_f_n1_r,'b','linewidth',4); hold on
plot(gamma_b_n1(:,1),lambda_b_n1_r,'b','linewidth',4);
plot(gamma_f_n2(:,1),lambda_f_n2_r,'k','linewidth',4);
plot(gamma_b_n2(:,1),lambda_b_n2_r,'k','linewidth',4);
plot(gamma_f_n3(:,1),lambda_f_n3_r,'g','linewidth',4);
plot(gamma_b_n3(:,1),lambda_b_n3_r,'g','linewidth',4);

```

```

plot(p(:,1),y1,'b','linewidth',3.5);
plot(n(:,1),y2,'b','linewidth',3.5);
plot(q(:,1),y3,'b','linewidth',3.5);
plot(r(:,1),y4,'b','linewidth',3.5);
plot(s(:,1),y5,'k','linewidth',3.5);
plot(t(:,1),y6,'k','linewidth',3.5);
plot(u(:,1),y7,'k','linewidth',3.5);
plot(v(:,1),y8,'k','linewidth',3.5);
plot([-5 5],[-2*1*pi^2 -2*1*pi^2], '--r','linewidth',2.5);
plot([-5 5],[-2*2^2*pi^2 -2*2^2*pi^2], '--r','linewidth',2.5);
plot([-5 5],[-2*3^2*pi^2 -2*3^2*pi^2], '--r','linewidth',3);
set(gca,'xtick',[-5 0 5],'fontsize',20);
set(gca,'ytick',[-100 -50 0],'fontsize',20);
text(3.7,-122,'z','fontsize',30);
%text(-5.47,0,'\lambda_1','fontsize',30);
set(gca,'linewidth',3.5,'fontsize',30);
title('Re(\lambda(z))');
axis([-5 5 -115 0]); hold off

%print -f1 -depsc2 lambda_real_z_pos.eps
%print -f2 -depsc2 lambda_im_z_pos.eps
print -f2 -depsc2 def_1.eps
print -f3 -depsc2 def_2.eps

```

A.4 CALCULATING THE EIGENVALUES FOR THE FPE OF THE IF MODEL

First, define the function file *nonlinear_FandG_if.m* which defines the nonlinear algebra problem $(F, G) = (0, 0)$. Next, run the Matlab file *gamma_and_evalues_IF.m* to calculate the γ and λ values listed in Tables 1-8.

Listing .17: M-file for calculating the Eigenvalues

```

% gamma_and_evalues_IF.m
% Goal: Calculate the gamma values (and hence evalues) of the IF when
% V_L=V_R=0 and V_T=theta.
%+++++
tic % Set the timer
mu=0.001; theta=1; sigma=5; % Set parameters
z1=mu*theta/(sigma*sigma); % Set z for gamma^star
gstar=log(exp(z1)+sqrt(exp(2*z1)-1)); %+++++
gamma1old=gstar; % Set Initial guesses
%gamma1old=0 % if mu<0
gamma2old=6.4; %+++++
%gamma2old=3.3 % if mu<0

```

```

numberofeigenvalues=10;      % How many eigenvalues do we want
% Set the solution matrices.
old=zeros(numberofeigenvalues ,5);
gammavalues=zeros(numberofeigenvalues ,4);
newsol=zeros(1,2);
% Set initialize Guesses
old(1,2)=gamma1old; old(1,3)=gamma2old;
gamma1old=old(1,2); gamma2old(1,3)=old(1,3);
for i=1:numberofeigenvalues
myf_1=@(gamma) nonlinear_FandG_IF(gamma,mu,theta ,sigma );
options=optimset('Display','off');
sol=fsolve(myf_1,[gamma1old gamma2old],options);
% Check we actually found a solution
Check=nonlinear_FandG_IF([sol(1) sol(2)],mu,theta ,sigma );
gammavalues(i,1)=sol(1);
gammavalues(i,2)=sol(2);
gammavalues(i,3)=Check(1);
gammavalues(i,4)=Check(2);
gamma1old=sol(1);
% gamma2old=sol(2)+6.4;
gamma2old=sol(2)+pi; % if mu<0
% Save the gamma values in the matrix old
old(i,1)=mu;
old(i,2)=sol(1);
old(i,3)=sol(2);
%check error
old(i,4)=Check(1);
old(i,5)=Check(2);
end
old; gammavalues;
% Define the gamma values
gammadata=[gammavalues(:,1) gammavalues(:,2)]
% Save the gamma values
save gammavalues_mu01_sigma5.dat -ascii gammadata
% Calculate the real parts of the eigenvalues
term1=sigma^(4).*(old(:,2).*old(:,2)-old(:,3).*old(:,3))...
-mu*mu*theta*theta;
term2=2*theta*theta*sigma*sigma;
lambdareal=term1./term2;
% Calculate the imaginary parts
term3=old(:,2).*old(:,3).*sigma*sigma;
lambdaim=term3/(theta*theta);
% Define the matrix of eigenvalues
eigenvalues=[lambdareal lambdaim]
% Save the eigenvalues
save values_mu01_sigma5.dat -ascii eigenvalues
toc

```

A.5 THE FIRING RATE FUNCTION

In this section we provide Matlab code to plot the theoretical firing rate and the population firing rate.

A.5.1 Calculating the Theoretical Firing Rate, $\nu(t)$

To reproduce Figure 12 five programs are needed. First we need three function files (see Listings .18-.19-.20).

Listing .18: Function file for the Eigenfunction $\phi'_n(V)$

```
% phiprime_general.m

% This function file is used in the file theory_firingrate_IF.m
% to determine the value of the derivative of the
% eigenfunction phi_n.
function y=phiprime_general(v,gammaval,mu,sigma,theta)
% Define z
z=mu.*theta./(sigma.*sigma);
% Begin defining phi_n
term1=exp(z.*v./theta);
term2=(z./theta).*sinh(gammaval.*(theta-v)./theta);
term3=(gammaval./theta).*cosh(gammaval.*(theta-v)./theta);
% Define the constant c_lambda
term4=gammaval.*z.*cosh(gammaval);
term5=(gammaval.*gammaval-z).*sinh(gammaval);
term6=theta.*(term4+term5);
csublambda=2.*gammaval./term6;
y=(csublambda).*term1.*(term2-term3);
```

Listing .19: Function file for the Eigenfunction $\phi'_0(V)$

```
% phizeroprime_general.m

% This function file is used in the file theory_firingrate_IF.m
% to determine the value of the derivative of the
% eigenfunction phi_zero.
function y=phizeroprime_general(v,mu,sigma,theta)
% Define z
z=mu.*theta./(sigma.*sigma);
% Define the constant
coef=(sigma.*sigma)./(2.*mu.*mu);
c1=coef.*(2.*mu.*theta./(sigma.*sigma)-1...
+exp(-2.*mu.*theta./(sigma.*sigma)));
cAA=1./c1;
```

```
term1000= -2.*(cAA./(sigma.*sigma)).*exp(-2.*z.*(theta-v)./theta);
y=term1000;
```

Listing .20: Function file for the Eigenfunction $\psi(V)$

```
% psi_general.m

% This function file is used in the file theory_firingrate_IF.m
% to determine the value of the of the function psi_n.
function y=psi_general(v,gammaval,mu,sigma,theta)
% Define z
z=mu.*theta./(sigma.*sigma);
term1=exp(-z.*v./theta);
termA=sinh(gammaval.*v./theta);
termB=cosh(gammaval.*v./theta);
y=term1.*(gammaval.*termB+z.*termA);
```

Next, export the eigenvalue data saved in Listing .17 to the following code:

Listing .21: Driver for Figure 12

```
% theory_firingrate_IF.m
% Goal: Calculate the theoretical firing rate nu(t) of the IF neuron
% when V_L=V_R=0. This program calls data from gamma_and_evalues_IF.m
% It uses the function files phizeroprime_general.m,
% phiprime_general.m and psi_general.m
%+++++
clf % Clear all figures and values
tic % Set the timer
%===== Load the gamma and lambda values=====
load gammavalues_mupt05_sigma5.dat
load evalues_mupt05_sigma5.dat
gammaval11=gammavalues_mupt05_sigma5;
lambdavalues11=evalues_mupt05_sigma5;
% Define the vectors of real parts of gamma/lambda
realgamma=gammaval11(:,1); reallambda=lambdavalues11(:,1);
% Define the vectors of imaginary parts of gamma/lambda
imaggamma=gammaval11(:,2); imaglambda=lambdavalues11(:,2);
% Define the vector of complex gamma values.
gammavals=gammaval11(:,1)+1i*gammaval11(:,2);
gammavals_conj=gammaval11(:,1)-1i*gammaval11(:,2);
% Define the vector of complex lambda values.
lambdavals=lambdavalues11(:,1)+1i*lambdavalues11(:,2);
lambdavals_conj=lambdavalues11(:,1)-1i*lambdavalues11(:,2);
%=====
t=0:.0001:100; % Set the domain of nu(t).
mu=.05; % Set the correct mu, theta and sigma values.
sigma=5; theta=1; v0=0;
%=====Define nu(t)=====
% Set the first term in the firing rate: -sigma^2/2
```

```

term1=-(sigma*sigma)/2;
% The first term in the expansion
term2=phizeroprime_general(theta,mu,sigma,theta);
% Check that our limiting value is correct
prediction=term1*term2
B=prediction;
% The first term in the expansion (and conj)
term3=exp(lambdavalconj(1)*t)*...
    phiprime_general(theta,gammavalconj(1),mu,sigma,theta);
term4=exp(lambdaval(1)*t)*...
    phiprime_general(theta,gammaval(1),mu,sigma,theta);
term5=psi_general(v0,gammaval(1),mu,sigma,theta);
term6=psi_general(v0,gammavalconj(1),mu,sigma,theta);

% The second term in the expansion (and conj)
term31=exp(lambdavalconj(2)*t)*...
    phiprime_general(theta,gammavalconj(2),mu,sigma,theta);
term41=exp(lambdaval(2)*t)*...
    phiprime_general(theta,gammaval(2),mu,sigma,theta);
term51=psi_general(v0,gammaval(2),mu,sigma,theta);
term61=psi_general(v0,gammavalconj(2),mu,sigma,theta);

% The third term in the expansion (and conj)
term32=exp(lambdavalconj(3)*t)*...
    phiprime_general(theta,gammavalconj(3),mu,sigma,theta);
term42=exp(lambdaval(3)*t)*...
    phiprime_general(theta,gammaval(3),mu,sigma,theta);
term52=psi_general(v0,gammaval(3),mu,sigma,theta);
term62=psi_general(v0,gammavalconj(3),mu,sigma,theta);

% The fourth term in the expansion (and conj)
term33=exp(lambdavalconj(4)*t)*...
    phiprime_general(theta,gammavalconj(4),mu,sigma,theta);
term43=exp(lambdaval(4)*t)*...
    phiprime_general(1,gammaval(4),mu,sigma,theta);
term53=psi_general(v0,gammaval(4),mu,sigma,theta);
term63=psi_general(v0,gammavalconj(4),mu,sigma,theta);

% Define the firing rate nu(t)
nu=term1*(term2+term3*term6+term4*term5+...
    term31*term61+term41*term51+...
    term32*term62+term42*term52+...
    term33*term63+term43*term53);
% This expansion is for the first four eigenvalues.
% This works but it is too long to put in.
% Need a more effecient way to enter the functions.

% Save the function nu(t) for each mu.
Sol_data=[1000*t; nu];
%save theory_firing_rate_mu_20.dat -ascii Sol_data
%save theory_firing_rate_mu_5.dat -ascii Sol_data
%save theory_firing_rate_mu_1.dat -ascii Sol_data
%save theory_firing_rate_mu_pt1.dat -ascii Sol_data
%save theory_firing_rate_mu_25_sigma_10.dat -ascii Sol_data

```

```

%save theory_firing_rate_mu_pt1_sigma_5.dat -ascii Sol_data

%+++++++Plot the firing rate+++++++
figure(1)
plot(Sol_data(1,:),Sol_data(2,:), 'linewidth',4.5); hold on
plot(Sol_data(1,:),0*Sol_data(1,:)+B, '—k', 'linewidth',3.5);
set(gca, 'ytick',[0 20 40 60], 'fontsize',25)
set(gca, 'xtick',[0 100 200 300], 'fontsize',25)
text(-25,58, '\nu', 'fontsize',30);
text(150,50, '\mu=0.1, \theta=1, \sigma=5', 'fontsize',25);
text(380,-7, 't', 'fontsize',30);
text(150,40, ['\nu(\infty)=', num2str(B)], 'fontsize',25);
set(gca, 'linewidth',3.5, 'fontsize',30);
axis([0 400 -2 60]);
hold off
%print -fl -depsc2 theory_fr_mup1.eps
toc

```

A.5.2 Simulation of the Population Firing Rate

To simulate a population of N IF neurons and calculate the population run the Matlab file *pop_firingrate_IF.m* below.

Caution: The simulation of 10000 neurons requires roughly 50 minutes.

Listing .22: Driver to Compute the Population Firing Rate

```

% pop_firingrate_if.m
% Goal: To calculate the population firing rate for N IF
% neurons. In particular, we use this file to plot the
% population firing rate and the theoretical firing rate
% on the same axis. This is similar to Figure 2 of Mattia
clf % Clear all figures
% Set the timer (for a population of 10000 neurons
% it takes roughly 60 minutes to compute)
tic
neurons=10; % Set the number of neurons
delta= 0.001; % Set the value delta t
h=delta/100; % Set the step size
V_T=1; % Set the threshold value V_T=theta where a spike occurs
V_0=0; % Set the initial condition V_0=V(0)
V_L=0; % Set the reflective boundary V_L
V_R=0; % Set the reset value V_R
mu=-1; % Set the parameters mu and sigma
sigma=5; % Initialize the number of spikes for the population
numberofspikes=0; % Initialize the number of spikes per neuron
count=0; % Initialize the initial TOTAL spike count
secs=.5; % How many seconds to simulate
II=secs/h; % Set the number of iterations for the Euler method.

```

```

times=linspace(0,secs,secs/h+1); % Set the vector of times for which
                                % the SDE is solved.
V=zeros(1,secs/h); % Set the solution vector V(t).
spiketimes=[]; % Set the vector whose entries are the spike times.

% Find the equilibrium value
term1=-(sigma*sigma)/2;
% The first term in the expansion
term2=phizeroprime_general(V_T,mu,sigma,V_T);
% Check that our limiting value is correct
nu_infinity=term1*term2
% Use Forward Euler to simulate a population of neurons
for i=1:neurons
    for k=1:II
        V(k+1)=V(k)+h*mu+sigma*sqrt(h)*randn;
        if (V(k+1)<V_L)
            V(k+1)=V_R;
        end;
        if (V(k+1)>V_T)
            V(k)=V_T;
            V(k+1)=V_R;
            spiketimes=[spiketimes times(k)];
            count=count+1;
            numberofspikes=numberofspikes+1;
        end;
    end;
end;
spiketimes=spiketimes;
numberofspikes=count % Print the number of spikes for the population.
% We need to find the number of spikes in each
% subinterval (t,t+h). Recall that
% n(t,t+h)=number of spikes in (t,t+h).
subints=secs/delta; % Set the number of subintervals.
values=zeros(1,subints); % Set the vector that shows the number of
                          % spikes in each of the subintervals.
% Count the number of spikes in each subinterval.
for m=1:subints
    for n=1:numberofspikes
        count_1=0;
        if ((m-1)*delta < spiketimes(n));
            count_1=count_1+1;
        end;
        if (spiketimes(n)>m*delta)
            count_1=count_1-1;
        end;
        values(m)=values(m)+count_1;
    end
end
values;
% Check that the number of spikes in each sub-
% interval add up to the total number of spikes.
this_better_be_zero=sum(values)-numberofspikes % you should get 0
% Define the population firing rate function.
num_firingrate=values/(neurons*delta);

```

```

% Define the vector of times to plot against the
% population firing rate function.
times_1=linspace(0,secs ,secs/delta );
% Multiply the domain by 1000 to get ms
Sol_data=[1000*times_1; num_firingrate ];
% ++++++
% Save the data to plot with theoretical.
% ++++++
% Make sure the correct mu is used!!!!
% ++++++
% save pop_firing_rate_mu_20.dat -ascii Sol_data
% save pop_firing_rate_mu_5.dat -ascii Sol_data
% save pop_firing_rate_mu_1.dat -ascii Sol_data
% save pop_firing_rate_mu_pt1.dat -ascii Sol_data
% save pop_firing_rate_mu_25_sigma_10.dat -ascii Sol_data
% save pop_firing_rate_mu_pt1_sigma_5.dat -ascii Sol_data
% save pop_firing_rate_mu_neg1_sigma_1.dat -ascii Sol_data
% save pop_firing_rate_mu_neg1_sigma_5.dat -ascii Sol_data
% ++++++
% Plot the population firing rate.
% ++++++
figure(1)
% Multiply the domain by 1000 to use ms
plot(1000*times_1 , num_firingrate )
%axis([0 secs*1000 -2 60])

load pop_firing_rate_mu_neg1_sigma_5.dat
pfr=pop_firing_rate_mu_neg1_sigma_5;

figure(2)
plot(pfr(1,:), pfr(2,:), 'linewidth', 3.5);hold on
axis([0 40 -2 35]);hold off
toc

```

How to Reproduce Figure 13: First, use Listing .17 to calculate the eigenvalues and store the data. Then run the Matlab file *IF_firingrate_pop_theory.m* below.

Listing .23: Driver to Plot Population and Theoretical Firing Rate

```

% IF_firingrate_pop_theory.m
tic; clf
% Load population and theory data.
load pop_firing_rate_mu_pt1_sigma_5.dat
load theory_firing_rate_mu_pt1_sigma_5.dat
load pop_firing_rate_mu_20.dat; load theory_firing_rate_mu_20.dat
load pop_firing_rate_mu_5.dat; load theory_firing_rate_mu_5.dat
load pop_firing_rate_mu_1.dat; load theory_firing_rate_mu_1.dat
load pop_firing_rate_mu_pt1.dat; load theory_firing_rate_mu_pt1.dat

% Rename the data.

```

```

p20=pop_firing_rate_mu_20'; t20=theory_firing_rate_mu_20';
p5=pop_firing_rate_mu_5'; t5=theory_firing_rate_mu_5';
p1=pop_firing_rate_mu_1'; t1=theory_firing_rate_mu_1';
pp1=pop_firing_rate_mu_pt1'; tp1=theory_firing_rate_mu_pt1';
pnp=pop_firing_rate_mu_pt1_sigma_5';
pnt=theory_firing_rate_mu_pt1_sigma_5';

% Define the Matrices p and t whose columns are the data
p=[p20(:,1),p20(:,2),p5(:,2),p1(:,2),pp1(:,2)];
t=[t20(:,1),t20(:,2),t5(:,2),t1(:,2),tp1(:,2)];
% Set the vector of mu values for labeling the plots
mu=[20,5,1,0.1];
% Plot the functions
for k=1:4
    figure(k)
    plot(p(:,1),p(:,k+1),'r','linewidth',4.5); hold on
    plot(t(:,1),t(:,k+1),'linewidth',4.5); hold on
    set(gca,'linewidth',3.5,'fontsize',25);
    set(gca,'ytick',[0 15 30 45],'fontsize',25)
    set(gca,'xtick',[0 100 200 300],'fontsize',25)
    text(-30,58,'\nu','fontsize',25);
    text(150,50,['\mu=' num2str(mu(k))],'fontsize',35);
    text(145,40,'\theta=1,\sigma=1','fontsize',35);
    text(350,-9.8,'t_\textsubscript{ms}','fontsize',25);
    axis([0 400 -5 60])
end
figure(5)
plot(pnp(:,1),pnp(:,2),'r','linewidth',4.5); hold on
plot(pnt(:,1),pnt(:,2),'linewidth',4.5); hold on
set(gca,'linewidth',3.5,'fontsize',25);
set(gca,'ytick',[0 10 20],'fontsize',25)
set(gca,'xtick',[0 10 20 30],'fontsize',25)
text(-3,29,'\nu','fontsize',25);
text(15,15,'\mu=0.1','fontsize',35);
text(14.5,10,'\theta=1,\sigma=5','fontsize',35);
text(35,-7,'t_\textsubscript{ms}','fontsize',25);
axis([0 40 -5 30])

% Save the plots
%print -f1 -depsc2 if_firingrate_both_mu_20.eps
%print -f2 -depsc2 if_firingrate_both_mu_5.eps
%print -f3 -depsc2 if_firingrate_both_mu_1.eps
%print -f4 -depsc2 if_firingrate_both_mu_pt1.eps
%print -f5 -depsc2 if_firingrate_both_mu_pt1_sigma_5.eps

toc

```

BIBLIOGRAPHY

- [1] E. D. Adrian, Y. Zotterman, *The impulses produced by sensory nerve-endings: Part ii. The response of a single end-organ*, J Physiol, 61(2):151171, Apr 1926.
- [2] E. D. Adrian, Y. Zotterman, *The impulses produced by sensory nerve endings: Part iii. Impulses set up by touch and pressure*, J Physiol, 61(4):465483, Aug 1926.
- [3] E. D. Adrian, D. W. Bronk, *The Discharge of Impulses in Motor Nerve Fibres. Part I. Impulses in single fibres of the phrenic nerve*, J. Physiol. 66:81-101, 1928
- [4] F. Apfaltrer, C. Ly, D. Tranchina, *Population density methods for stochastic neurons with realistic synaptic kinetics: Firing rate dynamics and fast computational methods*, Network: Computation in Neural Systems, Vol. 17: pp. 373-419 (2006)
- [5] J. S. Anderson, I. Lampl, D. Gillespie, D. Ferster, *The contribution of Noise to Contrast Invariance of Orientation Tuning in Cat Visual Cortex*, Science 8 December 2000, Vol. 290 no. 5498 pp. 1968-1972
- [6] N. Brunel, M.C. Van Rossum *Lapicque's 1907 paper: from frogs to integrate-and-fire*, Biol. Cybern. 97 (5-6): 337339, 2007
- [7] F. Chance, L. Abbott, A. Reyes, *Gain modulation from background synaptic input*, Neuron 35: 773782. 2002
- [8] J. Cronin, *Mathematical aspects of Hodgkin-Huxley neural theory*, Cambridge University Press, 1987
- [9] B. Doiron, J. Rinzel, and A. Reyes, *Stochastic Synchronization in Finite Size Spiking Networks*, Physical Review E 74, 2006
- [10] J. FitzHugh, *Impulses and physiological states in theoretical models of nerve membrane*, Biophysical Journal 1, 1961
- [11] S. Fusi, M. Mattia, *Collective Behavior of Networks with Linear Integrate-and-Fire Neurons*, Neural Computation 11, 633 1999
- [12] G.L. Gerstein, B. Mandelbrot, *Random walk models for the spike activity of a single neuron*, Biophys J. Jan;4:41-68. 1964

- [13] W. Gerstner, W.M. Kistler, *Spiking Neuron Models*, Cambridge University Press, August 2002
- [14] H. Haken, *Brain Dynamics: An Introduction to Models and Simulations*, Springer, 2008
- [15] J.L. Hindmarsh, R.M. Rose, *A model of neuronal bursting using three coupled first order differential equations*, Proc. R. Soc. London, Ser. B 221:87102. 1984
- [16] A.L. Hodgkin, A. Huxley, *A quantitative description of membrane current and its application to conduction and excitation in nerve*, Journal of Physiology 117, 1952
- [17] E.M. Izhikevich, *Which model to use for cortical spiking neurons?*, IEE transactions on neural networks, VOL. 15, NO. 5 2004
- [18] B. W. Knight, *Dynamics of Encoding in a Population of Neurons*, Journal of General Physiology 59, 734 1972
- [19] B. W. Knight, *Dynamics of Encoding in Neuron Populations: Some General Mathematical Features*, Neural Computation 12, 473 2000
- [20] A. Kuhn, A. Aertsen, S. Rotter, *Neuronal Integration of Synaptic Input in the Fluctuation-Driven Regime*, The Journal of Neuroscience, March 2004, 24(10):2345-2356
- [21] L. Lapicque, *Recherches quantitatives sur l'excitation lectrique des nerfs traite comme une polarisation*, J. Physiol. Pathol. Gen. 9: 620635, 1907
- [22] B. Lindner, *Coherence and Stochastic Resonance in Nonlinear Dynamical Systems*, (Ph.D Dissertation), Humboldt University Berlin, 2002
- [23] C. Ly, B. Doiron, *Divisive Gain Modulation with Dynamic Stimuli in Integrate-and-Fire Neurons*, PLoS Comput Biol 5, e1000365, 2009
- [24] M. Mattia, P. Del Giudice, *Population Dynamics of Interacting Spiking Neurons*, Physical Review E 66, 051917 (2002)
- [25] P. Mullenowney, S. Iyengar *Parameter estimation for a leaky integrate-and-fire neuronal model from ISI data*, Journal Computational Neuroscience, 24(2):179-94, 2008
- [26] J. Nagumo, S. Arimoto, S. Yoshizawa, *An active pulse transmission line simulating nerve axon*, Proceedings of the IEEE 50, 1962
- [27] H. Okamoto, T. Fukai, *Recurrent Network Models for Perfect Temporal Integration of Fluctuating Correlated Inputs*, PLOs Computational Biology, Vol 5. Issue 6., 2009
- [28] A. Reyes, *Synchrony-dependent propagation of firing rate in iteratively constructed networks in vitro*, Nature Neuroscience Vol. 6, 6. June 2003
- [29] J. Rinzel, *Excitation dynamics: insights from simplified membrane models*, Federation Proceedings 44, 1985

- [30] H. Risken, *The Fokker-Planck Equation, 2nd ed.*, Springer-Verlag, Berlin, 1989
- [31] J. M. Steele, *Stochastic Calculus and Financial Applications*, Springer, New York, 2001
- [32] R. Stein, *A theoretical analysis of neuronal variability*, Biophys. J. 5 , pp. 173194 1965
- [33] W. R. Softky, C. Koch, *The Highly Irregular Firing of Cortical Cells is Inconsistent with Temporal Integration of Random EPSPs*, The Journal of Neuroscience, January 1983, 13(1): 334-350
- [34] R. Leao, S. Li, B. Doiron, T. Tzounopoulos, *Diverse Expression of a Single Pottasium Conductance Generates Heterogeneous Neuronal Behavior in a Population of Pyramidal Neurons*
- [35] H.C. Tuckwell, *Introduction to Theoretical Neurobiology*, Cambridge University Press, 1988
- [36] H.R. Wilson, *Simplified dynamics of human and mammalian neocortical neurons*, Journal of Theoretical Biology 200, 1999